DRUG-CYTOKINE CYTOTOXIC INTERACTION: RELATIONSHIP TO IDIOSYNCRATIC, DRUG-INDUCED LIVER INJURY

Ву

Ashley Maiuri

A DISSERTATION

Submitted to
Michigan State University
in partial fulfillment of the requirements
for the degree of

Pharmacology and Toxicology – Environmental Toxicology – Doctor of Philosophy

2015

ABSTRACT

DRUG-CYTOKINE CYTOTOXIC INTERACTION: RELATIONSHIP TO IDIOSYNCRATIC, DRUG-INDUCED LIVER INJURY

By

Ashley Maiuri

Idiosyncratic, drug-induced liver injury (IDILI) occurs in a small fraction of susceptible patients and can be life threatening. Importantly, the current methods employed during preclinical safety evaluation of drug candidates fail to accurately identify those with IDILI liability before they reach the market. Accordingly, assays to identify drug candidates with the potential to cause IDILI early in the drug development process are greatly needed. Knowledge concerning mechanisms of IDILI is limited, but evidence in humans and animals implicates a role for immune mediators in the pathogenesis. Interestingly, several drugs associated with IDILI interact with cytokines, including tumor necrosis factor-alpha (TNF) and interferon gamma (IFN), in vitro to cause death of primary human hepatocytes and human-derived HepG2 cells. A major focus of this dissertation was to determine if cytotoxic synergy between drugs and cytokines can accurately classify drugs according to their IDILI liability. Indeed, cytotoxic synergy between drugs and TNF led to the generation of a statistical model that accurately classified a set of 24 drugs according to their IDILI potential. This result suggests a promising in vitro approach that is amenable to high throughput methodology and that could be used during preclinical safety evaluation to identify drug candidates with the potential to cause IDILI.

Another major focus of this dissertation was to gain a deeper understanding of the signaling mechanisms underlying the cytotoxic interaction between IDILI-associated drugs and TNF and IFN. Along with antibiotics, NSAIDs are among the most frequent causes of IDILI. The cytotoxic interaction between NSAIDs with various IDILI liabilities and the two cytokines was investigated, and dichotomous roles for several mitogen activated protein kinases (MAPKs) were found. The findings suggest that NSAIDs associated with IDILI synergize with cytokines to cause HepG2 cell death that is driven by different kinase signaling mechanisms. The differences appear to be related to chemical structure and IDILI liability.

The cytotoxic interaction between diclofenac (DCLF), an NSAID associated with IDILI, and TNF and IFN, was examined further. DCLF causes ER stress in HepG2 cells, which contributes to the cytotoxic interaction with TNF. Intracellular calcium (Ca⁺⁺) dysregulation, ER stress and MAPK activation are closely linked cellular responses. DCLF is known to promote intracellular Ca⁺⁺ dysregulation in hepatocytes. The contribution of free cytoplasmic Ca⁺⁺ to the DCLF/cytokine interaction was examined. Chelation of intracellular free Ca++ with BAPTA/AM reduced DCLF-mediated activation of the ER stress sensor protein kinase RNA-like endoplasmic reticulum kinase (PERK) and the activation of c-Jun N-terminal kinase (JNK) and extracellular signal-regulated kinase (ERK). Importantly, BAPTA/AM and an inositol trisphosphate (IP3) receptor antagonist reduced the cytotoxic interaction between DCLF and cytokines, suggesting that Ca++ contributes to the cytotoxic interaction. Additionally, interdependence of the activation of JNK and ERK was found. These findings provide insight concerning the cytotoxic interaction between DCLF and cytokines. Additionally, these results raise the possibility that Ca⁺⁺ contributes to the cytotoxic synergy between other drugs and the cytokines TNF and IFN, and might contribute to some cases of human IDILI.

ACKNOWLEDGEMENTS

There are so many people that deserve my thanks. The past five years that I have spent here at MSU in this Ph.D. program have probably been the most challenging of my life so far, but also the most exciting and rewarding. I absolutely could not have made it to this stage in my life and career without the support of the long list of people to follow.

First, I have to thank my mentors, Dr. Robert Roth and Dr. Patricia Ganey. If it was not for Bob's e-mail to me after my first time attending the Michigan Society of Toxicology (MISOT) meeting as an undergraduate, I might not have applied to the graduate program at MSU. Although I was interested in toxicology, with my academic background in ecology and evolutionary biology, I had never considered applying to a pharmacology/toxicology graduate program. My interactions with Bob at the MISOT meeting made me reconsider, and I'm so thankful that I did. When I joined the graduate program in the Department of Pharmacology and Toxicology I knew right away that I wanted to work with Bob and Patti. I was fortunate enough to be given the opportunity to do a research rotation in their lab. Needless to say, it was not difficult for me to decide to join the lab. Transitioning from my undergraduate program to the graduate program in pharmacology was quite a challenge, especially considering that fact that my academic background was not strong in the life sciences (physiology, molecular biology, etc.). Although I was intimidated at first, Bob and Patti were very encouraging and patient with me. They created an environment in the lab where I always felt comfortable engaging with them in discussion about my research. They have always been eager to listen to

my ideas and have encouraged me to think critically about my research and also to think outside the box. It is no secret in the lab that I am intimidated by public speaking to both large and small audiences. Thanks in large part to the positive feedback, encouragement and advice I have received from Bob and Patti, I am much more comfortable with this than I ever thought I could be. Their enthusiasm for research and mentoring students is really inspiring to me and has greatly contributed to my decision to continue to do research, and hopefully mentor students, after graduate school.

Outside the lab, Bob and Patti are as awesome as they are inside the lab. I always enjoy going to dinner with them or going out for happy hour. They work extremely hard but they also find time to enjoy themselves and spend time with their family.

The other members of my thesis committee, Dr. Pesta and Dr. Copple, deserve my thanks. Committee meetings can be intimidating, but Dr. Pestka and Dr. Copple always provided such good ideas and advice with regard to my research project. They thought about things that I would have never thought about on my own. Their involvement played an in instrumental role in the path that my project has taken over the years. My project has transformed considerably since I initially proposed it, in a really positive way, and this is thanks in large part to my meetings involving Dr. Pestka and Dr. Copple. Not only are they both great scientists, they are also just really wonderful people and I have always enjoyed my interactions with them.

I would also like to thank the Department of Pharmacology and Toxicology. I'm so proud to be a part of this department. I have enjoyed all of my interactions with the faculty members, students and administrative staff. The department has supported me both financially and in my academic and professional development over the years and I

am deeply thankful for that. Dr. Dorrance has been really instrumental in ensuring that the graduate students are satisfied. She has provided me with a lot of helpful advice over the years and has provided me with opportunities to grow professionally, especially via grad student forum. I am very thankful for her assistance. I am so thankful for the wonderful friends I have made here. Nikita Joshi has been such a wonderful friend to me; she constantly cheers me up when I have had a bad day and always knows what to say when things are not quite right. Thank you to Teri Lansdell, Keara Towery, Megan Carnaghi and Carly Gerhardt for being such great friends to me and for taking such good care of my dog when I have to go out of town.

I am also very thankful for the Center for Integrative Toxicology (CIT), as well as the administrative staff. The CIT has supported my travel to various national meetings including the Society of Toxicology (SOT) annual meeting and the Experimental Biology (EB) annual meeting. I am grateful for taking part in the Environmental and Integrative Toxicological Sciences program. This program provided opportunities for me to engage with students outside of my home department, whom I might not have met or interacted with. I also had to the opportunity to meet and engage with many outstanding toxicologists from various fields (industry, government, academia) because of my involvement with the CIT and EITS program.

I would like to thank the previous members of the Roth/Ganey laboratory. Dr. Kazuhiza Miyakawa has been a great friend and lab mate over the years, has given me great advice and has trained me to perform several techniques in the lab. Dr. Kevin Beggs, Dr. Kyle Poulsen and Dr. Aaron Fullerton made me laugh all the time. They provided me with a lot of encouragement especially as I was going through some of the

most difficult steps of the graduate program. They have given me some great advice over the years, both with regard to my research project, and with regard to life in general. Dr. Erica Sparkenbaugh has been such a great friend to me and although I was relatively new in the lab as she was graduating she has provided me with much support and advice over the years. She also provided me with a place to stay for three weeks when I traveled to North Carolina. I am thankful for my interactions with Nicole Crispe and Ryan Albee who provided much administrative and research support when I initially started working in the lab. Additionally, I have had the privilege of working closely with several extremely talented undergraduates, veterinary students, graduate students and rotating graduate students. Robert Parkins, Gurpreet Kaur, Teri Lansdell, Lukas Gora, Anna Breier and Jonathan Turkus have all made significant contributions to the work presented in this dissertation. I am so grateful for their assistance with my thesis project. Dr. Bronlyn Wassink also deserves my thanks; without her statistical expertise I could not have completed Chapter 2 of this dissertation. I am also very thankful for her patience with my lack of expertise in statistics, and for not laughing at me when I asked really basic questions.

I am thankful for the SOT and for the MISOT. I am thankful for the opportunities to attend and present at these meetings. These experiences allowed me to engage with many outstanding scientists and have allowed me to begin to build a professional network. Presenting research at these meetings has also improved my ability to communicate effectively to others about my research.

I am very thankful for the training grant support I have received over the years from the National Institutes of Health (NIH). I was fortunate enough to be supported for

three years of my predoctoral training with fellowships form the NIH. Bob and Patti have worked extremely hard to provide funding for all members of their lab and for this I am extremely thankful.

Thanks to my family for all of the support over the years. My parents, Martin and Janice Maiuri, have always been so supportive of me in all aspects of my life. They have always been my biggest source of encouragement. If it was not for them I truly would not be who I am today or where I am today. My siblings, Ryan and Julia, have also been extremely encouraging and supportive over the years. They are my best friends and soulmates and constantly lift me up when fall down.

I am also very thankful for the McCord family, Margo, Steve, Robbie and Tommy, who have welcomed me into their family. They have taken me on several of their family vacations with them. They constantly shower me with kindness and love and make me feel like part of their family.

My dog, Maeby, deserves a great deal of my gratitude, she constantly lights up my life. She is excited to see me every day when I come home from work and it doesn't matter if I have had a bad day or not, my mood instantly improves when I see her.

Lastly, my best friend and partner Paul has played a pivotal role in my success over the years. He has listened to me vent and gripe about failed experiments and has managed to help me through some of my most challenging obstacles thus far. Thank you for talking to me every single night for the past three and a half years; it really has helped get me through this. Thank you from the bottom of my heart for your constant supply of encouragement, support and love. I'm so excited to move to Bloomington with

you and I hope I am able to help you as you navigate the rest of your Ph.D. program, as much as you have helped me.

TABLE OF CONTENTS

LIST OF TABLES	xiv
LIST OF FIGURES	xvii
KEY TO ABBREVIATIONS	xx
CHAPTER 1: General Introduction and Specific Aims	
1.1 Overview of the liver and acute liver failure	
1.2 Types of drug-induced liver injury	
1.2.1 Drug-induced liver injury	
1.2.2 Idiosyncratic drug-induced liver injury.	
1.3 Hypothesized mechanisms of idiosyncratic drug-induced liver injury	
1.3.1 Genetic polymorphism hypothesis	
1.3.2 Failure-to-adapt hypothesis	
1.3.3 Hypotheses involving the immune system	
1.3.3.1 Adaptive immunity hypothesis	
1.3.3.2 Inflammatory stress hypothesis	
1.3.4 Inflammatory stress in the context of other hypotheses of idiosyncration	
drug-induced liver injury	
1.4 Involvement of cytokines in idiosyncratic drug-induced liver injury	
1.4.1 Tumor necrosis factor-alpha	
1.4.2 Interferon-gamma	
interferon gamma	
1.5 Mitogen activated protein kinase signaling pathways and their involvement	
injury	
1.5.1 c-Jun N-Terminal Kinase	28
1.5.2 Extracellular Signal-Regulated Kinase	32
1.5.3 p38	34
1.6 Calcium signaling, endoplasmic reticulum stress and cell death	37
1.7 Current status of preclinical safety evaluation of drugs in development	
1.8 Hypothesis and specific aims	
1.9 Significance of dissertation	50
CHAPTER 2: An In Vitro Approach to Classify Drugs According to their Pot	
to Cause Idiosyncratic Hepatotoxicity	
2.2 Introduction	
2.3 Materials and Methods	
2.3.1 Materials.	

	2.3.2 Cell Culture	56
	2.3.3 IDILI classification	56
	2.3.4 Cytotoxicity Assessment	
	2.3.5 Statistical Analysis	
	2.4 Results	
	2.4.1 Drug/cytokine cytotoxicity: concentration-response	
	2.4.2 Cmax is moderately associated with IDILI potential	
	2.4.3 ROC analysis of models incorporating the base covariates	
	2.4.5 ROC analysis of models incorporating various combinations of the bas	
	and derived covariates	
	2.4.6 Addition of IFN did not improve the classification of drugs according to	
	potential to cause IDILI	
	2.5 Discussion	92
	HAPTER 3: Cytotoxic Synergy Between Cytokines and NSAIDs Associated	
ld	iosyncratic Hepatotoxicity by Mitogen-activated Protein Kinases	
	3.1 Abstract	
	3.2 Introduction	
	3.3 Materials and Methods	
	3.3.1 Materials	
	3.3.2 Animals	
	3.3.3 Cell Culture	102
	3.3.4 IDILI Classification	.103
	3.3.5 Cytotoxicity Assessment	105
	3.3.6 Caspase-3 Activity	106
	3.3.7 Protein Isolation	106
	3.3.8 Western Analysis	107
	3.3.9 Statistical Analysis	
	3.4 Results	
	3.4.1 NSAID/cytokine-induced cytotoxicity concentration-response	
	3.4.2 Cytotoxic synergy between cytokines and NSAIDs requires caspases.	
	3.4.3 Cytotoxic synergy between cytokines and NSAIDs requires activation of	
	JNK	
	3.4.4 Cytotoxic synergy between cytokines and NSAIDs requires activation	
	ERK	
	3.4.5 p38 attenuates NSAID/cytokine-induced cytotoxic synergy	
	3.4.6 DCLF but not IBU promotes dual phosphorylation of STAT-1 in an ERI	
	dependent mannerdependent manner	
	3.5 Discussion	
	U.U DIOUUOOIUI I	ı¬- l

CHAPTER 4: Calcium Contributes to the Cytotoxic Interaction Between	4 47
Diclofenac and Cytokines	
4.1 Abstract	
4.2 Introduction	
4.3 Materials and Methods	
4.3.1 Materials	
4.3.2 Cell Culture	
4.3.3 Experimental Design and Cytotoxicity Assessment	
4.3.4 Caspase-3 Activity	
4.3.5 Protein Isolation	
4.3.6 Western Analysis	
4.3.7 Statistical Analysis	
4.4 Results	158
4.4.1 An intracellular Ca ⁺⁺ chelator reduced cytotoxicity mediated by	4 = 0
DCLF/cytokine cotreatment	
4.4.2 An IP3 receptor antagonist reduced cytotoxicity induced by DCLF/	-
cotreatment	
4.4.3 Ca ⁺⁺ contributes to DCLF/mediated activation of the ER stress ser	
PERK	_
4.4.4 Ca ⁺⁺ contributes to DCLF-mediated JNK activation	
4.4.5 Ca ⁺⁺ contributes to DCLF-mediated ERK activation	
4.4.6 Ca ⁺⁺ contributes to DCLF/IFN-mediated phosphorylation of STAT-	
727	
4.4.7 JNK promotes DCLF/IFN-mediated phosphorylation of STAT-1 at	
via activation of ERK	
4.4.8 Aspirin does not promote activation of JNK or ERK, or the ER stre	
sensor, PERK	
4.5 Discussion	179
CHAPTER 5: Summary, Implications and Future Directions	
5.1 Development of an in vitro approach with the potential to accurately pred	
liability of drugs in development	100 188
5.1.2 Implications for preclinical safety evaluation of drugs in development	
5.2 Elucidating mechanisms of cytotoxic synergy between drugs associated	
IDILI and the cytokines TNF and IFN: a focus on NSAIDs	
5.2.1 Involvement of caspases and MAPKs in NSAID/cytokine-induced	
cytotoxicity: summary of findings	190
5.2.2 Requirement of the availability of cytoplasmic free Ca ⁺⁺ in the cyto	
interaction between DCLF and cytokines: summary of findings	
idiosyncratic hepatotoxicity	3 01 197

5.3 Proposed future directions	200
APPENDIX	208
REFERENCES	228

LIST OF TABLES

Table 1: IDILI classification, Cmax concentration expressed in μM units and references from which the Cmax for a given drug was derived57
Table 2: The optimal cutoff threshold for the model incorporating the covariates TNF change, EC50 VEH, EC50 TNF, Delta VEH, and Cmax86
Table 3: Coefficients for the model incorporating the covariates TNF change, EC50 VEH, EC50 TNF, Delta VEH, and Cmax87
Table 4: The classification of the set of 24 drugs based on the model incorporating TNF change, EC50 VEH, EC50 TNF, Delta VEH, and Cmax89
Table 5: NSAID subclass and maximal plasma concentration (Cmax) from therapeutic doses in human patients104
Table 6: Minimum (min) LDH percentage values210
Table 7: Maximum (max) LDH percentage values211
Table 8: Concentration-response slope values212
Table 9: Concentration-response EC50 values213
Table 10: EC10 values: the [drug]/Cmax value corresponding to 10% of the difference between the max and min (max – min)
Table 11: D10 values for each drug/cytokine treatment combination215
Table 12: R10 values: the [drug]/Cmax at which a 10 percent increase in the LDH response above baseline occurs216
Table 13: EC50 quotient, EC10 quotient, R10 quotient and maxmindiff values for each drug/cytokine treatment combination
Table 14: The values for the categorical variable TNF change for each drug218
Table 15: Coefficients for the model incorporating the covariates TNF change, EC50 VEH, EC50 TNF, and Delta VEH219
Table 16: The optimal cutoff threshold for the model incorporating the covariates TNF change, EC50 VEH, EC50 TNF, and Delta VEH219

Table 17: Coefficients for the model incorporating the covariates TNF change, EC50 VEH, EC50 TNF, and Cmax220
Table 18: The optimal cutoff threshold for the model incorporating the covariates TNF change, EC50 VEH, EC50 TNF, and Cmax220
Table 19: Coefficients for the model incorporating the covariates maxmindiff, EC50 VEH, EC50 TNF, and Delta VEH221
Table 20: The optimal cutoff threshold for the model incorporating the covariates maxmindiff, EC50 VEH, EC50 TNF, and Delta VEH221
Table 21: Coefficients for the model incorporating the covariates maxmindiff, EC50 VEH, EC50 TNF, Delta VEH, Cmax222
Table 22: The optimal cutoff threshold for the model incorporating the covariates maxmindiff, EC50 VEH, EC50 TNF, Delta VEH and Cmax222
Table 23: Coefficients for the model incorporating the covariates TNF change, EC50 quotient, Delta VEH and Cmax223
Table 24: The optimal cutoff threshold for the model incorporating the covariates TNF change, EC50 quotient, Delta VEH and Cmax223
Table 25: Coefficients for the model incorporating the covariates TNF change, R10 VEH, R10 TNF, Delta VEH and Cmax224
Table 26: The optimal cutoff threshold for the model incorporating the covariates TNF change, R10 VEH, R10 TNF, Delta VEH and Cmax224
Table 27: Coefficients for the model incorporating the covariates maxmindiff, R10 VEH, R10 TNF and Delta VEH225
Table 28: The optimal cutoff threshold for the model incorporating the covariates maxmindiff, R10 VEH, R10 TNF and Delta VEH225
Table 29: Coefficients for the model incorporating the covariates TNF change, Delta VEH and Cmax226
Table 30: The optimal cutoff threshold for the model incorporating the covariates TNF change, Delta VEH and Cmax226
Table 31: Coefficients for the model incorporating the covariates TNF change, R10 quotient, Delta VEH and Cmax227

Table 32: The optimal cutoff threshold for the model incorporating the TNF change, R10 quotient, Delta VEH and Cmax	
Table 33: Coefficients for the model incorporating the covariates TNF EC50 quotient and Cmax	O ,
Table 34: The optimal cutoff threshold for the model incorporating the TNF change, EC50 quotient and Cmax	

LIST OF FIGURES

Figure. 1: Hepatocellular signaling pathways activated in response to TNF binding to the TNF receptor19
Figure 2: Signaling pathways activated in response to IFN binding to the IFN receptor24
Figure 3: Diagram of the MAPK signaling modules29
Figure 4: Causes and consequences of the endoplasmic reticulum stress response pathway43
Figure 5: Drug/cytokine-induced cytotoxicity; concentration-response66
Figure 6: Comparison of a model incorporating Cmax from a set of 24 drugs to a model incorporating Cmax from a set of 272 drugs72
Figure 7: Evaluation of models incorporating the base covariates75
Figure 8: Evaluation of models incorporating the derived covariates78
Figure 9: Evaluation of models incorporating combinations of the base and derived covariates82
Figure 10: ROC curves with an AUC > 0.9584
Figure 11: Comparison of models incorporating covariate(s) that describe the drug/TNF concentration response curve to those that include response to IFN
Figure 12: Cytokine concentration response studies111
Figure 13: Interaction of NSAIDs with cytokines leads to synergistic cytotoxicity
Figure 14: Bromfenac/cytokine-induced cytotoxic synergy in primary mouse hepatocytes115
Figure 15: Caspase activation in response to DCLF/cytokine and IBU/cytokine treatment117
Figure 16: Caspases are involved in the NSAID/cytokine-induced cytotoxic interaction

Figure 17: Time course of DCLF/cytokine-induced cytotoxic synergy121
Figure 18: DCLF and IBU treatment induce prolonged activation of JNK122
Figure 19: JNK is involved in the NSAID/cytokine-induced cytotoxic interaction125
Figure 20: DCLF and IBU treatment induce prolonged activation of ERK127
Figure 21: ERK is involved in the NSAID/cytokine-induced cytotoxic interaction130
Figure 22: Treatment with TNF, DCLF or IBU induces activation of p38132
Figure 23: P38 plays a protective role in NSAID/cytokine-induced cytotoxicity134
Figure 24: DCLF promotes ERK-dependent phosphorylation of STAT-1 in the presence of IFN
Figure 25: IBU treatment prevents IFN-mediated phosphorylation of STAT- 1139
Figure 26: Treatment with BAPTA/AM, a membrane-permeable Ca2+ chelator, reduced cytotoxicity mediated by DCLF/cytokine co-treatment159
Figure 27: Lack of Ca++ in culture medium did not affect the cytotoxic interaction between DCLF and cytokines161
Figure 28: Treatment with 2-APB, an IP3 receptor antagonist, almost completely eliminated cytotoxicity induced by DCLF/cytokine co-treatment163
Figure 29: Ca ⁺⁺ contributes to DCLF-mediated activation of the ER stress sensor, PERK165
Figure 30: Ca ⁺⁺ contributes to DCLF-mediated JNK activation167
Figure 31: Ca ⁺⁺ contributes to DCLF-mediated ERK activation170
Figure 32: Ca ⁺⁺ contributes to DCLF/IFN-mediated phosphorylation of STAT-1 at Ser 727172
Figure 33: JNK promotes DCLF/IFN-mediated phosphorylation of STAT1 at Ser 727 via activation of ERK175

Figure 34: Aspirin does not promote activation of the MAPKS, JNK and ER	K, or
the ER stress sensor, PERK	177
Figure 35: Proposed mechanism of DCLF/cytokine-induced cytotoxic	
synergy	185

KEY TO ABBREVIATIONS

ALT Alanine aminotransferase

2APB 2-aminophenoxydiphenyl borate

AP-1 Activator protein-1

ASK1 apoptosis signal regulating kinase 1

ASA Aspirin

BAPTA/AM acetoxymethyl-1,2-bis(2-aminophenoxy)ethane-N,N,N',N'-tetraacetic acid

BRM bromfenac

CYP cytochrome p450

Ca⁺⁺ calcium

DCLF diclofenac

DILI drug-induced liver injury

DOX doxorubicin

ERK extracellular signal-regulated kinase

FADD Fas-associated death domain

FDA Food and Drug Administration

GAS gamma associated sequenes

IBU ibuprofen

IDILI idiosyncratic drug induced liver injury

IFN interferon-gamma

IFNR IFN receptor

IkB inhibitor of kappa B

IKK inhibitor of kappa B kinase

IL interleukin

iNOS inducible nitric oxide synthase

IRF1 interferon regulatory factor 1

JAK Janus kinase

JNK c-Jun N-terminal kinase

LDH lactate dehydrogenase

LPS lipopolysaccharide

MAPK mitogen activated protein kinase

MKK MAPK kinase

MyD88 myeloid differentiation factor

MAL MyD88 adaptor-like protein

MPT mitochondrial permeability transition

NAP naproxen

NFkB nuclear factor-kappa B

NIH National Institutes of Health

NK natural killer

PBS phosphate buffered saline

RIP1 receptor interacting protein 1

PAMP pathogen associated molecular pattern

PRR pattern recognition receptor

ROS reactive oxygen species

Ser serine

SLD sulindac

STAT1 signal transducer and activator of transcription 1

TLR toll like receptor

TNF tumor necrosis factor-alpha

TNFR1 TNF receptor 1

TNFR2 TNF receptor 2

TRADD TNF receptor-associated death domain

TRAF2 TNF receptor-associated factor 2

TRAIL TNF-related apoptosis-inducing ligand

TRAM TRIF-related adaptor molecule

TRIF TIR-containing adaptor molecule

TVX trovafloxacin

Tyr tyrosine

VEH vehicle

CHAPTER 1:

General Introduction and Specific Aims

1.1 Overview of the liver and acute liver failure

The liver is the largest internal organ in the human body and it plays a pivotal role in metabolism and maintaining homeostasis. The liver receives approximately 80% of its blood supply from the gut via the portal venous system, and this blood is enriched with food-borne nutrients, drugs consumed orally, as well as bacterial products. Its anatomical location and role in xenobiotic metabolism render the liver vulnerable to various diseases and injury from chemical toxicants.

Acute liver failure (ALF), or loss of liver function, is a rare but deadly disease with a typically rapid onset. It often occurs in patients with no known underlying liver disease. Serious complications can arise during ALF including excessive bleeding due to the liver's impaired ability to produce coagulation factors, hepatic encephalopathy and kidney failure (Trey, et al., 1970). Although rare, ALF is a challenging problem clinically and the cause is often difficult to identify. The causes of ALF include viral hepatitis, autoimmune hepatitis, drug-induced toxicity, ischemia and other rare causes. The progression and outcome of ALF vary depending on the etiology. The mortality rate of ALF is high, and emergency liver transplantation is the only effective treatment available. Death without liver transplantation occurs in approximately 30% of adults with ALF (Lee, et al., 2008).

1.2 Types of drug-induced liver injury

1.2.1 Drug-induced liver injury

Drug-induced liver injury (DILI) is the leading cause of ALF in the United States (Aithal, et al., 2011, Ostapowicz, et al., 2002). It remains the most common adverse effect associated with failure to obtain U.S. Food and Drug Administration approval for new drugs (Aithal, et al., 2011, Watkins, 2005). DILI represents an important problem not only clinically but also for the pharmaceutical industry and regulatory agencies. Approximately 1,000 drugs have been implicated in causing liver injury (Zimmerman, 1999). DILI is an important therapeutic challenge for physicians due to a variety of factors. The clinical presentations of DILI can be hepatocellular, cholestatic or mixed and the pattern of liver injury can change over time. Moreover, the severity and lesion morphology of DILI varies depending on the offending drug. Variability in the severity and histopathology of DILI exists even among drugs within the same pharmacological class (O'Connor, et al., 2003, Teoh, et al., 2003). Patients presenting with symptoms of DILI are commonly misdiagnosed, and this is largely due to the fact that DILI can mimic many forms of acute and chronic liver injury (Larson, et al., 2005). Importantly, the difficulty in accurately diagnosing DILI makes it challenging to determine the incidence rate for a given drug.

1.2.2 Idiosyncratic drug-induced liver injury

An important subset of DILI is idiosyncratic drug-induced liver injury (IDILI). One study reported that 13% of DILI cases are attributed to IDILI (Ostapowicz et al. 2002).

IDILI is a condition that occurs in a small fraction of susceptible individuals but often results in severe liver injury that can lead to liver transplantation or death. Moreover, IDILI is the most common cause of post-marketing warnings and withdrawals of drugs from the pharmaceutical market (Aithal, et al., 2011, Kaplowitz, 2005, Watkins, 2005). Although drugs from various classes have been implicated in cases of IDILI, nonsteroidal anti-inflammatory drugs and antibiotics are the most common causes of IDILI. The occurrence of IDILI is influenced by patient susceptibility factors, either genetic, environmental or a combination of both.

IDILI remains a significant public health concern, and currently there are no effective preclinical procedures available to predict the potential of a drug to cause IDILI in humans (Aithal, et al., 2011, Kaplowitz, 2005). Important features of idiosyncratic adverse drug reactions include apparent lack of dose dependence and variability in the time-to-onset of toxicity. They often occur at doses that are safe in the majority of patients, and sometimes these reactions do not take place until the patient has been on maintenance therapy with a drug for several weeks or months. Moreover, drugs that cause IDILI in people do not typically cause liver injury in animals used in preclinical safety evaluation of drugs in development. These characteristics likely account for the difficulty in developing useful in vivo and in vitro models to predict the potential of a drug candidate to cause IDILI. There is a tremendous need for the development of assays to identify drug candidates with the potential to cause IDILI before they reach the marketplace. An increased understanding of mechanisms of IDILI will aid in the development of approaches that could be used during preclinical safety evaluation to screen for IDILI liability of drug candidates in development.

1.3 Hypothesized mechanisms of idiosyncratic drug-induced liver injury

Currently, there is limited knowledge concerning mechanisms of IDILI. However, several hypotheses have been proposed to explain its occurrence and pathogenesis. To date, no hypothesis has been proven or disproven and none are mutually exclusive.

The following sections will discuss several hypotheses of the etiology of IDILI in detail.

1.3.1 Genetic polymorphism hypothesis

A popular hypothesis to explain the pathogenesis of IDILI is that certain genetic polymorphisms can render individuals susceptible to toxicity from an otherwise innocuous dose of a drug. Polymorphisms in drug metabolizing enzymes, including the cytochrome p450 (CYP) enzymes, have been identified in humans. Such polymorphisms could lead to elevated levels of a potentially toxic parent drug or drug metabolite in the plasma thereby increasing a patient's susceptibility to injury. Isoniazid is a widely used drug used in the treatment of tuberculosis and is highly associated with IDILI. The mechanism of how isoniazid causes IDILI is unknown but it is highly speculated that genetic polymorphisms involving the enzymes that metabolize isoniazid are involved. Isoniazid is metabolized to acetylisoniazid via N-acetyltransferase 2 (NAT2) and then hydrolyzed to acetylhydrazine. Acetylhydrazine can be metabolized further by CYP2E1 to potentially hepatotoxic intermediates. Isoniazid can also be hydrolyzed directly to hydrazine, which is known to be toxic to the liver as well (Hughes, et al., 1954). Genetic polymorphisms in the NAT2 and CYP2E1 genes were found to be associated with isoniazid-induced liver injury in human patients (Sun, et al., 2008). However, other studies have failed to find such associations between the same genetic

polymorphisms and the occurrence of isoniazid-induced liver injury, making it difficult to establish cause and effect (Gurumurthy, et al., 1984). In addition to polymorphisms related to drug metabolizing enzymes, other genetic polymorphisms might play a role in influencing a patient's susceptibility to IDILI reactions. For instance, a polymorphism in a cytoprotective factor could increase a patient's likelihood of developing IDILI.

Associations between polymorphisms in human leukocyte antigen genes and the occurrence of IDILI have also been identified (Lucena, et al., 2011) and will be discussed in a later section. To date, no animal models based on the genetic polymorphism hypothesis have been developed that accurately reproduce the severity of IDILI that occurs in human patients. Further investigation with regard to the involvement of specific genetic polymorphisms in the pathogenesis of IDILI is warranted.

1.3.2 Failure to adapt hypothesis

The failure to adapt hypothesis states that patients who are susceptible to IDILI are those who are unable to adapt to modest liver damage caused by a drug (Watson, 2005). As with the genetic polymorphism hypothesis, this hypothesis is supported mainly by circumstantial evidence. For instance, many patients undergoing therapy with isoniazid experience elevated alanine aminotransferase levels in their serum yet only a very small fraction of these patients develops severe hepatotoxicity (Black, et al., 1975). This observation raises the possibility that isoniazid induces modest liver injury in most patients but only the individuals that lack the capacity to adapt to modest liver injury are susceptible to overt hepatotoxicity caused by drug exposure. The failure to adapt

hypothesis is consistent with all other hypotheses of IDILI in the sense that many factors including certain genetic polymorphisms, underlying disease states, and other conditions might interfere with an individual's capacity to repair modest liver damage caused by a drug exposure. Importantly, experimental evidence in animals supporting the failure to adapt hypothesis of IDILI is non-existent.

1.3.3 Hypotheses involving the immune system

Some hypotheses of IDILI exhibit a common theme: involvement of immune system activation in the precipitation of IDILI responses. The immune system can be divided into two categories. The innate immune system is tasked with providing the first line of defense against infection from initial exposure to pathogens. The adaptive immune system is responsible for providing specific defense against continued or repeated exposure to pathogens. The liver permanently houses both innate (eg, macrophages, natural killer (NK) cells, etc.) and adaptive immune cell types (eg, T cells) and upon injury or infection, infiltration of additional immune cells (innate and/or adaptive) can occur (Crispe, 2009). Each of these immune cell types can be activated in response to various stimuli including bacterial infection or tissue injury. Upon activation, immune cells release factors (e.g. cytokines and chemokines) that lead to the recruitment of other immune cell types to the site of injury and/or infection. Factors released from immune cells such as cytokines can cause injury to healthy cells by activating pathways that lead to cell death. Although activation of innate and adaptive immune responses is critical to protecting a host from infection, inappropriate activation of the innate and/or adaptive immune system can cause tissue injury in individuals.

Hypotheses of IDILI implicating a role for immune mediators are described in detail below.

1.3.3.1 Adaptive immunity hypothesis

A long-standing hypothesis of IDILI is the adaptive immunity hypothesis. According to this hypothesis, liver injury develops in response to a hypersensitivity reaction initiated by exposure to a drug. Liver injury induced by an adaptive immune response to a drug exposure sometimes involves the characteristic signs of an immune hypersensitivity reaction including fever, skin rash, eosinophilia, jaundice and rapid recurrence on rechallenge (Bissell, et al., 2001, Liu and Kaplowicz, 2002). Initiation of these reactions is hypothesized to occur by the covalent binding of a drug or its metabolite to an endogenous protein, creating a hapten. The hapten is seen as a foreign antigen and thereby elicits a harmful adaptive immune response. Drugs are typically not immunogenic on their own, but it is thought that their tendency to become immunogenic increases when bound to a macromolecule such as protein (Liu and Kaplowicz, 2002). When a hapten is formed, it becomes internalized by antigen presenting cells (APCs), such as macrophages and then processed and presented as antigens on the APC's surface. APCs present these antigens to naïve T cells containing major histocompatibility complex (MHC) molecules. In response to this, T cells undergo clonal expansion and subsequently activation upon re-exposure to the offending drug. Activation of T cells results in release of factors that lead to recruitment and activation of other potentially harmful immune cell types including cytotoxic T lymphocytes, antibody producing B cells and NK cells. Each of these cell types can release various cytokines including interferon gamma (IFN), tumor necrosis factor-alpha (TNF), interleukin (IL)-4,

IL-5 and IL-17. These cytokines are immune mediators that can activate intracellular pathways involved in cell survival, proliferation and cell death depending on the cell type and the state of the cell (Crispe, 2009).

There is circumstantial evidence to support the role of adaptive immunity in IDILI responses. Immune-mediated skin rashes have been reported to accompany human IDILI induced by some drugs (Devuyst, et al., 1993). Halothane was a widely used anesthetic in the 1980s, but due to the risk of IDILI associated with this drug its use was drastically limited in adults in the U.S. Liver biopsies from patients who died from halothane-induced hepatitis demonstrated infiltration of immune cells (Cousins, et al., 1989). A reactive metabolite of halothane, trifluoroacetyl chloride (TFA), was identified as being potentially involved in the hepatitis induced by halothane. TFA can form adducts with proteins and lipids in the liver (Bourdi, et al., 1996). It has been suggested that an antibody-mediated autoimmune reaction underlies cases of severe halothane-induced hepatitis. The presence of antibodies against a TFA hapten in the sera of patients afflicted with halothane hepatitis has been reported previously (Bird and Williams, 1989).

More recently, studies have demonstrated associations between human leukocyte antigen (HLA) polymorphisms and cases of IDILI. Some of the drugs for which associations between cases of IDILI and HLA polymorphisms have been identified include amoxicillin/clavulanate, flucloxacillin, ximelegatran, lapatinib and ticlopidine (Daly, et al., 2009, Hirata, et al., 2008, Kindmark, et al., 2008, Lucena, et al., 2011, Spraggs, et al., 2011).

Although there is circumstantial evidence supporting the involvement of adaptive immune responses in cases of IDILI, no animal models based on this hypothesis have been generated that recapitulate the severe liver injury that occurs in patients undergoing IDILI. This makes it difficult to understand the mechanisms of how adaptive immunity contributes to IDILI. That being said, in cases of IDILI that are driven by an adaptive immune response, it is likely that immune mediators such as cytokines released from immune cells contribute to hepatocellular killing.

Recently published studies reported that impaired immune tolerance might play a role in IDILI responses elicited by amodiaquine and halothane. Chakraborty, et al., (2015) produced an animal model of delayed-onset, halothane-induced hepatitis in mice depleted of myeloid derived suppressor cells (MDSCs). MDSCs comprise a population of immature and mature myeloid cells that play an important role in regulating immune responses during infection and/or injury. MDSCs regulate immune responses by suppressing T cell clonal expansion and activation (Gabrilovich and Nagaraj, 2009). Treatment of female balb/c mice with halothane resulted in a rapid increase in ALT which quickly resolved. Depletion of MDSCs prior to halothane treatment did not alter liver injury after the initial dose of halothane. However, when MDSC depleted mice were challenged with halothane 14 days after the initial treatment, mild liver injury was observed 9 days later (Chakraborty, et al., 2015). This animal study is one of the first to demonstrate a role for the involvement of the adaptive immune system in halothaneinduced hepatitis. That being said, in this model the injury produced in response to the second halothane exposure was much less severe than the injury produced in response to the first halothane exposure. This is counter-intuitive based on what is observed in

human patients who develop severe liver injury in response to multiple exposures to halothane. Moreover, the authors did not comment on why the severe toxicity induced by the first exposure to halothane was necessary for the less hepatotoxic response observed upon rechallenge. Dugan, et al., (2011) produced a model of acute halothaneinduced liver injury in female balb/c mice after a single administration of the drug. The injury occurred after 12 hours of treatment and this response was closely mimicked by the response that occurred after the first halothane administration in the study by Chakraborty, et al., (2015). The severe injury observed in the study conducted by Dugan, et al., (2011) was dependent on NK cells suggesting a requirement of the innate immune system in the pathogenesis. Although Chakraborty, et al., (2015) did not characterize the injury caused by the first administration of halothane; it is likely that an innate-immune mediated mechanism similar to what was observed in the study performed by Dugan, et al., (2011) was responsible, given the striking similarity in responses observed. The connection between the presumed innate immune-mediated liver injury elicited by the first halothane administration and the adaptive immunemediated injury caused by the second administration remains to be elucidated but may involve cross talk between the innate and adaptive immune systems.

In another study, depletion of cytotoxic T lymphocyte-associated protein 4 (CTL4) in mice resulted in delayed onset of mild, amodiaquine-induced liver injury (Metushi, et al., 2015a). In this study, programmed cell death-1 (PD1) knockout mice also developed liver injury in response to amodiaquine exposure. CTL4 and PD1 are known negative regulators of lymphocyte activation (Pardoll, 2012). These studies suggest that failure to maintain immune tolerance during drug exposure might underlie some cases of human

IDILI. Additionally, Metushi, et al., (2015b) found that depletion of NK cells attenuated the mild liver injury induced by amodiaquine exposure. When activated, NK cells release the cytokine interferon gamma (IFN) which is known to activate signaling pathways that lead to cell death. Additionally, Chakraborty, et al., (2015) found that depletion of CD4 T cells, which also release IFN, protected mice from the delayed onset of halothane hepatitis. It is possible that IFN by itself or in the presence of other cytokines promotes hepatocellular killing in cases of human IDILI induced by amodiaquine or halothane.

Although these recent animal studies shed light on the potential role of adaptive immunity in IDILI responses, it is worth emphasizing that the liver injury produced in these models is mild, unlike the severe liver injury that occurs in patients taking these drugs. This suggests that while adaptive immunity might be important in promoting IDILI responses in humans, other factors likely play a role in addition to activation of the adaptive immune system.

1.3.3.2 Inflammatory stress hypothesis

Inflammation is classically characterized by pain, redness, heat, swelling and loss of function. Tissue inflammation is characterized by the accumulation of immune cells at a site of infection or injury followed by immune cell activation and release of mediators including cytokines, chemokines, enzymes such as proteases and many other factors. Inflammatory responses can be induced by a variety of stimuli including infection, surgery, alcohol consumption and xenobiotic exposure. Hepatocytes comprise 80% of the liver volume, whereas 20% of the liver volume comprises nonparenchymal cells including endothelial cells, stellate cells, Kupffer cells and lymphocytes (Gao, et al.,

2008). Kupffer cells, the resident macrophages of liver, play an important role in initiating inflammatory responses in the liver. In mammalian organisms, Kupffer cells detect the presence of pathogens via specialized receptor complexes known as pattern recognition receptors (PRRs). PRRs recognize pathogen-associated molecular patterns (PAMPs) that are highly conserved molecular structures on the surfaces of microbes. Toll-like receptor-4 (TLR4) is a membrane-bound PRR found on the surfaces of Kupffer cells and initiates inflammatory responses in mammalian systems in response to certain PAMP stimuli (Bode, et al., 2012).

One of the best characterized PAMPs is lipopolysaccharide (LPS). LPS, a component of gram-negative bacterial cell walls, is a PAMP that is recognized by TLR4 (Fontana and Vance, 2011). Ligation of LPS to TLR4 leads to activation of macrophage effector functions, namely the production of cytokines and chemokines, which initiates an inflammatory response. Binding of LPS to TLR4 causes receptor oligomerization and recruitment of adaptor proteins including myeloid differentiation factor (MyD88), MyD88 adapter-like protein (MAL), TIR-containing adapter molecule (TRIF/TICAM-1), and TRIF-related adaptor molecule (TRAM). This leads to activation of nuclear factor kappa B (NFkB) and several mitogen activated protein kinases (MAPKs), including extracellular-signal-regulated kinase (ERK), p38, and c-Jun N-terminal kinase (JNK). Upon activation, NFkB translocates to the nucleus and binds to response elements on the DNA, ultimately leading to the induction of pro-inflammatory cytokines such as TNF, IL-6 and various chemokines (Bode, et al., 2012).

The inflammatory stress hypothesis states that a modest inflammatory episode can render an individual susceptible to toxicity from an otherwise nontoxic dose of a

drug (Roth and Ganey, 2011). Inflammatory episodes are commonplace in people and occur erratically throughout life. These factors can explain the unpredictable nature of IDILI responses. The observation that rheumatoid arthritis is a risk factor for IDILI in human patients suggests that immune mediators might contribute to IDILI pathogenesis (Garcia Rodriguez, et al., 1994). Several rodent models have been developed that suggest that inflammation plays an important role in IDILI (Shaw, et al., 2010). When LPS is administered at doses that cause noninjurious liver inflammation along with a nontoxic dose of a drug with idiosyncrasy liability, severe liver injury develops in rodents. Conversely, when the drug or LPS is administered alone, no liver injury occurs in these models. Drugs for which drug/LPS-induced liver injury models have been produced include trovafloxacin, ranitidine, halothane, amiodarone, chlorpromazine, doxorubicin, sulindac, and diclofenac (Buchweitz, et al., 2002, Deng, et al., 2006, Dugan, et al., 2010, Hassan, et al., 2008, Lu, et al., 2012, Luyendyk, et al., 2003, Shaw, et al., 2007, Zou, et al., 2009). Importantly, drugs without IDILI liability did not synergize with LPS to induce liver injury in rodents (Luyendyk, et al., 2003, Shaw, et al., 2007). Additionally, other PAMPs including peptidoglycan/lipoteichoic acid and poly I:C have been shown to synergize with IDILI-associated drugs to produce liver injury in rodents (Cheng, et al., 2009, Shaw, et al., 2009).

Inflammatory cytokines are expressed and mediate critical events in both adaptive and innate immune responses. The inflammatory mediators tumor necrosis factor-alpha (TNF) and IFN can be released from both innate and adaptive immune cell types. Not surprisingly, the levels of these two cytokines, as well as others, were found to be elevated in animals treated with LPS in combination with IDILI associated-drugs.

Interestingly, studies involving transgenic animals showed that the cytokines TNF and IFN are critical to the pathogenesis of liver injury that occurs in animal models of drug/LPS-induced liver injury (Deng, et al., 2007, Hassan, et al., 2008, Lu, et al., 2012, Shaw, et al., 2007, Shaw, et al., 2009b, Shaw, et al., 2009c, Tukov, et al., 2006, Zou, et al., 2009, Zou, et al., 2011). Involvement of the cytokines TNF and IFN in IDILI responses will be discussed in detail below.

1.3.4 Inflammatory stress in the context of other hypotheses of idiosyncratic drug-induced liver injury

It is worth noting that the inflammatory stress hypothesis is not mutually exclusive of other hypotheses of IDILI. Indeed, inflammation might be important in most if not all modes of action of IDILI. For example, inflammatory stress might interact with other patient susceptibility factors to lead to an IDILI response. A genetic polymorphism in pro-inflammatory or anti-inflammatory cytokine expression could make certain individuals susceptible to IDILI, and this would be consistent with both the inflammatory stress hypothesis and the genetic polymorphism hypothesis of IDILI. In fact, patients with polymorphisms in the anti-inflammatory genes IL-10 and IL-4 were at a greater risk of developing IDILI from DCLF (Aithal, 2004). Another study found an association between a polymorphism in the TNF gene and IDILI caused by amoxicillin clavulanate although this was not discussed in the study (Lucena, et al., 2011).

Inflammatory stress could prevent the liver from adapting to modest damage elicited by a drug that would normally resolve. This would be consistent with the failure to adapt hypothesis of IDILI, which states that patients susceptible to IDILI are ones

whose livers are unable to adapt to modest damage caused by a drug upon continued exposure (Watkins, 2005). Also consistent with the failure to adapt hypothesis is the fact that the inflammatory cytokines TNF and IFN are known to have anti-proliferative effects on the liver in response to injury (Sato, et al., 1993, Wullaert, et al., 2007). A scenario in which TNF and/or IFN are elevated in the liver to an extent that inhibits proliferative repair could underlie a failure to adapt to modest injury and lead to more pronounced cell death in response to a drug exposure.

The inflammatory stress hypothesis is also consistent with the adaptive immunity hypothesis. It is well understood that innate and adaptive immune responses are highly interdependent. Indeed, it has been shown that cytokines released form innate immune cells are critical to the proliferative expansion and activation of various adaptive immune cell types including Th17 cells (Schenten and Medzhitov, 2011). In the studies described above demonstrating involvement of adaptive immune responses in halothane and amodiaquine hepatotoxicity, it is possible that an innate immune response (i.e. an inflammatory response) was required to initiate the expansion of effector lymphocytes.

1.4 Involvement of immune mediators in idiosyncratic drug-induced liver injury

As mentioned above, there is evidence that inflammatory cytokines play a role in IDILI. Rodent models of drug/inflammatory stress-induced liver injury have implicated a role for the cytokines TNF and IFN in precipitating IDILI responses. Although various cytokines might contribute to IDILI, it is evident that TNF and IFN in particular play critical roles. An overview of the TNF and IFN signaling pathways, as well as evidence for the involvement of these cytokines in IDILI, will be discussed below.

1.4.1 Tumor necrosis factor alpha

Activation of immune cells including Kupffer cells, neutrophils, NK cells and others results in the release of a variety of growth factors, reactive oxygen species (ROS), and inflammatory cytokines such as TNF (Roberts, et al., 2007). TNF is a pleiotropic cytokine that plays an important role in liver physiology. TNF signaling can induce either hepatocyte proliferation or hepatocyte apoptosis. An appropriate balance between TNF-induced hepatocyte proliferation and apoptosis is critical to preserving homeostasis in the liver (Wullaert, et al., 2007). TNF exerts its biological effects by activating two distinct plasma membrane receptors, TNF receptors 1 and 2 (TNFR1 and TNFR2, respectively). TNFR1 is constitutively expressed in most cell types, whereas TNFR2 is typically expressed in immune cells, and its expression is highly regulated (Wajant, et al., 2003). This section will focus on signaling mediated by TNFR1 as it is responsible for initiating most of the biological activities of TNF (Chen and Goeddel, 2002).

Binding of TNF to TNFR1 can lead to activation of the transcription factor nuclear factor-κB (NFκB) or to induction of apoptosis (Wajant, et al., 2003). Whether TNFα

promotes cell survival signaling via NFκB or apoptotic signaling depends on the state of the cell. TNF binding to the extracellular domain of TNFR1 initiates recruitment of adaptor proteins including TNF receptor associated death domain (TRADD), receptor interacting protein (RIP), and TNF receptor associated factor (TRAF). Once this receptor complex (complex I) is formed, RIP and TRAF cooperate to recruit transforming growth factor-beta (TGF-β) activated kinase (TAK). TAK phosphorylates and activates inhibitor of κB kinase (IKK) which phosphorylates NFκB-bound inhibitor of κBα (IκBα), leading to its ubiquitination and subsequent proteosomal degradation.

Degradation of IκBα allows NFκB to translocate to the nucleus and bind to response elements on DNA, leading to transcription of NFκB responsive genes, many of which are involved in cell survival and proliferation (Wullaert, et al., 2007).

Alternatively, in addition to recruiting TRADD, TRAF, and RIP, activation of TNFR1 can lead to the recruitment of Fas-associated death domain (FADD) by TRADD (complex II) (Wullaert, et al., 2007). FADD can recruit proteins such as procaspase-8. Procaspase-8 undergoes autoactivation leading to the formation of active caspase-8, which is able to activate bcl-2 interacting protein (Bid) proteolytically, forming truncated Bid (tBid). Upon activation, tBid can translocate to the outer mitochondrial membrane leading to formation of the mitochondrial permeability transition (MPT) pore. MPT pore formation allows release of cytochrome c into the cytosol. Cytosolic cytochrome c facilitates apoptosome formation by recruiting apoptosis protease associated factor (Apaf-1) and procaspase-9. Activation of procaspase-9 leads to formation of initiator caspase-9 which can cleave and activate effector caspases-3 and 7, leading to apoptosis (Wullaert, et al., 2007) (Figure 1).

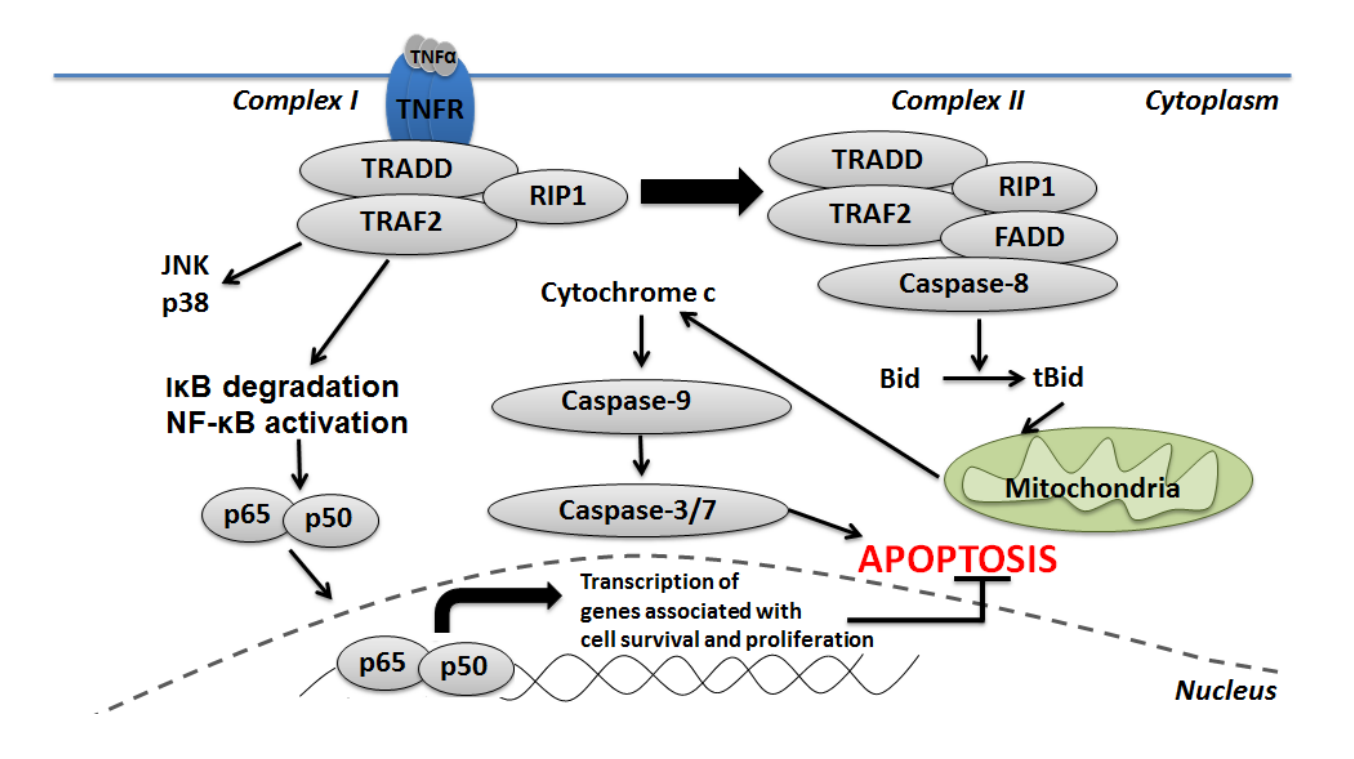


Figure. 1: Hepatocellular signaling pathways activated in response to TNF binding to the TNF receptor. TNF activates dichotomous signaling pathways in hepatocytes. The specific pathway activated in response to TNFα depends on the context. In healthy hepatocytes, TNF binding to its receptor leads to transient activation of JNK and p38. Additionally, IκB is degrading permitting activation of NF-κB followed by NF-κB translocation into the nucleus and transcription of genes associated with proliferation and cell survival. Under pathological conditions in the liver, or in stressed hepatocytes, TNF activates a signaling cascade that leads to activation of caspase 8 which cleaves the pro-apoptotic protein Bid. Truncated Bid (tBid) translocates to the mitochondrion and facilitates permeabilization of the mitochondrial membrane, release of cytochrome c, activation of initiator caspase 9 followed by cleavage and activation of the executioner caspase 3/7 and subsequently apoptosos. Figure adapted from Wullaert, et al., (2007).

TNF signaling is critical to the development of hepatotoxicity observed in rodent models of drug/LPS-induced liver injury (Roth and Ganey, 2011). Etanercept, a soluble TNF receptor, protected rodents from drug/LPS-induced liver injury (Lu, et al., 2012, Shaw, et al., 2009a, Zou, et al., 2009). TNFR1 or TNFR2 knockout mice were protected from liver injury induced by trovafloxacin(TVX)/LPS coexposure (Shaw, et al., 2009a). TNF augmented the cytotoxicity of sulindac sulfide in primary rat hepatocytes and in HepG2 cells (Zou, et al., 2009). It also potentiated cytotoxicity of chlorpromazine in primary mouse hepatocytes (Gandhi, et al., 2009). Moreover, several drugs associated with IDILI synergized with an inflammagen mixture containing TNF, IFN, IL-1alpha, and LPS, causing cytotoxicity in HepG2 cells and primary human hepatocytes (Cosgrove, et al., 2009). Another study demonstrated that diclofenac (DCLF) synergized with TNF to kill HepG2 cells, and this depended on caspase activation and c-Jun N-terminal kinase (JNK) activation (Fredriksson, et al., 2011). Additionally, various agents including drugs associated with IDILI have been shown to synergize with TNF-related apoptosisinducing ligand (TRAIL) to cause death of cells including hepatocytes (Hellwig and Rehm, 2012).

In most of the studies mentioned above, treatment with the drug or with TNF/TRAIL alone did not result in cytotoxicity. This suggests that certain drugs induce cellular stress that normally does not lead to cell death; however, after drug treatment the cells become sensitized such that in the presence of TNF, apoptosis occurs. Although animal studies implicated a role for TNF in IDILI, evidence in humans is lacking. One study found an association between a polymorphism in the promoter area of the TNF gene and incidence of anti-tubercular drug-induced hepatotoxicity (Kim, et

al., 2012). Various inflammatory diseases are associated with a guanine-to-adenine (G/A) transition 308 nucleotides upstream of the transcription initiation site in the TNF gene locus (Elahi, et al., 2009). Indeed, this nucleoside was associated with elevated TNF levels in the plasma. Interestingly, this particular polymorphism has been associated with hypersensitivity to carbamazepine, another drug associated with IDILI (Pirmohamed, et al., 2001). These findings in humans lend credence to the hypothesis that TNF plays an important role in the pathogenesis of human IDILI.

1.4.2 Interferon-gamma

Interferon-gamma (IFN) is a proinflammatory cytokine that is responsible for modulating a variety of immune and inflammatory responses (Farrar and Schreiber, 1993). T-lymphocytes and NK cells represent the major cellular sources of IFN. Specifically, CD8+ T-cells and CD4+ T-cells produce IFN following recognition of antigens associated with major histocompatibility complex (MHC) class I and II, respectively. Additionally, NK cells produce IFN in response to TNF released from activated macrophages and eosinophils (Farrar and Schreiber, 1993).

IFN exerts its biological actions via the activation of the Janus kinase/signal transducer and activator of transcription (JAK/STAT) signaling pathway (Stark, et al., 1998). Signaling via the JAK/STAT pathway is initiated when a cytokine such as IFN binds to its receptor (IFNR). Upon binding of IFN to the IFNR, the receptor dimerizes and undergoes autophosphorylation of specific tyrosine residues located on the intracellular portion of the receptor. The phosphorylated tyrosine residues serve as a docking site for the STAT1 transcription factor which, upon binding to the receptor, becomes phosphorylated and subsequently activated by JAK (Kisseleva, et al., 2002). Activation of STAT1 leads to its dimerization and translocation to the nucleus, where it binds to gamma-activated sites (GAS) on the DNA, evoking transcription of genes involved in regeneration, antiviral defense, cell cycle progression, and/or apoptosis (Kisseleva, et al., 2002). Genes involved in apoptosis, such as interferon regulatory factor-1 (IRF1), are upregulated in response to IFN-mediated STAT1 activation. Upon activation of the IFNR by IFN, JAK phosphorylates the STAT1 protein at tyrosine (Tyr) 701. It has been shown that mitogen activated protein kinases (MAPKs) promote

phosphorylation of STAT1 at serine (Ser) 727. Previously, it was thought that phosphorylation of STAT1 at Tyr 701 by JAK was enough to fully activate STAT1. However, it has been shown recently that maximal activation of the transcription factor STAT1 in response to IFN requires phosphorylation at both the Tyr 701 and Ser 727 positions (Wen, et al., 1995). It is thought that phosphorylation of STAT1 at Tyr 701 occurs in the cytoplasm, and then upon translocation of STAT1 to the nucleus it is phosphorylated at Ser 727 by MAPKs (Sadzak, et al., 2008) (Figure 2).

The JAK/STAT pathway is involved in most aspects if IFN signaling. However, IFN responsive genes can be regulated by alternative pathways (non-STAT-mediated pathways) (Horras, et al., 2011). For example, in STAT1-deficient mice, IFN treatment stimulates upregulation of IRF1. IRF1 is a transcription factor that can lead to expression of inducible nitric oxide synthase (iNOS) and p53, which regulate apoptosis and cell cycle progression (Horras, et al., 2011).

IFN is critical to the development of liver injury in several animal models of drug/LPS-induced hepatotoxicity (Dugan, et al., 2011, Hassan, et al., 2008, Shaw, et al., 2009b). Gene expression profiling revealed that genes involved in the IFN signaling pathway, such as interferon regulatory factor-1 (IRF-1), are selectively upregulated in response to TVX/LPS cotreatment of mice compared to either TVX or LPS treatment alone (Shaw, et al., 2009b). Moreover, IFN knockout mice treated with TVX/LPS were protected from liver injury (Shaw, et al., 2009b). Another study revealed that doxorubicin (DOX)/LPS cotreatment synergistically enhanced liver injury in rodents, and this enhancement depended on IFN (Hassan, et al., 2008). A neutralizing antibody to IFN protected rodents from DOX/LPS-induced hepatotoxicity (Hassan, et al., 2008). Gene

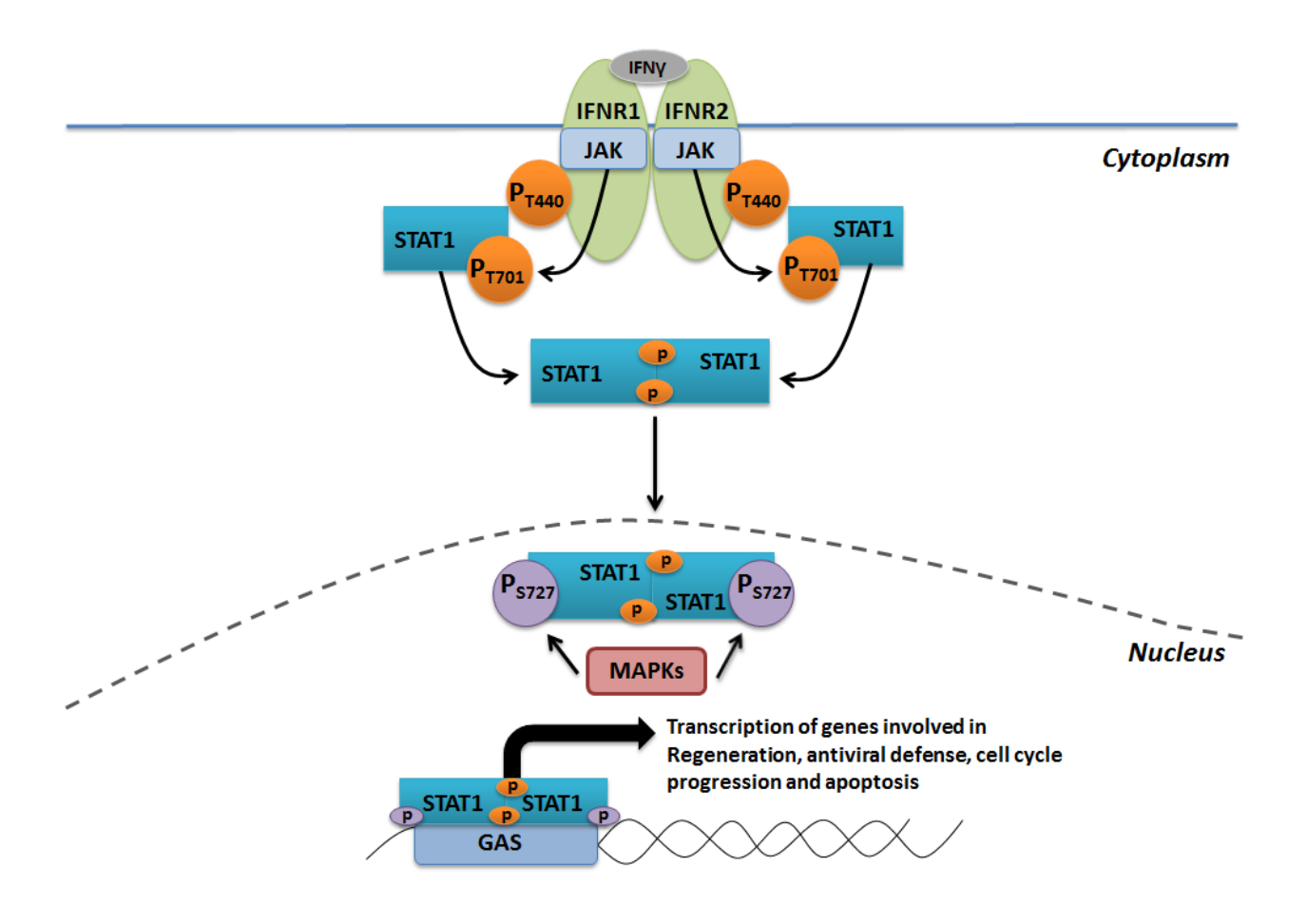


Figure 2. Signaling pathways activated in response to IFN binding to the IFN receptor. IFN activates the JAK/STAT signaling pathway. The IFN receptor is a heterodimer associated with Janus kinase (JAK). Activation of the IFN receptor by IFN leads to activation of JAK which phosphorylates the IFNγ receptor at tyrosine 440. Phosphorylation of the IFN receptor at this position provides a docking site for the transcription factor STAT1. Association of STAT1 with the IFN receptor permits phosphorylation of STAT1 by JAK at tyrosine 701. Phosphorylated STAT1 dimerizes followed by translocation of STAT1 to the nucleus. Once inside the nucleus, STAT1 can be phosphorylated by other kinases including MAPKs at serine 727. Phosphorylation of STAT1 at both the tyrosine 701 and serine 727 positions is required for maximal

Figure 2 (cont'd)

activation. Activated STAT1 binds to gamma associated sequences (GAS) on the DNA leading to transcription of genes involved in regeneration, antiviral defense, cell cycle progression and apoptosis. Figure adapted from Shuai, et al., (2003).

expression analysis of the livers from rodents treated with diclofenac (DCLF) demonstrated increased expression of various genes involved in both the TNF and IFN signaling pathways including TNF receptor superfamily member 1a (TNFRSF1a), signal transducer and activator of transcription-1 (STAT1) and the tumor suppressor protein p53 (Deng, et al., 2008). The specific mechanism by which IFN contributes to the hepatotoxicity observed in these drug/LPS animal models is unclear, but it is possible that IFN synergizes with the drug itself or with other inflammatory mediators such as TNF to cause hepatocellular death.

IFN plays a role in downregulating hepatocyte proliferation during liver regeneration (Sato, et al., 1993). It has been reported that IFNRs are expressed on hepatocytes in a liver stressed by inflammatory disease but not in a normal liver (Volpes, et al., 1991). Moreover, IFN suppressed liver regeneration following partial hepatectomy (Sato, et al., 1993). Accordingly, the anti-proliferative effects of IFN might promote the pathogenesis of liver injury in rodent models of drug/LPS-induced hepatotoxicity by inhibiting liver regeneration.

The findings from animal models discussed above implicate a role for IFN in the pathogenesis of IDILI. However, it is presently unclear whether IFN contributes to human IDILI. Additional studies evaluating the role of IFN in human IDILI are needed. It is interesting that a genetic polymorphism in the IFN gene was found to be associated with certain adverse drug reactions (Charli-Joseph, et al., 2013). This lends support to the hypothesis that IFN plays an important role in some cases of IDILI.

1.4.3 Mechanisms of cytotoxic synergy between tumor necrosis factor alpha and interferon gamma

IFN and TNF can synergize with each other, causing DNA fragmentation and apoptosis in primary cultured mouse hepatocytes (Morita, et al., 1995). IFN can synergize with LPS, TNF, or IL-1 to induce expression of the iNOS gene. Depending on the redox state of the cell, iNOS can either promote or inhibit hepatocyte apoptosis (Vodovotz, et al., 2004). For instance, in the absence of redox stress, iNOS production can lead to generation of cGMP and S-nitrosation of caspases, leading to inhibition of apoptosis. Conversely, in the presence of redox stress, iNOS production can lead to generation of oxidizing species that potentiate hepatocyte apoptosis (Vodovotz, et al., 2004). Exposure of pancreatic beta cells to TNF and IFN caused caspase-3 and STAT-1 dependent apoptosis (Cao, et al., 2013, Cao, et al., 2015). Taken together, these findings indicate that the TNF and IFN signaling pathways can interact with each other leading to synergistic cytotoxicity in various cell types including hepatocytes. Moreover, cytotoxic synergy between proinflammatory cytokines might play a role in some cases of IDILI.

1.5 Mitogen activated protein kinase signaling pathways

MAPKs are major components of signaling cascades that regulate a multitude of cellular processes including differentiation, proliferation and cell death (Johnson and Lapadat, 2002). MAPKs play a particularly important role in how cells respond to certain stresses. There are three distinct MAPK signaling modules which lead to activation of either c-Jun N-terminal kinase (JNK), extracellular signal-regulated kinase (ERK), or p38 kinase (Cowan and Storey, 2003). The MAPK signaling modules operate as a three-tiered cascade that can be initiated by either growth factor stimulation, stimulation by cellular stress or cytokine exposure. Stimulation by any of these initiates the activation of MAPK kinase kinases (MAPKKs). Subsequently, MAPKKKs phosphorylate and activate MAPK kinases (MAPKKs). Activation of the MAPKKs, MEK 1/2, MKK 4/7 or MKK 3/6, leads to activation of JNK, ERK 1/2 or p38, respectively (Figure 3).

1.5.1 c-Jun N-terminal kinase

Three genes that encode for JNK have been identified: JNK1, JNK2 and JNK3. In humans, JNK1 and JNK2 are ubiquitously expressed among tissues whereas expression of JNK3 is restricted to the brain, heart and testis (Davis, 2000). Alternative splicing of the three genes encoding for JNK results in the formation of 10 known JNK isoforms. In most instances translation of the JNK1 gene leads to a protein product that is 46 kDa whereas translation of the JNK2 gene leads to a protein product that is 55 kDa (Bogoyevitch, 2006). Phosphorylation of JNK generally occurs in response to

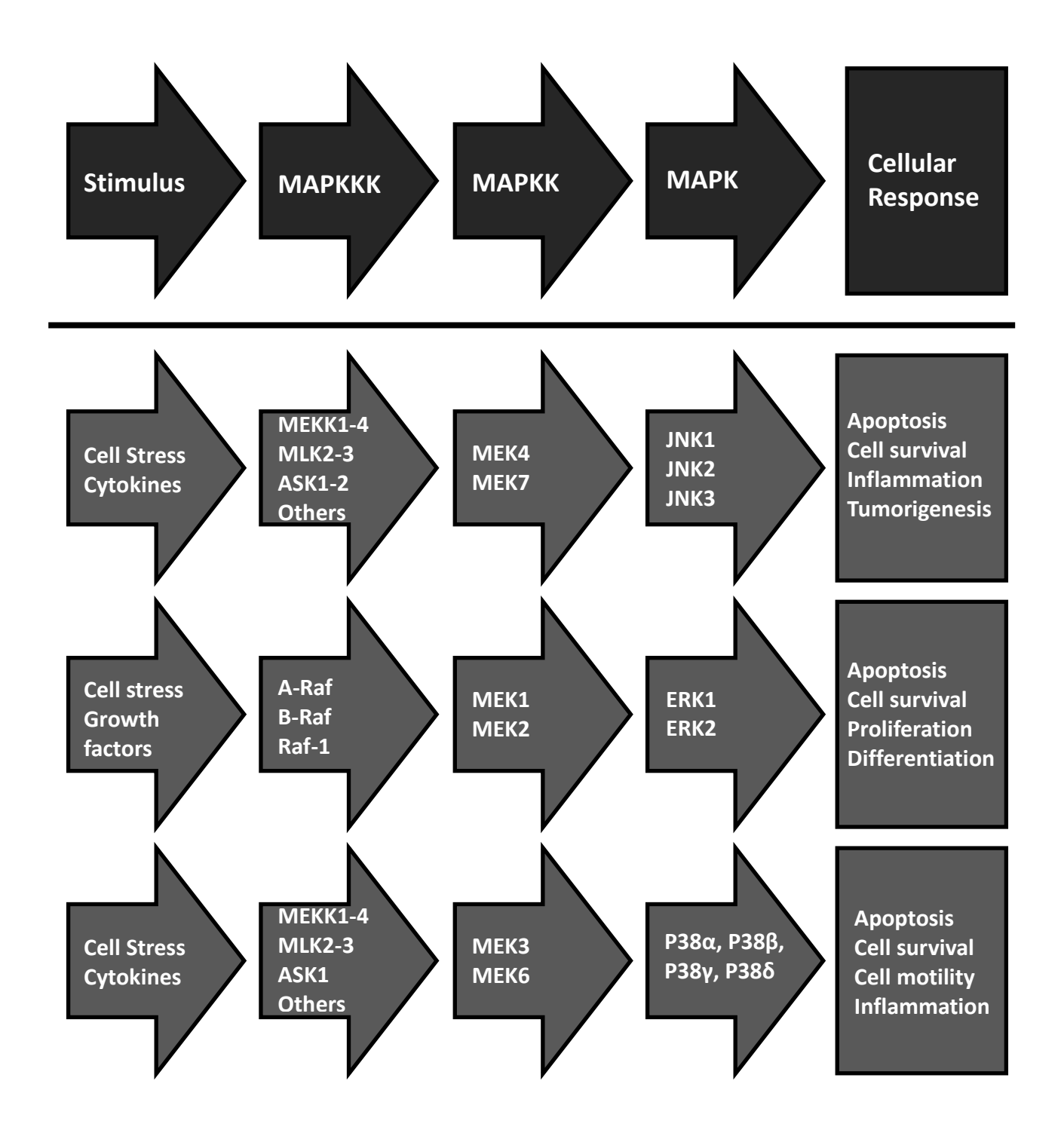


Figure 3. Diagram of the MAPK signaling modules. The MAPK signaling pathways operate as a three-tiered signaling cascade beginning with activation of MAPKKKs in response to some stimulus. The MAPKKKs that lead to activation of JNK and p38 are most commonly activated in response to cell stress or cytokine exposure whereas the

Figure 3 (cont'd)

MAPKKs that lead to activation of ERK are typically activated in response to cell stress or growth factor stimulation. Activation of the MAPKKs leads to activation of respective MAPKKs followed by activation of the MAPKs JNK, ERK and p38. Activation of each of these MAPKs can lead to cell survival or apoptosis depending on their duration of activation, subcellular localization, health state of the cell and other factors. Although depicted as linear pathways, crosstalk between the MAPK signaling cascades is known to occur. Figure adapted from Cowan and Storey, (2003).

stress such as inflammation (eg, exposure to pro-inflammatory cytokines) and is mediated by MKK4/7. Phosphorylation of JNK results in its dimerization and translocation to the nucleus where it phosphorylates transcription factors such as activated protein (AP)-1.

JNK activation leads to various cellular responses including transcription of cell survival genes, inflammation or apoptosis (Cowen and Storey, 2003). The consequences of JNK activation are influenced by several factors including its localization and duration of activation (Pearson, et al., 2001). In the absence of cellular stress, activation of JNK is usually transient and promotes activation of transcription factors, including AP-1 and NFkB, which translocate to the nucleus and activate transcription of cell survival genes (Hasselblatt, et al., 2007). However, certain types of stress such as the generation of reactive oxygen species (ROS) can promote persistent activation of JNK which can lead to activation of pathways leading to apoptosis.

Several pro-apoptotic substrates of JNK have been identified. JNK is known to phosphorylate the tumor suppressor protein p53, promoting its stability. Phosphorylation of p53 by JNK can inhibit its proteasomal degradation, thereby increasing the half-life of p53 (Fuchs, et al., 1998). Another target of JNK is the transcription factor c-MYC, which can promote apoptosis under certain conditions (Hoffman and Liebermann, 2008, Noguchi, et al., 1999). Persistent activation of the JNK pathway can cause a decrease in mitochondrial membrane potential which leads to permeabilization of the outer mitochondrial membrane and release of cytochrome c along with other pro-apoptotic factors. Association of the pro-apoptotic factors cytochrome c, Apaf-1 and procaspase-9 leads to activation of caspase 9 followed by cleavage and activation of executioner

caspase-3 and ultimately apoptosis. It remains unclear exactly how JNK promotes opening of the mitochondrial permeability transition (MPT) pore. JNK can phosphorylate anti-apoptotic proteins Bcl-2 and Bcl-XL thereby inhibiting their function. This might be one mechanism whereby JNK facilitates opening of the MPT pore, since the Bcl-2 proteins are known to regulate release of cytochrome c from mitochondria (Gross, et al., 1999, Maundrell, et al., 1997, Yamamoto, et al., 1999).

Findings from studies in vivo and in vitro point to an important role for JNK in the pathogenesis of DILI and IDILI. Various drugs associated with IDILI induced persistent activation of JNK in transformed human hepatocytes (Beggs, et al., 2014, Fredriksson, et al., 2011). Additionally, inhibition of the JNK pathway protected transformed and primary hepatocytes from toxicity mediated by drugs associated with IDILI (Beggs, et al., 2014, Fredriksson, et al., 2011, Gandhi, et al., 2010). Furthermore, JNK activation plays a critical role in the pathogenesis of acetaminophen-induced liver injury in rodents by inducing mitochondrial permeability transition (Saberi, et al., 2014). Treatment of primary hepatocytes with acetaminophen resulted in persistent activation of JNK and translocation of JNK and bax to the outer mitochondrial membrane, leading to formation of the MPTP (Gunawan, et al., 2006). Generation of reactive oxygen species (ROS) in response to acetaminophen treatment led to inhibition of JNK phosphatases which promoted prolonged activation of JNK. Indeed, it is possible that similar mechanisms underlie persistent activation of JNK and hepatocellular death induced by drugs associated with IDILI.

1.5.2 Extracellular signal-regulated kinase

ERK is activated in a manner analogous to the activation of JNK. There are two isoforms of ERK: ERK 1 and ERK2. Both are ubiquitously expressed and are nearly identical. Ras, a small GTPase associated with the plasma membrane, recruits the MAPKKK, Raf, and subsequently phosphorylates and activates it. Activated Raf phosphorylates the MAPKK, MEK1/2, at two serine positions leading to its activation. Activation of MEK1/2 then directly phosphorylates and activates ERK1/2. Once activated, ERK is able to phosphorylate various cytoplasmic and nuclear targets (Cagnol, et al., 2009). Like JNK, ERK controls various cell responses including proliferation, differentiation and cell death. The magnitude and duration of ERK activity as well as its cellular localization determine how ERK signals within a cell.

Under certain conditions, ERK signaling can lead to apoptosis via activation of the intrinsic (mitochondrial) or the extrinsic (death receptor-mediated) apoptotic pathway. ERK can promote activation of caspase 8 by increasing the level of death receptor ligands such as TNF and/or Fas (Jo, et al., 2005, Ulisse, et al., 2000).

Additionally, ERK can upregulate the expression of death receptors, including the TNF receptor, the Fas ligand receptor and TRAIL receptors (Drosopoulos, et al., 2005, Tewari, et al., 2008). Moreover, activation of ERK can decrease mitochondrial membrane potential leading to MPTP formation, release of cytochrome c, activation of caspases and ultimately apoptosis (Wang, et al., 2000). Consistent with this is that ERK can localize to the outer mitochondrial membrane under certain conditions (Nowak, et al., 2002). It can upregulate proapoptotic factors such as Bax, Bak, and p53 upregulated modulator of apoptosis (PUMA). ERK can also downregulate antiapoptotic factors such as Bcl-2 and Bcl-XL (Liu, et al., 2008). Furthermore, it can promote p53 stability and

activation by phosphorylating p53 at serine 15. Phosphorylation of p53 at serine 15 by ERK inhibits its association with the ubiquitin ligase Mdm2, thereby preventing its proteasomal degradation (She, et al., 2000).

The role of ERK in the pathogenesis of IDILI is not well understood. Several studies demonstrated that ERK plays a protective role in various models of liver disease. ERK is known to become activated in various rodent models of liver injury, and it appears to be involved in liver regeneration (Czaja, et al., 2003, Desbois-Mouthon, et al., 2006, Svegliati-Baroni, et al., 2003). This is consistent with ERK's ability to promote proliferation and cell survival. In contrast, activation of ERK promoted hepatocellular injury in an in vitro model of IDILI. Trovafloxacin, an antibiotic associated with IDILI, synergized with the cytokine TNF to cause death of HepG2 cells, and this depended on activation of ERK (Beggs, et al., 2015). The involvement of ERK in IDILI remains to be determined, and depending on the situation and offending drug, ERK might play different roles in the pathogenesis.

1.5.3 p38

The p38 MAPK module is activated in response to various stressors including oxidative stress, UV radiation, hypoxia, ischemia and cytokines such as IL-1 and TNF (Roux and Blenis, 2004). Activation of the p38 MAPK pathway begins with activation of MAPKKK, MEKK1-4, in response to the stressors listed above. MEKK1-4 phosphorylate the MAPKKs, MEK3/6. MEK3/6 specifically phosphorylates the various p38 isoforms. There are four known p38 isoforms: p38α, p38β, p38γ, and p38δ. The p38α pathway is the best characterized, although the functional significance of each of these isoforms is

not well understood. MEK6 activates all four p38 isoforms, whereas MEK3 preferentially activates p38α and p38β (Enslen, et al., 2000). Upon activation, p38 phosphorylates many different substrates, including proteins such as cytoplasmic phospholipase A2 (cPLA2) and various transcription factors such as Elk1, NFκB, ATF1/2 and p53 (Kyriakis and Avruch, 2001).

The p38 MAPK signaling pathway is well known for its involvement in regulating immune responses and activating pathways that lead to cell death. p38 plays an important role in the initiation of the inflammatory response by regulating inflammatory cytokine expression through activation of the transcription factor NFkB. Consequently, p38 is involved in the pathogenesis of various diseases involving the immune system including asthma and autoimmune diseases (Johnson and Lapadat, 2002).

Similar to the other MAPKs, p38 can activate either cell survival or apoptotic signaling pathways, and the outcome of p38 signaling is context-dependent. Treatment of ovarian carcinoma cells with cisplatin resulted in persistent activation of p38.

Additionally, persistent activation of p38 promoted induction of Fas ligand which, upon binding to the Fas ligand receptor, promoted caspase activation and apoptosis (Mansouri, et al., 2003). p38 can also translocate to the mitochondria and promote apoptosis via activation of the intrinsic apoptotic pathway by promoting MPTP formation, release of cytochrome c and caspase activation (Rosini, et al., 2000).

In contrast to its role in mediating cell death, p38 can also promote cell survival under certain conditions. Unlike many other cancer-derived cell types, KYM-1 human myosarcoma cells are sensitive to TNF-mediated apoptosis. Treatment of KYM-1 cells with TNF resulted in biphasic activation of p38 MAPK (Roulston, et al., 1998). Inhibition

of the p38 pathway with SB203580 enhanced TNF-induced death of KYM-1 cells suggesting that p38 activation in response to TNF treatment mediates cell survival signaling.

Much remains unknown about the role of p38 in IDILI. In many in vivo models of liver disease, p38 plays a detrimental role. Levels of phosphorylated p38 (pp38) were elevated in the livers of mice treated either with pyrazole and LPS or with pyrazole in combination with TNF. Treatment of mice with pyrazole/LPS or pyrazole/TNF resulted in severe liver injury that depended on activation of p38. Inhibition of the p38 pathway with SB203580 protected mice from liver injury induced by pyrazole/LPS or pyrazole/TNF (Wu and Cederbaum, 2008). In addition to contributing to activation of cell death pathways, p38 also plays a role in inhibiting proliferation of hepatocytes after partial hepatectomy by stabilizing the cyclin-dependent kinase (cdk) inhibitor p21 (Stepniak, et al., 2006). Although p38 plays a role in various models of liver disease, more research is needed to determine the role of p38 in the pathogenesis of IDILI.

Exposure to inflammatory cytokines or other mediators produced during IDILI responses can prompt the activation of MAPK signaling pathways. Each of these pathways can lead to activation of either cytoprotective or cell death signaling pathways depending on the context.

1.6 Calcium signaling, endoplasmic reticulum stress and cell death

Calcium (Ca⁺⁺) is one of the most important signaling molecules in the human body. It plays a pivotal role in regulating many different cellular processes including cell survival, proliferation, differentiation and cell death. Normally, Ca⁺⁺ levels are very low in the cytoplasm (~100 nM) compared to the extracellular space (> 1 mM) (Orrenius, et al., 2003). Ca⁺⁺ can enter the cytoplasm via two routes: from the extracellular space and from intracellular stores. The primary intracellular source of Ca⁺⁺ is the endoplasmic reticulum (ER) but Ca⁺⁺ can also be stored in the mitochondrion and other organelles. Voltage-operated, store-operated and receptor-operated Ca⁺⁺ channels are expressed on the plasma membrane of cells and tightly control the influx of Ca⁺⁺ from the extracellular space into the cytoplasm. Release of Ca⁺⁺ from the ER is also a tightly regulated process. Ryanodine receptors and inositol trisphosphate (IP3) receptors are expressed on the ER membrane and upon activation allow release of Ca⁺⁺ from the ER into the cytoplasm (Berridge, et al., 1998).

Proper regulation of influx and/or release of Ca⁺⁺ is essential to maintaining normal cell function. Typically, Ca⁺⁺ enters the cytoplasm in the form of plumes which locally activate processes in the immediate vicinity of the channel from which Ca⁺⁺ entered. Oftentimes, the cell requires global activation of processes, in which case additional Ca⁺⁺ channels are recruited to the plasma membrane and/or ER and promote global influx and/or release of Ca⁺⁺ into the cytoplasm (Berridge, et al., 1998). The influx/release of too much Ca⁺⁺ into the cytoplasm can lead to cell death. In order to avoid this, Ca⁺⁺ signals are often delivered transiently or in an oscillatory fashion. This helps the cell maintain control over the cytoplasmic Ca⁺⁺ concentration. The cell also

expresses enzymes such as Ca⁺⁺/calmodulin kinase II which can modulate the frequency of Ca⁺⁺ signals by varying its activity (phosphorylation status) depending on the level of Ca⁺⁺ present in the cytoplasm (Berridge, et al., 1998).

Although Ca⁺⁺ is essential for normal cell function, too much Ca⁺⁺ in the cytoplasm for too long can lead to either oncosis or apoptosis. Intracellular Ca⁺⁺ dysregulation can lead to oncosis via activation of Ca⁺⁺-dependent proteases, lipases and endonucleases which digest cellular proteins, lipids and DNA, respectively. Ca⁺⁺ has also been implicated in promoting apoptosis via the intrinsic (mitochondrial) route. Normally, when Ca⁺⁺ is released from the ER, it is sequestered by the mitochondria and then shuttled back to the ER (Berridge, et al., 1998). However, if the ER Ca⁺⁺ store is rapidly depleted, the mitochondria become overloaded with Ca⁺⁺, which can result in apoptosis.

As mentioned above, the ER is the primary intracellular source of Ca⁺⁺ and it is also tasked with the synthesis, maturation, folding and transport of cellular proteins. The process of protein folding is particularly sensitive to a variety of insults. Intracellular Ca⁺⁺ dysregulation, oxidative stress, energy deprivation and other disturbances can lead to the accumulation of misfolded proteins in the ER causing ER stress. Accumulation of misfolded proteins in the ER lumen leads to activation of a program which promotes adaptation to and/or recovery from the initiating insult. This response is known is the unfolded protein response (UPR) (Rutkowski, 2004). The ER contains several transmembrane proteins which have the capacity to sense the accumulation of unfolded proteins and initiate the UPR. The three best characterized ER stress sensors are inositol requiring enzyme 1 (IRE1), protein kinase RNA-like endoplasmic reticulum

kinase (PERK) and activating transcription factor 6 (ATF6). The activation of these proteins occurs rapidly in response to the accumulation of unfolded proteins; however, the kinetics of their activation differs, and they each have distinct roles. PERK is the most rapidly activated sensor, and it is responsible for promoting repression of protein synthesis. This prevents the influx of additional proteins into the highly congested ER lumen. Activation of PERK directly phosphorylates and activates eukaryotic initiation factor 2 (EIF2) which inhibits the 80S ribosomal subunit, resulting in inhibition of translation (Rutkowski, 2004). ATF6 is a transcription factor that is rapidly activated in response to accumulation of unfolded proteins. The accumulation of unfolded proteins leads to translocation of ATF6 to the Golgi apparatus where it is proteolytically cleaved, thereby freeing its cytoplasmic domain and allowing it to behave as a transcription factor and activate transcription of genes to relieve ER stress (Ye, et al., 2000). IRE1 is activated rapidly in response to ER stress but typically later than PERK and ATF6 (Yoshida, et al., 2003). Similar to ATF6, activation of IRE1 also promotes transcription of genes that alleviate ER stress.

In quiescent (nonstressed) cells, PERK, ATF6 and IRE1 are constitutively bound to the luminal ER chaperone BiP. BiP prevents the homodimerization and autophosphorylation of PERK and IRE1 and also the translocation of ATF6 to the Golgi apparatus. It has been hypothesized that when the ER lumen becomes overloaded with unfolded proteins, BiP dissociates from the ER stress sensors and preferentially binds to unfolded proteins, thereby allowing for homodimerization and autophosphorylation of PERK and IRE1 and also allowing ATF6 to translocate to the Golgi apparatus (Rutkowski, 2004) (Figure 4A).

The presumed function of the UPR is to relieve the cell from the stress caused by accumulation of unfolded proteins in the ER lumen; however, persistent activation of the UPR can be detrimental to cells. Positive and negative feedback loops regulate the length of activation of the ER stress sensors. One important negative feedback loop controlling the activation of PERK is P58^{IPK}. P58^{IPK} is upregulated later than PERK in response to ER stress and physically interacts with PERK promoting its dephosphorylation and subsequent decreased activation (Yan, et al., 2002).

If the UPR is not shut off at the appropriate time, it can promote activation of various pathways leading to cell death. One such pathway is triggered by release of Ca⁺⁺ from the ER in response to ER stress. Although intracellular Ca⁺⁺ dysregulation can cause ER stress, it can also be caused by ER stress. ER stress can lead to release of Ca⁺⁺ from the ER lumen into the cytoplasm. Release of Ca⁺⁺ from the ER into the cytosol promotes uptake of Ca⁺⁺ from the cytoplasm into the mitochondria (Deniaud, et al., 2008). If the amount of Ca⁺⁺ taken up by the mitochondria reaches a critical threshold, permeabilization of the mitochondrial membrane will occur, leading to cytochrome c release, caspase activation and apoptosis. Interactions between the ER and mitochondria play a pivotal role in the initiation of apoptosis in response to ER stress. In various cell types, the IP3 receptor interacts physically with the voltage-dependent anion channel (VDAC) and adenine nucleotide translocase (ANT), which are located on the outer mitochondrial membrane, to facilitate the transfer of Ca⁺⁺ from the ER lumen into the mitochondria (Deniaud, et al., 2008, Verrier, et al., 2004) (Figure 4B).

ER stress and release of Ca⁺⁺ from the ER are also associated with activation of MAPKs including JNK, which can promote apoptosis under certain conditions. The ER

stress sensor IRE1 can promote activation of JNK by binding to TNF receptor-associated factor 2. Activated JNK can subsequently phosphorylate and inactivate the antiapoptotic protein Bcl-2, thereby promoting cell death (Ron and Walter, 2007). Various agents that induce intracellular Ca⁺⁺ dysregulation and ER stress, such as thapsigargin and tunicamycin, cause activation of the stress activated proteins kinases, JNK and p38 MAPK (Oh-hashi, et al., 2002, Urano, et al., 2000). Additionally, PERK activation in response to disruption of ER Ca⁺⁺ homeostasis leads to activation of JNK in mouse embryonic fibroblasts (Liang, et al., 2006).

Intracellular Ca⁺⁺ dysregulation and ER stress play important roles in many pathological liver conditions, including ischemia/reperfusion injury, cholestatic liver disease, viral hepatitis, alcoholic liver disease, nonalcoholic fatty liver disease and DILI (Dara et al. 2011). Several studies have demonstrated a role for ER stress in acetaminophen (APAP)-induced liver injury (Nagy, et al., 2007, Uzi, et al., 2013). Sublethal doses of APAP activated ER stress markers ATF6 and C/EBP CCAAT/enhancer binding protein homologous protein (CHOP) in mice. CHOP is a proapoptotic transcription factor activated in response to PERK activation of EIF2 followed by activation of ATF4. Additionally, CHOP knockout reduced APAP-induced liver injury in mice (Uzi, et al., 2013).

Efavirenz, ritonavir and lopinavir, antiretroviral drugs associated with IDILI, induced ER stress in primary human and transformed hepatocytes (Apostolova 2013, Kao et al. 2012). Several protease inhibitors used for the treatment of HIV induced activation of CHOP, ATF4 and several other ER chaperones in human HepG2 cells. The ER stress induced by these antiretroviral drugs was attributed to their ability to

inhibit the proteasome (Parker, et al., 2005). Diclofenac, an NSAID associated with IDILI, caused ER stress in HepG2 cells and sensitized HepG2 cells to killing mediated by TNF (Fredriksson, et al., 2014). Ciglitazone, a drug not marketed due to liver toxicity, and troglitazone, a drug removed from the market due to IDILI, induced Ca⁺⁺ dependent MAPK activation and ER stress in rat liver cells (Gardner, et al., 2005). In addition, the activation of MAPKs correlated with the activation of the UPR in this study. Furthermore, two other drugs in the same pharmacologic class but which are not associated with IDILI, pioglitazone and rosiglitazone, did not activate MAPKs or the UPR pathway (Gardner, et al., 2005). Taken together, these studies suggest that intracellular Ca⁺⁺ dysregulation is associated with ER stress and both play important roles in liver diseases including DILI.

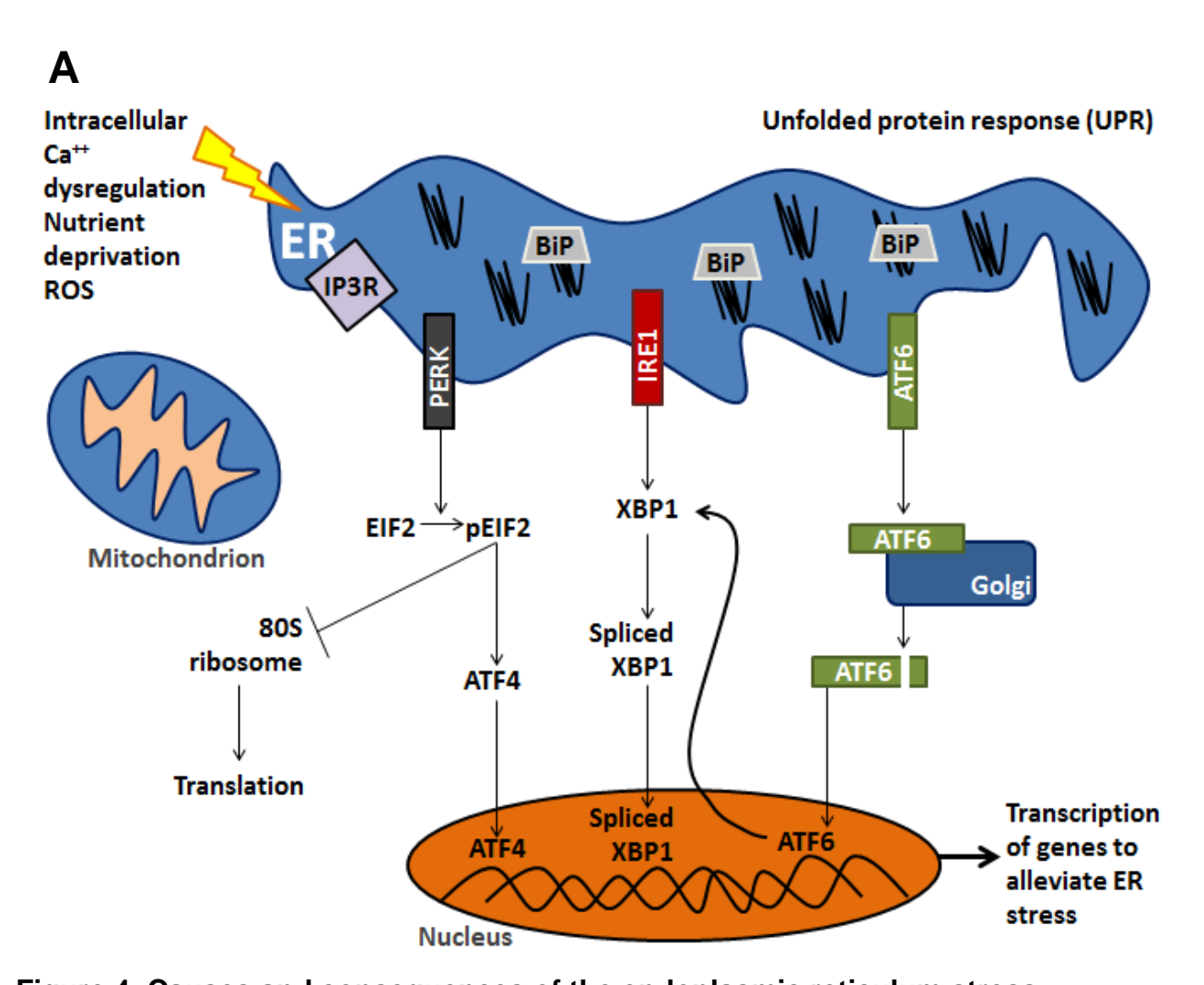
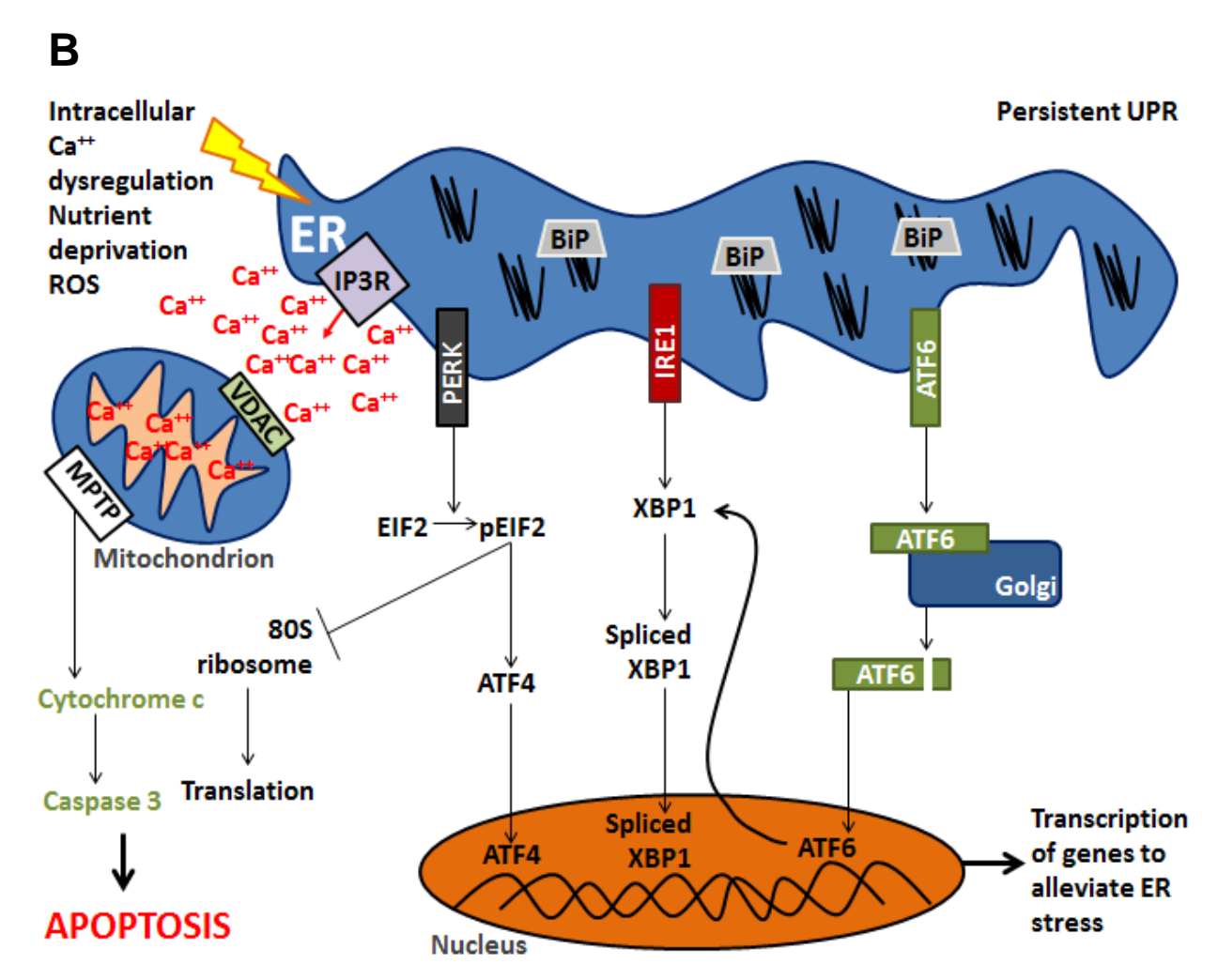


Figure 4. Causes and consequences of the endoplasmic reticulum stress response pathway. A) Intracellular Ca⁺⁺ dysregulation, nutrient deprivation, ROS and other stressful situations can lead to activation an adaptive program known as the UPR. The ER membrane contains various integral membrane proteins some of which sense perturbations to the ER. These are known as ER stress sensors and include inositol requiring enzyme 1 (IRE1), protein kinase RNA-like endoplasmic reticulum kinase (PERK) and activating transcription factor 6 (ATF6). Under homeostatic conditions, the ER stress sensors are bound to the chaperone protein Bip which keeps the ER stress sensors in an inactivated

Figure 4 (cont'd)



state. Dysfunction of the ER leads to accumulation of misfolded proteins permitting dissociation of Bip from the ER stress sensors and subsequently autophosphorylation and activation of the ER stress sensors. Activated PERK leads to activation of EIF2 which inhibits translation. PERK also activations the transcription factor ATF4 which controls activation of genes to alleviate ER stress. When activated, IRE1 and ATF6 promote transcription of genes to alleviate ER stress as well. To become activated ATF6 must translocate to the Golgi apparatus where it is activated by proteolytic cleavage. Mitigation of ER stress leads to downregulation of the UPR. B) If ER stress

Figure 4 (cont'd)

persists, the UPR remains persistently activated which can lead to apoptosis. Failure of the UPR to properly shut down can lead to depletion of Ca⁺⁺ stored within the ER via IP3 receptors which further perpetuates the UPR. Ca⁺⁺ released from the ER is rapidly taken up by the mitochondrion. Too much Ca⁺⁺ taken up into the mitochondrion can lead to permeabilization of the mitochondrial membrane, release of cytochrome c, caspase activation and apoptosis. Adapted from Chen, et al., (2014).

1.7 Current status of preclinical safety evaluation of drugs in development

It takes 10-15 years and close to one billion dollars to develop a new drug (Adams and Brandtner, 2006). Due in part to the tremendous cost associated with developing a drug, and more importantly to the health issues associated with IDILI, it is crucial that drugs and drug candidates with idiosyncrasy liability are identified as early as possible during the development process. Early identification of compounds with the potential to cause toxicity would protect patients in the long run and improve the productivity of pharmaceutical companies. Current methods employed during preclinical safety evaluation of drug candidates are quite successful in identifying those that cause dose-dependent (i.e., "intrinsic") hepatotoxicity. However, drugs that are found to cause IDILI only after reaching the market do not typically show signs of hepatotoxicity during the preclinical and clinical trial phases of the drug development process. Moreover, preclinical assays effective in predicting the potential of a drug to cause IDILI in humans are lacking.

Several decades ago, preclinical safety evaluation of drugs in development was not particularly extensive, and mainly consisted of a few basic in vitro toxicity assays (Kramer, et al., 2007). Consequently, toxicity was the principal cause of attrition of drugs during all phases of development. In the last decade or so, considerable efforts have been made to improve the safety assessment of drugs during the preclinical phase of drug development. Although substantial improvements have been made, hepatotoxicity is still the leading cause of failure to obtain US FDA approval for new drugs, and the most common cause for postmarketing warnings and withdrawals of drugs from the market.

Currently, preclinical safety evaluation of drugs involves a battery of in vitro and in vivo assays to evaluate the intrinsic toxicity of drugs. Preclinical studies are designed to assess three criteria: 1) the dose-limiting toxicity of a drug, 2) if the dose-limiting toxicity of a drug is reversible and 3) if the dose-limiting toxicity can be monitored clinically (Stevens and Baker, 2009). A goal of these initial assessments is to establish the margin of safety for a given drug, that is, the ratio of the maximum safe level of exposure divided by the exposure required to produce a desired pharmacological effect (Kramer, et al., 2007). Preclinical safety evaluation of drugs in development includes a combination of both prospective and retrospective in vitro assays as well as in vivo tests to evaluate the potential for drugs to cause target organ toxicity. Prospective in vitro toxicology assays are the first assays to be conducted during the drug development process and are designed to test drugs for the potential to cause cytotoxicity and other development-limiting toxicities, i.e., toxicity for which there is no acceptable margin of safety (e.g. genotoxicity). Knowledge from these initial studies is used to customize safety assessment in vivo and also to design retrospective, in vitro studies to evaluate target organ toxicities (Kramer, et al., 2007).

Target organ toxicity is difficult to predict using prospective in vitro assays largely due to the difficulty in predicting a given drug's margin of safety in vitro. The purpose of early, in vivo toxicology studies is to identify the potential for a drug to cause dosedependent target organ toxicity. If the potential for a drug to cause dose-dependent target organ toxicity in vivo exists, a variety of factors are taken into consideration to determine if development of the drug should be halted. These factors include the margin

of safety, the nature of the toxicity (reversibility), the route of administration, and the intended therapeutic indication of the drug.

The drug development paradigm described above makes no attempt to identify drug candidates with the potential to cause idiosyncratic, adverse drug reactions such as IDILI. In light of this, assays that can be employed during preclinical safety evaluation of drug candidates are greatly needed to identify drugs with idiosyncrasy liability before they reach the marketplace. The limited knowledge available concerning mechanisms of IDILI is largely to blame for the lack of assays available to predict IDILI liability. Although knowledge concerning the etiology of IDILI is sparse, several risk factors associated with IDILI have been identified. Some of these risk factors identified include underlying inflammatory diseases such as rheumatoid and osteoarthritis. Other risk factors for IDILI that have been identified include genetic polymorphisms in drug metabolizing enzyme genes, certain human leukocyte antigen genes and cytokine genes (Hussaini and Farrington, 2014). Knowledge concerning risk factors and mechanisms underlying IDILI will be useful in developing an approach that could be employed during preclinical safety evaluation to identify drug candidates with the potential to cause IDILI.

1.8 Hypothesis and specific aims

There are two primary objectives of this dissertation: 1) to develop an in vitro approach which accurately classifies drugs according to their IDILI liability and 2) to elucidate the signaling mechanisms involved in the cytotoxic interaction between NSAIDs associated with IDILI and the cytokines TNF and IFN. An in vitro approach that has the potential to accurately identify drug candidates with the potential to cause IDILI would tremendously improve preclinical safety evaluation of drugs in development. Furthermore, an understanding of the signaling mechanisms underlying drug/cytokine-induced cytotoxic synergy will deepen our understanding of the pathogenesis of IDILI. The objectives described above will be evaluated in the following specific aims:

Aim 1 Hypothesis: A drug's ability to synergize with the cytokines TNF and/or IFN correlates with the drug's ability to cause IDILI (Chapter 2).

Aim 2 Hypothesis: NSAIDs associated with IDILI synergize with the cytokines TNF and/or IFN by a mechanism involving caspases and MAPKs (Chapter 3).

Aim 3 Hypothesis: Cytotoxic synergy between diclofenac and the cytokines TNF and IFN requires calcium (Chapter 4).

Aim 4 Hypothesis: Calcium released from the ER promotes diclofenac-induced ER stress and MAPK activation and consequent cytotoxic synergy with cytokines (Chapter 4).

1.9 Significance of dissertation

This dissertation describes the development and evaluation of an in vitro approach to accurately classify drugs according to their potential to cause IDILI in humans. This approach is amenable to high-throughput testing and could be easily employed as a prospective or retrospective in vitro assay to identify drug candidates with the potential to cause IDILI. Furthermore, the studies described in this dissertation provide substantial insight regarding the mechanisms of human IDILI. Indeed, critical gaps in the understanding of how drugs associated with IDILI synergize with mediators of the immune system to cause hepatocellular death are filled.

CHAPTER 2:

An In Vitro Approach to Classify Drugs According to their Potential to Cause Idiosyncratic Hepatotoxicity. Maiuri, A.R., Wassink, B., Turkus, J.D., Breier, A.B., Lansdell, T., Kaur, G., Ganey, P.E., Roth, R.A.

2.1 Abstract

Idiosyncratic, drug-induced liver injury (IDILI) typically occurs in a small fraction of patients and has resulted in removal of otherwise efficacious drugs from the market. Currently, preclinical methods to predict which drugs will have IDILI liability are lacking. Recent results suggest that immune mediators such as TNF and IFN interact with drugs that cause IDILI to kill hepatocytes. Accordingly, the purpose of this study was to test the hypothesis that a drug's ability to synergize with these inflammatory cytokines to cause hepatocellular death in vitro can classify dugs according to their potential to cause idiosyncratic hepatotoxicity in humans. Human hepatoma (HepG2) cells were treated with drugs associated with IDILI or with drugs lacking IDILI liability and cotreated with TNF and/or IFN. Out of 14 drugs associated with IDILI, 11 synergized with TNF to kill HepG2 cells. IFN enhanced the toxicity mediated by some IDILI-associated drugs in the presence of TNF. In contrast, of 10 drugs with little/no IDILI liability, none synergized with inflammatory cytokines to kill HepG2 cells. Concentration response curves were modeled to permit calculation of parameters such as the maximal cytotoxic effect, slope and EC50. These parameters were weighted and incorporated into various probability models to identify the combination of parameters that most accurately classified the drugs according to their potential to cause IDILI. This resulted in models with very high specificity and sensitivity that proved to be highly effective at accurately classifying drugs according to their IDILI liability.

2.2 Introduction

Idiosyncratic, drug-induced liver injury (IDILI) is a typically rare reaction that occurs at drug doses that are safe in the majority of patients. Cases of IDILI can be severe, leading to liver transplantation or death. In addition to public health concerns, IDILI is the most common cause of removal of drugs from the pharmaceutical market due to the occurrence and severity of these reactions and the poor ability of standard toxicity tests to identify drugs with IDILI liability before they reach the market. The causes of IDILI are unknown, but it is thought that genetic and/or environmental factors predispose patients to toxicity from an otherwise safe dose of a drug. Because these reactions are usually rare, drugs with IDILI potential are often not identified during clinical trials that employ limited numbers of human subjects. More effective preclinical strategies to identify drug candidates with IDILI potential could inform decisions about whether to allow a candidate to proceed through the development process. An in vitro approach that uses cells that are readily available and easily grown in culture, requires little compound, employs a single, relevant endpoint and is amenable to high-throughput format would be highly desirable.

Development of such an approach has been challenging due to the limited knowledge about mechanisms underlying IDILI. It is commonly believed that activation of the innate and/or adaptive immune responses underlies IDILI pathogenesis.

Activation of cells from the innate and adaptive immune systems culminates in the release of immune mediators such as cytokines. Some recently developed animal models suggest that adaptive immunity might play a role in the precipitation of IDILI responses. Mice that have impaired immune tolerance developed liver injury after

several administrations of IDILI-associated drugs such as halothane and amodiaquine (Chakraborty, et al., 2015, Pardoll, et al., 2012). Although these models involving activation of the adaptive immune system resulted in only mild liver injury, they could represent an advance in understanding IDILI pathogenesis. So far, the only animal models of IDILI that recapitulate the severity of hepatocellular injury observed in human patients are based on the interaction of drugs with an activated innate immune system (Roth and Ganey, 2011). The inflammatory mediators tumor necrosis factor-alpha (TNF) and/or interferon-gamma (IFN) were critical to the pathogenesis of liver injury in these models (Dugan, et al., 2011, Hassan, et al., 2008, Lu, et al., 2012, Shaw, et al., 2009a, Shaw, et al., 2009b, Zou, et al., 2009).

Both innate and adaptive immune responses culminate in the release of potentially cytotoxic, pro-inflammatory cytokines such as TNF and IFN. Findings from the animal studies raised the possibility that IDILI-associated drugs interact with cytokines in causing death of hepatocytes (Roth and Ganey, 2011). Indeed, using a series of drugs Cosgrove, et al., (2009) found a correlation between IDILI liability and ability of drugs to synergize with immune mediators to kill primary human hepatocytes in vitro. Using a smaller subset of drugs, they also found that their results in primary human hepatocytes could be reproduced using HepG2 cells, suggesting that the latter cells hold promise in classifying drugs according to IDILI liability. These and other studies suggest that IDILI-associated drugs act in part by causing stress to hepatocytes, such that they become susceptible to killing mediated by cytokines (Beggs, et al., 2014, Beggs, et al., 2015, Cosgrove, et al., 2009, Fredriksson, et al., 2011, Fredriksson, et al., 2014, Maiuri, et al., 2015, Zou, et al., 2009).

Using HepG2 cells, we recently studied the cytotoxic interaction of TNF/IFN with a series of NSAIDs with various IDILI liabilities and also with an antibiotic, trovafloxacin, and found dichotomous roles for several mitogen activated protein kinases in the cell killing (Beggs, et al., 2014, Beggs, et al., 2015, Maiuri, et al., 2015). In this study, we expanded on those findings of drug-cytokine interactions with a larger set of drugs. Importantly, elucidation of detailed concentration-response relationships permitted calculation and weighting of various parameters (e.g. EC50, maximal response, slope, etc.), which we then incorporated into statistical models to evaluate the ability of this approach to classify drugs according to their IDILI liabilities. The results suggest a highly promising, in vitro approach to predict IDILI liability.

2.3 Materials and Methods

2.3.1 Materials

All drugs were purchased from Sigma-Aldrich (St. Louis, MO) unless otherwise noted. Recombinant human TNF and IFN were purchased from R & D Systems (Minneapolis, MN) or Millipore (Billerica, MA). Phosphate-buffered saline (PBS), Dulbecco's Modified Eagles Medium (DMEM), fetal bovine serum (FBS), Antibiotic-Antimycotic (ABAM) and 0.25% Trypsin-EDTA were purchased from Life Technologies (Carlsbad, CA).

2.3.2 Cell Culture

Human hepatoma HepG2 cells (American Type Culture Collection, Manassas, VA) were grown in 25-cm² tissue culture flasks, maintained in DMEM supplemented with 10% FBS and 1% ABAM in a humidified incubator at 37°C under 95% air and 5% CO₂. Cells were passed or used for experiments when they reached approximately 80% confluence.

2.3.3 IDILI classification

The set of 24 drugs evaluated in this study were classified as being associated with (IDILI+) or not associated with IDILI (IDILI-). Classification of drugs according to their potential to cause IDILI was based on a set of criteria established by Xu, et al., (2008). Table 1 lists all of the drugs evaluated in this study, their maximal plasma concentration (Cmax) in human patients expressed in µM concentration and their IDILI classification.

2.3.4 Cytotoxicity Assessment

HepG2 cells were plated at a density of 4 X 10⁴ cells per well in black-walled, 96well tissue culture plates and were allowed to attach overnight prior to treatment with

Drug	IDILI liability	Cmax µM	Reference
Aspirin	IDILI-	47	Brandon et al. 1986
Azithromycin	IDILI-	0.5	Xu et al. 2008
Buspirone	IDILI-	0.005	Xu et al. 2008
Idarubicin	IDILI-	0.02	Xu et al. 2008
Levofloxacin	IDILI-	15.7	Xu et al. 2008
Moxifloxacin	IDILI-	6.2	Stass et al. 1998
Pioglitazone	IDILI-	2.67	Xu et al. 2008
Promethazine	IDILI-	0.06	Xu et al. 2008
Rofecoxib	IDILI-	1	Gottesdeiner et al. 2003
Sertraline	IDILI-	0.06	Xu et al. 2008
Bromfenac	IDILI+	13.5	Gumbhir-Shah et al. 1997
Chlorpromazine	IDILI+	0.84	Xu et al. 2008
Diclofenac	IDILI+	7.44	Xu et al. 2008
Doxorubicin	IDILI+	1	Barpe et al. 2010
Flucloxacillin	IDILI+	72.6	Roder et al. 1995
Flutamide	IDILI+	0.36	Xu et al. 2008
Ibuprofen	IDILI+	164	Bramlage et al. 2008
Isoniazid	IDILI+	77	Xu et al. 2008
Naproxen	IDILI+	300	Setiawati et al. 2009
Nimesulide	IDILI+	21.08	Xu et al. 2008
Clavulanate	IDILI+	12	Hu et al. 2002
Telithromycin	IDILI+	2.77	Xu et al. 2008
Trovafloxacin	IDILI+	5	Xu et al. 2008
Valproic Acid	IDILI+	175	Rha et al. 1993

Table 1. IDILI classification, Cmax concentration expressed in μ M units and references from which the Cmax values were derived. IDILI classification was determined by a set of criteria described in Xu, et al., (2008); IDILI(-) = the drug is not associated with IDILI, and IDILI(+)= the drug is associated with IDILI.

compounds. Drugs were reconstituted in vehicles consisting of sterile water or DMSO (no greater than 0.5%). Cells were treated with various concentrations of the drug or its vehicle (control) alone or in combination with the cytokines TNF (10 ng/ml) and/or IFN (10 ng/ml) or their PBS vehicle (VEH). Concentration-response curves were generated for 24 drugs, 14 of which are associated with IDILI and 10 of which are not. Cells were treated with drug concentrations ranging from 0 to 100 times the Cmax observed in human patients. The cytokine concentrations used in this study are within 10-fold of the concentrations found in serum of human patients undergoing an inflammatory response (Pinsky, et al., 1993, Taudorf, et al., 2007). If a cytotoxic response was observed but did not reach a plateau by the 100 times Cmax concentration, further testing was performed with larger concentrations of drug to generate a complete (sigmoidal) concentrationresponse curve. Typically, the range of drug concentrations included at least two that were without effect, two defining the maximal effect and two surrounding the EC50. This was necessary because four-parameter logistic modeling used in the statistical analysis requires well defined, sigmoidal concentration-response curves. Cells were exposed to drug/cytokine combinations for 24 hours. Cytotoxicity was evaluated as lactate dehydrogenase (LDH) activity released from the cells into culture medium using the Homogeneous Membrane Integrity Assay kit from Promega (Madison, WI). In cases where the drug interfered with this fluorescence-based assay, a spectrophotometric method was used to measure LDH release (Vanderlinde, 1985).

2.3.5 Statistical analysis

The statistical approach used in this study can be divided into three phases. In the first phase, variables (covariates) were defined. First, a one-way analysis of variance (ANOVA) was used to determine if a particular treatment (e.g. drug alone or in combination with either TNF and/or IFN) caused a significant change in LDH release relative to baseline (i.e., LDH release after treatment with 0 μ M drug). The criterion for significance for the ANOVA was set at α =0.01. For treatments that did not result in a significant change in LDH above baseline (p > 0.01), the following characteristics were assumed for the purpose of modeling: (1) the minimum LDH response (min) = the maximum LDH response (max); (2) the slope = 0; and (3) the EC50 = 0. For drug/cytokine treatment combinations that did result in a statistically significant LDH response, the concentration response data were modeled using a four parameter logistic function:

$$LDH(x) = \min + \frac{\max - \min}{1 + (x/EC50)^{slope}}$$

where LDH(x) is the percentage of LDH released at a given concentration x, where x = [drug]/Cmax, min = the % LDH release at 0 drug concentration (i.e. baseline) and max = the maximal LDH response.

The base covariates, Delta (max – min), slope, EC50 and EC10, were calculated for each of the 96 drug/cytokine treatment combinations evaluated in this study (24 drugs X 4 cytokine combinations) (See Appendix, Table 6-14). The four-parameter logistic models were generated using R statistical software (R package "drc") (R Core Team, 2015, Ritz and Streibig, 2005). EC10, similar to EC50, represents the

[drug]/Cmax value associated with a 10% increase above baseline relative to the maximal response and was determined by the equation:

$$EC10 = D10 \cdot EC50 \cdot 9^{1/_{slope}}$$

D10 is a categorical variable and is defined as a threshold LDH response above which a drug is classified as positively associated with IDILI and relates to the difference in 10 percent LDH activity between the max and min responses for a particular treatment. D10 is defined as 0 if max – min \leq 10 % LDH and D10 is defined as 1 if max – min > 10 % LDH.

From covariates discussed above, several other covariates were derived; these included a combination of categorical and quantitative covariates including R10, EC50 quotient, EC10 quotient, R10 quotient, Delta difference (maxmindiff) and TNF change. Each of the derived covariates is explained in more detail below.

R10 represents the [drug]/Cmax value associated with an increase in 10 LDH percentage points above min for a particular treatment condition and was determined by the equation:

$$R10 = EC50 \cdot \left[\frac{\text{max} - min}{10} - 1 \right]^{1/\text{slope}}$$

R10 was considered to be 0 when the max – min \leq 10 % LDH (i.e. when D10 = 0).

EC50quotient, EC10quotient and R10quotient represent the ratio between the EC50, EC10 or R10 of the drug/TNF concentration-response curve and the respective

values for the drug/VEH concentration-response curve. In other words, EC50quotient = EC50 TNF/EC50 VEH, EC10quotient = EC10 TNF/EC10 VEH and R10quotient = R10 TNF/R10 VEH.

Maxmindiff represents the difference between the Delta (max – min) of the drug/TNF concentration-response curve and the Delta of the drug/VEH concentration response curve. In other words, maxmindiff = (Delta TNF) – (Delta VEH).

The other categorical variable employed in the statistical analysis is TNF change, which relates to the alteration in the drug-induced cytotoxic response in the presence and absence of TNF. Since we hypothesized that only drugs associated with IDILI, and not negative comparators, would synergize with cytokines to cause LDH release, it was important to establish covariates that could account for the scenarios we expect to be associated with IDILI liability, as this was expected to aid in the correct classification of drugs according to their potential to cause IDILI. With regard to cytotoxic synergy between drugs and TNF, we hypothesized that the following scenarios might be associated with IDILI liability: 1) a cytotoxic response in the presence of drug/TNF with a concomitant lack of cytotoxic response in the presence of drug/VEH and, 2) a cytotoxic response in the presence of drug/TNF and drug/VEH with the condition that the drug/TNF concentration-response curve lay to the left of the drug/VEH curve. These scenarios have been observed previously in HepG2 cells with some drugs and TNF (Beggs, et al., 2014, Cosgrove, et al., 2009, Fredriksson, et al., 2011, Maiuri, et al., 2015).

The first scenario is represented by the covariate, TNF change, and was determined by the equation:

The second scenario is accounted for when including in the models factors such as EC50 VEH and EC50 TNF, EC10 VEH and EC10 TNF, R10 VEH and R10 TNF, EC50 quotient, EC10 quotient, R10 quotient, Delta VEH, Delta TNF or maxmindiff. See Tables 6-14 in the Appendix for the values of all covariates calculated in this study.

In the second phase, covariates were chosen to set criteria for the model for classifying a drug as being associated with IDILI (1=yes) or not associated with IDILI (0=no). Covariates were evaluated individually and in combination with each other. Combinations of covariates were selected to maximize the ability of the model to distinguish between drugs associated or not with IDILI. Covariates were first evaluated individually to determine how well a particular covariate classified drugs according to IDILI liability, and then covariates were evaluated in combination.

To model the probability that a drug is associated with IDILI (1=yes/associated and 0=no/not associated), a logistic regression was used following the equation:

$$prob(IDILI = 1|y) = \frac{e^{\beta_0 + \Sigma \beta_i y_i}}{1 + e^{\beta_0 + \Sigma \beta_i y_i}}$$

where prob(IDILI = 1|y) is the probability that a drug with covariates y is associated with IDILI. β_0 is the regression intercept and $\beta_i y_i$ is the regression coefficient (β_i) multiplied by the i'th covariate for a given drug. The regression coefficients (β_i) were calculated using Firth's method, which eliminates bias when estimating the value β_i (Firth 1993). Many of the covariates used in this study exhibited quasi-complete

separation. This occurs when a covariate almost perfectly separates observations into the appropriate categories. In this study, several covariates almost completely separated drugs according to their IDILI liability. When separation or quasi-complete separation occurs, use of the standard method (i.e., maximum likelihood estimation) provides biased, unreliable estimates of β_i . Firth's method uses a penalized likelihood regression to rectify this issue and is an appropriate method to use for estimating β_i when quasi-complete separation of data occurs (Firth, 1993). All coefficients were computed using R statistical software (R package "logistf") (R Core Team, 2015, Heinze, et al., 2013).

In the third phase of the statistical approach, the probability models using single covariates or combinations of covariates were evaluated by receiver operating characteristic (ROC) analysis to determine which sets of covariates led to the most accurate classification of drugs according to their potential to cause IDILI. ROC curves are created for a given model by graphing the true positive rate (sensitivity; proportion of drugs correctly classified as associated with IDILI) against the false positive rate (1-specificity; proportion of drugs incorrectly classified as associated with IDILI) at various probability cutoff thresholds. ROC curves generated using the R package pROC (R Core Team, 2015, Robin, et al., 2011). The AUCs and confidence intervals for all ROC curves were also computed using the pROC. Plots depicting the AUCs and confidence intervals of the ROC curves were generated using the R package metafor (Viechtbauer, et al., 2010).

Because there were too many possible combinations of covariates to report, a small set was selected for evaluation based on what was deemed to lead to the most

accurate classification of drugs. Plots and ROC curves were generated to illustrate graphically the ability of each selected set of covariates to classify drugs. This allowed for selection of optimal set(s) of covariates (e.g., the set(s) that resulted in the most accurate classification of drugs according to IDILI liability). DeLong's method was used to determine if there were statistically significant differences among ROC curves (DeLong, et al., 1988). A model that is able to classify drugs perfectly according to their potential to cause IDILI has an ROC curve with an area under the curve (AUC) = 1. Our goal was to achieve a model (set of covariates) with an AUC as close to 1 as possible with the narrowest confidence interval.

2.4 Results

2.4.1 Drug/cytokine cytotoxicity: concentration-response

Detailed cytotoxicity concentration-response curves were generated with 24 drugs (Table 1); 14 drugs that are associated with IDILI (Figure 1A-C) and 10 drugs that are not (negative comparators) (Figure 1D-E). HepG2 cells were treated with various concentrations of drug alone or in combination with TNF and/or IFN, and cytotoxicity was assessed 24 hours later. Of the 14 drugs associated with IDILI, 11 synergized with cytokines in causing cell death (Figure 5 A, B). Interestingly, 4 IDILI-associated drugs (diclofenac, bromfenac, nimesulide and trovafloxacin) caused no cytotoxicity on their own but synergized with TNF to caused cytotoxicity. Several IDILI associated drugs were cytotoxic on their own (valproic acid, doxorubicin, telithromycin, ibuprofen, naproxen, chlorpromazine and isoniazid) and TNF enhanced this effect. The cytotoxic interaction between some drugs (diclofenac, bromfenac, trovafloxacin, chlorpromazine, telithromycin and isoniazid) and TNF was enhanced by treatment with IFN. Three IDILIassociated drugs (potassium clavulanate, flutamide and flucloxacillin) did not synergize with any combination of cytokines to kill HepG2 cells (Figure 5C). In contrast, none of 10 negative comparators synergized with either cytokine to cause cytotoxicity (Figure 5D, E).

2.4.2 Cmax is moderately associated with IDILI potential

IDILI reactions were once thought not to be dose-related; however, the observation that most drugs that have been withdrawn from the market or have received a black box warning due to IDILI were prescribed at doses greater than 50 mg/day suggested that daily dose plays some role in the propensity of a drug to cause IDILI

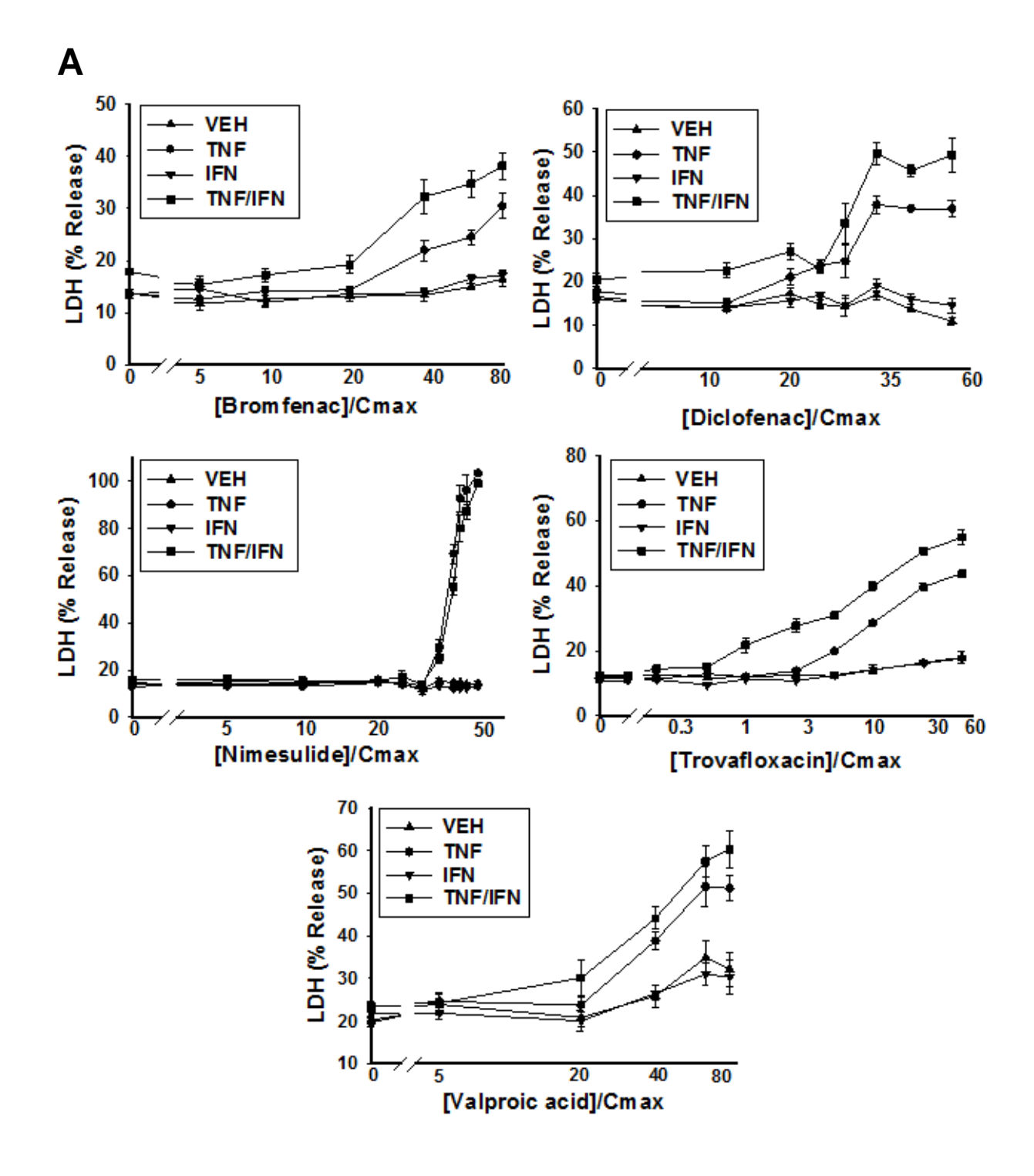
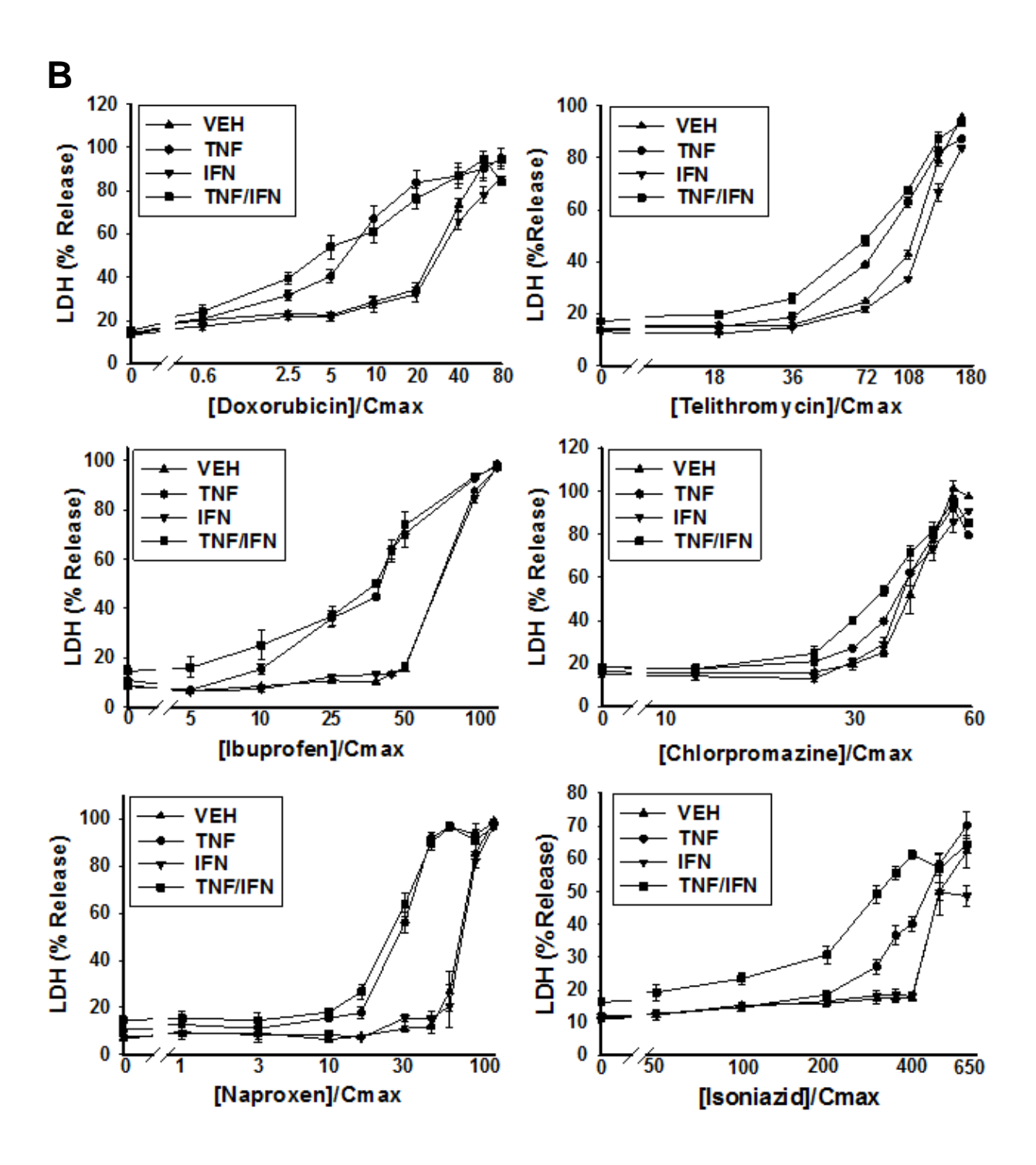


Figure 5. Drug/cytokine-induced cytotoxicity: concentration-response.

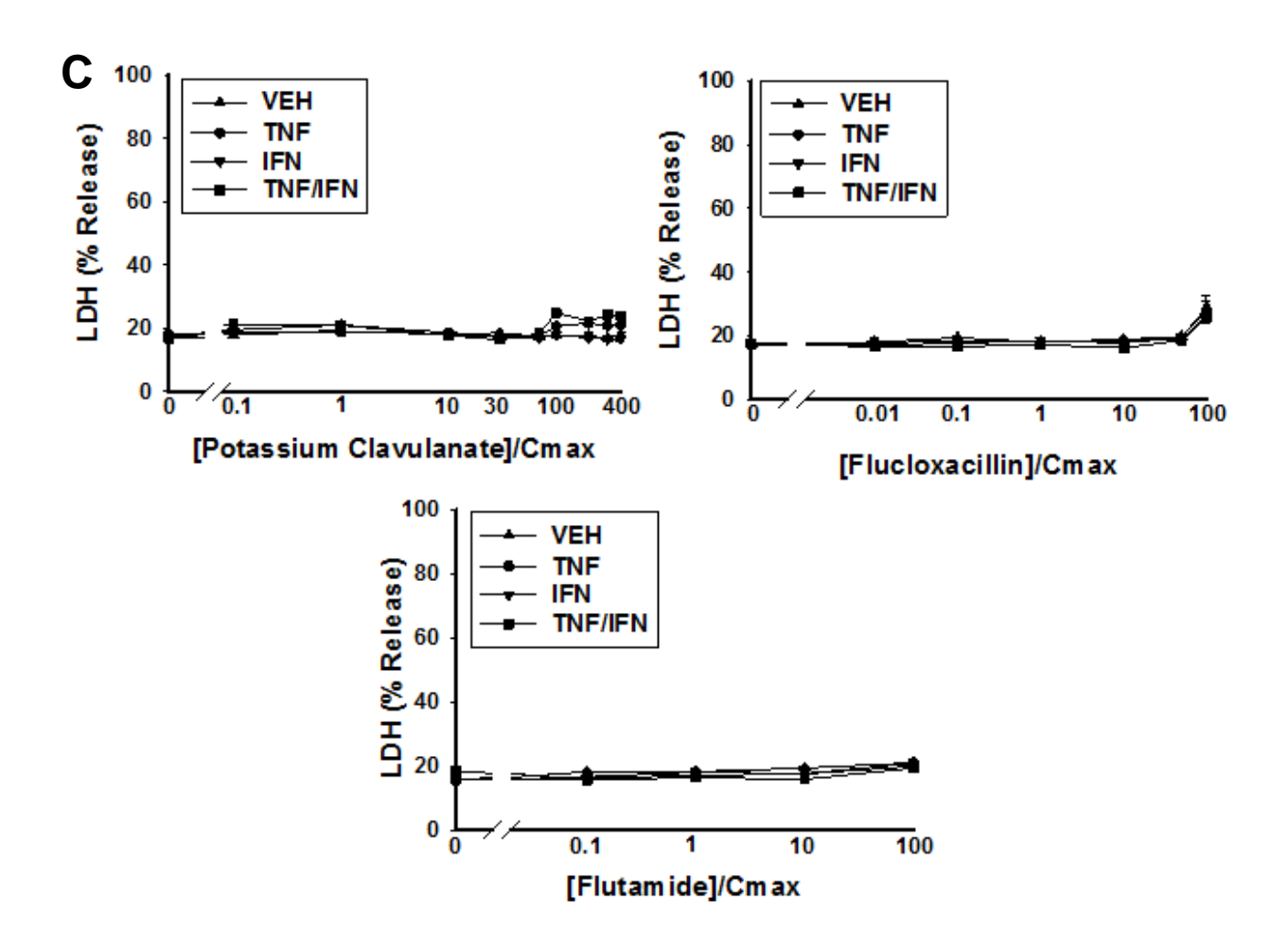
HepG2 cells were treated with 14 drugs associated with IDILI (A-C) or with 10 drugs not associated with IDILI (D-E) alone or in combination with TNF and/or IFN. Cytotoxicity (%

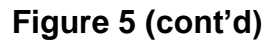
Figure 5 (cont'd)

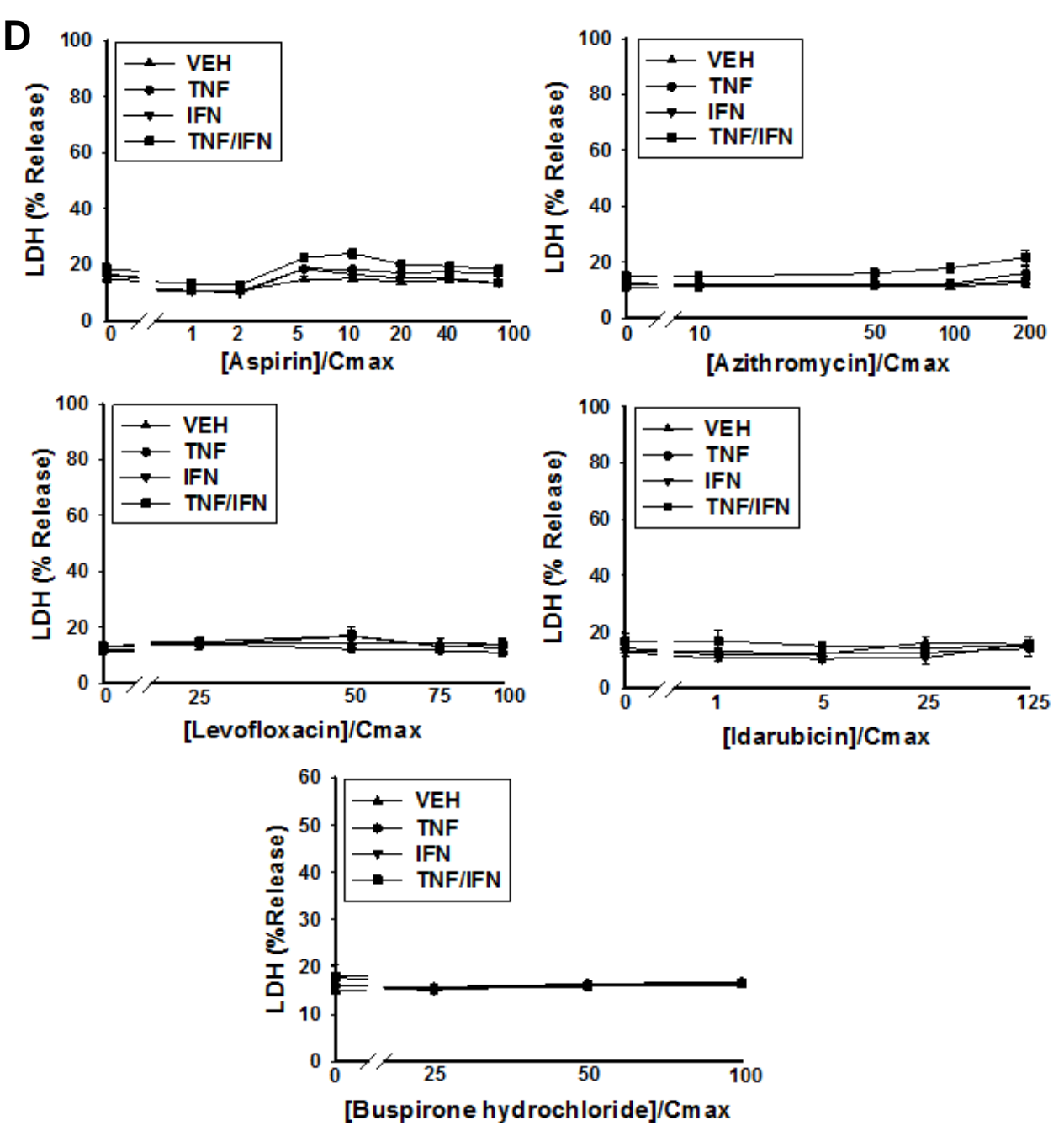


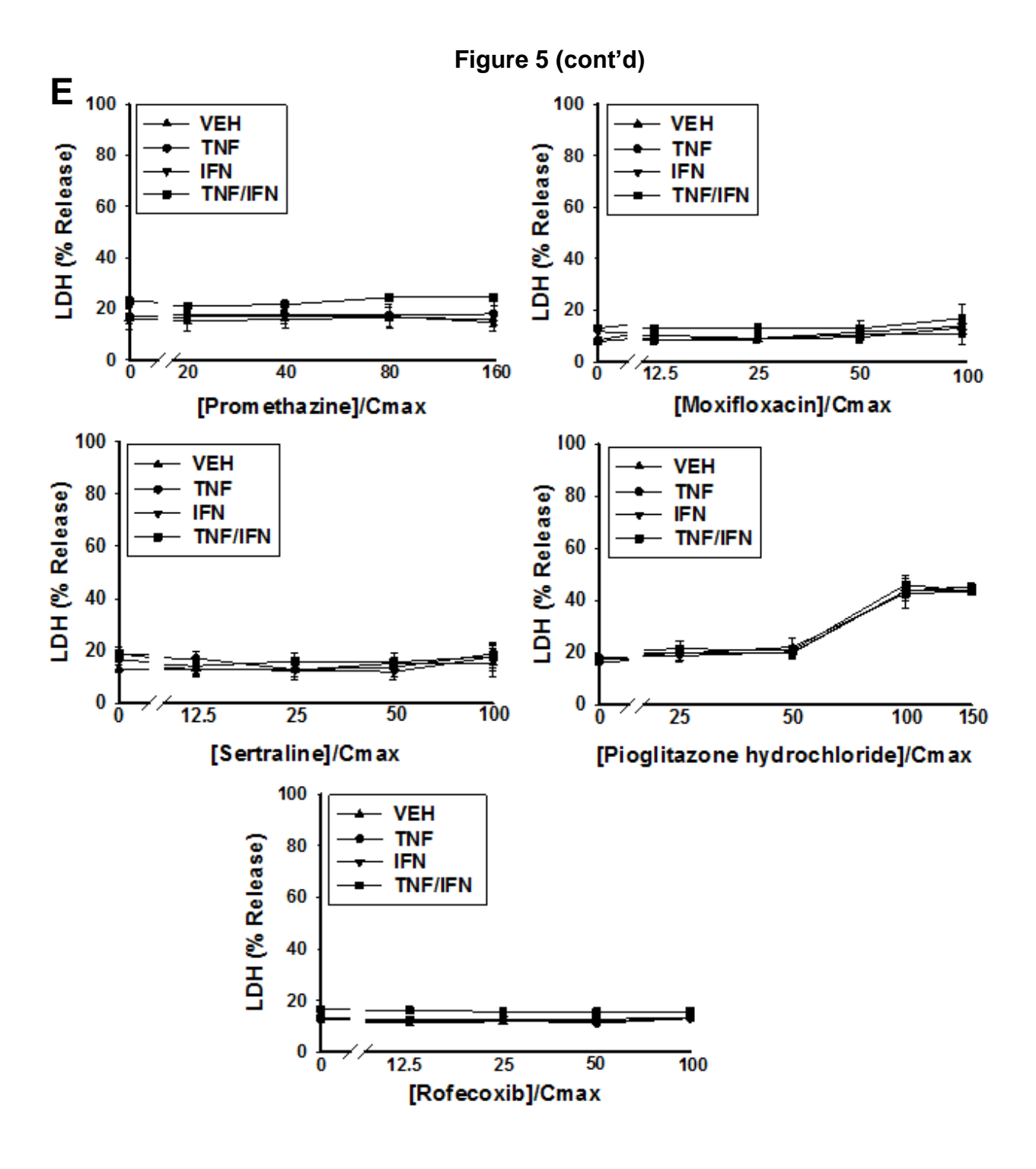
LDH release) was evaluated 24 hours after treatment. Each data point represents the mean ± standard error of the mean (S.E.M.) of at least n=3 separate experiments.

Figure 5 (cont'd)









(Uetrecht 1999). Based on this observation, we evaluated how accurately the Cmax of a drug classifies drugs in the dataset in Figure 1 according to their potential to cause IDILI.

The coefficients (β_0 and β_{Cmax}) were determined as described in Methods, and the following equation was used to calculate from its Cmax the estimated probability that a drug, from the set of 24 drugs, causes IDILI:

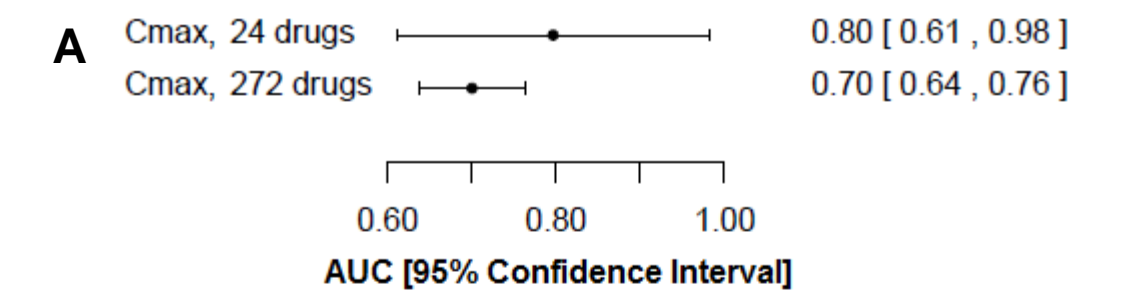
$$Prob (IDILI = 1 | Cmax) = \frac{\exp\{-0.119 + 0.014(Cmax)\}}{1 + \exp\{-0.119 + 0.014(Cmax)\}}$$

The AUC of the ROC curve generated to evaluate the ability of this model to classify drugs according to their IDILI potential is 0.80, with a 95% confidence interval of [0.61, 0.98] (Figure 6).

To determine if our set of 24 drugs is representative of a larger set of drugs, Cmax values were obtained for 272 drugs from a study conducted by Xu, et al., (2008) and converted to μ M units. The coefficients (β_0 and β_{Cmax}) were computed as described in Methods section and the following equation was used to calculate the estimated probability that a drug, from the set of 272 drugs, causes IDILI based on its Cmax:

$$Prob (IDILI = 1|Cmax) = \frac{\exp\{-0.02 + 0.044(Cmax)\}}{1 + \exp\{-0.02 + 0.044(Cmax)\}}$$

The AUC of the ROC curve generated from the large set of drugs is 0.70 with a confidence interval of [0.64, 0.76]. The ROC curves derived from the set of 24 drugs and from the set of 272 drugs are depicted along with their 95% confidence intervals



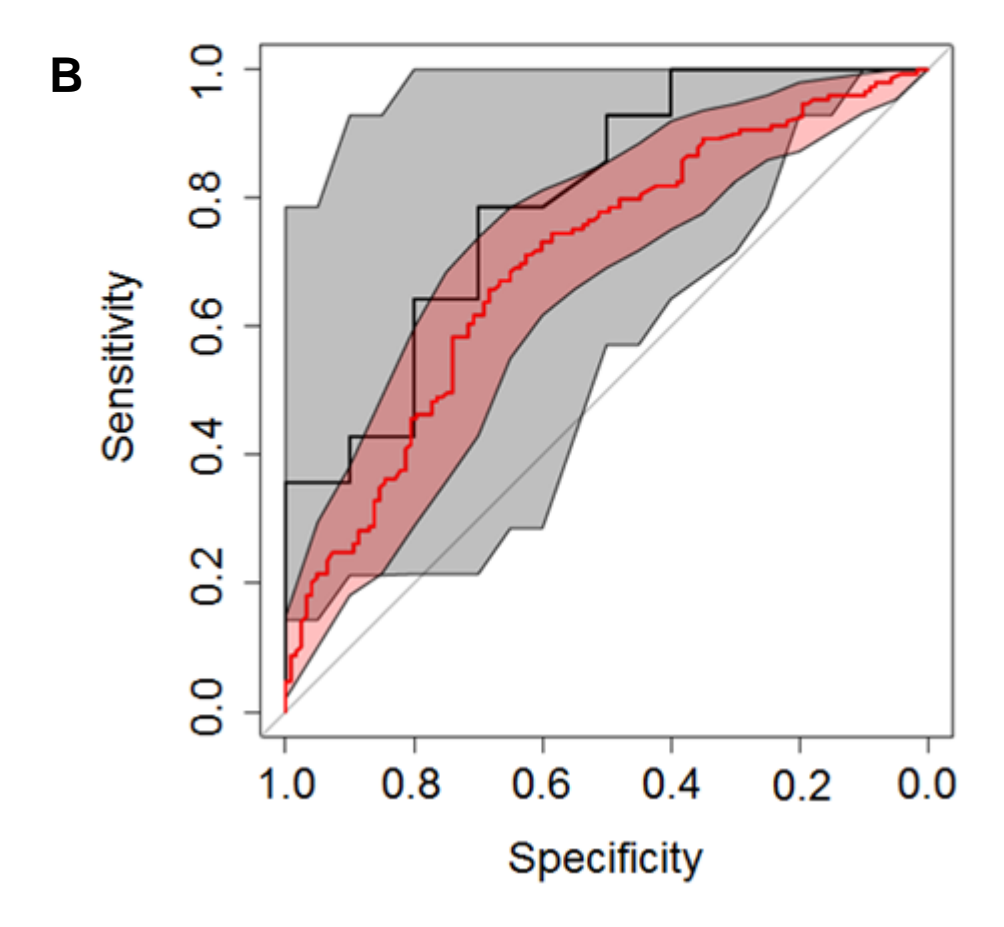


Figure 6. Comparison of a model incorporating Cmax from a set of 24 drugs to a model incorporating Cmax from a set of 272 drugs. A) AUCs and 95% confidence intervals are depicted for the ROC curves derived from the models incorporating either Cmax from a set of 24 drugs or Cmax from a set of 272 drugs. B) The ROC curves for the set of 24 drugs and the set of 272 drugs are indicated by the black line and red line,

Figure 6 (cont'd)

respectively. The confidence intervals for the model describing the set of 24 drugs and for the model describing the set of 272 drugs are shaded grey and red, respectively.

(Figure 6A, B). The confidence interval corresponding to the ROC curve derived from the set of 272 drugs (shaded red) is contained within the confidence interval for the ROC curve derived from the set of 24 drugs (shaded grey) suggesting that the smaller set of drugs is a representative sample of a much larger set of drugs.

2.4.3 ROC analysis of models incorporating the base covariates

Almost all of the IDILI-associated drugs evaluated in this study synergized with TNF to cause death of HepG2 cells. None of the drugs synergized with IFN in the absence of TNF to cause cytotoxicity, but several IDILI-associated drugs synergized with IFN in the presence of TNF (Figure 5A-E). These results indicated that cytotoxic synergy with TNF in particular might be correlated with IDILI liability. Based on these results, models were constructed using covariates that describe the concentrationresponse curves to determine whether the presence of TNF can improve a model's ability to classify drugs according to IDILI liability. The base covariates were modeled individually, and those evaluated included Delta VEH, Delta TNF, EC50 VEH, EC50 TNF, EC10 VEH and EC10 TNF. Each of these covariates was at least moderately associated with IDILI liability (i.e. the confidence intervals for the various models do not contain the value 0.5). The model incorporating Delta TNF produced the ROC curve with the greatest AUC (0.93) and narrowest 95% confidence interval (0.83, 1.00) suggesting that, of these models, it provided the most accurate classification of drugs (Figure 7A). The base covariates that described the response to drug/TNF led to models that produced ROC curves that had significantly greater AUCs with narrower confidence intervals than those that described the response to drug alone (i.e. drug/VEH) (Figure 7A, B).

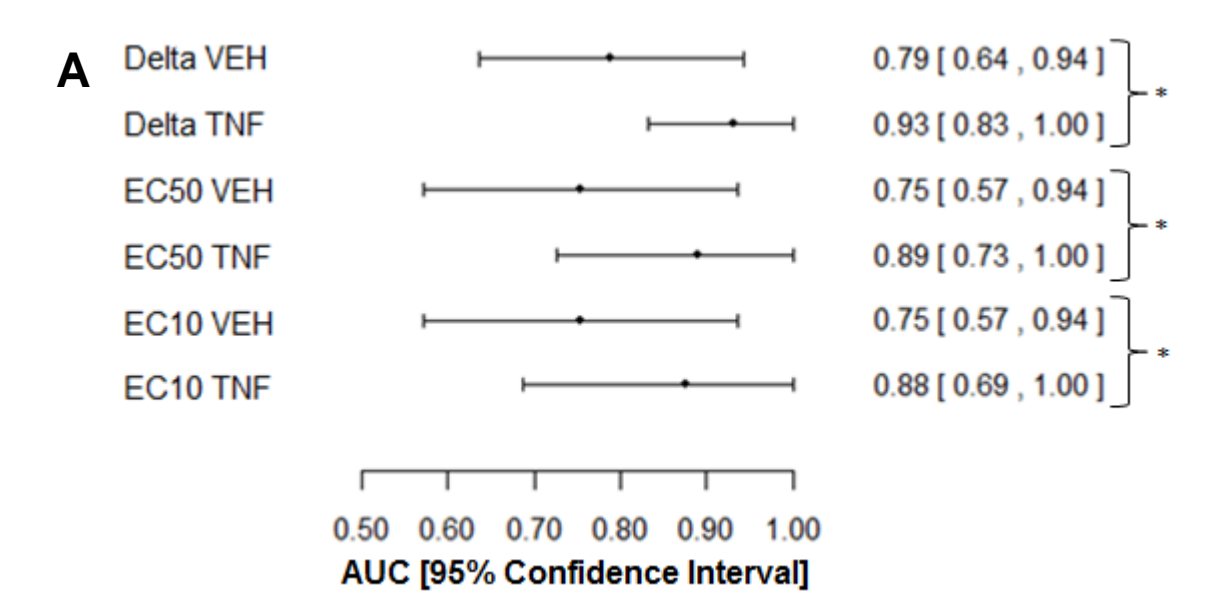
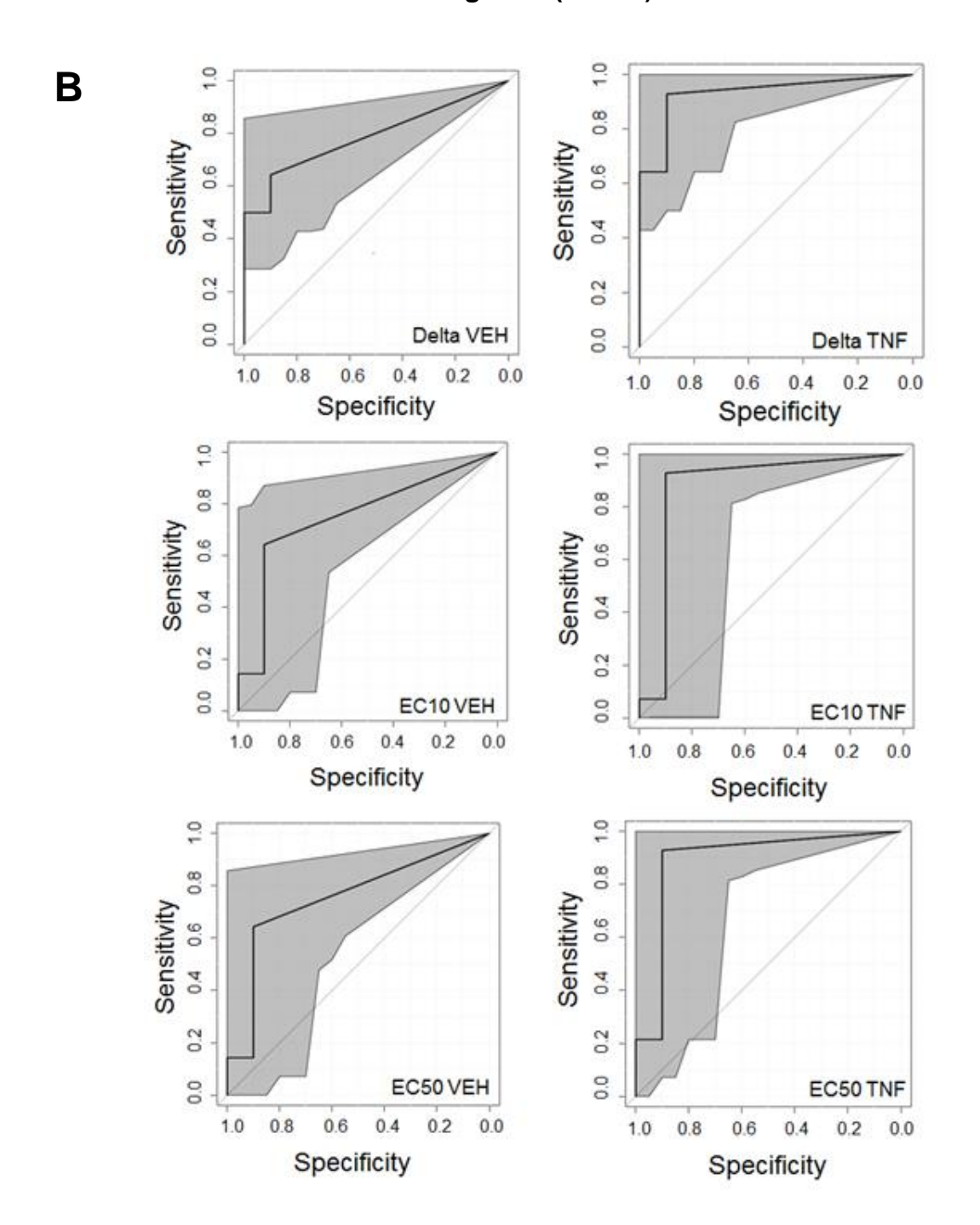


Figure 7. Evaluation of models incorporating the base covariates.

A) AUCs and 95% confidence intervals are illustrated for the ROC curves derived from the models incorporating the base covariates Delta VEH, Delta TNF, EC50 VEH, EC50 TNF, EC10 VEH or EC10 TNF. Depicted are the AUC of the ROC curve and 95% confidence interval for each model.

Figure 7 (cont'd)



B) ROC curves were generated for each model, with the 95% confidence interval shaded in grey. The covariate incorporated into the model is listed on the bottom right

Figure 7 (cont'd)

corner of each ROC curve. *, denotes a statistically significant difference as determined by DeLong's test (p<0.05).

2.4.4 ROC analysis of models incorporating derived covariates

Probability models were also generated using individual covariates that were derived from the base covariates. These models included R10 VEH, R10 TNF, EC50 quotient, EC10 quotient, R10 quotient, maxmindiff or TNF change. Each of these covariates was moderately associated with IDILI liability; however, the ROC curves generated based on these models (Figure 8A, B) did not have greater AUCs or narrower confidence intervals than the models produced by incorporating the base covariates (compare Figure 8 and Figure 7).

2.4.5 ROC analysis of models incorporating combinations of the base and derived covariates

Although it was necessary to evaluate the base and derived covariates individually, it was not surprising that incorporation of a single covariate into a model did not provide enough information to permit the most accurate classification of drugs. Evaluation of the covariates individually did, however, provide some hints as to which covariates when paired together might provide the most accurate classification of drugs according to their IDILI liability. Accordingly, various combinations of the base and derived covariates were evaluated to identify a set of covariates that permitted the most accurate drug classification. Specifically, covariates that were thought to emphasize the difference between treatment with drug/VEH and drug/TNF were paired and evaluated. Combining base and derived covariates led to several models with greater AUCs and narrower confidence intervals than the models incorporating only a single base or a single derived covariate (Figure 9A). Furthermore, when Cmax was added as a covariate, it tended to

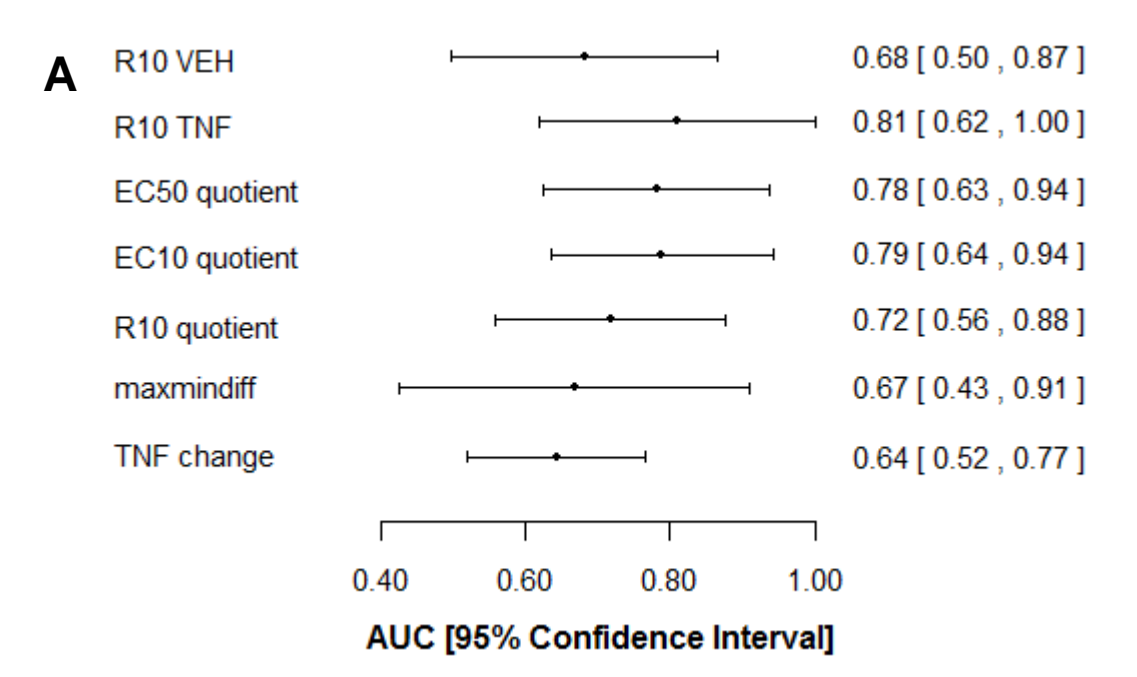
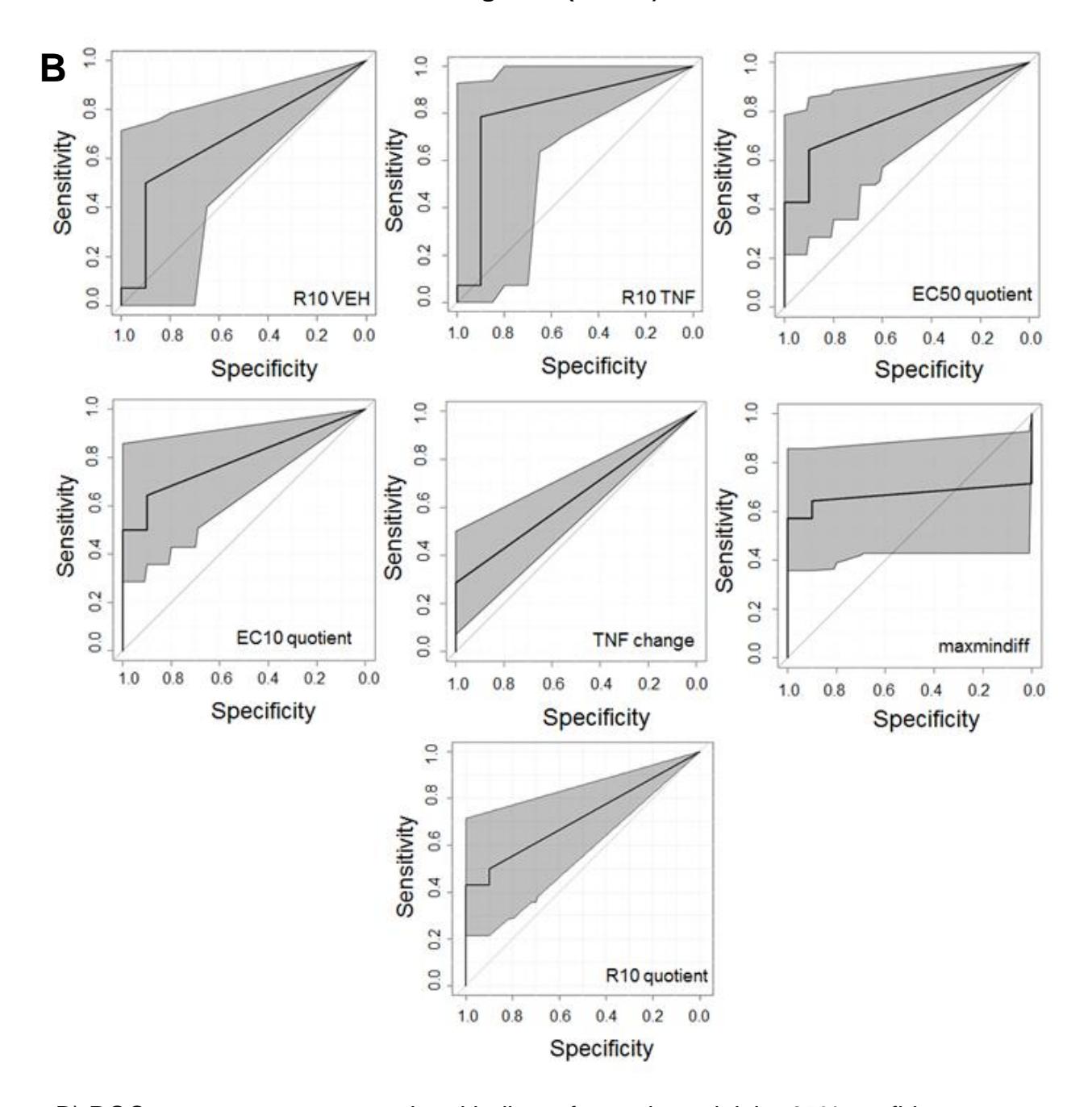


Figure 8. Evaluation of models incorporating the derived covariates.

A) AUCs and 95% confidence intervals for the ROC curves are depicted for the models incorporating the derived covariates individually.

Figure 8 (cont'd)



B) ROC curves were generated and indicate for each model the 95% confidence interval shaded in grey. The covariates incorporated in the model are listed on the bottom right corner of each ROC curve.

improve the performance (AUC and confidence interval) of some models but not others (Figure 9B).

Some of the combined models were associated with remarkably high AUCs, and some of these were associated with small confidence intervals. There were no statistically significant differences among the models with an AUC > 0.95 as determined by DeLong's method for comparing ROC curves (p > 0.05). The ROC curves that met this criterion (AUC > 0.95) are shown in Figure 10.

The optimal cutoff threshold is the probability cutoff threshold that permits the most accurate classification of drugs according to IDILI liability for a given model, i.e., the point on the ROC curve closest to the coordinate (1,1). If one of these models were to be used in the future to classify a set of drugs according to IDILI liability, the optimal cutoff value is the estimated probability above which a drug would be classified as associated with IDILI (1 = associated with IDILI) and below which a drug would be classified as not associated with IDILI (0 = not associated with IDILI). Table 2 shows the optimal cutoff threshold (K*) for the model incorporating the combination of the covariates TNF change, EC50 VEH, EC50 TNF, Delta VEH and Cmax as well as the model's sensitivity (true positive rate) and specificity (true negative rate) when employing the optimal cutoff value. The coefficients (β_0 and β_i) for this model are shown in Table 3 and were incorporated into the following equation:

Prob(IDILI = 1|TNFchange, EC50VEH, EC50TNF, DeltaVEH, Cmax) =

 $\exp\{-2.169+3.247(TNFchange)-0.055(EC50VEH)+0.049(EC50TNF)+0.056(DeltaVEH)+0.014(Cmax)\}$

 $1 + \exp\{-2.169 + 3.247 (TNF change) - 0.055 (EC50VEH) + 0.049 (EC50TNF) + 0.056 (DeltaVEH) + 0.014 (Cmax)\}$

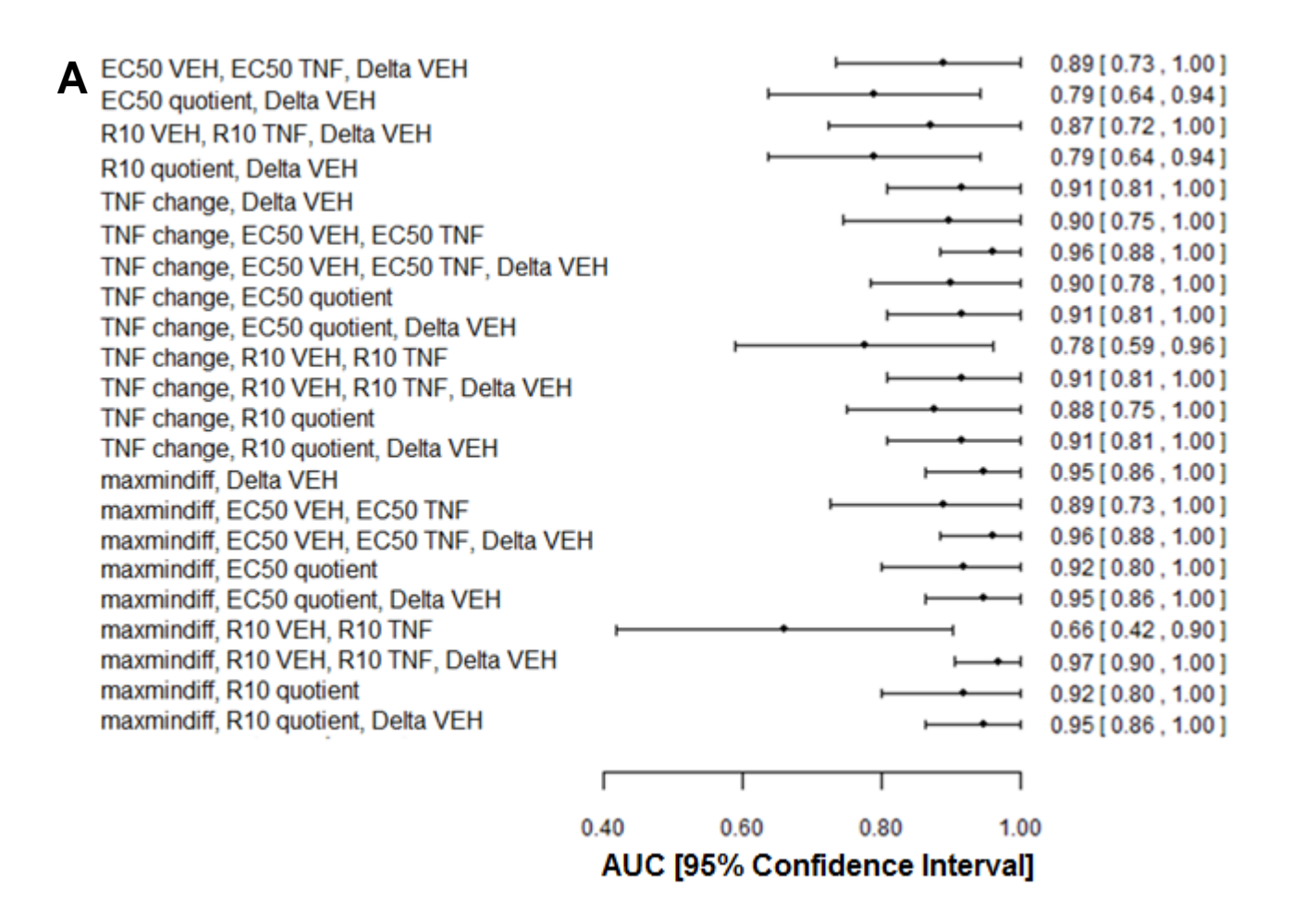
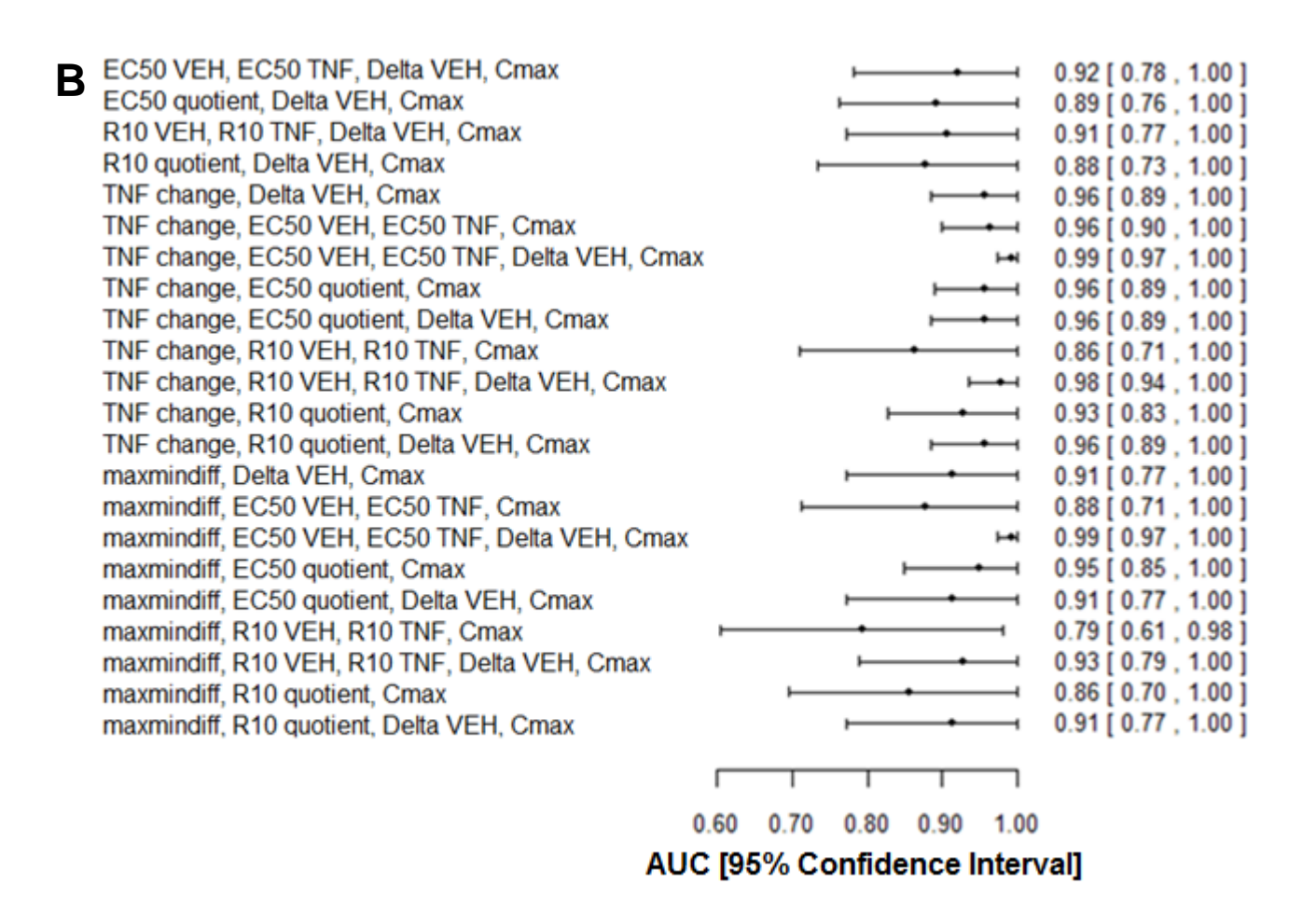


Figure 9. Evaluation of models incorporating combinations of the base and derived covariates. A) AUCs and 95% confidence intervals for the ROC curves are depicted for the models incorporating various combinations of base and derived covariates.

Figure 9 (cont'd)



B) AUCs and 95% confidence intervals are shown for all of the models from A) plus Cmax.

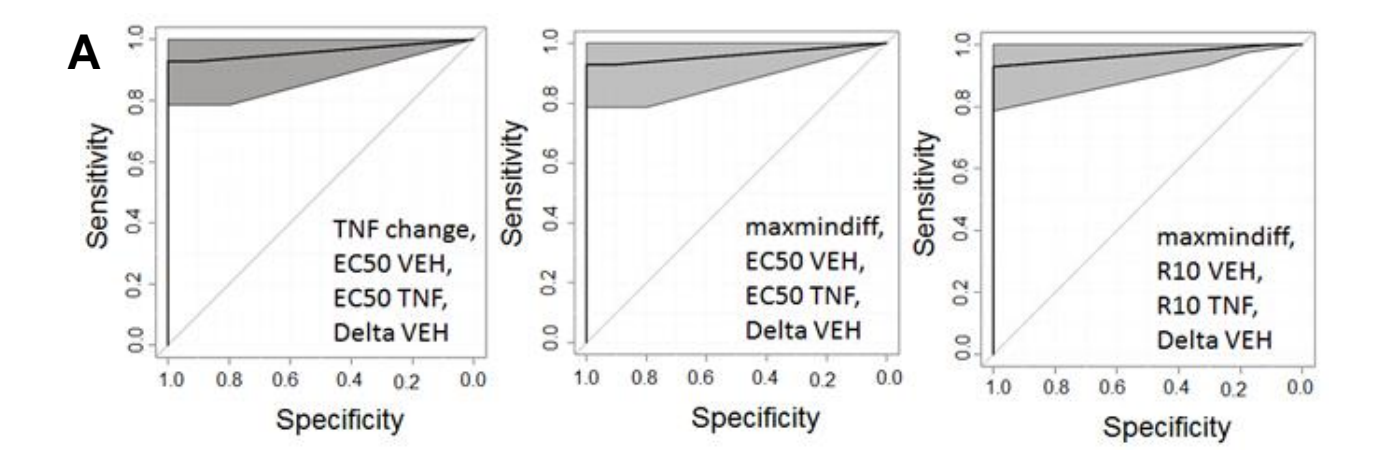
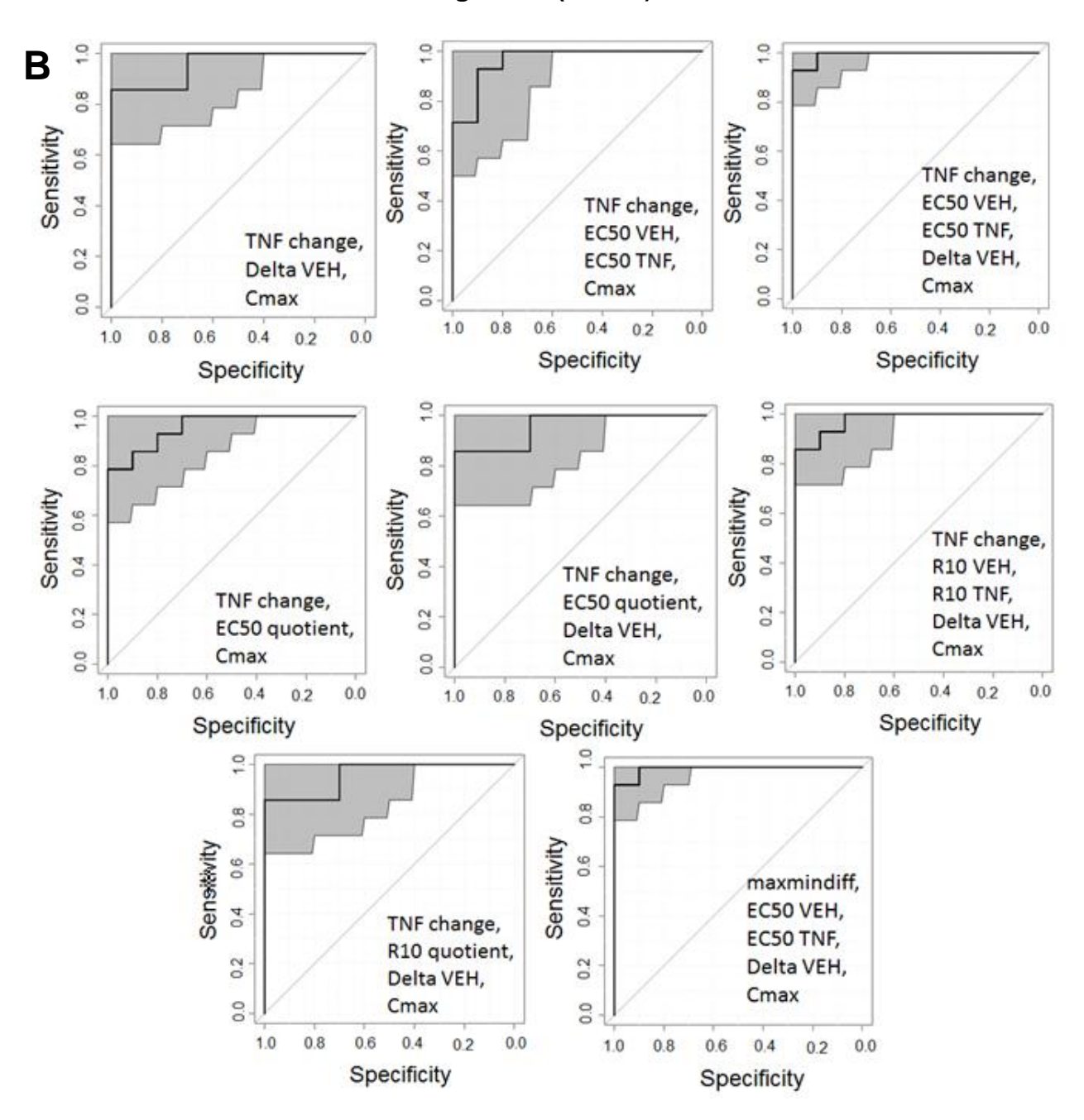


Figure 10. ROC curves with an AUC >0.95.

ROC curves for which AUC > 0.95 are depicted. The 95% confidence interval is shaded grey. The covariates incorporated into the model are listed at the bottom right corner of each ROC curve. The ROC curves shown were not significantly different from each other as determined by DeLong's test (p > 0.05). A) ROC curves incorporating various covariates excluding Cmax.

Figure 10 (cont'd)



B) ROC curves incorporating various covariates including Cmax.

		95% confidence interval
Optimal cutoff threshold, k*	0.46	
True negative rate (specificity)	1	(0.7, 1)
using threshold k*		
True positive rate (sensitivity)	0.93	(0.79, 1)
using threshold k*		
AUC	0.99	(0.97, 1)

Table 2. The optimal cutoff threshold for the model incorporating the covariates TNF change, EC50 VEH, EC50 TNF, Delta VEH, and Cmax.

Covariates	Beta
Intercept	-2.169
TNF change	3.247
EC50 VEH	-0.055
EC50 TNF	0.049
Delta VEH	0.058
Cmax	0.014

Table 3. Coefficients for the model incorporating the covariates TNF change, EC50 VEH, EC50 TNF, Delta VEH, and Cmax. The beta values (coefficients) were computed using Firth's approach as described in the methods.

For each drug, from this equation, the estimated probability that a drug is associated with IDILI was computed. Applying the optimal cutoff value of 0.46 led to almost perfect classification of drugs. The exception was flucloxacillin, which was incorrectly classified as not associated with IDILI (Table 4). This model had an impressive AUC of 0.99 with an extremely narrow confidence interval (0.97, 1.00) (Figure 9B and Figure 10). Table 4 shows the classification of drugs according to their IDILI liability that this particular model provided when employing the optimal cutoff value of 0.46. For all of the models that led to generation of an ROC curve with an AUC > 0.95, the coefficients for each model as well as each model's optimal cutoff threshold (k*) are indicated in the Appendix (Tables 15-34).

2.4.6 Addition of IFN data did not improve the classification of drugs

Treatment of cells with IFN did not result in cytotoxic synergy with any of the drugs in the absence of TNF. However, for several IDILI-associated drugs, the cytotoxic drug/TNF interaction was enhanced by the presence of IFN (Figure 1). The models that incorporated covariates that described the response to drug/TNF/IFN led to ROC curves that were either similar to or less desirable than those generated from models that incorporated covariates that described the response to drug/TNF. The drug/TNF/IFN models tended to have smaller AUCs and larger confidence intervals than the drug/TNF models (Figure 11), indicating that the addition of data describing the IFN response did not enhance the ability of models to classify drugs.

Drug	Estmated	Modeled	True	Classified
	probability	Classification	classification	correctly?
Buspirone	0.1026	0	IDILI –	Y
Idarubicin	0.1026	0	IDILI –	Υ
Promethazine HCL	0.1027	0	IDILI –	Υ
Sertraline	0.1027	0	IDILI –	Υ
Azithromycin	0.1033	0	IDILI –	Υ
Rofecoxib	0.1039	0	IDILI –	Υ
Moxifloxacin	0.1112	0	IDILI –	Υ
Levofloxacin	0.1255	0	IDILI –	Υ
Aspirin	0.1843	0	IDILI –	Υ
Flucloxacillin	0.2467	0	IDILI +	Ν
Pioglitazone	0.2754	0	IDILI –	Υ
Flutamide	0.6461	1	IDILI +	Υ
Isoniazid	0.7492	1	IDILI +	Υ
Telithromycin	0.7566	1	IDILI +	Y
Trovafloxacin	0.7592	1	IDILI +	Υ
Doxorubicin	0.8154	1	IDILI +	Υ
Valproic Acid	0.9026	1	IDILI +	Υ
Potassium Clavulanate	0.9211	1	IDILI +	Υ
Diclofenac	0.9306	1	IDILI +	Y
Chlorpromazine	0.9375	1	IDILI +	Y
Nimesulide	0.9612	1	IDILI +	Y
Ibuprofen	0.9628	1	IDILI +	Y
Bromfenac	0.9685	1	IDILI +	Y
Naproxen	0.9893	1	IDILI +	Υ

Table 4. The classification of the set of 24 drugs based on the model incorporating TNF change, EC50 VEH, EC50 TNF, Delta VEH, and Cmax. 0 indicates the drug was classified by the model as not associated with IDILI and 1 indicates the drug was classified by the model as associated with IDILI. With regard to the true IDILI classification, IDILI(-) = the drug is not associated with IDILI and IDILI (+) = the drug is associated with IDILI. The dark line indicates the optimal cutoff threshold. Y=yes, N=no.

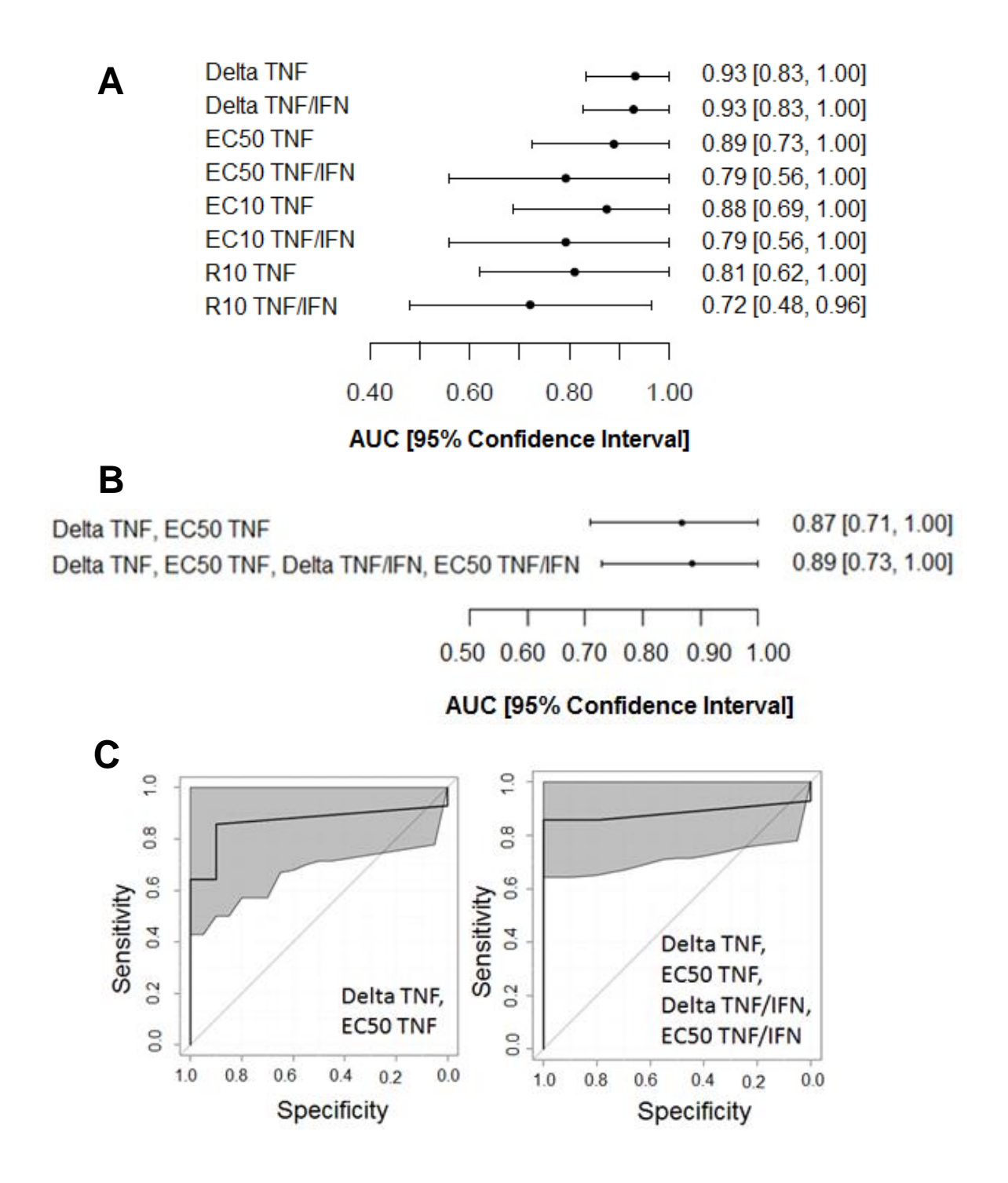


Figure 11. Comparison of models incorporating covariate(s) that describe the drug/TNF concentration response curve to those that include response to IFN.

Figure 11 (cont'd)

A) AUCs and 95% confidence intervals are shown for the models containing the individual covariates Delta TNF, Delta TNF/IFN, EC50 TNF, EC50 TNF/IFN, EC10 TNF, EC10 TNF, EC10 IFN, R10 TNF and R10 TNF/IFN and B) the models combining the covariates Delta TNF and EC50 TNF or Delta TNF, EC50 TNF, Delta TNF/IFN and EC50 TNF/IFN.

C) ROC curves are shown for the models listed in B) and indicate the 95% confidence interval shaded in grey. The covariates incorporated into the model are listed at the bottom right corner of each ROC curve.

2.5 Discussion

The purpose of this study was to develop and evaluate an in vitro approach to classify drugs according to their potential to cause IDILI. The overall hypothesis tested was that the ability of a drug to synergize with the cytokines TNF and/or IFN to kill HepG2 cells is associated with the drug's propensity to cause IDILI in humans. Detailed concentration response curves were generated, and this proved to be critical for elucidation of a model with the capacity to classify drugs correctly.

Since it has been suggested that the daily dose of a drug might be associated with its potential to cause IDILI and since dose is often related to Cmax, we evaluated how well Cmax classifies drugs according to their IDILI liability. To our knowledge, this has not been reported previously. Interestingly, Cmax was somewhat effective at classifying a small set of drugs (24 drugs) according to their IDILI potential; however, it was clear that this was not a perfect model and that there was room for improvement (Figure 6). Since Cmax information is readily available for many drugs, we assessed whether a similar ROC curve would result from incorporating the Cmax of a much larger drug set. Cmax information extracted from Xu, et al., (2008) for 272 drugs was converted to micromolar concentration, and an ROC curve was generated. The AUC of the ROC curve derived from the larger set of drugs was 0.70, which was comparable to the AUC of the ROC curve derived from the smaller set of 24 drugs evaluated in this study (AUC=0.80), and the confidence intervals overlapped (Figure 6A, B). This result suggests that our set of 24 drugs is representative of a larger set of drugs. Moreover, the AUC result suggests that plasma drug concentration contributes to risk of IDILI.

As a prelude to exploring whether cytotoxic synergy between drugs and cytokines is important in classifying drugs according to IDILI liability, we determined whether cytotoxicity induced by treatment with drugs in the absence of cytokines could produce a model that accurately classifies drugs. We first evaluated models that incorporated a single, base covariate related to the drug/VEH concentration response curves and compared them with models that incorporated a single, base covariate derived from the drug/TNF concentration response curves (Figure 3A, B). The latter models incorporating TNF performed significantly better in classifying drugs. Most of the single, base covariate models did not perform better than the Cmax model (compare Figure 7 with Figure 6). The exception was the model incorporating Delta TNF, which had a greater AUC (0.93) and a narrower confidence interval than the other base covariate models or the Cmax model.

With regard to cytotoxic synergy between drugs and TNF, several responses are possible: (1) no cytotoxic response from the drug alone but cytotoxicity after treatment with drug/TNF (i.e. sigmoidal TNF curve and flat VEH curve), (2) cytotoxic responses after treatment both with drug alone and drug/TNF but with greater killing efficacy (i.e., greater Delta) and/or potency (e.g., smaller EC50) in the presence of TNF. Covariates were derived from the base covariates to account for these scenarios. As defined, TNF change categorizes drugs that follow the first scenario as positively associated with IDILI, but drugs that follow the second scenario are classified as not associated with IDILI. As expected, this covariate alone did not produce a desirable ROC curve (Figure 8A, B). Similarly, other derived covariates, when evaluated individually, did not produce desirable ROC curves (Figure 8A, B). However, when paired with covariates (i.e.

maxmindiff, EC50quotient, R10 quotient, etc.) that do account for TNF-induced changes in potency or efficacy, much better models resulted (Figure 9A, Figure 10), Furthermore, incorporating Cmax into a few of these models led to the ROC curves with the greatest AUCs and narrowest confidence intervals (Figure 9B, Figure 10).

IFN contributed to hepatotoxicity in several animal models of drug/inflammatory stress-induced liver injury (Shaw et al. 2009, Hassan et al. 2007, Dugan et al. 2011). Interestingly, in the absence of TNF, IFN did not synergize with any of the drugs in vitro to cause cell death (Figure 1). However, IFN enhanced the cytotoxic interaction between several IDILI-associated drugs and TNF. We evaluated whether a change in the concentration response curves due to exposure to IFN could improve the classification of drugs. The probability model developed from the covariates that describe the response to drug/TNF/IFN produced ROC curves that were not improved from those incorporating covariates that describe the response to drug/TNF (Figure 7). These results indicate that cytotoxic synergy between IDILI-associated drugs and TNF is sufficient to produce a statistical model that accurately classifies drugs according to their potential to cause human IDILI, irrespective of the presence of IFN. We reported recently that IFN-mediated enhancement of NSAID/TNF-induced cytotoxicity occurs with some IDILI-associated NSAIDs but not others, and this effect was related to chemical structure and to the magnitude of clinical concern for IDILI liability (Maiuri, et al., 2015). Specifically, several acetic acid derivatives, which are associated with IDILI of clinical concern, synergized with TNF to cause HepG2 cell death, and IFN enhanced this effect, whereas two propionic acid derivatives, which are associated with IDILI that is of less clinical concern, also synergized with TNF, but IFN was without effect. It would be interesting if the ability of drugs to sensitize cells to the harmful effects of IFN could distinguish drugs of greater concern clinically for IDILI from those of less concern.

Clearly, larger numbers of drugs would need to be analyzed to evaluate this.

Although HepG2 cells are human-derived, their use for drug toxicity evaluation has been criticized because they have limited capacity to bioactivate drugs to toxic metabolites via cytochrome P450-mediated pathways. Despite this potential limitation, Cosgrove, et al., (2009) found that HepG2 cells behave similar to primary human hepatocytes in their cytotoxic responses to drug-cytokine combinations. We have also observed comparable responses in primary hepatocytes (Zou, et al., 2009, Beggs, et al., 2014, Maiuri, et al., 2015). These findings suggest either that (1) metabolic activation of drugs by HepG2 cells, although limited, is sufficient to stress cells so that they respond to cytokine exposure by dying or (2) metabolism is not generally needed for the cytotoxic interaction of drugs with cytokines.

In summary, the results add to evidence that drug-induced stress can sensitize hepatocytes to the killing actions of cytokines such as TNF and IFN. Moreover, this could be requisite for the pathogenesis of IDILI, since numerous IDILI-associated drugs have this capacity and many do so in vitro at concentrations near those that occur during drug therapy. Currently, effective assays to screen preclinically for IDILI potential are lacking. A method that accurately identifies drug candidates with the potential to cause IDILI could revolutionize preclinical testing strategies. Our results suggest an in vitro assay that could do just that, i.e., by delineating drug concentration-response curves in the absence and presence of TNF and applying an appropriate statistical model for classification. This approach is attractive because it (1) uses a cell type that

is easily obtained and maintained in culture and yields consistent results, (2) requires minimal amounts of test compound, (3) employs an easily and inexpensively measured phenotypic endpoint that is directly relevant to IDILI (hepatocellular death) and (4) is adaptable to high throughput technology. Validation of this approach as a screening tool will require the evaluation of additional drugs, but the results presented herein seem quite promising.

CHAPTER 3:

Cytotoxic Synergy Between Cytokines and NSAIDs Associated with Idiosyncratic Hepatotoxicity is Driven by Mitogen-activated Protein Kinases. Toxicol. Sci. (2015). Maiuri, A.R., Breier, A.B., Gora, L.F.P., Parkins, R.V., Ganey, P.E., Roth, R.A.

3.1 Abstract

Non-steroidal, anti-inflammatory drugs (NSAIDs) are among the most frequent causes of idiosyncratic, drug-induced liver injury (IDILI). Mechanisms of IDILI are unknown, but immune responses are suspected to underlie them. In animal models of IDILI, the cytokines tumor necrosis factor-alpha (TNF) and interferon-gamma (IFN) are essential to the pathogenesis. Some drugs associated with IDILI interact with cytokines to kill hepatocytes in vitro, and mitogen activated protein kinases (MAPKs) might play a role. We tested the hypothesis that caspases and MAPKs are involved in NSAID/cytokine-induced cytotoxicity. NSAIDs that are acetic acid (AA) derivatives and associated with IDILI synergized with TNF in causing cytotoxicity in HepG2 cells, and IFN enhanced this interaction. NSAIDs that are propionic acid (PA) derivatives and cause IDILI that is of less clinical concern also synergized with TNF, but IFN was without effect. Caspase inhibition prevented cytotoxicity from AA and PA derivative/cytokine treatment. Treatment with a representative AA or PA derivative induced activation of the MAPKs c-Jun N-terminal kinase (JNK), extracellular signalregulated kinase (ERK), and p38. Inhibition of either JNK or ERK reduced cytotoxicity from cytokine interactions with AA derivatives. In contrast, an ERK inhibitor potentiated cytotoxicity from cytokine interactions with PA derivatives. An AA derivative but not a PA derivative enhanced IFN-mediated activation of STAT-1, and this enhancement was ERK-dependent. These findings raise the possibility that some IDILI reactions result from drug/cytokine synergy involving caspases and MAPKs and suggest that, even for drugs within the same pharmacologic class, synergy with cytokines occurs by different kinase signaling mechanisms.

3.2 Introduction

Drug-induced liver injury (DILI) is the leading cause of acute liver failure in the United States and remains the most common adverse effect associated with failure to obtain U.S. Food and Drug Administration approval for new drugs (Aithal et al., 2011). Idiosyncratic drug-induced liver injury (IDILI), a subset of DILI, occurs in a small fraction of patients taking a drug and can result in severe liver injury or death. These reactions have resulted in removal of many drugs from the market that are efficacious and safe in the majority of patients.

Mechanisms underlying IDILI remain unproven, and the reactions are not predicted by typical preclinical toxicity testing. The infrequency of most IDILI responses suggests that individual susceptibility as well as characteristics of the offending drug are needed to elicit a response. A longstanding hypothesis is that IDILI-associated drugs activate a damaging adaptive immune response (Uetrecht, 1999). Specific human leukocyte antigen (HLA) polymorphisms are associated with liver injury induced by some drugs, suggesting an important role for adaptive immune responses in the pathogenesis of IDILI (Tujios and Fontana 2011). Another hypothesis suggests that activation of the innate immune system during drug therapy can render an individual susceptible to injury from an otherwise nontoxic dose of the drug (Roth and Ganey, 2011). Importantly, inflammatory cytokines are expressed and mediate critical events in both adaptive and innate immune responses. Indeed, in several rodent models of IDILI based on interaction of drugs with an immune response, the cytokines tumor necrosis factor-alpha (TNF) and interferon-gamma (IFN) proved to be critical to the pathogenesis

of hepatocellular injury (Dugan et al., 2011, Shaw et al., 2009a, Shaw et al., 2009b, Zou et al., 2009).

Recently published studies suggest that toxic cytokine/drug synergy can be recapitulated in vitro. For example, some drugs associated with IDILI synergize with TNF to kill hepatocytes in vitro, and a role for aberrant mitogen activated protein kinase (MAPK) signaling has been implicated in this response (Beggs et al., 2013, Cosgrove et al., 2009, Cosgrove et al. 2010, Fredriksson et al., 2011). TNF is known to activate the MAPKs JNK and p38 transiently (Wullaert et al. 2007). MAPKs are commonly activated in response to cellular stress, and if their activation is prolonged cell death can ensue (Anderson 1997). IFN activates the Janus kinase-signal transducer and activator of transcription (JAK-STAT) pathway, which can also mediate cell death (Stephanou et al. 2003). Exactly how drugs associated with IDILI synergize with cytokines to cause hepatocellular damage remains incompletely understood, although it is likely that activation of caspases and MAPKS play a role (Beggs et al. 2013, Fredriksson et al. 2011).

Nonsteroidal anti-inflammatory drugs (NSAIDs) and antibiotics are the most frequent causes of IDILI. The observation that rheumatoid arthritis increases the risk of NSAID-induced liver injury more than 10-fold in human patients suggests that immune mediators contribute to IDILI pathogenesis from drugs in this pharmacologic class (García Rodríguez et al., 1994). This suggestion is supported by results in animal models. In one such model, rodents treated with diclofenac (DCLF) in combination with lipopolysaccharide (LPS), an activator of the innate immune system, developed hepatocellular injury which did not occur after treatment with either DCLF or LPS alone

(Deng et al., 2006). Additionally, DCLF potentiated LPS-mediated expression of TNF and IFN genes in rats (Ramm et al., 2013). Similarly, sulindac (SLD), another NSAID associated with IDILI, produced TNF-dependent liver injury in rats cotreated with LPS (Zou et al., 2009).

Nearly all NSAIDs have been implicated in causing IDILI; however, the severity and lesion morphology of NSAID-induced hepatotoxicity varies substantially, likely due at least in part to the diversity of chemical structures within this drug class (O'Connor et al., 2003, Teoh et al., 2003). In this study, we tested the hypothesis that NSAIDs with idiosyncrasy liability synergize with TNF and IFN to cause hepatocellular toxicity in vitro. To gain insight into the mechanism of the NSAID/cytokine-induced cytotoxic interaction, the involvement of caspases and MAPKs was examined.

3.3 Materials and Methods

3.3.1 Materials

NSAIDs and MAPK inhibitors were purchased from Sigma-Aldrich (St. Louis, MO). Z-VAD-FMK and recombinant human TNF and IFN were purchased from R & D Systems (Minneapolis, MN). Phosphate-buffered saline (PBS), Dulbecco's Modified Eagles Medium (DMEM), William's Medium E, L-glutamine, fetal bovine serum (FBS), Antibiotic-Antimycotic (ABAM) and 0.25% Trypsin-EDTA were purchased from Life Technologies (Carlsbad, CA). All antibodies were purchased from Cell Signaling Technology (Beverly, MA).

3.3.2 Animals

Male C57BI/6J mice purchased from Jackson Laboratory (Bar Harbor, ME) were allowed to acclimate for at least 1 week upon arrival. They were housed in a 12-hour light/dark cycle, were fed a standard chow (8640 Teklad 22/5 Rodent Diet, Harlan Laboratories, Madison, WI) and had continual access to bottled spring water. All procedures were conducted with the approval of the Michigan State University Institutional Animal Care and Use Committee.

3.3.3 Cell Culture

Human hepatoma HepG2 cells (American Type Culture Collection, Manassas, VA) were chosen because they are insensitive to the harmful effects of cytokines yet express both TNF and IFN receptors (Hershey et al., 1989, Stonans et al., 1998).

Moreover, HepG2 cells respond similarly to primary mouse hepatocytes and primary human hepatocytes with regard to the cytotoxic interaction between IDILI-associated drugs and cytokines (Beggs et al., 2014, Cosgrove et al., 2009). It is known that HepG2

cells have low expression of phase 1 drug metabolizing enzymes compared to primary human hepatocytes. However, compared to primary human hepatocytes, they have similar expression of phase 2 drug metabolizing enzymes (Westerink and Schoonen, 2007a, Westerink and Schoonen, 2007b). The only NSAID used in this study for which it is suspected that phase 1 metabolism is required for liver injury is SLD. In this study the active metabolite of SLD, SLD sulifde, was used. We previously demonstrated that SLD sulfide, but not the parent compound, synergized with cytokines to cause cytotoxicity in HepG2 cells and primary rat hepatocytes (Zou et al. 2009). With regard to the remaining NSAIDs used in this study, there is not convincing evidence that bioactivation is required for liver injury in humans. Cells were grown in 25-cm² tissue culture treated flasks and maintained in DMEM supplemented with 10% FBS and 1% ABAM. They were cultured at 37°C in 95% air and 5% CO₂ in a humidified incubator. They were passaged when they reached approximately 80% confluence.

Primary murine hepatocytes were isolated as described previously by Klaunig et al. (1981). Hepatocytes were isolated using a 2-step collagenase perfusion method. Viability of isolated hepatocytes was assessed by trypan blue exclusion. Only cells with greater than 85% viability were used for experiments. Hepatocytes were plated with Williams' Medium E supplemented with 10% FBS, 1% ABAM, 2 mM L-glutamine and 100 nM insulin. After plating, they were cultured at 37°C in 95% air and 5% CO₂ in a humidified incubator and allowed 3 hours to attach prior to treatment.

3.3.4 IDILI Classification

NSAIDs were classified according to their ability to cause IDILI (Table 5).

NSAID	Structural sub-class	IDILI potential	Cmax (µg/ml)	Molecular Weight (g/mol)	Cmax reference
Diclofenac	Acetic acid derivative	Yes	2.4	296.15	Xu <i>et al.</i> 2008
Sulindac sulfide	Acetic acid derivative	Yes	1.6	340.41	Reid <i>et al.</i> 2008
Bromfenac	Acetic acid derivative	Yes	4.8	356.15	Gumbhir- Shah <i>et al.</i> 1997
Ibuprofen	Propionic acid derivative	Yes	32.9	206.29	Bramlage et al. 2008
Naproxen	Propionic acid derivative	Yes	75.9	252.23	Setiawati et al. 2009
Aspirin	Salicylic acid derivative	No	7.6	180.16	Brandon <i>et</i> <i>al.</i> 1986

Table 5. NSAID subclass and maximal plasma concentration (Cmax) from therapeutic doses in human patients

The criteria used to classify the drugs in this study was established by Xu et al. (2008) and takes into consideration post-marketing label information as well as numbers of published clinical case reports.

3.3.5 Cytotoxicity Assessment

HepG2 cells were plated at a density of 4 X 10⁴ cells per well in black-walled, 96well tissue culture plates and were allowed to attach overnight before treatment with compounds. DCLF, bromfenac (BRM), ibuprofen (IBU) and naproxen (NAP) were reconstituted in sterile water. SLD sulfide and aspirin were reconstituted in DMSO. Cells were treated with various concentrations of each NSAID or its vehicle, and simultaneously with TNF (10 ng/ml) and/or IFN (10 ng/ml) or their vehicles (PBS). Cells were treated with NSAID concentrations ranging from 0 to 100 times the maximal plasma concentration (Cmax) observed in human patients. The Cmax value for each NSAID is presented in Table 1. One hundred fold of the Cmax was considered a pharmacologically relevant dosing limit for this in vitro study and was derived from scaling factors described in Xu et al. (2008). Cells were exposed to drug/cytokine combinations for 24 hours, and cytotoxicity was evaluated by measuring lactate dehydrogenase (LDH) release from the cells into culture medium using the Homogeneous Membrane Integrity Assay kit from Promega (Madison, WI). For drugs that interfered with the fluorescence-based assay (IBU and NAP), a spectrophotometric method was used to measure LDH release (Vanderlinde, 1985).

To investigate the roles of caspases and the MAPKs, pharmacological inhibitors of these pathways were used (40 μ M Z-VAD-FMK for caspases, 20 μ M SP600125 for JNK, 20 μ M U0126 for ERK and 20 μ M SB203580 for p38). Inhibitors were reconstituted in DMSO, resulting in a maximal final concentration of 0.4% DMSO in experiments

involving SLD sulfide/z-VAD-FMK or 0.2% DMSO in all other experiments. In brief, cells were treated with an inhibitor alone or in combination with TNF and/or IFN and with one concentration of NSAID that produced strong cytotoxic synergy in the presence of cytokines. LDH release was measured 24 hours after treatment.

Primary mouse hepatocytes were plated at a density of 1.25 X 10⁵ cells per well in collagen-coated 24-well tissue culture treated plates. Cells were allowed 3 hours to attach followed by two washes with warm PBS then were treated with bromfenac alone or in combination with TNF and/or IFN prepared in serum-free Williams' Medium E supplemented with 1% ABAM and 2mM L-glutamine. After 24 hours of exposure to drugs and/or cytokines, cell supernatant was collected, and attached cells were lysed with 1% triton-X. The supernatant and lysate were transferred to 96-well plates and analyzed for alanine aminotransferase (ALT) activity as described by Luyendyk et al. (2005).

3.3.6 Caspase-3 activity

Caspase-3 activity was measured using the Caspase-3 Fluorometric Assay Kit purchased from R&D Systems (Minneapolis, MN). HepG2 cells were plated at 1.2 X 10⁶ cells per well in 6-well tissue culture plates. Cells were treated with an NSAID alone or in combination with TNF and/or IFN. Cells were lysed and centrifuged after 24 hours of exposure. 50 µl of lysate was added to black-walled, 96-well plates and incubated with assay reaction buffer and fluorogenic substrate for 1 hour. The plate was then read on a fluorescent plate reader at an excitation wavelength of 400 nm and an emission wavelength of 505 nm.

3.3.7 Protein isolation

Cells (1.2 X 10⁶ per well) were plated in 6-well tissue culture plates and allowed to adhere overnight. They were exposed to one concentration of NSAID and its vehicle alone or in combination with TNF and/or IFN for 12 hours or 18 hours. Cells were rinsed with cold PBS followed by addition of 150 µl of radioimmunoprecipitation assay (RIPA) buffer containing HALT protease and phosphatase inhibitor cocktails (Thermo Scientific, Rockford, IL). Cells were scraped, collected, placed in microcentrifuge tubes and incubated on ice for 10 minutes. During the 10-minute incubation, the tubes were vortexed intermittently. Lysates were centrifuged for 25 minutes at 20,000 X g. The supernatants containing whole cell extracts were collected, placed in fresh, chilled tubes and stored at -80°C until use. Protein concentrations were quantified using the bicinchoninic acid assay (Thermo Scientific).

3.3.8 Western analysis

For detection of MAPKs and phosphorylated STAT-1 (pSTAT-1) in whole cell lysates, protein (30 μg for JNK and 15 μg for ERK, p38 and STAT-1) was loaded onto pre-cast NuPAGE 12% Bis-Tris gels (Life Technologies) and subjected to electrophoresis. Proteins were transferred onto polyvinylidene fluoride (PVDF) membranes (Millipore, Billerica, MA). Membranes were blocked for one hour with 5% bovine serum albumin (BSA) reconstituted in 1% tris-buffered saline (TBS) containing 0.1% tween-20 (TBSt) for detection of JNK, p38 and STAT-1 or blocked with TBS-based LI-COR blocking buffer (Lincoln, NE) for detection of ERK. Membranes were probed with antibodies directed against phosphorylated JNK (pJNK), total JNK, phosphorylated ERK (pERK), total ERK, phosphorylated p38 (pp38), total p38, pSTAT-1 (Tyrosine 701), pSTAT-1 (Serine 727), and α-tubulin. Primary antibodies were diluted in

appropriate buffers to 1:1000. Membranes were incubated with primary antibodies overnight at 4°C, after which they were washed with TBSt followed by addition of secondary antibodies. Goat anti-rabbit horseradish peroxidase (HRP)-conjugated secondary antibody was diluted in 5% BSA in TBSt at a concentration of 1:2500 for pJNK, 1:5000 for total JNK, 1:5000 for pp38, 1:5000 for total p38, 1:5000 for pSTAT-1 (Tyrosine 701), 1:5000 for pSTAT-1 (Serine 727) and 1:5000 for α-tubulin. Clarity Western ECL substrate (Bio-rad, Hercules, CA) was used to visualize HRP and the substrate was developed on HyBlot CL film (Denville Scientific, Metuchen, NJ). For detection of ERK, donkey anti-mouse or goat anti-rabbit infrared (IR) dye-conjugated secondary antibodies were diluted in LI-COR blocking buffer to 1:3000, and IR fluorescence was detected using the LI-COR Odyssey IR Imaging System. All images were quantified by performing densitometry using image J software.

3.3.9 Statistical analysis

All results are expressed as mean \pm standard error of the mean (S.E.M.). Data were subjected to log transformation as necessary to achieve normality and equal variance. Data were analyzed via a one-way or two-way analysis of variance (ANOVA). Tukey's post-hoc test was used to perform multiple, pair-wise comparisons between treatment groups. The criterion for significance was set at α =0.05.

3.4 Results

3.4.1 NSAID/cytokine-induced cytotoxicity: concentration-response

The NSAIDs chosen for this study are diclofenac (DCLF), bromfenac (BRM), SLD sulfide (the active metabolite of SLD), naproxen (NAP), ibuprofen (IBU) and aspirin. Aspirin is the only one of these drugs that has not been associated with IDILI. Within the NSAID class of pharmaceuticals, there are a variety of subclasses based on chemical structure. There are three NSAID subclasses represented among the drugs used in our study. DCLF, BRM and SLD sulfide are acetic acid derivatives, IBU and NAP are propionic acid derivatives, and aspirin is a salicylic acid derivative. It is worth noting that acetic acid (AA) derivatives and propionic acid (PA) derivatives are among the most hepatotoxic NSAIDs (Teoh, et al., 2003). Moreover, among the IDILI-associated drugs used in this study, the AA derivatives are of greater clinical concern than the PA derivatives (Unzueta and Vargas, 2013).

Preliminary concentration-response studies were conducted with each cytokine to find a concentration that produced a robust cytotoxic interaction in the presence of DCLF. Treatment of HepG2 cells with 10 ng/ml of TNF led to a robust cytotoxic interaction with DCLF and treatment of cells with 10 ng/ml of IFN enhanced DCLF/TNF-mediated cytotoxicity (Figure 12). These cytokine concentrations were used for all remaining experiments in this study and are within 10-fold of the concentrations found in serum of human patients undergoing an inflammatory response (Pinsky, et al., 1993; Taudorf, et al., 2007). As expected, treatment of cells with TNF and/or IFN in the absence of drug did not result in release of LDH (Figure 12 and Figure 13). With the exception of SLD sulfide, treatment with NSAID alone did not result in cytotoxicity. All

five IDILI-associated NSAIDs synergized with TNF in a concentration-dependent manner to cause cytotoxicity (Figure 13A, B). IFN by itself did not influence drug-induced cytotoxicity; however, in the presence of TNF it enhanced the cytotoxicity mediated by DCLF, BRM and SLD sulfide (Figure 13A) but had no effect on the toxicity of IBU and NAP (Figure 13B). Aspirin did not synergize with TNF or IFN alone or in combination to kill HepG2 cells (Figure 13C).

Some of the NSAIDs used in this study, in addition to dozens of other IDILI associated drugs, synergize with cytokines to cause death of primary human hepatocytes (Cosgrove, et al., 2009). Drug/cytokine-induced cytotoxic synergy observed in primary human hepatocytes was recapitulated in HepG2 cells in spite of the low phase 1 metabolism observed in this cell line (Cosgrove, et al., (2009). The cytotoxic interaction observed here in HepG2 cells between BRM and TNF, as well as the IFN-mediated enhancement of BRM/TNF-induced cytotoxicity (Figure 13A), was observed in primary mouse hepatocytes as well (Figure 14).

3.4.2 Cytotoxic synergy between cytokines and NSAIDs requires caspases

Fredriksson, et al., (2011) reported that DCLF/TNF-mediated cytotoxicity in HepG2 cells depends on caspases. Additionally, Zou, et al., (2009) demonstrated that SLD sulfide synergizes with TNF to cause caspase activation that led to cell death. We tested the hypothesis that this holds true for other NSAIDs and for the IFN-mediated enhancement of NSAID/TNF-induced cytotoxicity.

Of the three NSAID subclasses used in this study, two of them (the AA derivatives and PA derivatives) interacted with cytokines to kill cells. Although these two subclasses differed in the manner in which they synergized with the cytokines, within

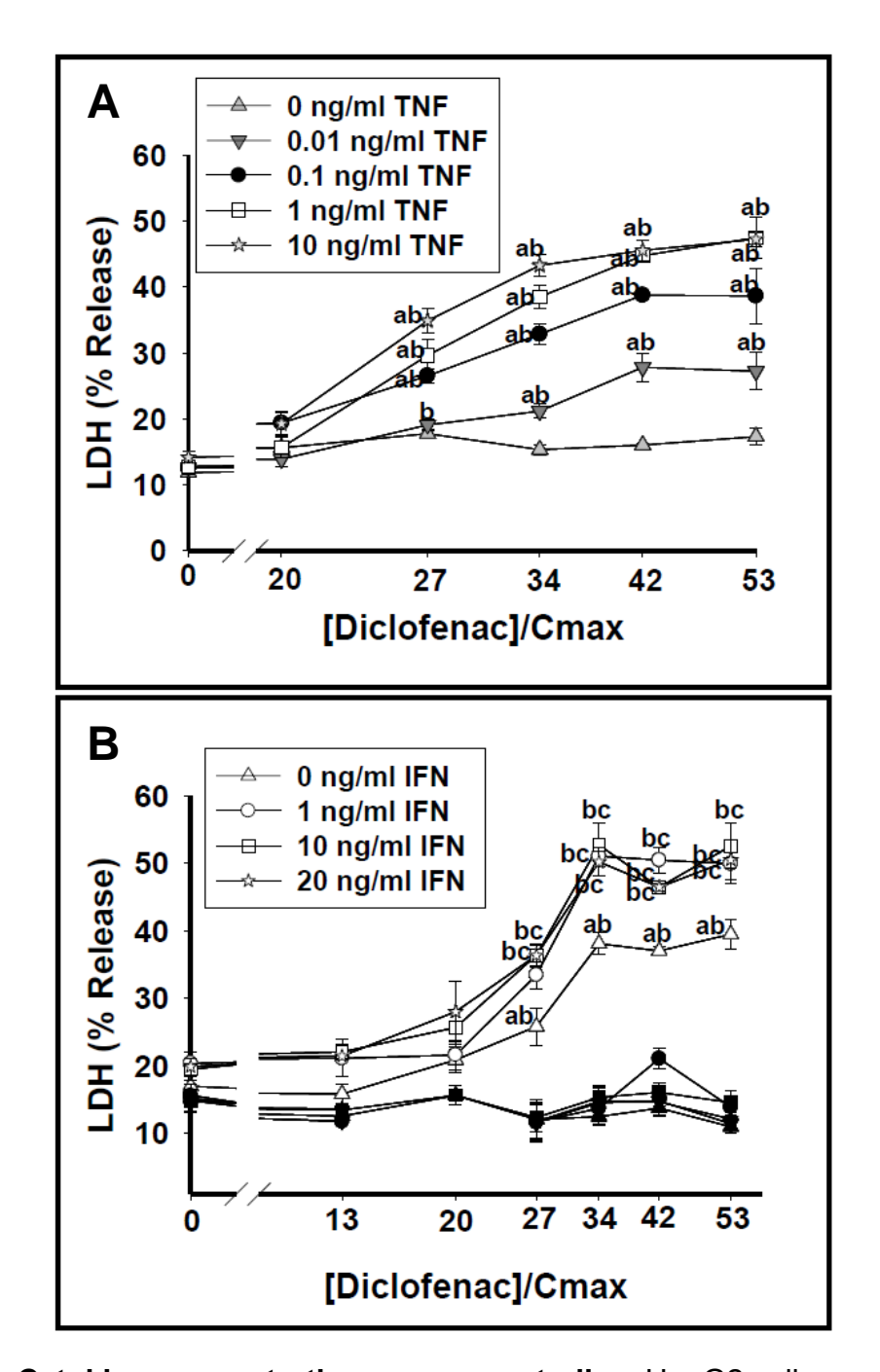


Figure 12. Cytokine concentration response studies. HepG2 cells were treated with DCLF alone or in combination with various concentrations of A) TNF or B) IFN \pm 10 ng/ml TNF. For panel B, open symbols indicate treatment with IFN + TNF

Figure 12 (cont'd)

(10 ng/ml) and closed symbols indicate treatment with IFN in the absence of TNF. a, significantly different from VEH (no cytokine) within a DCLF concentration. b, significantly different from 0 μ M DCLF within a cytokine concentration. c, significantly different from TNF alone (0 ng/ml IFN) within a DCLF concentration. Data are represented as mean \pm S.E.M of at least 5 separate experiments. Abbreviations: VEH, vehicle; TNF, tumor necrosis factor-alpha; IFN, interferon-gamma; LDH, lactate dehydrogenase.

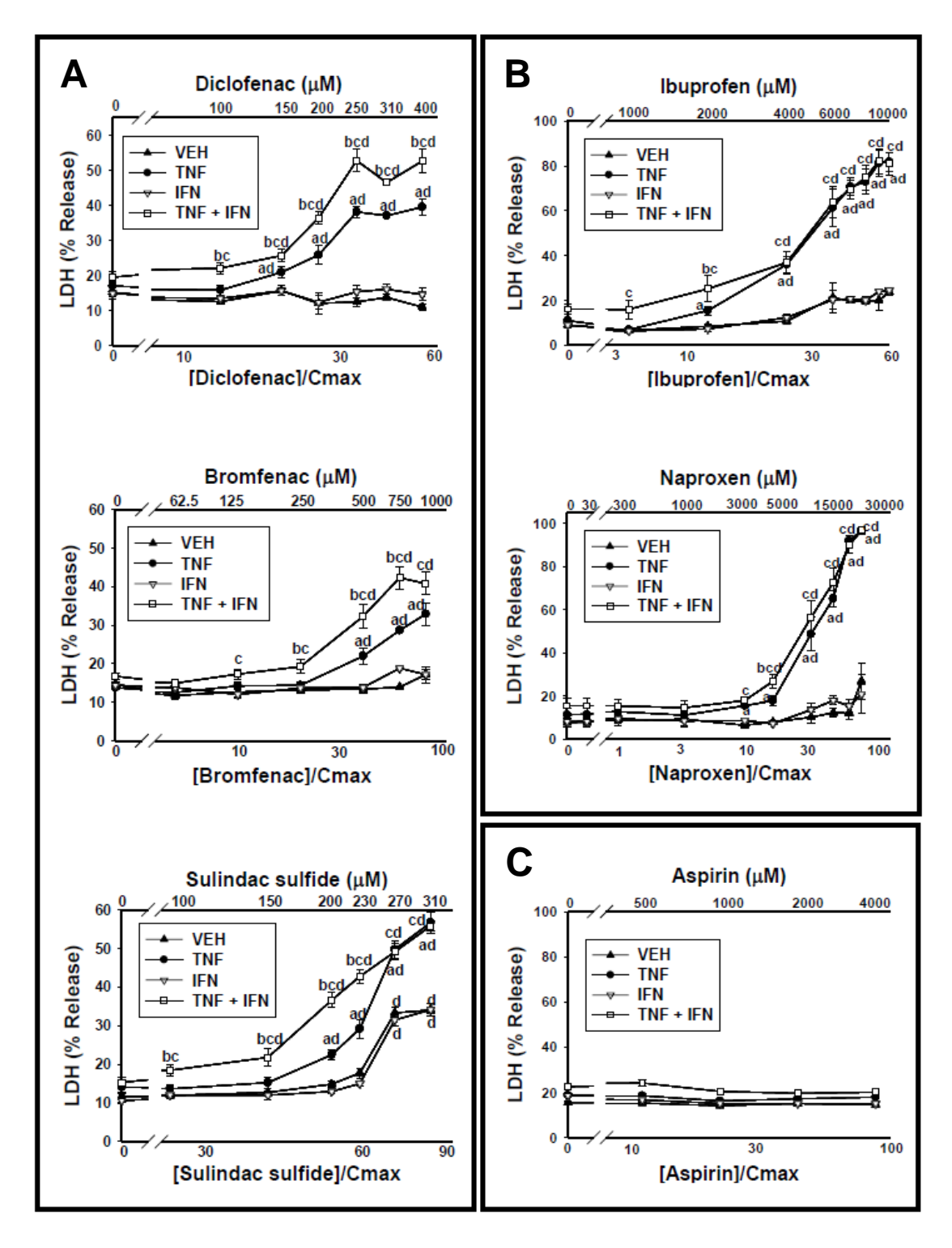


Figure 13. Interaction of NSAIDs with cytokines leads to synergistic cytotoxicity.

HepG2 cells were treated with NSAIDs that have (A,B) or do not have (C) IDILI liability

Figure 13 (cont'd)

alone or in combination with TNF (10 ng/ml) and/or IFN (10 ng/ml). The NSAIDs that have IDILI liability are grouped according to structural subclass: (A) AA derivatives; (B) PA derivatives; (C) salicylic acid derivative. a, significantly different from VEH (no cytokine) within an NSAID concentration. b, significantly different from TNF within an NSAID concentration. c, significantly different from IFN within an NSAID concentration. d, significantly different from 0 µM NSAID within a cytokine group. Data are represented as mean ± S.E.M of at least 5 separate experiments. Abbreviations: VEH, vehicle; TNF, tumor necrosis factor-alpha; IFN, interferon-gamma; LDH, lactate dehydrogenase.

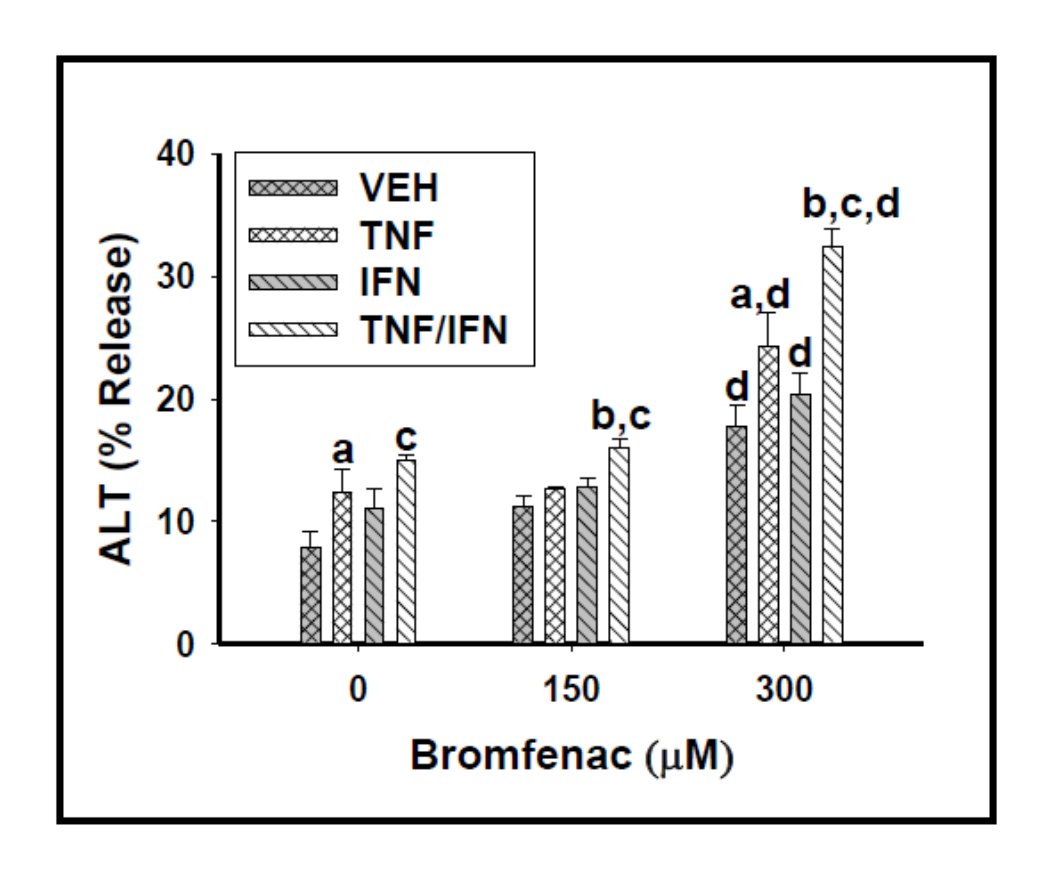


Figure 14. Bromfenac/cytokine-induced cytotoxic synergy in primary mouse hepatocytes. Primary mouse hepatocytes were treated with bromfenac alone or in combination with TNF and/or IFN. ALT release was measured 24 hours after treatment. a, significantly different from VEH (within a bromfenac concentration). b, significantly different from TNF (within a bromfenac concentration). c, significantly different from IFN (within a bromfenac concentration). d, significantly different from 0 μM bromfenac (within a cytokine treatment). Data are represented as mean ± S.E.M of 4 mice. Abbreviations: VEH, vehicle; TNF, tumor necrosis factor-alpha; IFN, interferon gamma; ALT, alanine aminotransferase.

subclass they responded similarly to each other. Consequently, we selected a representative AA derivative (DCLF) and PA derivative (IBU) to evaluate caspase involvement in the NSAID/cytokine-induced cytotoxic interaction. For this experiment and all subsequent ones, we selected an NSAID concentration that resulted in strong cytotoxic synergy with TNF and/or IFN. Both DCLF and IBU induced caspase 3 activation within 24 hours of treatment (Figure 15). Addition of TNF potentiated caspase 3 activation by the drugs. Consistent with the cytotoxicity data presented in Figure 13, IFN enhanced caspase 3 activation induced by DCLF/TNF but not by IBU/TNF (Figure 15). Treatment with the pan-caspase inhibitor Z-VAD-FMK completely protected cells from NSAID/TNF-induced cytotoxicity. Additionally, the IFN-mediated enhancement of cytotoxicity in cells treated with AA derivatives/TNF was eliminated by Z-VAD-FMK treatment (Figure 16).

3.4.3 Cytotoxic synergy between cytokines and NSAIDs involves activation of JNK

As described above, a representative AA derivative (DCLF) and PA derivative (IBU) were selected to examine the expression of phosphorylated (activated) JNK (pJNK). Based on the time-course of cytotoxicity after treatment with DCLF and cytokines (Figure 17), two times were selected: a time at which there was no cytotoxicity (12 hours) and a time at which cytotoxicity was observed (18 hours). Treatment with TNF in the absence of drug (Control) caused expression of pJNK at 12 hours (Figure 18A). In the absence of drug, expression of pJNK was unchanged by treatment with TNF, IFN, or TNF/IFN at 18 hours (Figure 18A, B). At 12 hours, treatment with DCLF caused phosphorylation of JNK which was strongly enhanced in the presence of TNF.

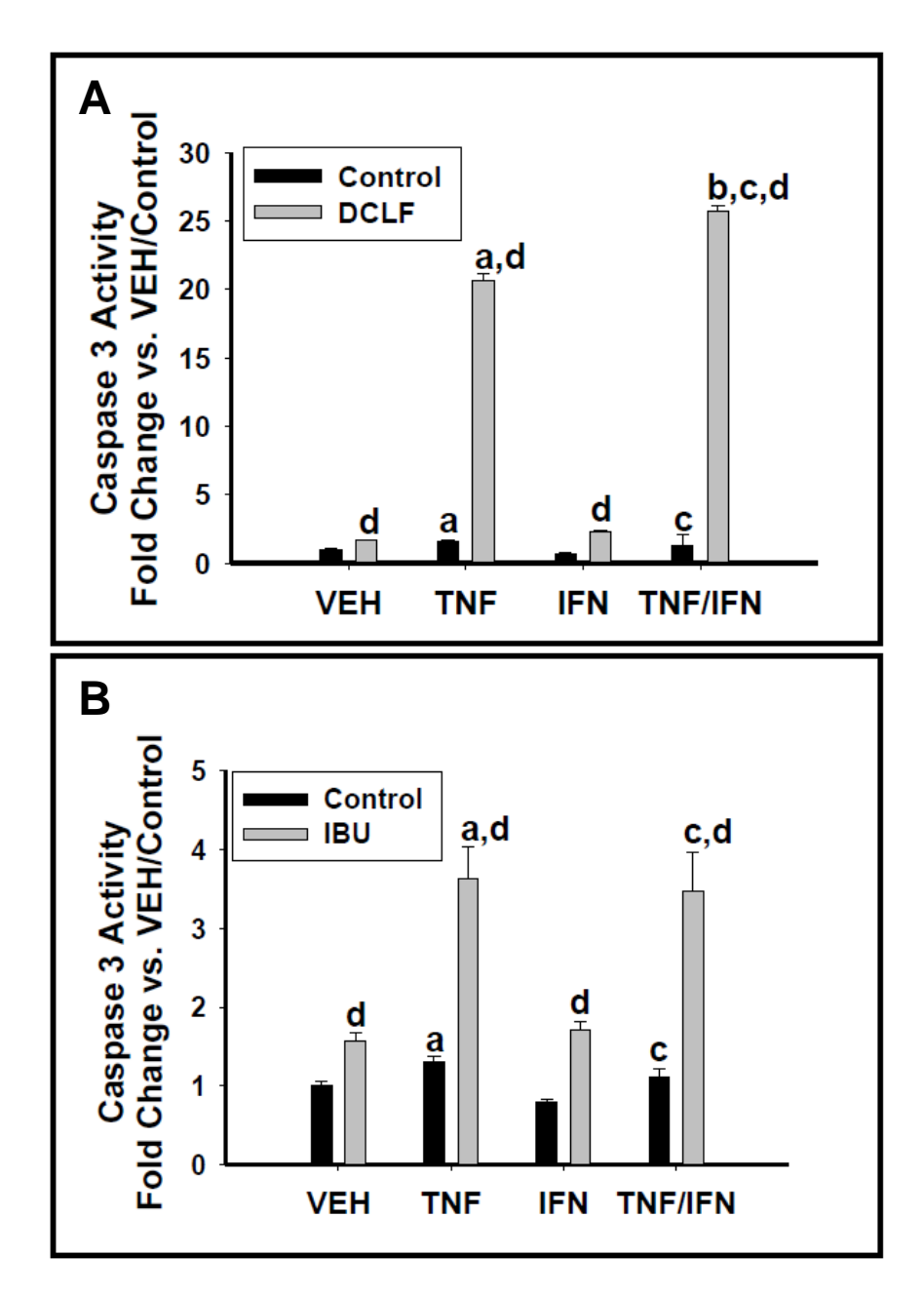


Figure 15. Caspase activation in response to DCLF/cytokine and IBU/cytokine treatment. HepG2 cells were treated with (A) a representative AA derivative (DCLF: 250 μM) or (B) a representative PA derivative (IBU: 6 mM) alone or in combination with TNF and/or IFN, and cell lysates were collected 24 hours after treatment for measurement of caspase 3 activity. a, significantly different from VEH. b, significantly

Figure 15 (cont'd)

different from TNF. c, significantly different from IFN. d, significantly different from Control. Data are represented as mean ± S.E.M of at least 3 separate experiments.

Abbreviations: VEH, vehicle; TNF, tumor necrosis factor-alpha; IFN, interferon-gamma; DCLF, diclofenac; IBU, ibuprofen.

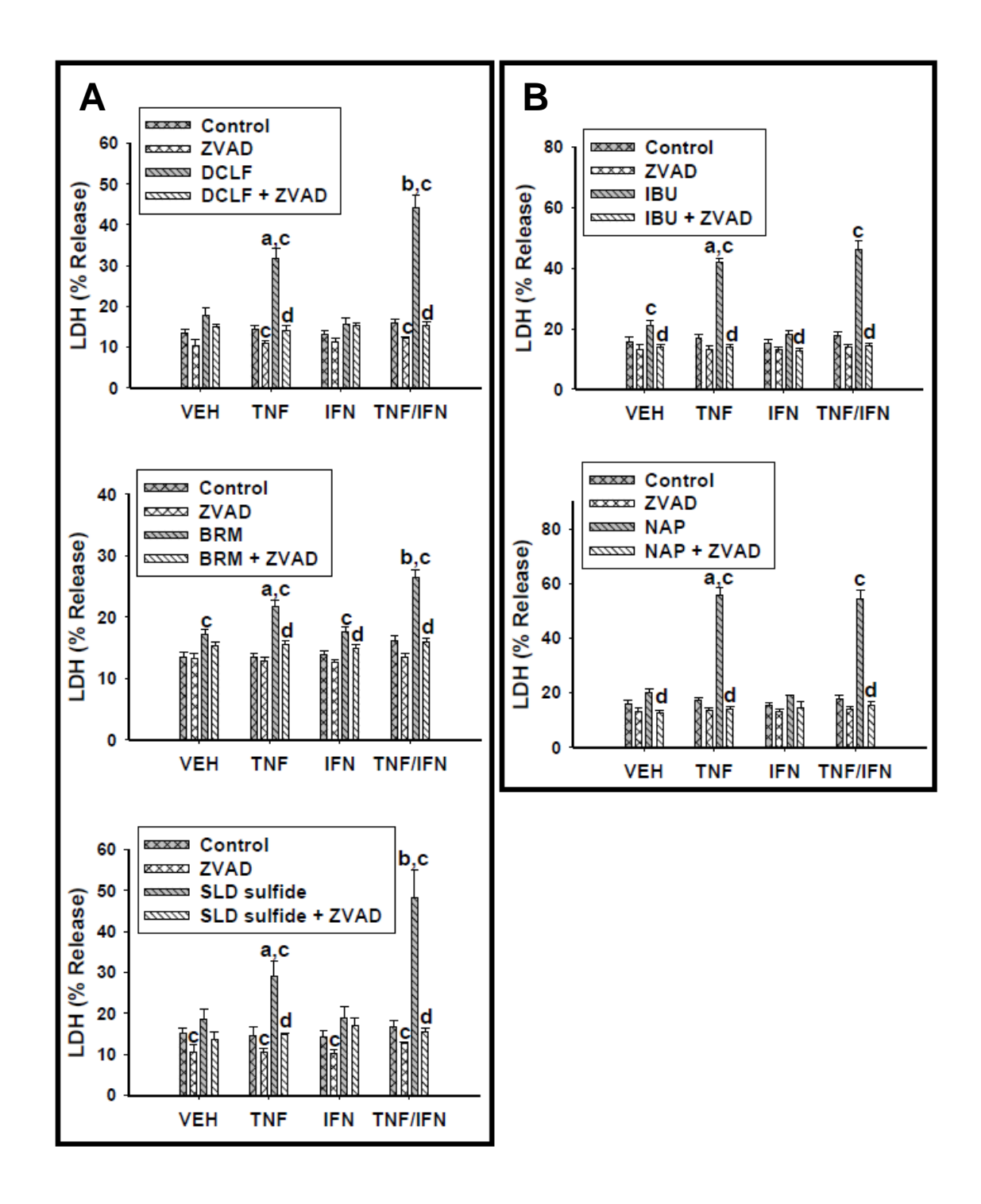


Figure 16. Caspases are involved in the NSAID/cytokine-induced cytotoxic interaction. HepG2 cells were treated with (A) AA derivatives (DCLF: 250 μ M, BRM: 750 μ M or SLD sulfide: 200 μ M), or (B) PA derivatives (IBU: 6 mM or NAP: 10 mM)

Figure 16 (cont'd)

alone or in combination with TNF and/or IFN. Cells were also incubated in the presence and absence of the pan-caspase inhibitor ZVAD-FMK (40 µM). Cytotoxicity was measured 24 hours later. a, significantly different from VEH within NSAID/inhibitor treatment. b, significantly different from TNF within NSAID/inhibitor treatment. c, significantly different from Control within a cytokine group. d, significantly different from NSAID without inhibitor within a cytokine group. Data are represented as mean ± S.E.M of at least 5 separate experiments. Abbreviations: VEH, vehicle; TNF, tumor necrosis factor-alpha; IFN, interferon-gamma; LDH, lactate dehydrogenase; DCLF, diclofenac; BRM, bromfenac; SLD, sulindac; IBU, ibuprofen; NAP, naproxen.

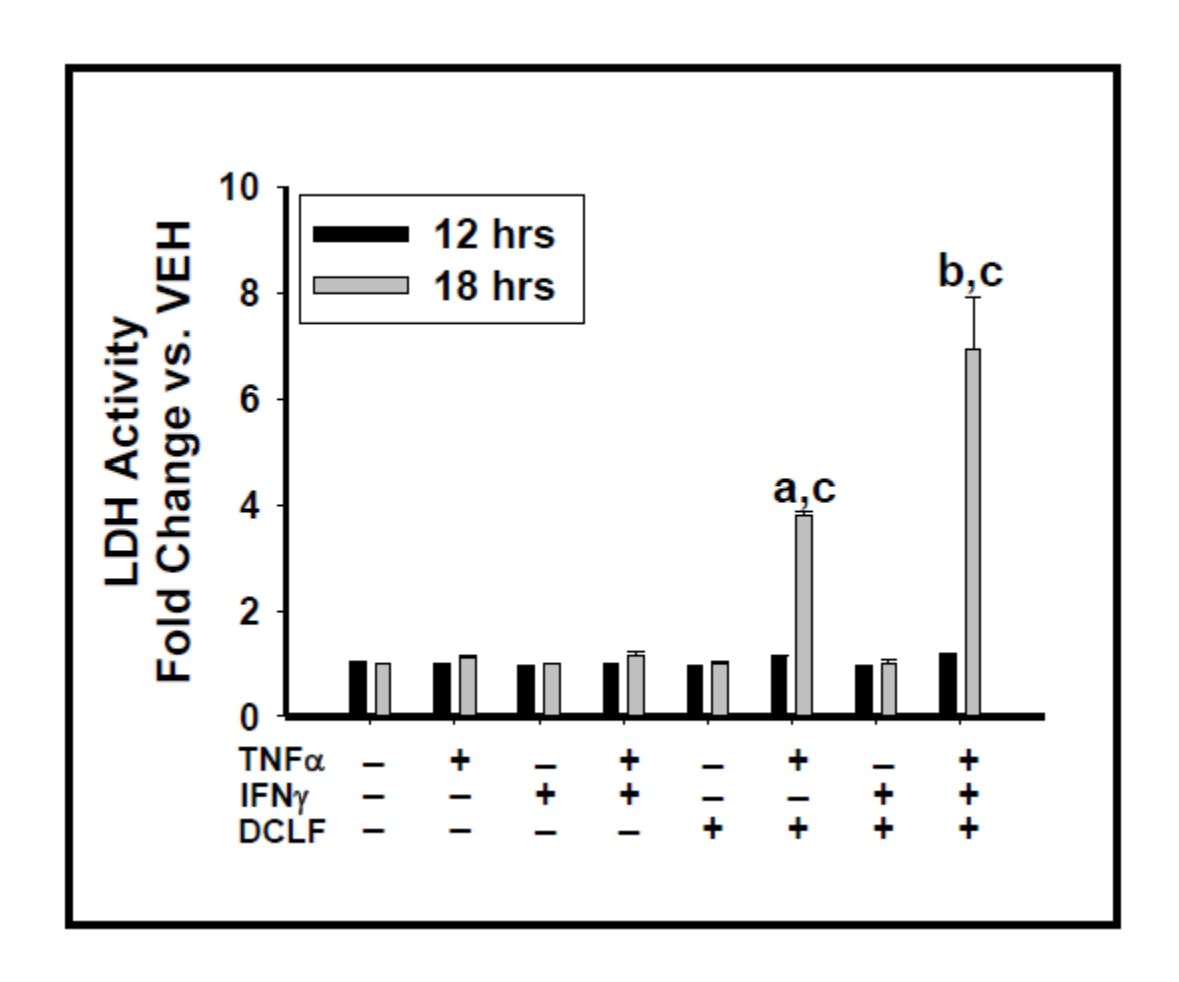


Figure 17. Time course of DCLF/cytokine-induced cytotoxic synergy. HepG2 cells were treated with DCLF (250 μ M) alone or in combination with TNF (10ng/ml) and/or IFN (10 ng/ml). Activity of LDH released from cells was measured 12 and 18 hours after treatment. a, significantly different from VEH (absence of drug/cytokines). b, significantly different from DCLF/TNF. c, significantly different from 12 hour time point. Data are represented as mean \pm S.E.M of 3 experiments. Abbreviations: LDH, lactate dehydrogenase; hrs, hours; VEH, vehicle; TNF, tumor necrosis factor-alpha, IFN, interferon-gamma; DCLF, diclofenac.

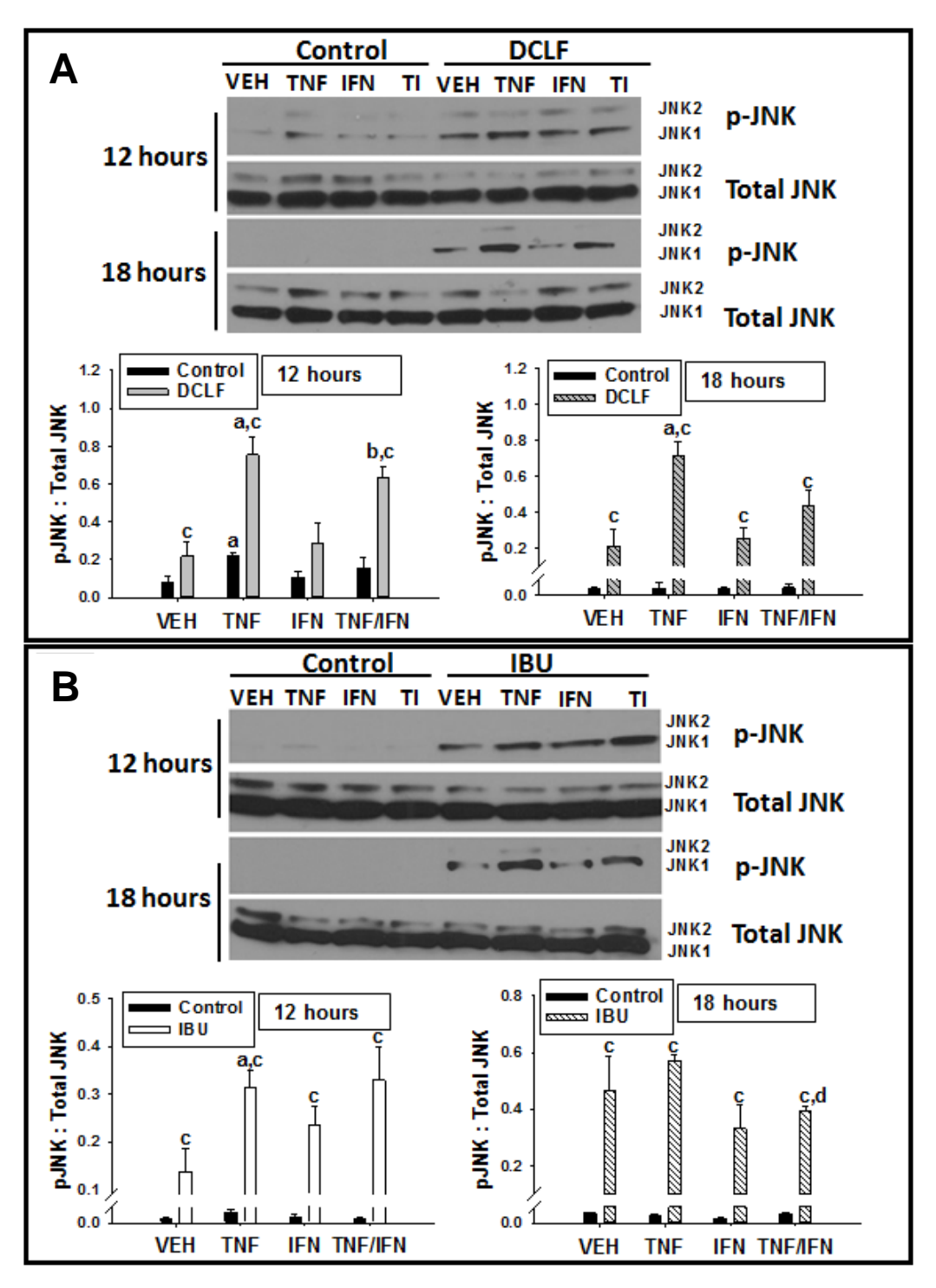


Figure 18. DCLF and IBU treatment induce prolonged activation of JNK. HepG2 cells were treated with (A) a representative AA derivative (DCLF: 250 µM) or (B) a

Figure 18 (cont'd)

representative PA derivative (IBU: 6 mM) alone or in combination with TNF and/or IFN, and protein extracts were collected 12 or 18 hours after treatment. p-JNK and total JNK protein were detected via western analysis. Representive blots are shown.

Densitometry was performed using image J software. a, significantly different from VEH within an NSAID treatment. b, significantly different from IFN within an NSAID treatment. c, significantly different from Control within a cytokine treatment. d, significantly different from TNF within an NSAID treatment Data are represented as mean ± S.E.M of 3 separate experiments. Abbreviations: VEH, vehicle; TNF, tumor necrosis factor-alpha; IFN, interferon gamma; TI, tumor necrosis factor-alpha and interferon-gamma; DCLF, diclofenac; IBU, ibuprofen.

Treatment with IFN did not alter DCLF/TNF-induced JNK phosphorylation. By 18 hours, DCLF caused JNK activation in the absence of TNF. In the presence of TNF this response was enhanced, but IFN did not alter JNK activation either alone or in the presence of DCLF/TNF. In contrast, IBU significantly activated JNK by itself at both 12 and 18 hours (Figure 18B). IBU-mediated JNK activation was enhanced in the presence of TNF at 12 hours, whereas IFN was without effect.

We next examined the involvement of JNK in NSAID/cytokine-induced cytotoxicity. Treatment with SP600125, an inhibitor of JNK activation, significantly reduced cytotoxicity mediated by cytokines in combination with NSAIDs containing an AA moiety (Figure 19A). In contrast, SP600125 treatment did not alter the cytotoxic interaction for NSAIDs containing a PA moiety (Figure 19B). Interestingly, treatment with SP600125 eliminated VEH- and DCLF-induced JNK activation but was ineffective at eliminating IBU-mediated JNK activation (Figure 19C).

3.4.4 Cytotoxic synergy between cytokines and NSAIDs involves activation of ERK

Treatment with cytokines in the absence of drug (Control) did not result in ERK activation (Figure 20). Treatment with DCLF caused activation of ERK at 12 hours that was still evident at 18 hours (Figure 20A). Neither TNF nor IFN alone or in combination affected DCLF-mediated activation of ERK. Similarly, treatment with IBU caused persistent ERK activation that was unaltered by the presence of cytokines (Figure 20B).

U0126 prevents ERK phosphorylation by inhibiting the MAPK kinase (MEK) that directly phosphorylates ERK. Treatment with U0126 did not affect cytotoxicity mediated by AA derivatives in combination with TNF; however, it significantly reduced the IFN-

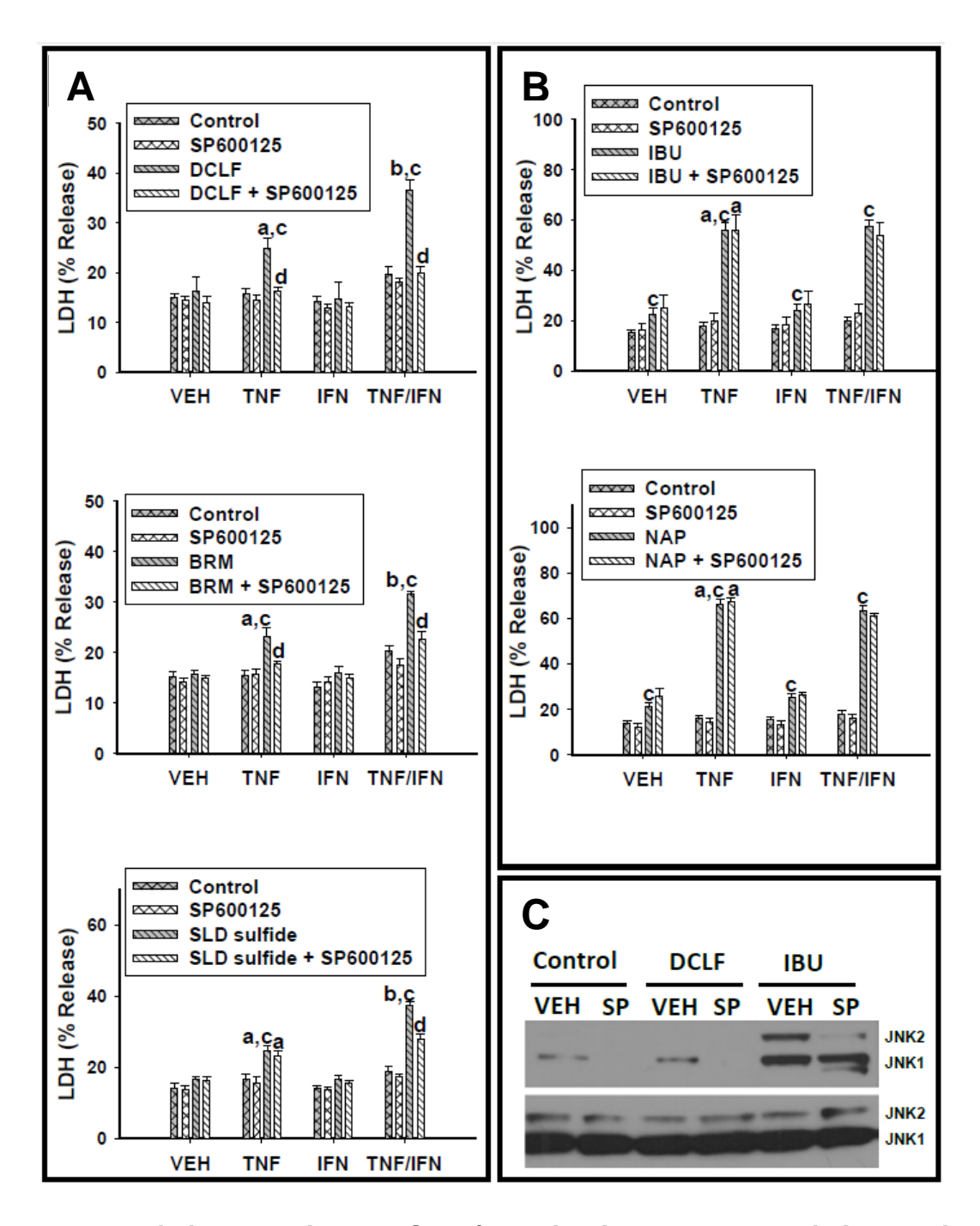


Figure 19. JNK is involved in the NSAID/cytokine-induced cytotoxic interaction.

HepG2 cells were treated with (A) AA derivatives (DCLF: 250 μ M, BRM: 750 μ M or SLD sulfide: 200 μ M), or (B) PA derivatives (IBU: 6 mM or NAP: 10 mM) alone or in combination with TNF and/or IFN. Cells were also incubated in the presence and

Figure 19 (cont'd)

absence of the JNK inhibitor SP600125 (20 µM). Cytotoxicity was measured 24 hours later. (C) Cells were treated with a representative AA derivative (DCLF: 250 µM) or a representative PA derivative (IBU: 6mM) in the presence or absence of SP600125 for 12 hours, and p-JNK and total JNK protein were detected via western analysis. a, significantly different from VEH within NSAID/inhibitor treatment. b, significantly different from TNF within NSAID/inhibitor treatment. c, significantly different from Control within a cytokine group. d, significantly different from NSAID without inhibitor within a cytokine group. Data are represented as mean ± S.E.M of at least 5 separate experiments. Abbreviations: VEH, vehicle; TNF, tumor necrosis factor-alpha; IFN, interferon-gamma; LDH, lactate dehydrogenase; DCLF, diclofenac; BRM, bromfenac; SLD, sulindac; IBU, ibuprofen; NAP, naproxen; SP, SP600125.

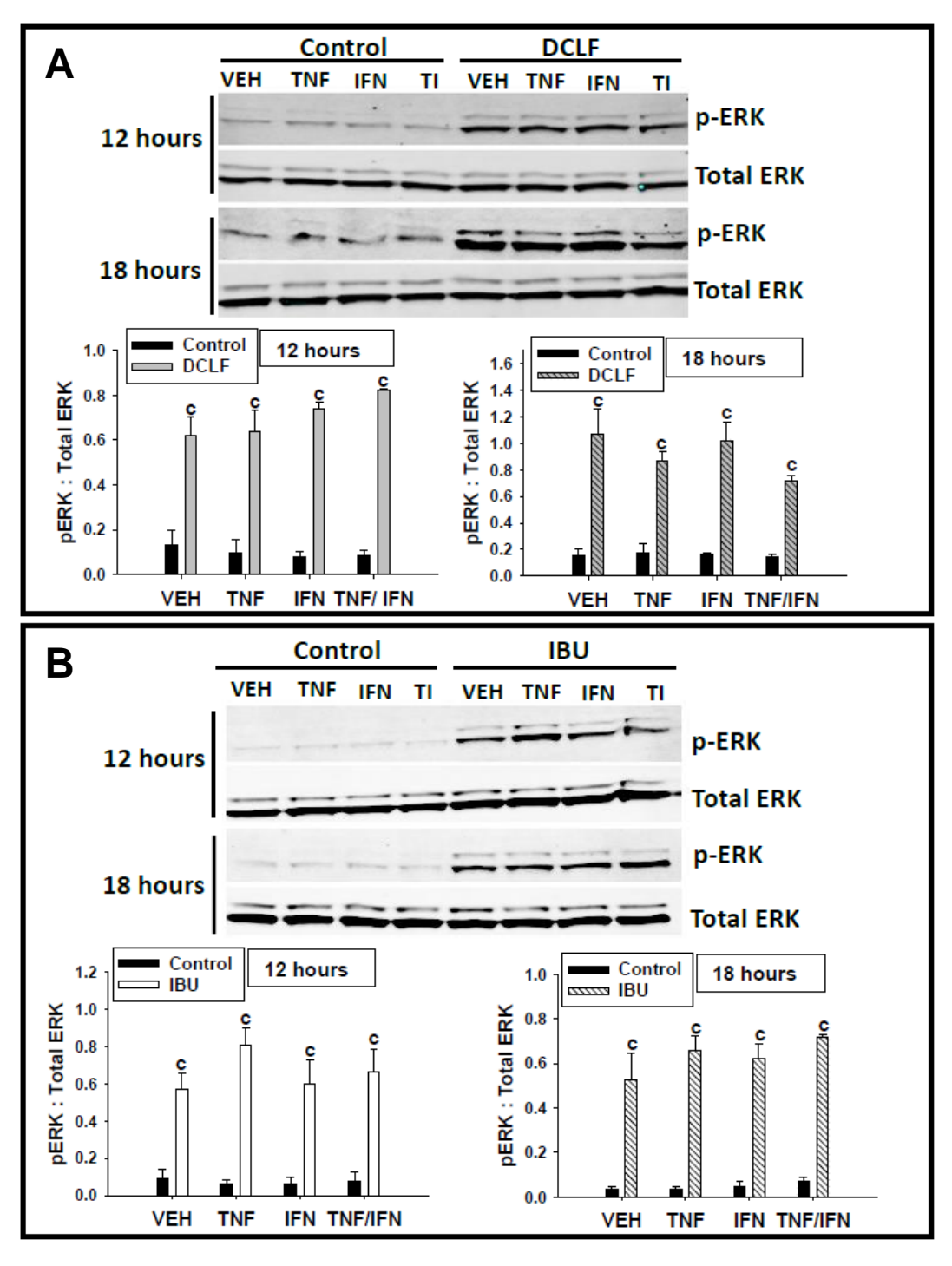


Figure 20. DCLF and IBU treatment induce prolonged activation of ERK. HepG2 cells were treated with (A) a representative AA derivative (DCLF: 250 μM) or (B) a

Figure 20 (cont'd)

representative PA derivative (IBU: 6 mM) alone or in combination with TNF and/or IFN, and protein extracts were collected 12 or 18 hours after treatment. p-ERK and total ERK protein were detected via western analysis. Representative blots are shown.

Densitometry was performed using image J software. c, significantly different from Control within a cytokine treatment. Data are represented as mean ± S.E.M of 3 separate experiments. Abbreviations: VEH, vehicle; TNF, tumor necrosis factor-alpha, IFN, interferon-gamma; TI, tumor necrosis factor-alpha and interferon-gamma; DCLF, diclofenac; IBU, ibuprofen.

mediated enhancement of AA derivative/TNF-mediated cytotoxicity (Figure 21A). In contrast, treatment with U0126 potentiated cytotoxicity caused by PA derivatives in combination with cytokines (Figure 21B). The MEK inhibitor U0126 was effective at eliminating ERK activation induced by DCLF and IBU (Figure 21C).

3.4.5 p38 attenuates NSAID/cytokine-induced cytotoxic synergy

Treatment with either TNF alone or DCLF alone induced phosphorylation of p38 at 12 hours but not at 18 hours (Figure 22A). There was no change in DCLF-induced p38 activation in the presence of TNF at 12 hours, and treatment with DCLF/TNF/IFN increased p38 phosphorylation relative to DCLF/IFN or TNF/IFN treatment (Figure 22A). IBU strongly induced p38 activation relative to VEH at 12 hours and 18 hours (Figure 22B). Cytokine treatment did not significantly alter IBU-mediated p38 activation (Figure 22B).

Activation of p38 is typically associated with activation of pathways leading to cell death. Surprisingly, with the exception of DCLF/TNF exposure, treatment with the p38 inhibitor SB203580 enhanced cytotoxicity mediated by AA derivative/TNF exposure in the presence and absence of IFN (Figure 23A). Treatment with SB203580 potentiated cytotoxicity from PA derivative/TNF exposure as well, irrespective of IFN exposure (Figure 23B). These data suggest that p38 plays a protective role in NSAID/cytokine-induced cytotoxicity.

3.4.6 DCLF but not IBU promotes dual phosphorylation of STAT-1 in an ERK-dependent manner

Upon binding to its receptor, IFN is well known to activate the JAK-STAT pathway. As expected, treatment with IFN resulted in phosphorylation of STAT-1 at

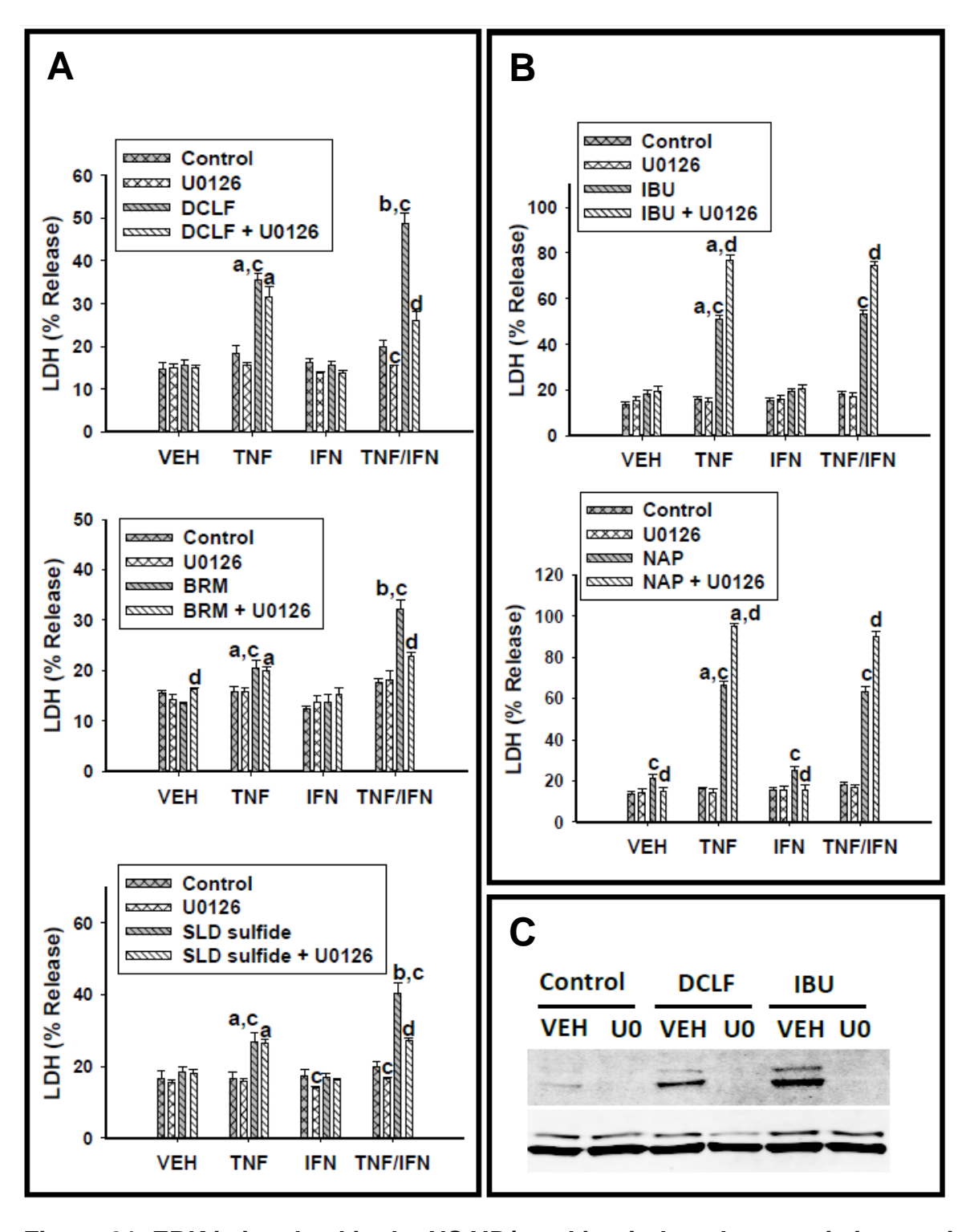


Figure 21. ERK is involved in the NSAID/cytokine-induced cytotoxic interaction.

HepG2 cells were treated with (A) AA derivatives (DCLF: 250 μ M, BRM: 750 μ M or SLD

Figure 21 (cont'd)

sulfide: 200 µM), or (B) PA derivatives (IBU: 6 mM or NAP: 10 mM) alone or in combination with TNF and/or IFN. NSAID/cytokine combinations were also incubated in the presence and absence of the ERK inhibitor U0126 (20 µM). Cytotoxicity was measured 24 hours later. (C) Cells were treated with a representative AA derivative (DCLF: 250 µM) or a representative PA derivative (IBU: 6 mM) in the presence or absence of U0126 for 12 hours and p-ERK and total ERK protein was detected via western analysis. a, significantly different from VEH within NSAID/inhibitor treatment. b, significantly different from TNF within NSAID/inhibitor treatment. c, significantly different from Control within a cytokine group. d, significantly different from NSAID without inhibitor within a cytokine group. Data are represented as mean ± S.E.M of at least 5 separate experiments. Abbreviations: VEH, vehicle; TNF, tumor necrosis factoralpha; IFN, interferon-gamma; LDH, lactate dehydrogenase; DCLF, diclofenac; BRM, bromfenac; SLD, sulindac; IBU, ibuprofen; NAP, naproxen; U0, U0126.

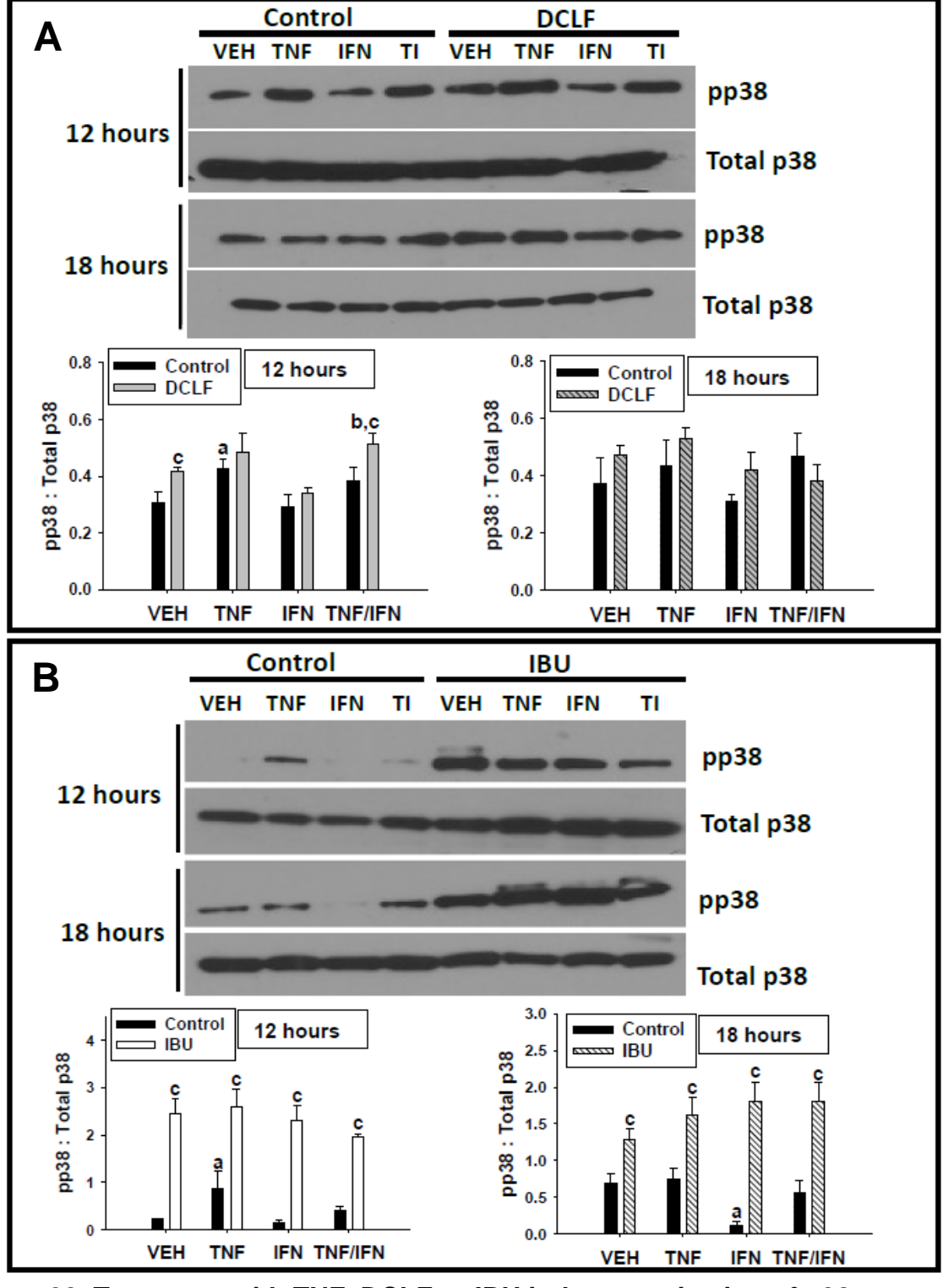


Figure 22. Treatment with TNF, DCLF or IBU induces activation of p38.

Figure 22 (cont'd)

HepG2 cells were treated with (A) a representative AA derivative (DCLF: 250 μM) or (B) a representative PA derivative (IBU: 6 mM) alone or in combination with TNF and/or IFN, and protein extracts were collected 12 or 18 hours after treatment. pp38 and total p38 protein were detected via western analysis. Representative blots are shown. Densitometry was performed using image J software. a, significantly different from VEH. b, significantly different from IFN. c, significantly different from Control. Data are represented as mean ± S.E.M of 3 separate experiments. Abbreviations: VEH, vehicle; TNF, tumor necrosis factor-alpha, IFN, interferon-gamma; TI, tumor necrosis factor-alpha and interferon-gamma; DCLF, diclofenac; IBU, ibuprofen.

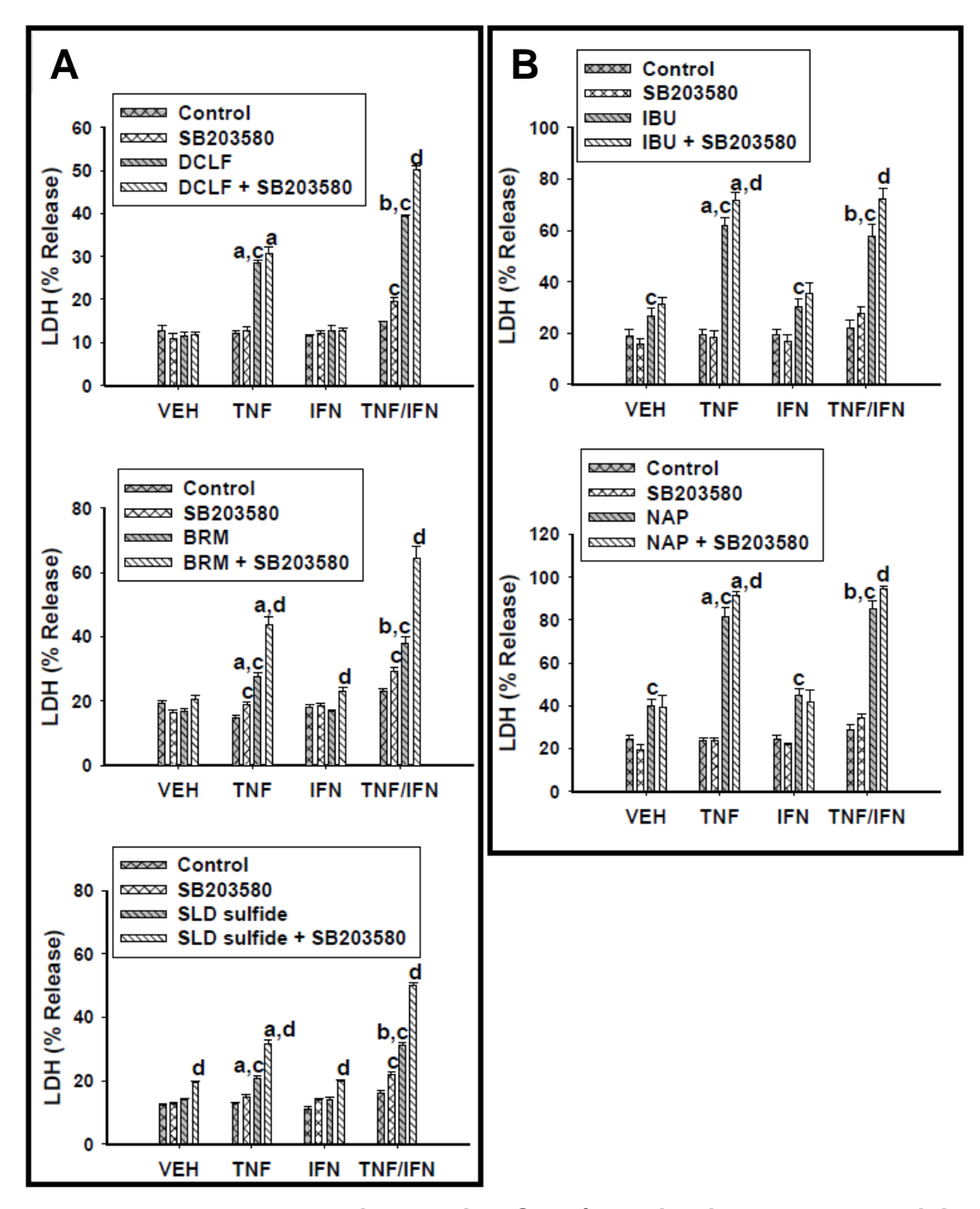


Figure 23. P38 plays a protective role in NSAID/cytokine-induced cytotoxicity.

HepG2 cells were treated with (A) AA derivatives (DCLF: 250 μ M, BRM: 750 μ M or SLD sulfide: 200 μ M), or (B) PA derivatives (IBU: 6 mM or NAP: 10 mM) alone or in

Figure 23 (cont'd)

combination with TNF and/or IFN. NSAID/cytokine combinations were also incubated in the presence and absence of the p38 inhibitor SB203580 (20 μ M). Cytotoxicity was measured 24 hours later. a, significantly different from VEH within NSAID/inhibitor treatment. b, significantly different from TNF within NSAID/inhibitor treatment. c, significantly different from Control within a cytokine group. d, significantly different from NSAID without inhibitor within a cytokine group. Data are represented as mean \pm S.E.M of at least 4 separate experiments. Abbreviations: VEH, vehicle; TNF, tumor necrosis factor-alpha; IFN, interferon-gamma; LDH, lactate dehydrogenase; DCLF, diclofenac; BRM, bromfenac; SLD, sulindac; IBU, ibuprofen; NAP, naproxen.

tyrosine (Tyr) 701, irrespective of TNF exposure (Figure 24). DCLF treatment did not influence Tyr 701 phosphorylation. It has been reported that phosphorylation of STAT-1 at serine (Ser) 727 in addition to Tyr 701 is required for maximal activation (Varinou et al. 2003). There was a modest increase in phosphorylation of STAT-1 at Ser 727 in response to IFN treatment, irrespective of TNF treatment. Interestingly, treatment with DCLF markedly enhanced the IFN-mediated phosphorylation at Ser 727 (Figure 24). JAK is responsible for phosphorylating Tyr 701 on STAT-1. It is unclear which specific kinases are responsible for phosphorylating Ser 727, but it has been suggested that MAPKs, specifically ERK, can perform this phosphorylation (Zhang et al. 2004). Treatment with the ERK inhibitor U0126 did not alter phosphorylation of Tyr 701 but completely prevented phosphorylation of Ser 727 (Figure 24). Treatment with IBU prevented IFN-mediated phosphorylation of STAT-1 at both Tyr 701 and Ser 727 (Figure 25).

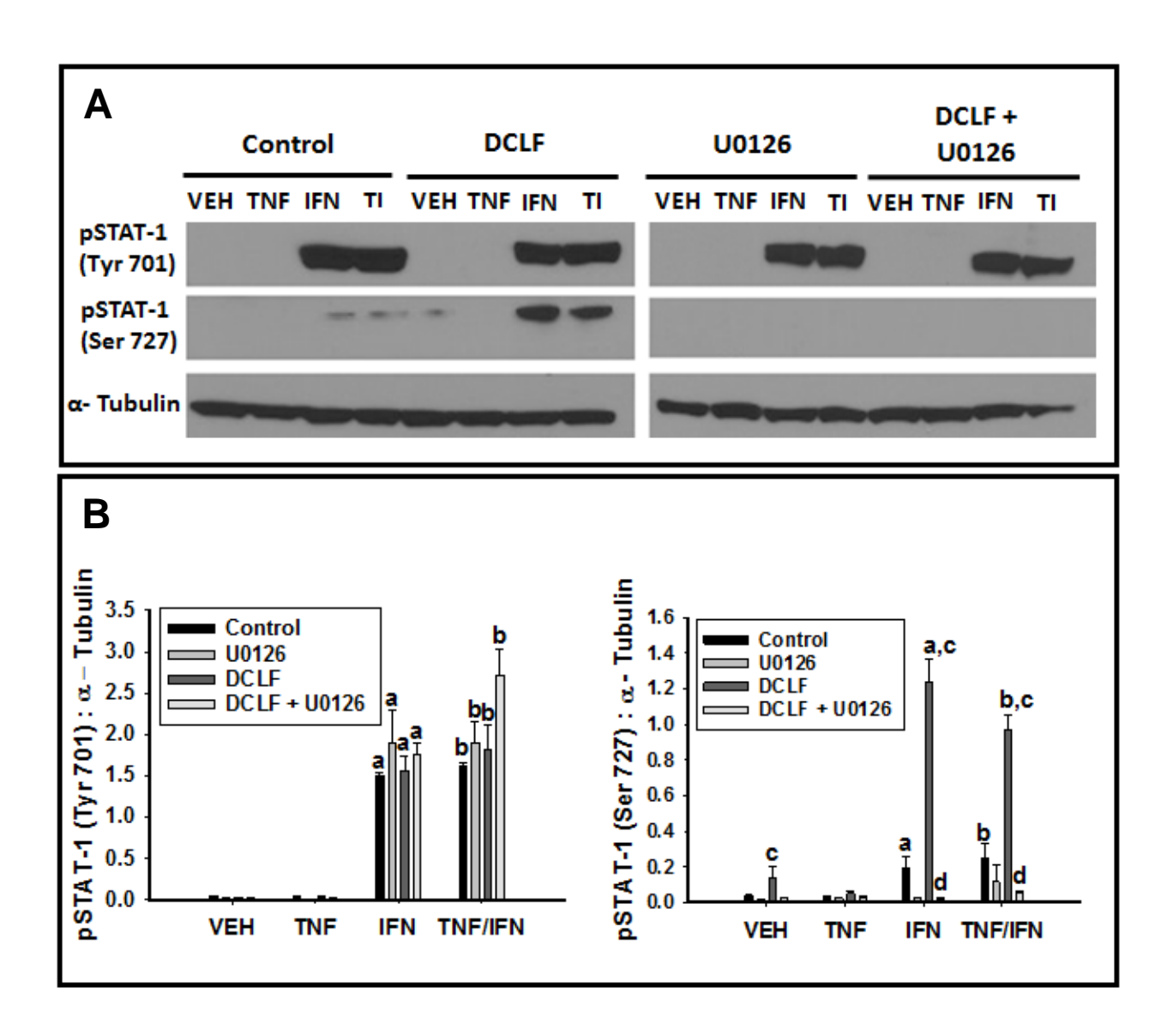
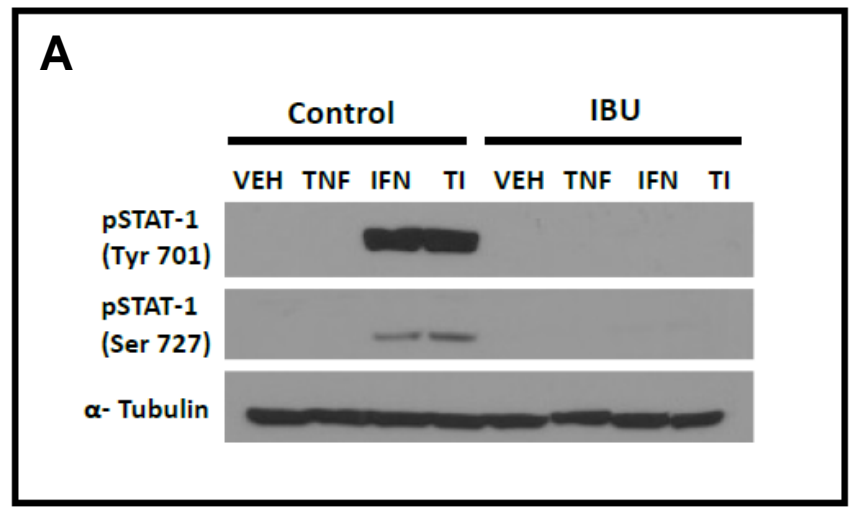


Figure 24. DCLF promotes ERK-dependent phosphorylation of STAT-1 in the presence of IFN. HepG2 cells were treated with (A) a representative AA derivative (DCLF: 250 μM) alone or in combination with TNF and/or IFN and incubated in the presence or absence of U0126. Protein extracts were collected 18 hours after treatment. pSTAT-1 (Tyrosine 701), pSTAT-1 (Serine 727) and α-tubulin protein levels were detected via western analysis. Representative blots are shown. (B) Densitometry was performed using image J software. a, significantly different from VEH. b,

Figure 24 (cont'd)

significantly different from TNF. c, significantly different from Control. d, significantly different from DCLF (without inhibitor). Data are represented as mean ± S.E.M of 3 separate experiments. Abbreviations: VEH, vehicle; TNF, tumor necrosis factor-alpha, IFN, interferon-gamma; TI, tumor necrosis factor-alpha and interferon-gamma; DCLF, diclofenac; Tyr, tyrosine; Ser, serine.



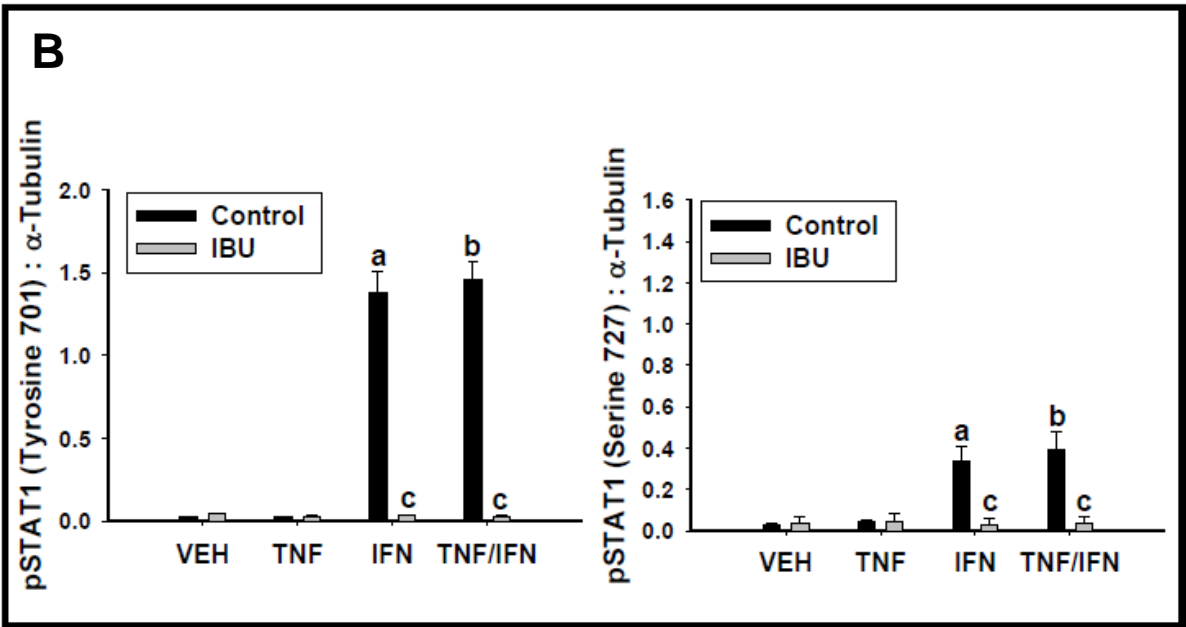


Figure 25. IBU treatment prevents IFN-mediated phosphorylation of STAT-1.

HepG2 cells were treated with (A) a representative PA derivative (IBU: 6 mM) alone or in combination with TNF and/or IFN. Protein extracts were collected 18 hours after treatment. pSTAT 1 (Tyrosine 701), pSTAT-1 (Serine 727) and α-tubulin protein levels, were detected via western analysis. Representative blots are shown. (B) Densitometry was performed using image J software. a, significantly different from VEH. b, significantly different from TNF. c, significantly different from Control. Data are

Figure 25 (cont'd)

represented as mean \pm S.E.M of 3 separate experiments. Abbreviations: VEH, vehicle; TNF, tumor necrosis factor-alpha, IFN, interferon-gamma; TI, tumor necrosis factor-alpha and interferon-gamma; IBU, ibuprofen; Tyr, tyrosine; Ser, serine.

3.5 Discussion

In this study, we showed that NSAIDs associated with IDILI synergize with TNF to kill HepG2 cells in vitro and that treatment with an additional cytokine, IFN, enhanced the NSAID/TNF-induced cytotoxic interaction. These results are consistent with what has been reported previously in studies involving animal models of drug/inflammatory stress-induced liver injury (Dugan, et al., 2011, Shaw, et al., 2009a, Shaw, et al., 2009b, Zou, et al., 2009). The IFN-mediated enhancement of NSAID/TNF-induced cytotoxicity was observed with the AA derivatives (DCLF, BRM and SLD sulfide) but not with the PA derivatives (IBU or NAP), suggesting that this is a phenomenon related to chemical structure.

To gain insight into the mechanism underlying NSAID/cytokine-induced cytotoxic synergy, the roles of caspases and MAPKs were examined. Caspase enzymes are crucial to the initiation of apoptosis (Porter, et al., 1999), and results of previous studies suggested a role for caspases in drug/cytokine-induced cytotoxic synergy (Beggs, et al., 2014, Fredriksson, et al., 2011, Zou, et al. 2009). Treatment with a representative AA derivative or PA derivative resulted in activation of caspase 3, which was increased further in the presence of TNF (Figure 15). Treatment with IFN enhanced caspase 3 activation in the presence of DCLF/TNF but not IBU/TNF (Figure 15), consistent with its effect on cytotoxicity (Figure 13). Treatment with the caspase inhibitor Z-VAD-FMK eliminated the NSAID/TNF-mediated cytotoxic interaction and also eliminated the IFN-mediated enhancement of NSAID/TNF cytotoxicity (Figure 16). These results suggest that caspase-mediated apoptosis is the mode of cell death in NSAID/cytokine cytotoxic synergy.

Prolonged activation of JNK is associated with signaling through pathways leading to cell death (Wullaert, et al., 2007), and JNK activation contributes to cytotoxicity mediated by TNF in combination with trovafloxacin, another IDILI-associated drug, and, as mentioned previously, also by DCLF/TNF (Beggs, et al., 2014, Fredriksson, et al., 2011). In the present study, DCLF and IBU caused similar patterns of JNK activation (Figure 18). That is, both drugs caused persistent JNK activation that was enhanced in the presence of TNF but unaffected by IFN exposure. A JNK inhibitor eliminated activation of JNK and completely prevented the cytotoxic synergy caused by DCLF/TNF in the absence and presence of IFN (Figure 19). This is consistent with IFN interacting somehow with the cell death pathway initiated by TNF. Inhibition of JNK similarly prevented cytotoxicity from other AA derivative NSAID/cytokine combinations (Figure 19A).

In contrast to the AA derivatives, JNK inhibition did not affect cytotoxicity mediated by PA derivative/cytokine combinations (Figure 19B). At first glance, these results suggest that JNK plays a role in cytotoxic synergy mediated by AA derivatives but not PA derivatives. However, treatment with the JNK inhibitor did not eliminate phosphorylation of JNK induced by IBU treatment, which might explain the lack of effect on cytotoxicity (Figure 19). Moreover, since SP600125 acts as a reversible, ATP-competitive inhibitor (Bennett, et al., 2001), it is possible that IBU physically interacts with SP600125 or with JNK, thereby preventing SP600125 from completely inhibiting ATP binding to JNK. Treatments with larger concentrations of SP600125 were attempted but were unsuccessful due to solubility limitations at concentrations greater than 30 µM.

ERK phosphorylation is typically associated with activating cell survival signaling pathways; however, it has become clear that under some conditions, ERK activates cell death pathways (Cagnol, et al., 2009). The duration of ERK activation can be an important factor in determining cellular fate. It has been suggested that prolonged ERK signaling can lead to cell death (Cagnol, et al. 2009). The involvement of ERK in the cytotoxic synergy mediated by IDILI-associated drugs in combination with cytokines has not been reported previously. The representative AA and PA derivatives induced very similar patterns of ERK activation (Figure 20), and these were not affected by cytokine treatment. U0126 treatment effectively inhibited both DCLF- and IBU-mediated ERK activation (Figure 21C) but had opposite effects on the synergistic cytotoxicity caused by AA and PA derivatives. U0126 eliminated the IFN-mediated enhancement of AA derivative/TNF-induced cytotoxicity (Figure 21A), suggesting that the cytotoxic effect of IFN required ERK activity. In contrast, U0126 treatment potentiated cytotoxicity mediated by the PA derivative/cytokine combinations (Figure 21B). These results suggest that ERK signaling plays a protective role in this case. Together, the findings indicate that persistent ERK activation can promote either cell survival or cell death, depending on the particular NSAID involved in its activation.

The involvement of p38 in drug/cytokine-induced cytotoxic synergy has not been reported. TNF transiently activates p38 in a variety of cell types (Anderson, 1997), as was seen here in HepG2 cells (Figure 22). DCLF also caused a transient activation of p38 that was modestly affected by the addition of cytokines (Figure 22A). In contrast, IBU caused activation of p38 that was longer lived but unaffected by cytokine treatment (Figure 22B). The observation that inhibition of p38 enhanced the NSAID/cytokine-

induced cytotoxic interaction (Figure 23) suggests that p38 dampens this toxic response. Activation of p38 is commonly associated with activation of cell death pathways (Anderson, 1997); however, it can promote cell survival under certain conditions. For example, transient activation of p38 by TNF is essential to mediating signals that protect cells from apoptosis (Roulston, et al. 1998).

As mentioned above, AA derivatives and PA derivatives responded differently in terms of their interaction with cytokines to kill cells. Although both subclasses interacted with TNF to cause cytotoxicity, IFN enhanced the synergy from TNF and AA derivatives but not PA derivatives. This observation raises the questions of how AA derivatives sensitize cells to the harmful effects of IFN and why are cells treated with PA derivatives not sensitive to IFN. To answer these questions, we evaluated the phosphorylation status of STAT-1, a critical component of the IFN signaling pathway. The IFN receptor is a heterodimer associated intracellularly with JAK. When bound to IFN, the receptor becomes activated, leading to activation of JAK which phosphorylates STAT-1 at Tyr 701. Upon phosphorylation, STAT-1 dimerizes and translocates to the nucleus, where it binds to specific DNA sequences (Farrar and Schreiber, 1993). Phosphorylation at Ser 727 is required for maximal STAT-1 activation (Varinou, et al., 2003). The kinases responsible for phosphorylation at Ser 727 include MAPKs, specifically ERK (Li, et al., 2010). IFN caused pronounced phosphorylation of STAT-1 at Tyr 701 but had only a modest effect at Ser 727 (Figure 24 and Figure 25). Conversely, DCLF was without effect on Tyr 701 phosphorylation but in the presence of IFN caused a pronounced increase in phosphorylation at Ser 727 which depended on ERK (Figure 24). These findings might explain why inhibition of ERK prevented the IFN-mediated enhancement

of DCLF/TNF-induced cytotoxicity. Interestingly, phosphorylation of STAT-1 at Tyr 701 in response to IFN treatment was necessary for robust DCLF-induced phosphorylation of Ser 727. Consistent with this observation, in several cell types phosphorylation at Tyr 701 by JAK was required for Ser 727 phosphorylation (Sadzak, et al., 2008).

In stark contrast to DCLF, treatment with IBU prevented IFN-mediated phosphorylation of STAT-1 at both Tyr 701 and Ser 727 (Figure 25). These results are consistent with the observation that IFN failed to enhance cytotoxicity mediated by PA derivatives in combination with TNF. Given that phosphorylation of Ser 727 was dependent on ERK, it is puzzling that both DCLF and IBU treatment induced the same pattern of ERK activation, yet only DCLF led to phosphorylation of Ser 727. Our findings suggest that treatment with DCLF and IFN unmasks a substrate for ERK at Ser 727 of STAT-1, which is not available in cells treated with IBU. Additionally, the observation that inhibition of ERK increased cytotoxicity from PA derivatives/TNF treatment suggests that ERK activated by IBU treatment interacts with a cytoprotective substrate rather than one that leads to enhanced cytotoxicity.

In summary, NSAIDs associated with IDILI synergize with TNF to cause death of HepG2 cells. IFN treatment enhances the cytotoxicity mediated by some NSAIDs in the presence of TNF. Aspirin, an NSAID that is not associated with IDILI, did not synergize with any combination of cytokines to kill cells. These findings raise the possibility that drug/cytokine cytotoxic synergy contributes to human IDILI from NSAIDs.

With regard to mechanism, NSAID/cytokine-induced cytotoxicity requires caspases, suggesting an apoptotic mode of cell death. Persistent JNK activation plays an important role in the cytotoxic synergy. Prolonged ERK activation plays either a

cytotoxic or a protective role, depending on NSAID chemical structure, whereas p38 is cytoprotective. Cosgrove, et al., (2010) evaluated the signaling pathways involved in drug/cytokine-induced cytotoxic synergy in primary human hepatocytes. They found that various drugs associated with IDILI (including NSAIDs) synergized with cytokines to cause MAPK signaling dysregulation and consequently death of primary human hepatocytes, which lends support to our findings concerning involvement of MAPKs in NSAID/cytokine-induced cytotoxic synergy in HepG2 cells. NSAIDs from different structural classes differentially modify the phosphorylation status of STAT-1, and this appears to explain why IFN potentiates the cytotoxic interaction with TNF for some NSAIDs but not others.

These findings suggest that cytotoxic synergy of drugs with cytokines occurs through different kinase signaling mechanisms, even for drugs within the same pharmacologic class, and that these differences are related to chemical structure and IDILI liability. Knowledge generated from this study could be useful in developing an in vitro approach to classify drugs according to their potential to cause IDILI in humans.

CHAPTER 4:

Calcium Contributes to the Cytotoxic Interaction Between Diclofenac and Cytokines. Maiuri, A.R., Breier A.B., Turkus, J.D., Breier, Ganey, P.E., Roth, R.A.

4.1 Abstract

Diclofenac (DCLF) is a widely used NSAID that is associated with idiosyncratic drug-induced liver injury (IDILI) in humans. The mechanism of DCLF-induced liver injury is unknown; however, patients with certain inflammatory diseases have an increased risk of developing IDILI, which raises the possibility that immune mediators play a role in the pathogenesis. DCLF synergizes with the cytokines tumor necrosis factor alpha (TNF) and interferon gamma (IFN) to cause hepatocellular apoptosis in vitro. DCLF activates the endoplasmic reticulum (ER) stress response pathway and the mitogen activated protein kinases (MAPKs), c-Jun N-terminal kinase (JNK) and extracellular signal regulated kinase (ERK), and these pathways are critical to the cytotoxic synergy mediated by DCLF/cytokine cotreatment. DCLF also caused intracellular calcium (Ca⁺⁺) dysregulation in hepatocytes, but the role of this effect in cytotoxic synergy between DCLF and cytokines is unknown. We tested the hypothesis that Ca⁺⁺ contributes to DCLF/cytokine-induced cytotoxic synergy. Treatment of HepG2 cells with the intracellular Ca⁺⁺ chelator BAPTA/AM reduced cytotoxicity and caspase 3 activation caused by DCLF/cytokine cotreatment. BAPTA/AM treatment also significantly reduced DCLF-induced activation of the ER stress sensor protein kinase, RNA-like endoplasmic reticulum kinase (PERK), as well as activation of JNK and ERK. Treatment of cells with an inositol trisphosphate (IP3) receptor antagonist almost completely eliminated DCLF/cytokine-induced cytotoxic synergy and decreased DCLF-induced activation of PERK, JNK and ERK. These findings indicate that Ca⁺⁺ contributes to DCLF/cytokineinduced cytotoxic synergy by promoting activation of the UPR pathway and JNK and ERK.

4.2 Introduction

Drug-induced liver injury (DILI) is the leading cause of acute liver failure in the United States and the most common adverse event associated with failure to obtain U.S. Food and Drug Administration approval for new drugs (Aithal et al. 2011). Most DILI reactions are dose-dependent and predictable using routine animal testing; however, a subset of DILI reactions is idiosyncratic. Idiosyncratic DILI (IDILI) reactions are often rare but sometimes severe and are the most common cause of post-marketing warnings and withdrawal of drugs from the pharmaceutical market. IDILI is a poorly understood phenomenon, but susceptibility to these reactions is likely due to actions of the drug in the context of environmental and genetic factors within patients (Boelsterli 2002).

Along with antibiotics, nonsteroidal anti-inflammatory drugs (NSAIDs) are the most frequent causes of IDILI (Unzueta and Vargas 2013). The frequency and severity of IDILI among drugs differ within this pharmacologic class (Teoh and Farrell 2003), and patients with certain underlying diseases are susceptible to IDILI induced by some NSAIDs but not others (García Rodríguez et al. 1994). These observations further suggest the possibility that both patient-specific susceptibility factors and drug-specific factors are important determinants of susceptibility.

Diclofenac (DCLF) is one of the most widely used NSAIDs worldwide although its use has been restricted in the United States due to association with IDILI. The mechanisms of DCLF-induced hepatotoxicity are unknown, but immune mediators might play a role. A retrospective cohort study found that rheumatoid arthritis was a risk factor for NSAID-induced idiosyncratic hepatotoxicity (García Rodríguez et al. 1994). Additionally, osteoarthritis was found to be a risk factor for IDILI induced by DCLF in

particular (Banks et al. 1995). These observations suggest a role for inflammation in IDILI caused by NSAIDs, particularly DCLF.

Studies in rodents also revealed a role for immune mediators in DILI caused by various drugs, including DCLF (Deng et al. 2006, Deng et al. 2008, Dugan et al., 2011, Shaw et al., 2009a, Shaw et al., 2009b, Zou et al., 2009). When rodents were administered a nonhepatotoxic dose of the inflammagen lipopolysaccharide (LPS) in combination with a nonhepatotoxic dose of DCLF, they developed pronounced hepatocellular injury (Deng et al. 2006). Similar animal models employing other IDILIassociated drugs revealed a critical role for the proinflammatory cytokines tumor necrosis factor-alpha (TNF) and interferon-gamma (IFN) in the pathogenesis of liver injury (Dugan et al., 2011, Shaw et al., 2009a, Shaw et al., 2009b, Zou et al., 2009, Hassan et al. 2007). These cytokines are well known to activate pathways leading to cell death. Gene expression analysis of the livers from rodents treated with DCLF revealed increased expression of various genes involved in both the TNF and IFN signaling pathways, including TNF receptor superfamily member 1a (TNFRSF1a), signal transducer and activator of transcription-1 (STAT1) and the tumor suppressor protein p53 (Deng et al. 2008). The protein products of these genes are known to promote apoptosis (Shen and Pervaiz 2006, Hussain and Harris 2006, Gorina et al. 2005). These findings in animals suggest that DCLF can synergize with immune mediators to cause death of hepatocytes and might explain why humans with certain underlying inflammatory diseases are more susceptible to toxicity from DCLF.

In vitro, DCLF synergized with inflammatory cytokines including TNF and IFN to kill human primary hepatocytes (Cosgrove et al. 2009). Similarly, DCLF synergized with

TNF to cause death of HepG2 cells, and this depended on caspase activation and activation of the mitogen activated protein kinase (MAPK), c-Jun N-terminal kinase (JNK) (Fredriksson et al. 2011). Additionally, IFN treatment enhanced cytotoxicity mediated by DCLF/TNF treatment, and this required activation of caspases, JNK and extracellular signal-regulated kinase (ERK) (Maiuri et al. 2015). Fredriksson et al. (2014) demonstrated that DCLF treatment caused activation of the endoplasmic reticular (ER) stress sensors, inositol requiring enzyme-1 (IRE1) and protein kinase RNA-like endoplasmic reticulum kinase (PERK), and this was followed by upregulation of the proapoptotic transcription factor CCAAT/-enhancer-binding protein homologous protein (CHOP). Silencing of the ER stress mediators PERK and CHOP using siRNA reduced apoptosis induced by DCLF/TNF treatment (Fredriksson et al. 2014). These studies in vitro provided mechanistic insight into the pathways activated in response to DCLF that promote a cytotoxic interaction with TNF. However, how DCLF/cytokine treatment promotes the activation of these stress response pathways and how the pathways interact with each other in causing cell death remain unknown.

It is been reported that DCLF treatment induces intracellular calcium (Ca⁺⁺) dysregulation in rat (500 µM DCLF) and human hepatocytes (1mM DCLF), and this contributes to cytotoxicity induced by DCLF in these cell types (Bort et al. 1999, Lim et al. 2006). Intracellular Ca⁺⁺ dysregulation is known to contribute to the activation of MAPKs and also activation of the unfolded protein response (UPR) (Kim et al. 2004, Bollo et al. 2010). In this study we tested the hypothesis that Ca⁺⁺ contributes to DCLF/cytokine-induced cytotoxic synergy by promoting ER stress and also activation of

JNK, ERK, STAT1 and caspase 3. Additionally, we explored the interdependence of DCLF-induced JNK, ERK and STAT1 activation.

4.3 Materials and Methods

4.3.1 Materials

All drugs were purchased from Sigma-Aldrich (St. Louis, MO) unless otherwise noted. Recombinant human TNF and IFN were purchased from Millipore (Billerica, MA). Phosphate-buffered saline (PBS), Dulbecco's Modified Eagles Medium (DMEM), Ca⁺⁺-free DMEM, fetal bovine serum (FBS), Antibiotic-Antimycotic (ABAM) and 0.25% Trypsin-EDTA were purchased from Life Technologies (Carlsbad, CA). The phosphorylated PERK antibody was purchased from Santa Cruz Biotechnology (Dallas, TX). All other antibodies were purchased from Cell Signaling Technology (Beverly, MA).

4.3.2 Cell Culture

Human hepatoma HepG2 cells (American Type Culture Collection, Manassas, VA) were chosen because they respond similarly to primary human hepatocytes with regard to the cytotoxic interaction between DCLF and cytokines (Cosgrove *et al.*, 2009). Although HepG2 cells have low expression of phase 1 drug metabolizing enzymes compared to primary human hepatocytes, they express phase II enzymes (Westerink and Schoonen, 2007a, Westerink and Schoonen, 2007b). Importantly, HepG2 cells metabolize DCLF into both acylglucuronide and hydroxymetabolites (Fredriksson et al. 2011), which are the metabolites that have been suggested to mediate DCLF-induced hepatotoxicity (Boelsterli, 2003). Cells were grown in 25-cm² tissue culture treated flasks, maintained in DMEM supplemented with 10% FBS and 1% ABAM (complete DMEM) and cultured at 37°C in 95% air and 5% CO₂ in a humidified incubator. They were passaged when they reached approximately 80% confluence.

4.3.3 Experimental design and cytotoxicity assessment

HepG2 cells were plated at a density of 4 X 10⁴ cells per well in black-walled, 96well, tissue culture plates and allowed to attach overnight before treatment with compounds. DCLF was reconstituted in sterile water. Cells were treated with 250 µM DCLF or its vehicle, and simultaneously with TNF (10 ng/ml) and/or IFN (10 ng/ml) or their vehicle (PBS). Treatment of cells with 250 µM DCLF in combination with TNF (10 ng/ml) was shown to cause a robust cytotoxic response in HepG2 cells that was enhanced by IFN (10 ng/ml), whereas treatment of cells with each component individually did not result in death of HepG2 cells (Maiuri et al. 2015). Cells treated with DCLF/cytokine combinations were also incubated in the presence or absence of the intracellular Ca⁺⁺ chelator acetoxymethyl-1,2-bis(2-aminophenoxy)ethane-N,N,N',N'tetraacetic acid (BAPTA/AM, 10 µM, 4 h pretreatment) or the IP3 receptor antagonist 2aminophenoxydiphenyl borate (2-APB, 100 µM, addition simultaneous with DCLF/cytokines). Cells were exposed to the drug/cytokine/inhibitor combination for 24 hours, and cytotoxicity was evaluated by measuring release of lactate dehydrogenase (LDH) from the cells into culture medium using the Homogeneous Membrane Integrity Assay kit from Promega (Madison, WI). BAPTA/AM and 2-APB were reconstituted in DMSO, resulting in a final concentration of 0.1% DMSO in all experiments involving treatment with BAPTA/AM and 2-APB.

To examine the involvement of extracellular Ca⁺⁺ in the cytotoxic interaction between DCLF and cytokines, DCLF/cytokine combinations were prepared in Ca⁺⁺-free medium. At the time of drug treatment, complete DMEM was replaced with Ca⁺⁺-free medium, which was prepared using FBS-free and Ca⁺⁺-free DMEM supplemented with sodium pyruvate (1 mM) and L-glutamine (4 mM).

4.3.4 Caspase-3 activity

Caspase-3 activity was measured using the Caspase-3 Fluorometric Assay Kit purchased from R&D Systems (Minneapolis, MN). HepG2 cells were plated at 1.2 X 10⁶ cells per well in 6-well tissue culture plates. They were treated with DCLF alone or in combination with TNF and/or IFN and also in the presence or absence of BAPTA/AM or 2-APB. For all studies involving BAPTA/AM, cells were pretreated with BAPTA/AM for four hours prior to the addition of DCLF and cytokines. For all studies involving 2-APB, cells were treated with 2-APB simultaneously with DCLF and cytokines. Cells were lysed and centrifuged after 24 hours of exposure. 50 µl of lysate was added to blackwalled, 96-well plates and incubated with assay reaction buffer and fluorogenic substrate for 1 hour. The plate was then read in a fluorescence plate reader at an excitation wavelength of 400 nm and an emission wavelength of 505 nm.

4.3.5 Protein isolation

Cells (1.2 X 10⁶ per well) were plated in 6-well tissue culture plates and allowed to adhere overnight. They were exposed to 250 µM DCLF and its vehicle alone or in combination with TNF and/or IFN for 18 hours. For some experiments, cells treated with DCLF/cytokine combinations were also incubated in the presence of BAPTA/AM, 2-APB or SP600125. SP600125 was prepared in DMSO resulting in a final concentration of 0.1% DMSO in all experiments involving treatment with SP600125. Cells were rinsed with cold PBS followed by addition of 150 µl of radioimmunoprecipitation assay (RIPA) buffer containing HALT protease and phosphatase inhibitor cocktails (Thermo Scientific, Rockford, IL). Cells were scraped, collected, placed in microcentrifuge tubes and incubated on ice for 10 minutes. During the 10-minute incubation, the tubes were

vortexed intermittently. Lysates were centrifuged for 25 minutes at 20,000 X g. The supernatants containing whole cell protein extracts were collected and stored at -80°C until use. Protein concentrations were quantified using the bicinchoninic acid assay (Thermo Scientific).

4.3.6 Western analysis

For detection of phosphorylated JNK (pJNK), phosphorylated ERK (pERK), phosphorylated PERK (pPERK) and phosphorylated STAT-1 (pSTAT-1) in whole cell lysates, 20 µg protein was loaded onto precast NuPAGE 12% Bis-Tris gels (Life Technologies) and subjected to electrophoresis. Proteins were transferred onto polyvinylidene fluoride (PVDF) membranes (Millipore, Billerica, MA). Membranes were blocked for one hour with 5% bovine serum albumin (BSA) reconstituted in 1% trisbuffered saline (TBS) containing 0.1% tween-20 (TBSt). They were then probed with antibodies directed against pJNK, pERK, pPERK, pSTAT-1 (Tyrosine 701), pSTAT-1 (Serine 727), and α -tubulin. Primary antibodies were diluted in 2% BSA in TBSt. Membranes were incubated with primary antibodies overnight at 4°C, after which they were washed with TBSt followed by addition of secondary antibody. Goat anti-rabbit or goat anti-mouse horseradish peroxidase (HRP)-conjugated secondary antibody was diluted in 5% BSA in TBSt at a concentration of 1:2500 for pJNK and 1:5000 for all others. Clarity Western ECL substrate (Bio-Rad, Hercules, CA) was used to visualize HRP, and the substrate was developed on HyBlot CL film (Denville Scientific, Metuchen, NJ). All images were quantified by performing densitometry using Image J software.

4.3.7 Statistical analysis

All results are expressed as mean \pm standard error of the mean (S.E.M.). Data were subjected to log transformation as necessary to achieve equal variance and normality. Data were analyzed by either a one-way or two-way analysis of variance (ANOVA), as appropriate. For one-way and two-way ANOVAs, Tukey's post-hoc test was used for multiple, pair-wise comparisons between treatment groups. The criterion for significance was set at α =0.05.

4.4 Results

4.4.1 An intracellular Ca⁺⁺ chelator reduced cytotoxicity mediated by DCLF/cytokine cotreatment.

Pretreatment of cells with the intracellular Ca⁺⁺ chelator BAPTA/AM had no effect on LDH release from VEH/Control-treated cells but markedly reduced cytotoxicity induced by DCLF/cytokine treatment, as well as the IFN-mediated enhancement of DCLF/TNF-induced cytotoxicity (Figure 26A).

DCLF/TNF-induced cytotoxicity and the IFN-mediated enhancement of this cytotoxicity are caspase-dependent (Maiuri, et al., 2015, Fredriksson, et al., 2011).

BAPTA/AM pretreatment markedly reduced DCLF/cytokine-induced caspase-3 activation, suggesting that Ca⁺⁺ released from an intracellular source contributes to DCLF/cytokine-induced apoptosis (Figure 26B). In contrast, incubating cells in culture medium depleted of Ca⁺⁺ did not significantly alter the DCLF/cytokine-induced cytotoxic interaction, suggesting that extracellular Ca⁺⁺ is not important in the cytotoxic interaction (Figure 27).

4.4.2 An IP3 receptor antagonist reduced cytotoxicity induced by DCLF/cytokine cotreatment.

The results from the BAPTA/AM experiment suggest that Ca⁺⁺ released from an intracellular source contributes to DCLF/cytokine-induced cytotoxic synergy. The ER is widely known for its role in Ca⁺⁺ storage, and Ca⁺⁺ can be released from the ER via activation of IP3 receptors and ryanodine receptors located on the ER membrane.

Treatment of HepG2 cells with 2-APB, an IP3 receptor antagonist, almost completely eliminated DCLF/TNF-induced cytotoxicity as well as the IFN-mediated enhancement of

cytotoxicity (Figure 28A). Additionally, treatment of HepG2 cells with 2-APB markedly reduced DCLF/cytokine-induced caspase-3 activation (Figure 28B).

4.4.3 Ca⁺⁺contributes to DCLF-mediated activation of the ER stress sensor, PERK

The UPR and intracellular Ca⁺⁺ dysregulation are intricately linked phenomena. ER stress is known to promote intracellular Ca++ dysregulation, and this can in turn promote persistent activation of the UPR leading to apoptosis (Fribley, et al., 2009). We evaluated whether Ca⁺⁺ contributes to DCLF-mediated, persistent ER stress. Treatment with cytokines alone did not cause activation (phosphorylation) of PERK (Figure 29A, B). Treatment with DCLF led to phosphorylation of PERK, and addition of TNF and/or IFN did not significantly alter DCLF-mediated PERK activation. Treatment with either BAPTA/AM (Figure 29A) or 2-APB (Figure 29B) significantly decreased the activation of PERK at 18 hours.

4.4.4 Ca⁺⁺ contributes to DCLF-mediated JNK activation

DCLF/TNF-mediated cytotoxicity and the IFN-mediated enhancement of that cytotoxicity are JNK-dependent processes (Maiuri, et al., 2015, Fredriksson, et al., 2011). DCLF caused activation of JNK, consistent with previous findings, and this effect was unaltered by cytokine treatment (Figure 30A, B). DCLF/cytokine-mediated JNK activation was reduced by pretreatment with BAPTA/AM (Figure 30A) and almost completely eliminated by treatment with 2-APB (Figure 30B).

4.4.5 Ca⁺⁺contributes to DCLF-mediated ERK activation

The IFN-mediated enhancement of DCLF/TNF-induced cytotoxicity depends on ERK (Maiuri, et al., 2015). DCLF treatment promoted strong activation of ERK that was

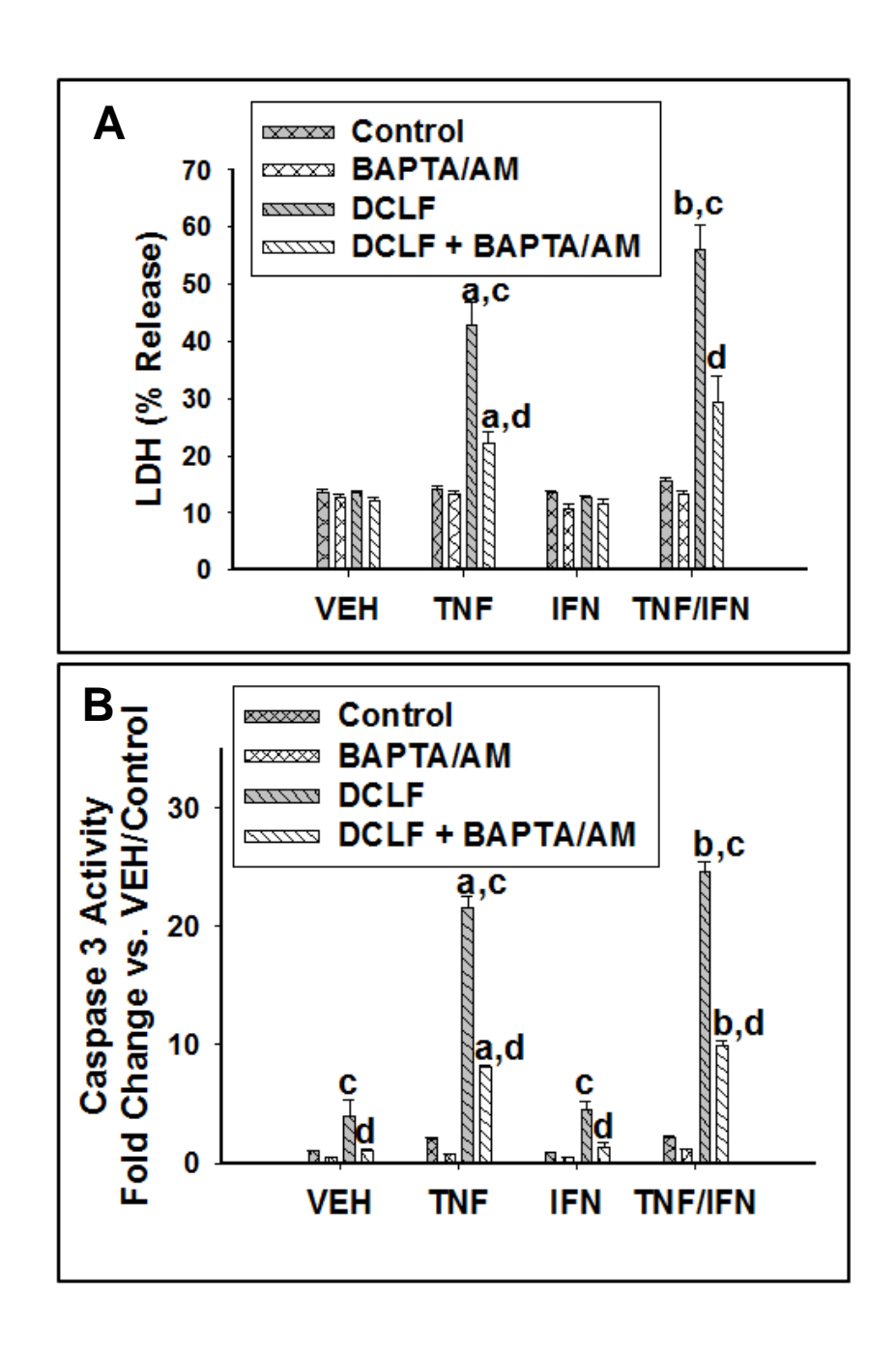


Figure 26. Treatment with BAPTA/AM, a membrane-permeable Ca2+ chelator, reduced cytotoxicity mediated by DCLF/cytokine cotreatment. HepG2 cells were pretreated with VEH (0.1% DMSO) or BAPTA/AM (10 μ M) for four hours. After the four hour pretreatment, cells were treated with DCLF (250 μ M) alone or in combination with

Figure 26 (cont'd)

TNF and/or IFN, and (A) cytotoxicity or (B) caspase-3 activity was measured 24 hours later. a, significantly different from corresponding bar within VEH. b, significantly different from corresponding bar within TNF. c, significantly different from Control within a cytokine group. d, significantly different from DCLF without BAPTA/AM within a cytokine group. Data are represented as mean ± S.E.M of at least n=3. Abbreviations: VEH, vehicle; TNF, tumor necrosis factor-alpha; IFN, interferon-gamma; LDH, lactate dehydrogenase; DCLF, diclofenac; BAPTA/AM, acetoxymethyl-1,2-bis(2-aminophenoxy)ethane-N,N,N',N'-tetraacetic acid; APB, aminophenoxydiphenyl borate.

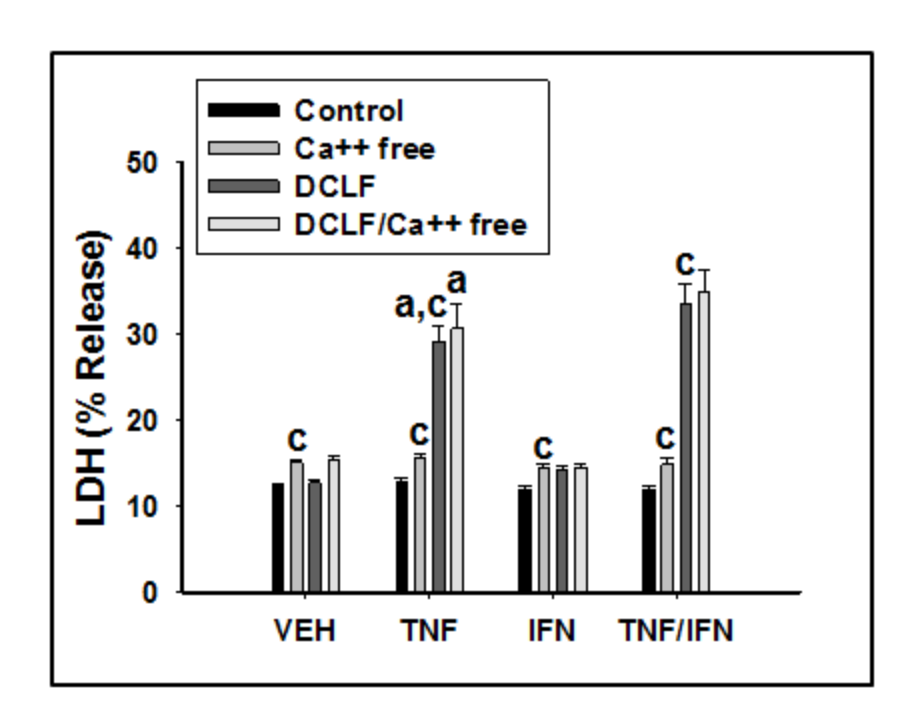


Figure 27. Elimination of Ca++ in culture medium did not affect the cytotoxic interaction between DCLF and cytokines. HepG2 cells were treated with VEH (sterile water) or DCLF (250 μM) alone or simultaneously with TNF (10 ng/ml) and/or IFN (10 ng/ml). Cells were plated in complete DMEM and then treated with DCLF/cytokine combinations using Ca⁺⁺-free medium. The Ca⁺⁺-free medium was prepared using FBS-free and Ca⁺⁺-free DMEM supplemented with sodium pyruvate (1 mM) and L-glutamine (4 mM). Percent LDH release was measured 24 hours after treatment. Data are represented as mean ± S.E.M of at least n=4. a, significantly different from corresponding bar within VEH. b, significantly different from corresponding bar within TNF. c, significantly different from Control within a cytokine group. d, significantly from DCLF. Abbreviations: LDH, lactate dehydrogenase; DCLF, diclofenac; Ca, calcium; VEH, vehicle; TNF, tumor necrosis factor-alpha; IFN, interferon gamma.

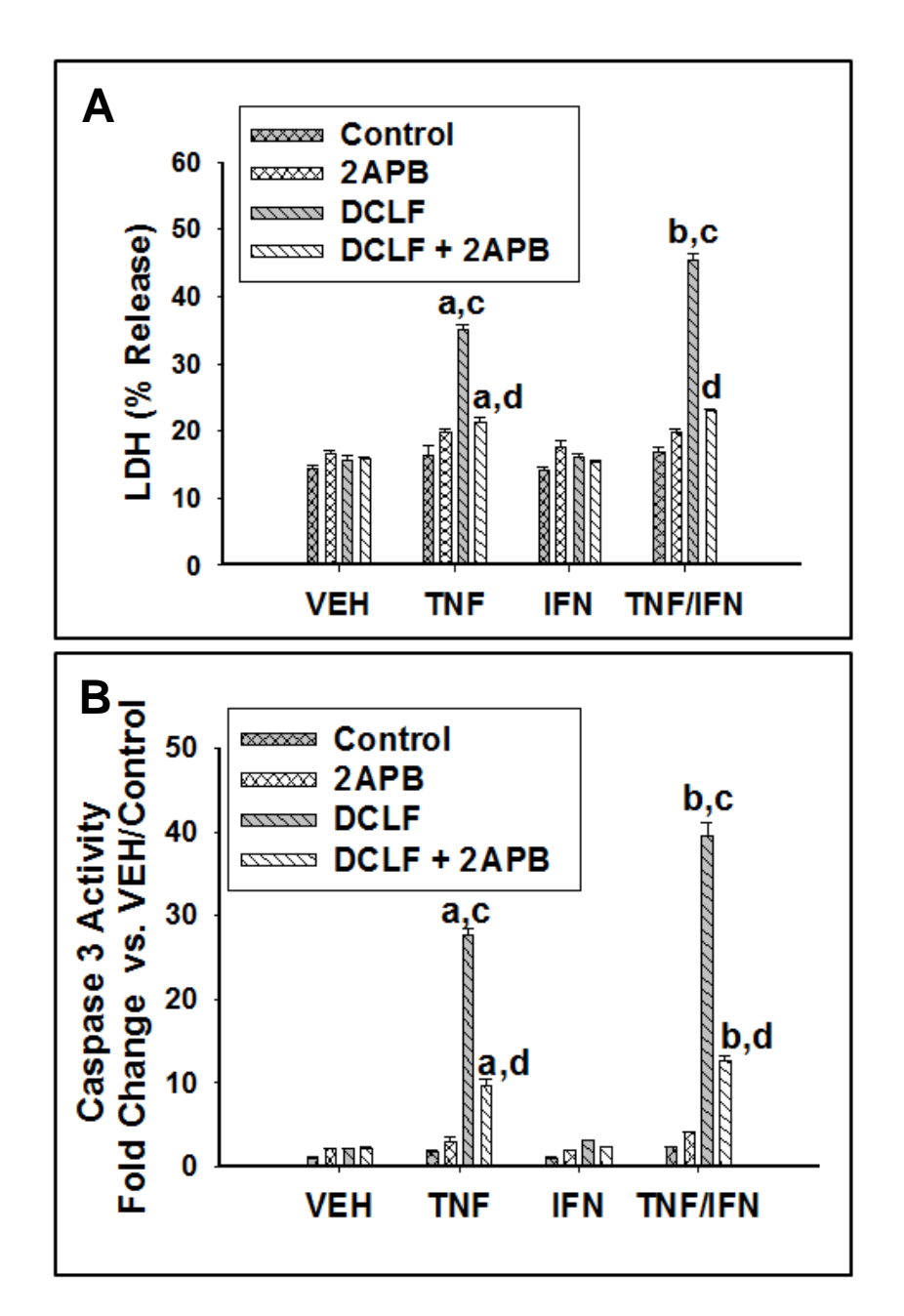


Figure 28. Treatment with 2-APB, an IP3 receptor antagonist, almost completely eliminated cytotoxicity induced by DCLF/cytokine cotreatment. HepG2 cells were treated with VEH (0.1% DMSO) or 2-APB (100 μM) and treated simultaneously with DCLF (250 μM) alone or in combination with TNF and/or IFN. (A) Cytotoxicity or (B) caspase-3 activity was measured 24 hours later. a, significantly different from VEH.

Figure 28 (cont'd)

b, significantly different from corresponding bar within TNF treatment group. c, significantly different from Control within a cytokine group. d, significantly different from DCLF without 2-APB within a cytokine group. Data are represented as mean ± S.E.M of at least n=3. Abbreviations: VEH, vehicle; TNF, tumor necrosis factor-alpha; IFN, interferon-gamma; LDH, lactate dehydrogenase; DCLF, diclofenac; BAPTA/AM, acetoxymethyl-1,2-bis(2-aminophenoxy)ethane-N,N,N',N'-tetraacetic acid; APB, aminophenoxydiphenyl borate.

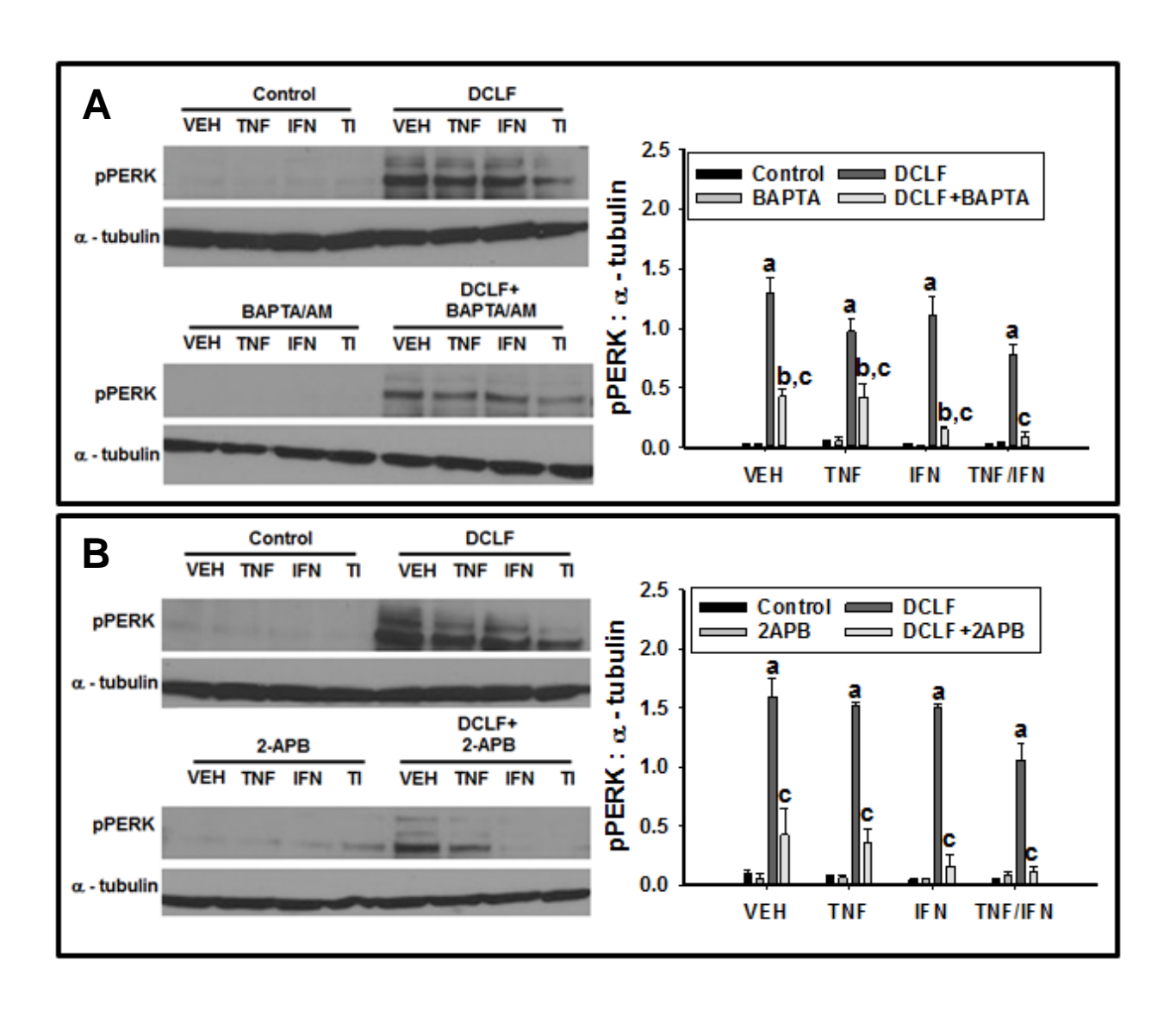


Figure 29. Ca⁺⁺contributes to DCLF-mediated activation of the ER stress sensor, PERK. HepG2 cells were treated with VEH (0.1% DMSO), (A) BAPTA/AM (10 μM, 4h before addition of DCLF/cytokines) or (B) 2-APB (100 μM, simultaneously addition with DCLF/cytokines) and treated with Control (sterile water) or DCLF (250 μM) alone or in combination with TNF (10 ng/ml) and/or IFN (10 ng/ml). Proteins were collected 18 hours after drug treatment. pPERK and α-tubulin levels were detected via western analysis. a, significantly different from Control group within a cytokine treatment. b,

Figure 29 (cont'd)

significantly different from BAPTA/AM (A) or 2-APB (B) within a cytokine treatment group. c, significantly different from DCLF within a cytokine treatment. Data are represented as mean ± S.E.M of n=3. Abbreviations: VEH, vehicle; DCLF, diclofenac; pPERK, phosphorylated protein kinase RNA-like endoplasmic reticulum kinase; BAPTA/AM, acetoxymethyl-1,2-bis(2-aminophenoxy)ethane-N,N,N',N'-tetraacetic acid; APB, aminophenoxydiphenyl borate.

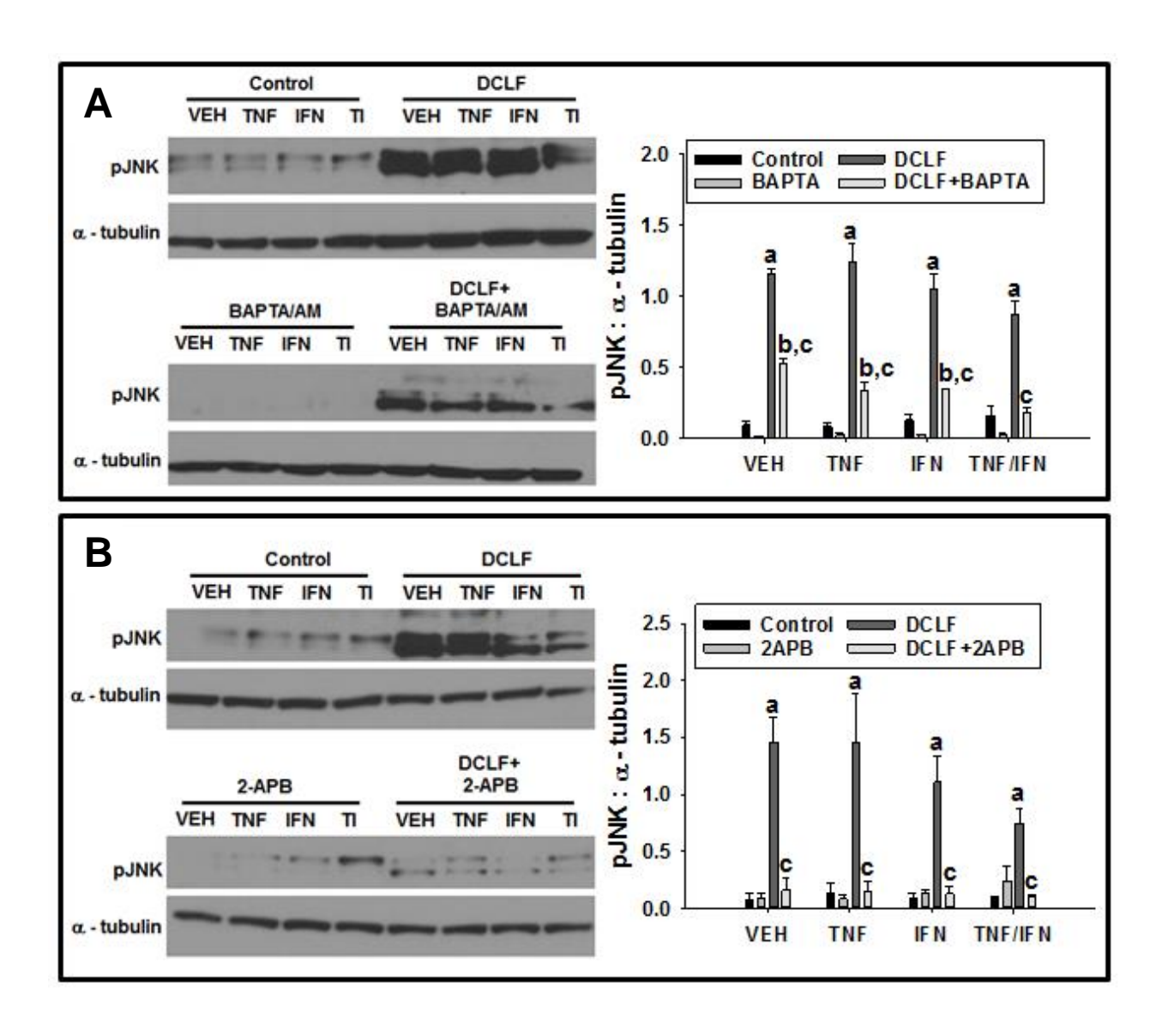


Figure 30. Ca⁺⁺contributes to DCLF-mediated JNK activation. HepG2 cells were treated with VEH (0.1% DMSO), (A) BAPTA/AM (10 μM, 4h before addition of DCLF/cytokines) or (B) 2-APB (100 μM, simultaneous addition with DCLF/cytokines) and treated with Control (sterile water) or DCLF (250 μM) alone or in combination with TNF (10 ng/ml) and/or IFN (10 ng/ml). Proteins were collected 18 hours after drug treatment. pJNK and α-tubulin levels were detected via western analysis. a, significantly different from Control group within a cytokine treatment.

Figure 30 (cont'd)

b, significantly different from BAPTA/AM (A) or 2-APB (B) within a cytokine treatment group. c, significantly different from DCLF within a cytokine treatment. Data are represented as mean ± S.E.M of n=3. Abbreviations: VEH, vehicle; DCLF, diclofenac; pJNK, phosphorylated c-Jun N-terminal kinase; BAPTA/AM, acetoxymethyl-1,2-bis(2-aminophenoxy)ethane-N,N,N',N'-tetraacetic acid; APB, aminophenoxydiphenyl borate.

unaffected by cytokine treatment (Figure 31), confirming our earlier observation.

Pretreatment of cells with BAPTA/AM significantly reduced ERK activation induced by DCLF (Figure 31A). Similarly, treatment of HepG2 cells with 2-APB markedly reduced DCLF-mediated activation of ERK (Figure 31B).

4.4.6 Ca⁺⁺ contributes to DCLF/IFN-mediated phosphorylation of STAT1 at Ser

Janus kinase (JAK)-mediated phosphorylation of STAT1 at Tyr 701 and ERK-mediated phosphorylation of STAT1 at Ser 727 are required for maximal activation of STAT1 and STAT1-mediated apoptosis (Varinou, et al., 2003). We demonstrated previously that DCLF-mediated ERK activation promotes phosphorylation of STAT1 at Ser 727 in the presence of IFN and that the IFN-mediated enhancement of DCLF/TNF-induced cytotoxicity is driven by ERK (Maiuri, et al., 2015). Since Ca⁺⁺ contributed to DCLF-mediated ERK activation, we evaluated whether Ca⁺⁺ also contributes to DCLF/IFN-induced phosphorylation of STAT1 at Ser 727. As reported previously, treatment with IFN led to phosphorylation of Tyr 701 of STAT1 in the absence and presence of DCLF, but Ser 727 of STAT1 was only phosphorylated in the presence of both IFN and DCLF (Figure 32). Interestingly, treatment of HepG2 cells with either BAPTA/AM or 2-APB significantly reduced DCLF/IFN-mediated phosphorylation of STAT1 at Ser 727 without affecting phosphorylation of STAT1 at Tyr 701 (Figure 32).

4.4.7 JNK promotes DCLF/IFN-mediated phosphorylation of STAT1 at Ser 727 via activation of ERK

Activation of JNK and ERK both contributed to the IFN-mediated enhancement of DCLF/TNF-induced cytotoxicity (Maiuri, et al., 2015). ERK contributed to the

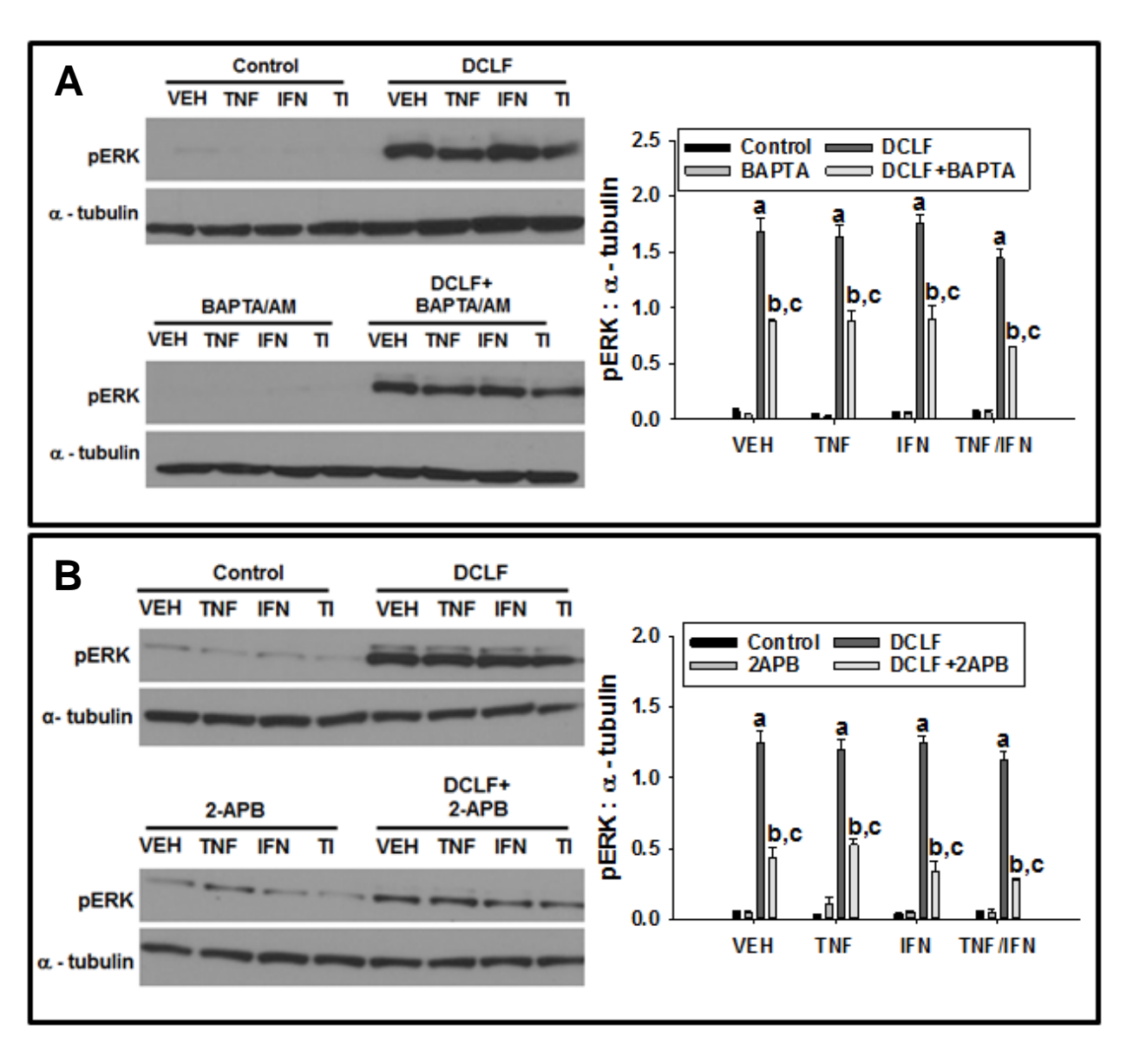


Figure 31. Ca⁺⁺contributes to DCLF-mediated ERK activation.

HepG2 cells were treated with VEH (0.1% DMSO), (A) BAPTA/AM (10 μ M, 4h before addition of DCLF/cytokines) or (B) 2-APB (100 μ M, simultaneous addition with DCLF/cytokines) and treated with Control (sterile water) or DCLF (250 μ M) alone or in combination with TNF (10 ng/ml) and/or IFN (10 ng/ml). Proteins were collected 18 hours after drug treatment. pERK and α -tubulin were detected via western analysis. a, significantly different from Control group within a cytokine treatment. b,

Figure 31 (cont'd)

significantly different from BAPTA/AM (A) or 2-APB (B) within a cytokine treatment group. c, significantly different from DCLF within a cytokine treatment. Data are represented as mean ± S.E.M of n=3. Abbreviations: VEH, vehicle; DCLF, diclofenac; pERK, phosphorylated extracellular signal-regulated kinase; BAPTA/AM, acetoxymethyl-1,2-bis(2-aminophenoxy)ethane-N,N,N',N'-tetraacetic acid; APB, aminophenoxydiphenyl borate.

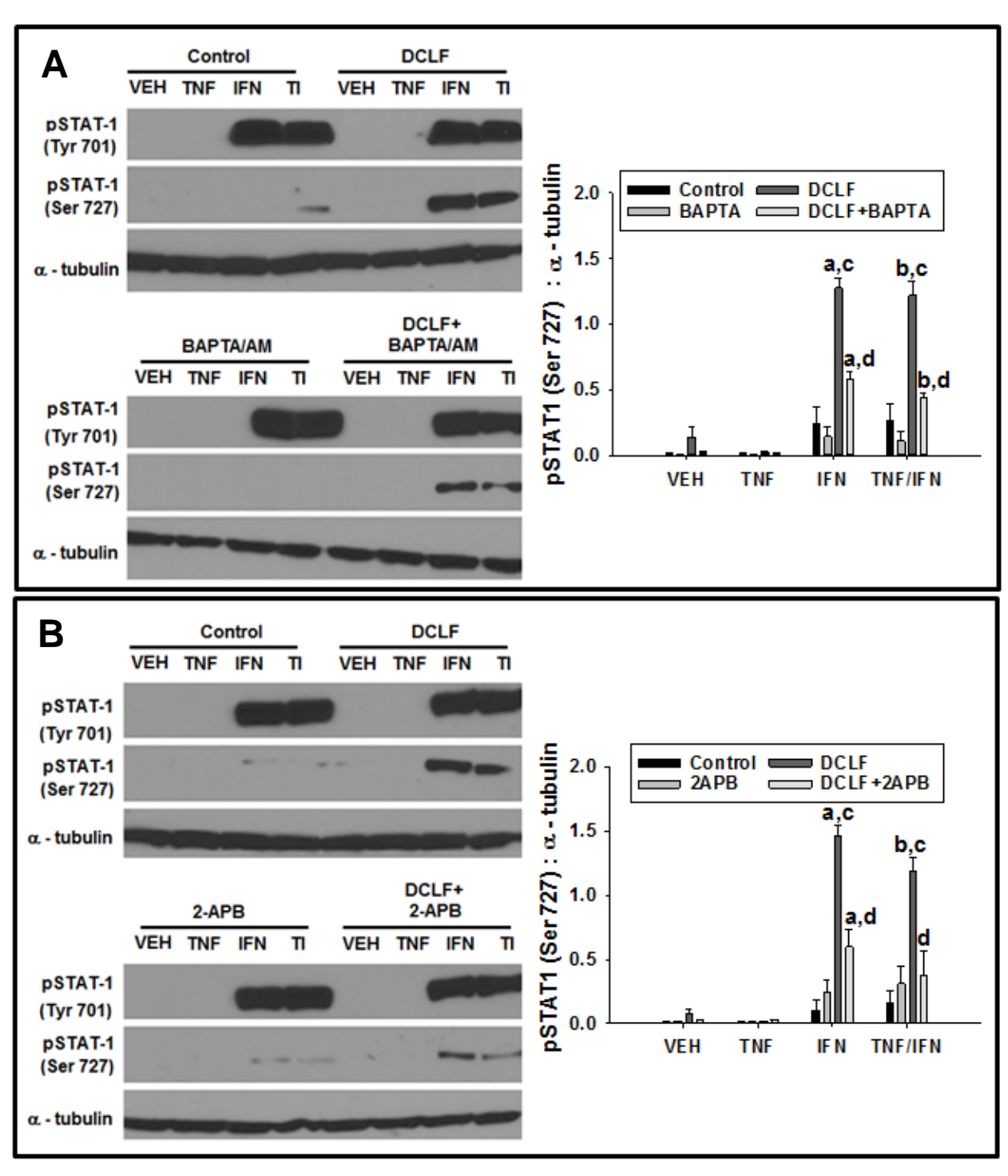


Figure 32. Ca⁺⁺ contributes to DCLF/IFN-mediated phosphorylation of STAT-1 at Ser 727. HepG2 cells were treated with VEH (0.1% DMSO), (A) BAPTA/AM (10 μM, 4h before addition of DCLF/cytokines) or (B) 2-APB (100 μM, simultaneously addition with

Figure 32 (cont'd)

DCLF/cytokines) and treated with Control (sterile water) or DCLF (250 μM) alone or in combination with TNF and/or IFN. Proteins were collected 18 hours after drug treatment. pSTAT1 (Tyr 701), pSTAT1 (Ser 727), and α-tubulin levels were detected via western analysis. a, significantly different from corresponding bar in VEH group. b, significantly different from corresponding bar in TNF group. c, significantly different from Control within a cytokine group. d, significantly different from DCLF within a cytokine group. Data are represented as mean ± S.E.M of n=3. Abbreviations: VEH, vehicle; DCLF, diclofenac; pSTAT1, phosphorylated signal transducer and activator of transcription-1; Tyr, tyrosine; Ser, serine; BAPTA/AM, acetoxymethyl-1,2-bis(2-aminophenoxy)ethane-N,N,N',N'-tetraacetic acid; APB, aminophenoxydiphenyl borate.

phosphorylation of STAT1 at Ser 727 (Maiuri, et al., 2015), but the role of JNK in this response is unknown, as is whether there is interdependence of JNK and ERK activation. Treatment of HepG2 cells with the JNK inhibitor SP600125 prevented DCLF/IFN-mediated phosphorylation of STAT1 at Ser 727 (Figure 33A). Moreover, treatment with SP600125 significantly reduced DCLF-induced activation of ERK (Figure 33B).

4.4.8 Aspirin does not promote activation of JNK or ERK, or the ER stress sensor, PERK

Aspirin is an NSAID that is not associated with human IDILI, and it does not synergize with cytokines to kill HepG2 cells (Maiuri, et al., 2015). Since DCLF-induced activation of JNK, ERK and the ER stress sensor PERK is required for cytotoxic synergy mediated by DCLF/cytokine cotreatment, we evaluated whether aspirin treatment promotes activation of JNK, ERK and PERK. The concentration of aspirin chosen relative to its maximal plasma concentration observed in human patients (Cmax) is comparable to that chosen for DCLF relative to its Cmax (Brandon, et al., 1986, Xu, et al., 2008). Treatment of HepG2 cells with aspirin did not result in activation of any of these factors (Figure 34).

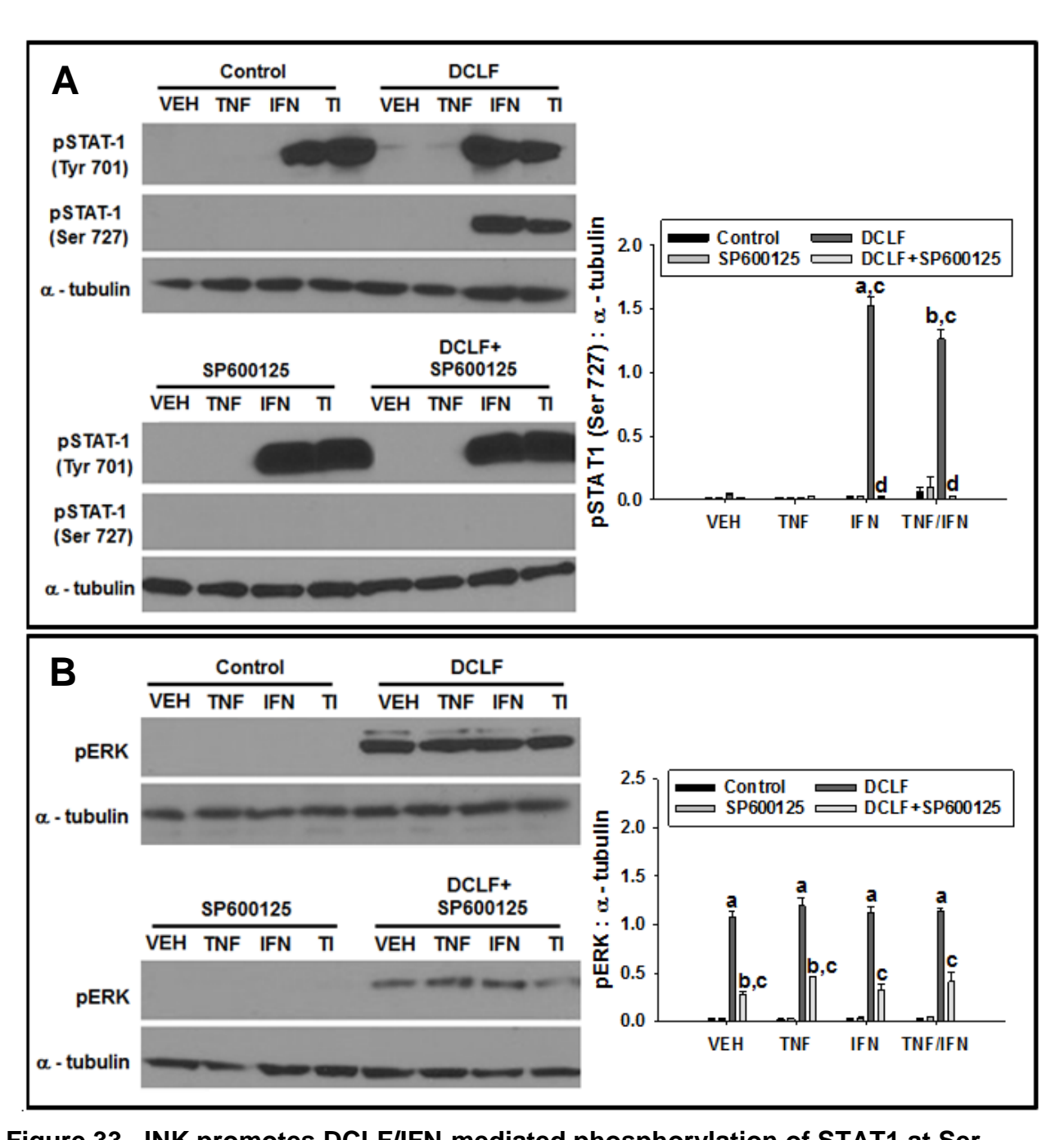


Figure 33. JNK promotes DCLF/IFN-mediated phosphorylation of STAT1 at Ser 727 via activation of ERK. HepG2 cells were treated with VEH (0.1% DMSO) or SP600125 (20 μM) and simultaneously treated with Control (sterile water) or DCLF (250 μM) alone or in combination with TNF and/or IFN. Whole cell lysates were collected 18 hours after treatment. (A) pSTAT1 (Tyr 701), pSTAT1 (Ser 727), α-tubulin and (B) pERK and α-tubulin levels were detected via western analysis. (A) a, significantly

Figure 33 (cont'd)

different from corresponding bar in VEH group. b, significantly different from corresponding bar in TNF group. c, significantly different from Control within a cytokine group. d, significantly different from DCLF within a cytokine group. (B) a, significantly different from Control within a cytokine group. b, significantly different from SP600125 within a cytokine group. c, significantly different from DCLF within a cytokine group. Data are represented as mean ± S.E.M of n=3. Abbreviations: VEH, vehicle; DCLF, diclofenac; pSTAT1, phosphorylated signal transducer and activator of transcription-1; Tyr, tyrosine; Ser, serine; pERK, phosphorylated extracellular signal-regulated kinase.

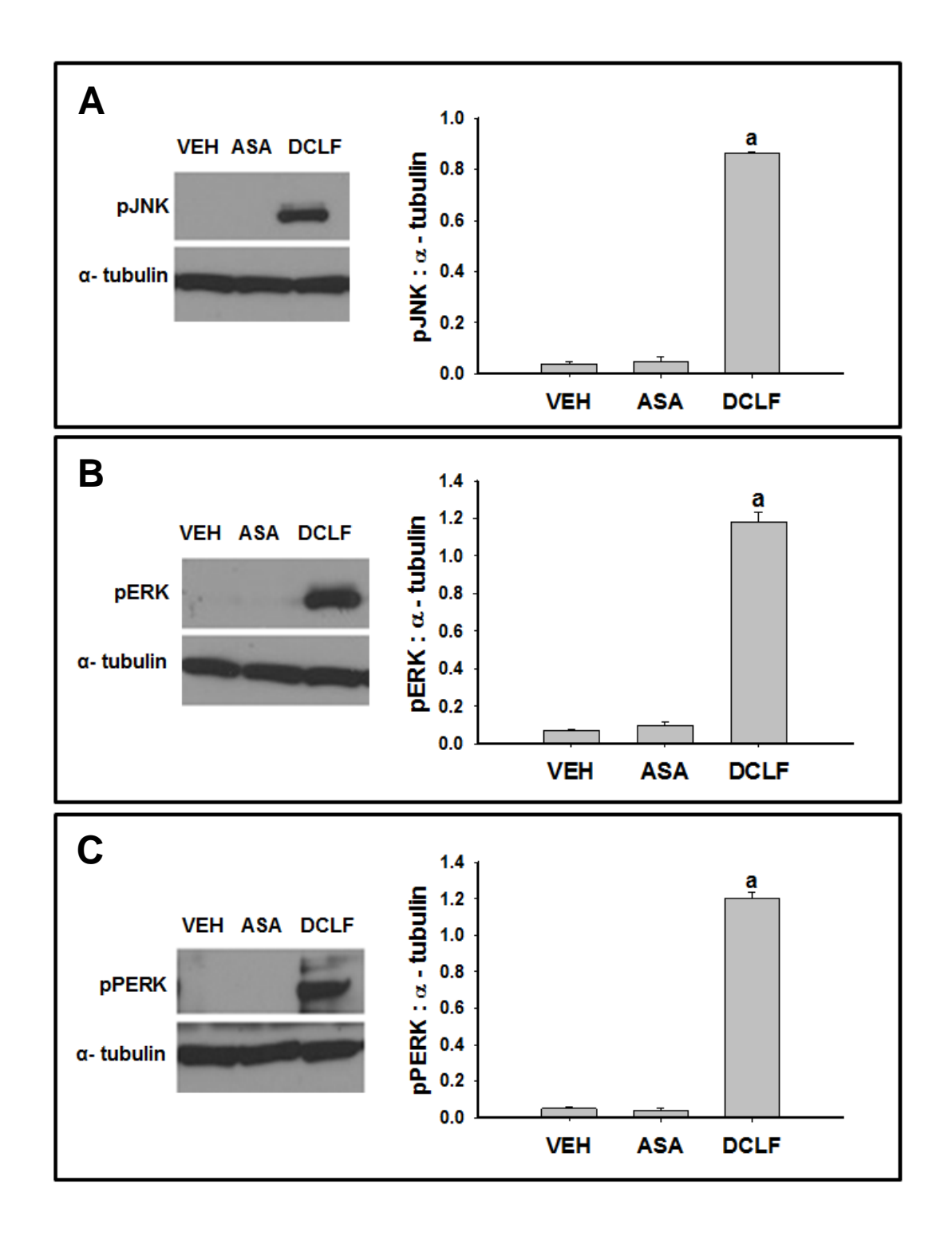


Figure 34. Aspirin does not promote activation of the MAPKS, JNK and ERK, or the ER stress sensor, PERK. HepG2 cells were treated with VEH (0.1% DMSO), ASA (2 mM) or DCLF (250 μM). Protein was collected 18 hours after treatment. A) pJNK, B)

Figure 34 (cont'd)

pERK and C) pPERK levels were measured via western analysis. a, significantly different from all treatment groups. Data are represented as mean ± S.E.M of n=3. Abbreviations: VEH, vehicle; ASA, aspirin; pJNK, phosphorylated c-Jun N-terminal kinase; pERK, phosphorylated extracellular signal-regulated kinase; pPERK, phosphorylated protein kinase RNA-like endoplasmic reticulum kinase.

4.5 Discussion

We and others have shown that DCLF synergizes with cytokines to cause cytotoxicity in primary human hepatocytes (Cosgrove, et al., 2009) and HepG2 cells (Fredriksson, et al., 2011, Maiuri, et al., 2015) by a mechanism involving the MAPKs, JNK and ERK. Moreover, Fredriksson, et al., (2014) reported that DCLF caused ER stress in HepG2 cells as early as 2 hours after treatment, and this response was unaffected by TNF but required for DCLF/TNF-induced cytotoxic synergy. Additionally, DCLF induced a delayed increase in intracellular Ca⁺⁺ in transformed human hepatocytes and primary rat hepatocytes after 6 or 8 hours of exposure, respectively (Bort, et al., 1999, Lim, et al., 2006). Since ER stress is strongly associated with intracellular Ca⁺⁺ dysregulation, and since DCLF treatment can induce both of these responses in liver cells, we hypothesized that Ca⁺⁺ contributes to DCLF/cytokine-induced cytotoxic synergy.

Chelation of intracellular Ca⁺⁺ markedly reduced cytotoxicity and caspase-3 activation induced by DCLF/cytokine treatment (Figure 26), whereas removal of extracellular Ca⁺⁺ did not affect the cytotoxic interaction (Figure 27). These findings suggest that Ca⁺⁺ released from an intracellular source underlies the cytotoxic interaction mediated by DCLF/cytokine cotreatment.

Ca⁺⁺ is primarily stored in the ER, but it can also be stored in other intracellular compartments including the mitochondria (Berridge, et al., 1998). Ryanodine receptors and IP3 receptors are the most well characterized Ca⁺⁺ channels localized to the ER membrane. Moreover, IP3 receptor activation is associated with Ca⁺⁺-mediated apoptosis via the intrinsic (mitochondrial) pathway (Deniaud, et al., 2008, Verrier, et al.,

2004). 2-APB, a commonly used IP3 receptor antagonist, greatly reduced the cytotoxic interaction mediated by DCLF/TNF cotreatment, prevented the IFN-mediated enhancement of cytotoxicity, and greatly reduced DCLF/cytokine-induced caspase 3 activation (Figure 28).

Activation of the ER stress sensor PERK contributed to cytotoxicity mediated by DCLF/TNF (Fredriksson, et al., 2014). Although TNF treatment did not affect the activation of PERK in response to DCLF, the participation of IFN in activation of PERK had not been investigated. As observed with TNF, IFN did not modulate the activation of PERK in response to DCLF treatment (Figure 29). It is well understood that ER stress can cause intracellular Ca⁺⁺ dysregulation. Conversely, intracellular Ca⁺⁺ dysregulation can engage in a positive feedback amplification loop, thereby promoting persistent activation of the UPR (Timmins, et al., 2009). Treatment with either BAPTA/AM or 2-APB reduced DCLF-induced PERK phosphorylation. These findings indicate that intracellular free Ca⁺⁺ contributes to persistent ER stress in response to DCLF exposure.

DCLF/cytokine-induced cytotoxic synergy requires JNK (Fredriksson, et al., 2011, Maiuri, et al., 2015). JNK is activated in response to a variety of stressors, including TNF exposure, UV radiation, ROS exposure, ER stress and intracellular Ca⁺⁺ dysregulation (Seki, et al., 2012, Kim, et al., 2004). The kinetics of the activation of JNK can vary depending on the inducer, and the duration of JNK activation is critical to determining the fate of a cell. For instance, TNF promotes transient activation of JNK, which is associated with cell survival. Other stressors can induce persistent activation of JNK, which is associated with caspase activation and apoptosis (Seki, et al., 2012).

TNF activated JNK as early as 12 hours after treatment in HepG2 cells, and this response was transient in the absence of DCLF. In the presence of DCLF, activation of JNK persisted until at least 18 hours after treatment (Maiuri, et al., 2015). The mechanism by which DCLF promotes persistent activation of JNK is unknown, but it might involve ER stress and intracellular Ca⁺⁺ dysregulation. Support for this comes from the observation that treatment of cells with BAPTA/AM reduced activation of JNK in response to DCLF, and 2-APB eliminated DCLF-induced JNK activation (Figure 30). Since 2-APB also greatly reduced cytotoxicity induced by DCLF/cytokine cotreatment, these results are consistent with our previous findings which suggested that JNK is necessary and sufficient for DCLF/cytokine-induced cytotoxic synergy (Maiuri, et al., 2015).

Ca⁺⁺ can lead to activation of JNK via several routes, one of which involves activation of Ca⁺⁺/calmodulin-dependent protein kinase II (CaMKII) in response to ER stress and to increases in intracellular free Ca⁺⁺. CaMKII can directly phosphorylate apoptosis signal-regulating kinase 1 (ASK1), a MAPK kinase kinase that promotes downstream sustained activation of JNK (Brnjic, et al., 2010). Taken together, these findings indicate that DCLF-mediated activation of JNK requires availability of Ca⁺⁺. Furthermore, IP3-mediated release of Ca⁺⁺ from the ER drives DCLF-induced JNK activation.

The IFN-mediated enhancement of DCLF/TNF-induced cytotoxicity involves ERK (Maiuri, et al., 2015). DCLF treatment caused activation of ERK as early as 12 hours; this persisted until after 18 hours and was unaffected by TNF and/or IFN treatment (Maiuri, et al., 2015). The observation that either BAPTA/AM or 2-APB reduced ERK

activation (Figure 31) suggests that Ca⁺⁺ released from the ER via IP3 receptors contributes to ERK activation induced by DCLF. It remains unclear exactly how Ca⁺⁺ causes activation of ERK; however, in some transformed cell types, Ca⁺⁺ can promote activation of ERK via activation of the upstream MAPK kinase kinase (MAPKKK) Ras (Li, et al., 2005).

Activation of STAT1 plays an important role in IFN-dependent apoptosis (Cao, et al., 2015). Dual phosphorylation of STAT1 is required for maximal activation (Varinou, et al., 2003) and this occurred in cells treated with DCLF/IFN but not in cells treated with IFN alone (Maiuri, et al., 2015 and Figure 32). Not surprisingly, treatment of HepG2 cells with IFN caused phosphorylation of STAT1 at Tyr 701 (Maiuri, et al., 2015 and Figure 32) presumably via activation of JAK. DCLF in the presence of IFN promoted phosphorylation of STAT1 at Ser 727 via activation of ERK (Maiuri, et al., 2015). Consistent with their effects on DCLF-induced ERK activation, treatment with either BAPTA/AM or 2-APB reduced DCLF/IFN-induced phosphorylation of STAT1 at Ser 727 (Figure 32). These results indicate that free cytoplasmic Ca⁺⁺ contributes to STAT1 activation induced by DCLF/IFN cotreatment. Interestingly, treatment with BAPTA/AM or 2-APB did not affect IFN-induced phosphorylation of STAT1 at Tyr 701 (Figure 32).

JNK can also phosphorylate STAT1 at Ser 727 (Zhang, et al., 2004). Indeed, treatment of HepG2 cells with a JNK inhibitor eliminated the IFN-mediated enhancement of DCLF/TNF-induced cytotoxicity, suggesting that, along with ERK, JNK drives the IFN component of the DCLF/cytokine interaction (Maiuri, et al., 2015). Treatment with the JNK inhibitor SP600125 eliminated DCLF/IFN-induced phosphorylation of STAT1 at Ser 727 without affecting IFN-mediated phosphorylation of

STAT1 at Tyr 701 (Figure 33A). These results indicate that in addition to ERK, JNK mediates activation of STAT1 in response to DCLF/IFN and raises the question: does JNK contribute to the activation of ERK in response to DCLF treatment? The kinetics of DCLF-induced JNK activation correlated with the kinetics of DCLF-induced ERK activation (Maiuri, et al., 2015). Accordingly, we evaluated whether JNK activation drives DCLF-induced ERK activation (Figure 33B). Treatment with SP600125 reduced DCLF-induced ERK activation, suggesting that JNK is involved in the activation of ERK in response to DCLF treatment but is not solely responsible for it. Additionally, these results raise the possibility that JNK contributes to the phosphorylation of STAT1 at Ser 727 by promoting the activation of ERK.

We and others have shown that aspirin, an NSAID not associated with IDILI, does not synergize with cytokines to kill primary human hepatocytes (Cosgrove, et al., 2009) or HepG2 cells (Maiuri, et al., 2015). Since activation of PERK, JNK and ERK play critical roles in the cytotoxic DCLF/cytokine interaction, we examined whether aspirin can induce activation of these pathways. As expected, DCLF treatment promoted activation of PERK, JNK and ERK, whereas treatment with aspirin did not (Figure 34).

Collectively, these findings indicate that availability of Ca⁺⁺ in the cytoplasm, likely due to release from the ER via IP3 receptors, underlies most, if not all, aspects of DCLF/cytokine-induced cytotoxic synergy and raise the possibility that increase in intracellular Ca⁺⁺ contributes to hepatocellular injury that occurs in cases of human IDILI. Additionally, results from this study tie together critical components of the mechanism underlying the cytotoxic interaction mediated by DCLF and cytokines

(Figure 35). Understanding the mechanisms by which drugs sensitize hepatocytes to the harmful effects of immune mediators will be helpful in developing an approach for preclinical identification of drug candidates with the potential to cause IDILI in human patients.

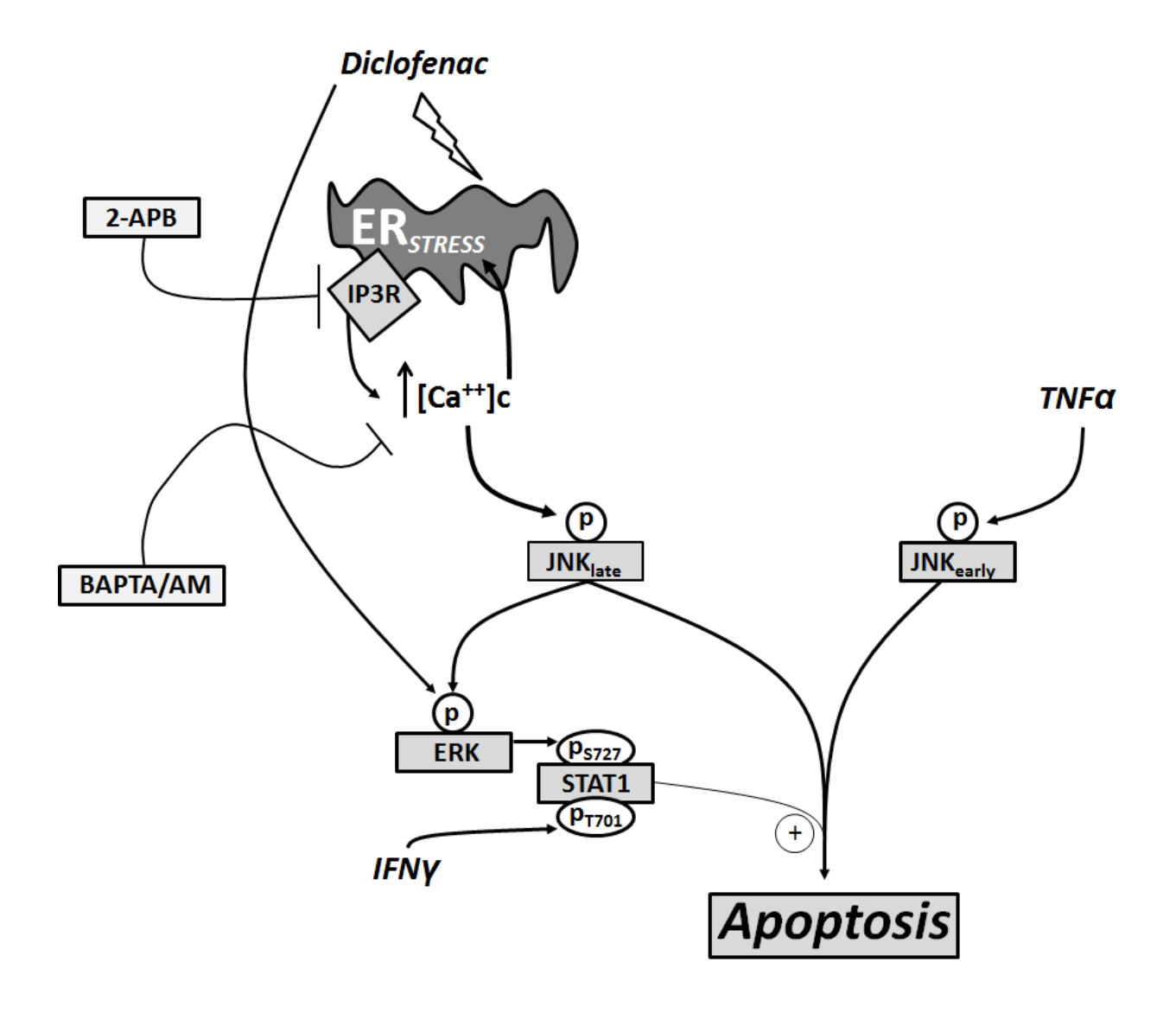


Figure 35. Proposed mechanism of DCLF/cytokine-induced cytotoxic synergy.

DCLF treatment causes ER stress in HepG2 cells as early as 2 h after treatment (Fredriksson, et al., 2014). ER stress is known to cause release of Ca⁺⁺ from the ER via IP3 receptors leading to an increase in cytoplasmic free Ca⁺⁺ ([Ca⁺⁺]c) that is associated with apoptosis (Deniaud, et al., 2008). Ca⁺⁺ released from the ER during ER stress can participate in a positive feedback amplification loop that leads to persistent ER stress (Timmins, et al., 2009). Results obtained using agents (BAPTA/AM and 2-APB) that

Figure 35 (cont'd)

inhibit the accumulation of cytoplasmic Ca⁺⁺ indicate that Ca⁺⁺ released from an intracellular source, likely IP3 receptor-coupled Ca⁺⁺ channels located on the ER membrane, contributes to the cytotoxic synergy mediated by DCLF/cytokine cotreatment by promoting DCLF-induced activation of the UPR pathway as well as the MAPKs, JNK and ERK. TNF treatment causes modest early activation of JNK that is transient in the absence of DCLF but persistent in its presence (Maiuri, et al., 2015). Persistent activation of JNK is essential for the DCLF/TNF-induced cytotoxic interaction. In this study we also determined that DCLF-induced activation of JNK contributes to activation of ERK and subsequently to phosphorylation of STAT1 at Serine 727 in the presence of IFN. The phosphorylation of STAT1 at Serine 727 by ERK is responsible for the IFN-mediated enhancement of DCLF/TNF-induced cell death as (indicated by the plus sign; Maiuri, et al., 2015). Abbreviations: ER, endoplasmic reticulum; IP3R, inositol trisphosphate receptor; APB, aminophenoxydiphenyl borate; [Ca⁺⁺]c, concentration of cytoplasmic calcium; BAPTA/AM, acetoxymethyl-1,2-bis(2-aminophenoxy)ethane-N,N,N',N'-tetraacetic acid; JNK, c-Jun N-terminal kinase; TNF, tumor necrosis factoralpha; ERK, extracellular signal-regulated kinase; STAT1, signal transducer and activator of transcription; S727, serine 727; T701, tyrosine 701; IFN, interferon gamma.

CHAPTER 5:

Summary, Implications and Future Directions

5.1 Development of an in vitro approach with the potential to predict IDILI liability of drugs in development

5.1.1 Summary of assay development and evaluation

A major goal of the work described in this dissertation was to develop and evaluate an in vitro approach with the ability to classify drugs according to their potential to cause IDILI. The approach developed incorporates a potential patient susceptibility factor that might underlie human IDILI: the presence of inflammation (inflammatory cytokines) in the context of a drug exposure. Briefly, human derived HepG2 cells were treated with various concentrations of a set of drugs associated with or not associated with IDILI, alone or simultaneously in combination with the cytokines TNF and/or IFN. Cell death was evaluated 24 hours after drug and/or cytokine treatment. The hypothesis tested was that drugs associated with IDILI would synergize with cytokines to cause death of HepG2 cells, whereas drugs not associated with IDILI would not synergize with cytokines to cause cell death. Various statistical models were used to evaluate the ability of this approach to classify a set of drugs according to their known IDILI potential. Importantly, this assay proved to be highly effective at classifying a test set of drugs.

5.1.2 Implications for preclinical safety evaluation of drugs in development

There is a remarkable need for the development of a high throughput approach to identify accurately during preclinical safety evaluation those drug candidates with the potential to cause human IDILI. An ideal approach would possess the following features: human cell type, relevant phenotypic endpoint (cell death), incorporation of

susceptibility factors that underlie human IDILI, ability to accurately discriminate between drugs that cause IDILI and do not cause IDILI, cost effective and amenable to high throughput testing. Current approaches employed during preclinical safety evaluation of drug candidates in development attempt to determine the intrinsic toxicity of a given drug candidate but fail to consider patient susceptibility factors that might underlie human IDILI. Several factors that underlie susceptibility to IDILI have been identified including certain conditions that are known to involve elevated plasma levels of immune mediators such as cytokines in patients. The approach described in this dissertation is the first to our knowledge that comprises all of the above-listed desired features of a useful in vitro approach to identify drug candidates with the potential to cause IDILI. Several important attractive features of this assay are that it involves use of a human cell line (HepG2) that is amenable to high throughput testing and is already used during preclinical safety evaluation of drugs in development. Moreover, the simplicity of the assay, simultaneous addition of test compounds and evaluation of a single relevant endpoint (percent LDH release, cell death) make it a desirable approach for employment during preclinical safety evaluation of drugs in development. Employment of such an approach could revolutionize the current paradigm in place during preclinical safety evaluation. Employing assays, such as the one described in this dissertation, which take susceptibility factors associated with IDILI into consideration could lead to identification of drugs with the potential to cause IDILI early on in the drug development process. This could reduce the financial burden of IDILI on the pharmaceutical industry and most importantly reduce suffering and the loss of human lives due to IDILI.

5.2 Elucidating mechanisms of cytotoxic synergy between drugs associated with IDILI and the cytokines TNF and IFN: a focus on NSAIDs

5.2.1 Involvement of caspases and MAPKs in NSAID/cytokine-induced cytotoxicity: summary of findings

The second major goal of the work described in this dissertation was to elucidate mechanisms underlying the cytotoxic interaction between IDILI-associated drugs and the cytokines, TNF and IFN. Since NSAIDs are among the most frequent causes of IDILI (Unzueta and Vargas, 2013), they were the primary focus of the mechanistic studies discussed in this dissertation. The human hepatoma HepG2 cell line was used in these studies. Importantly, HepG2 cells respond similarly to primary human hepatocytes with regard to the cytotoxic interaction between IDILI-associated drugs and cytokines, including TNFα and IFNy (Cosgrove, et al., 2009). A previous study showed that caspase activation and MAPK signaling dysregulation are involved in this interaction in primary human hepatocytes (Cosgrove, et al., 2009, Cosgrove, et al., 2010). In HepG2 cells, cytotoxic synergy between some IDILI-associated drugs and cytokines also depends on caspases and the MAPK JNK (Fredriksson, et al., 2011, Beggs, et al., 2014, Cosgrove, et al., 2009). Based on these previous findings, the involvement of MAPKs and caspases in NSAID/cytokine-induced cytotoxic synergy was examined.

Six NSAIDs were selected and stratified according to their chemical structure and potential to cause IDILI. Briefly, HepG2 cells were treated with various concentrations (0 to 100 times Cmax) of an NSAID alone or in combination with the cytokines TNF and/or

IFN. Cytotoxicity was measured 24 hours after treatment. Interestingly, three responses were observed, and these responses correlated with the drug's chemical structure and IDILI liability. The AA derivatives DCLF, SLD sulfide and BRM, which are associated with IDILI, synergized with TNF to cause HepG2 cell death, and IFN enhanced this cytotoxic response (Figure 13A). The PA derivatives NAP and IBU, which are associated with IDILI but are of less clinical concern, also synergized with TNF to cause cytotoxicity, but IFN was without effect (Figure 13B). The salicylic acid derivative aspirin, which is not associated with IDILI, did not synergize with any combination of cytokines to kill HepG2 cells (Figure 13C). The cytotoxic interaction between IDILI-associated NSAIDs and TNF was caspase-dependent. Moreover, the IFN-mediated enhancement of AA derivative/TNF-induced cytotoxicity was also a caspase-dependent process (Figure 15 and Figure 16).

Activation of MAPK signaling pathways can lead to apoptosis (Johnson and Lapadat, 2002). Treatment of HepG2 cells with TNF led to transient activation of JNK and p38. Treatment with a representative AA derivative (DCLF) or PA derivative (IBU) resulted in activation of JNK after 12 hours that was markedly enhanced by treatment with TNF, unaffected by IFN, and persisted until at least 18 hours after treatment (Figure 18). Treatment with DCLF or IBU also caused prolonged ERK activation that was unaltered by treatment with TNF or IFN (Figure 20). DCLF treatment caused early activation of p38 that was neither prolonged nor affected by cytokine treatment, whereas IBU caused persistent activation of p38 that was unaffected by cytokine treatment (Figure 22).

Inhibition of the JNK pathway with the pharmacologic inhibitor SP600125 completely protected cells from cytotoxicity induced by AA derivatives in combination with TNF as well as from the IFN-mediated enhancement of cytotoxicity (Figure 19A). In contrast, treatment with SP600125 had no effect on the cytotoxicity mediated by PA derivatives in combination with TNF (Figure 19B).

Treatment with U0126, an inhibitor of the ERK pathway, did not affect AA derivative/TNF-induced cytotoxicity but eliminated the IFN-mediated enhancement of AA derivative/TNF-induced cytotoxicity (Figure 21A). These results suggested that the mechanism by which IFN enhances AA derivative/TNF-induced cytotoxicity requires ERK. In contrast, inhibition of the ERK pathway enhanced PA derivative/cytokine-induced cytotoxicity, suggesting that ERK plays a protective role in this cytotoxic interaction mediated by PA derivatives and TNF (Figure 21B).

Inhibition of the p38 pathway potentiated cytotoxicity mediated by AA derivative/cytokine and PA derivative/cytokine treatment combinations, indicating that p38 plays a protective role (Figure 23).

One interesting observation in this study was that AA derivative/TNF-treated cells were sensitive to toxicity mediated by IFN whereas PA derivative/TNF-treated cells were insensitive. This suggested that the IFN-mediated enhancement of NSAID/TNF-induced cytotoxicity is a phenomenon related to chemical structure and to the magnitude of clinical concern regarding IDILI. This observation provided a unique platform on which to investigate further the mechanism underlying the IFN-mediated enhancement of NSAID/TNF-induced cytotoxicity. To identify the IFN mechanism, the phosphorylation status of the transcription factor STAT1, an important component of the

IFN signaling pathway, was examined after treatment with a representative AA derivative (DCLF) or PA derivative (IBU). As suspected, treatment with IFN in the absence of drug promoted phosphorylation of STAT1 at tyrosine 701. Treatment with DCLF in combination with IFN caused phosphorylation of STAT1 at serine 727, a phenomenon that was not observed after treatment with IBU/IFN (Figure 24 and Figure 25). In fact, treatment with IBU prevented phosphorylation of STAT1 at both tyrosine 701 and serine 727 (Figure 25). Since phosphorylation of STAT1 at both tyrosine 701 and serine 727 is required for full STAT1 activation (Varinou, et al., 2003), these results explain the increased sensitivity of AA derivative/TNF-treated cells to toxicity mediated by IFN and the lack of sensitivity of PA derivative/TNF-treated cells to death mediated by IFN.

Interestingly, DCLF/IFN-mediated phosphorylation of STAT1 at serine 727 was ERK-dependent, consistent with the observation that an ERK inhibitor eliminated the IFN-mediated enhancement of DCLF/TNFα-induced cytotoxicity (Figure 24). It was interesting that treatment with an AA or PA derivative resulted in remarkably similar patterns of ERK activation, yet treatment with an ERK inhibitor had a protective effect in one case (AA derivative/cytokine treatment) but a cytotoxic effect in another (PA derivative/cytokine treatment). The findings suggest that treatment with AA derivatives and IFN unmasks a substrate for ERK at Ser 727 of STAT1, which is not available in cells treated with PA derivatives, and that ERK activated in response to PA derivative treatment activates a cytoprotective substrate rather than one that is cytotoxic.

Overall, these findings indicate that NSAIDs associated with IDILI synergize with the cytokines TNF and/or IFN to cause hepatocellular death in vitro. Moreover,

depending on the chemical structure, some NSAIDs are more likely than others to sensitize cells to the harmful effects of IFN. It would be interesting if the capacity of AA derivatives to sensitize cells to toxicity mediated by IFN in the presence of TNF could explain why these NSAIDs are of more clinical concern with regard to IDILI than the PA derivatives. More research is required to test this hypothesis. Lastly, these findings indicate that IDILI-associated NSAIDs synergize with cytokines to cause hepatocellular death by different kinase signaling mechanisms and these differences might be related to chemical structure and IDILI liability.

5.2.2 Requirement of the availability of cytoplasmic Ca⁺⁺ in the cytotoxic interaction between DCLF and cytokines: summary of findings

The mechanisms by which NSAIDs associated with IDILI promote caspase activation and prolonged activation of the MAPKs JNK and ERK was investigated. DCLF was chosen as a representative IDILI-associated NSAID to investigate further the mechanisms underlying cytotoxic synergy between NSAIDs and the cytokines TNF and IFN. DCLF caused ER stress in HepG2 cells, and this played a role in cytotoxic interaction between DCLF and TNF (Fredriksson, et al., 2014). DCLF promoted activation of the ER stress sensors PERK and CHOP, and siRNA-mediated silencing of PERK and CHOP reduced the cytotoxicity mediated by DCLF/TNF cotreatment (Fredriksson, et al., 2014). The ER stress response pathway, also known as the unfolded protein response (UPR), is closely associated with dysregulation of intracellular Ca⁺⁺ (Fribley, et al., 2009) which can lead to activation of pathways that lead to apoptosis (Berridge, et al., 1998). This prompted investigation of the

involvement of Ca⁺⁺ in prolonged activation of the UPR, JNK and ERK pathways in response to treatment with DCLF in the absence or presence of TNF and/or IFN.

Chelation of intracellular Ca⁺⁺ using BAPTA/AM significantly decreased cytotoxicity and caspase 3 activation caused by cotreatment with DCLF and cytokines (Figure 26). Moreover, removal of Ca⁺⁺ from the culture medium did not affect the cytotoxic interaction between DCLF and cytokines (Figure 27). These results indicated that Ca⁺⁺ is involved in the cytotoxic interaction mediated by DCLF and cytokines, and that it is released from an intracellular source as opposed to entering the cell from the extracellular space.

Ca⁺⁺ is primarily stored in the ER, and its release from the ER is largely controlled by two channels: ryanodine receptors and IP3 receptors. Release of Ca⁺⁺ from IP3 receptors can result in apoptosis in various cell types including hepatocytes (Jeschke, et al. 2009, Lail-Trecker, et al. 2000). IP3 receptor activation can lead to apoptosis via several routes, one of which involves a physical interaction with the mitochondria to facilitate transfer of Ca⁺⁺ from the ER to the mitochondria, ultimately leading to apoptosis (Deniaud, et al. 2008, Verrier, et al., 2004, Szalai, et al., 1999). The involvement of IP3 receptors in the cytotoxic interaction between DCLF and cytokines was evaluated using a pharmacologic antagonist of IP3 receptors known as 2-APB. Treatment of cells with 2-APB almost completely prevented the cytotoxic interaction between DCLF and cytokines (Figure 28).

To determine to role of Ca⁺⁺ in DCLF/cytokine-induced cytotoxic synergy, the effect of chelation of intracellular Ca⁺⁺ on activation of the ER stress sensor PERK and the MAPKs JNK and ERK was evaluated. Chelation of intracellular Ca⁺⁺ using

BAPTA/AM greatly reduced DCLF-mediated activation of the ER stress sensor PERK and the MAPKs, JNK and ERK (Figure 29A, Figure 30A and Figure 31A). Furthermore, treatment of HepG2 cells with the IP3 receptor antagonist 2-APB significantly reduced DCLF-mediated activation of PERK, JNK and ERK (Figure 29B, Figure 30B and Figure 31B). Collectively, these findings indicate that the availability of cytoplasmic Ca⁺⁺, most likely due to release of Ca⁺⁺ from the ER via IP3 receptors, is essential for the prolonged activation of PERK, JNK and ERK pathways in response to treatment with DCLF.

ERK is responsible for the IFN-mediated enhancement of DCLF/TNF-induced cytotoxicity, presumably by phosphorylating STAT1 at serine 727 (Maiuri et al. 2015, Figure 24). Since Ca⁺⁺ contributed to the activation of ERK in response to DCLF treatment, the involvement of Ca⁺⁺ in phosphorylation of STAT1 at serine 727 in response to DCLF/IFN treatment was tested. Interestingly, treatment of HepG2 cells with either BAPTA/AM or 2-APB significantly reduced phosphorylation of STAT1 at serine 727 in response to DCLF/IFN treatment (Figure 32A, B). These findings indicate that Ca⁺⁺ contributes to the activation of STAT1 possibly by promoting activation ERK.

In addition to ERK, JNK was required for the IFN-mediated enhancement of DCLF/TNFα-induced cytotoxicity (Maiuri, et al., 2015). Inhibition of the JNK pathway eliminated DCLF/IFN-mediated phosphorylation of STAT1 at serine 727 (Figure 33A). This is consistent with what has been reported regarding pathways that lead to the phosphorylation of STAT1 at serine 727 (Zhang, et al., 2004). Since JNK and ERK are both required for phosphorylation of STAT1 at serine 727 in response to DCLF/IFN treatment, interdependence of JNK and ERK activation was investigated. Interestingly,

inhibition of the JNK pathway significantly reduced DCLF-mediated activation of the ERK pathway (Figure 33B) indicating that there is indeed crosstalk between the JNK and ERK pathways in the context of DCLF/cytokine-induced cytotoxic synergy. This is consistent with other reports of crosstalk between the ERK and JNK MAPK signaling pathways (Dong and Bode, 2003, Chen, et al. 2001).

Taken together, these findings implicate a role for Ca⁺⁺ in the cytotoxic interaction between DCLF and the cytokines TNF and IFN. Importantly, Ca⁺⁺ plays an essential role in the prolonged activation of the UPR pathway and the activation of the MAPKs, JNK and ERK, in response to DCLF treatment. Additionally, crosstalk between the JNK and ERK signaling pathways is vital to the cytotoxic interaction mediated by DCLF/cytokine cotreatment.

5.2.3 Implications of this work with regard to understanding mechanisms of idiosyncratic hepatotoxicity

To say that the mechanisms underlying the pathogenesis of human IDILI are complex would be a massive understatement. As alluded to earlier in this dissertation, a combination of modes of action are likely required to explain the pathogenesis of IDILI, and the specific combination of susceptibility factors likely varies from case to case. With regard to explaining the occurrence of IDILI, it is important to consider susceptibility factors associated with the individual as well as characteristics of the offending drug. Not all patients that possess a particular attribute associated with IDILI susceptibility will experience IDILI, and likewise not all drugs will lead to a hepatotoxic response in individuals that are susceptible. It cannot be emphasized enough that both

individual susceptibility factors and properties related to the offending drug are chief components that contribute to the occurrence of IDILI. The studies discussed in this dissertation aided in identifying some characteristics of drugs that make some more likely than others to interact with a host-specific factor that might render patients susceptible to IDILI.

The individual susceptibility factor of interest to this dissertation is inflammation, which is characterized by elevated levels of inflammatory cytokines in the plasma and often in the liver. There are many conditions that can result in elevated levels of circulating cytokines including underlying inflammatory diseases and various genetic polymorphisms in the human leukocyte antigen (HLA) genes or cytokine genes. Indeed, patients with either of these conditions have a greater risk of developing IDILI than patients who do not have them (Garcia Rodriguez, et al., 1994, Lucena, et al., 2011).

The studies described in this dissertation detail how NSAIDs associated with IDILI interact with the inflammatory cytokines TNF and IFN to cause hepatocellular death. The specific pathways activated by NSAIDs associated with IDILI that led to enhanced sensitivity of liver cells to the cytotoxic effects of cytokines were elucidated. Activation of caspases and MAPK signaling pathways in response to treatment with NSAIDs associated with IDILI played a pivotal role in the cytotoxic interaction between NSAIDs associated with IDILI and the cytokines TNF and IFN (Maiuri, et al., 2015). Importantly, the involvement of caspases and MAPKs in drug/cytokine-induced cytotoxic synergy expands beyond NSAIDs. Trovafloxacin, a fluoroquinolone antibiotic associated with IDILI, synergized with TNF to cause death of HepG2 cells by a mechanism involving the MAPKs, JNK and ERK (Beggs, et al., 2014, Beggs, et al., 2015).

Moreover, caspase activation and MAPK signaling dysregulation was involved in cytotoxic synergy between IDILI-associated drugs from various pharmacologic classes and cytokines in primary human hepatocytes (Cosgrove, et al., 2009, Cosgrove, et al., 2010).

Another stress-activated pathway that plays a central role in drug/cytokine-induced cytotoxic synergy is the UPR and associated intracellular Ca⁺⁺ dysregulation.

DCLF treatment causes delayed intracellular Ca⁺⁺ dysregulation in hepatocytes (Bort, et al., 1999, Lim, et al., 2006) most likely as a consequence of early activation of the UPR (Fredriksson, et al., 2014). The availability of intracellular free Ca⁺⁺ was paramount to the prolonged activation of the UPR and the prolonged activation of the MAPKs, JNK and ERK, in response to DCLF exposure as well as the ensuing cell death due to cotreatment with DCLF and cytokines.

Importantly, aspirin, a drug that is not associated with IDILI, did not lead to activation of the UPR or activation of the MAPKs, JNK and ERK. Additionally, aspirin did not synergize with any combination of inflammatory cytokines to cause death of HepG2 cells. Findings from the mechanistic studies described in this dissertation shed light on the specific properties of drugs that make some drugs more likely than others to promote hepatocellular toxicity in the context of inflammation. This knowledge might be useful in the design and development of safer drugs. Additionally, knowledge concerning which drugs are more likely than others to interact with inflammation to cause hepatocellular toxicity could aid clinicians in choosing the safest course of treatment for their patients.

5.3 Proposed future directions

The in vitro approach discussed in this dissertation proved to be highly effective at accurately classifying drugs according to their potential to cause IDILI. That being said, out of 14 drugs associated with IDILI, 3 of them did not synergize with cytokines to kill HepG2 cells. Although this number is small, it is an important reminder that this approach, as to be expected with any approach, has flaws that permit misclassification of some drugs with regard to IDILI liability. As of yet, it is unclear what these specific flaws are, but one explanation might be that some drugs do not promote IDILI by synergizing with immune mediators to cause hepatocellular toxicity. Another possibility is that some drugs might synergize with a different combination of immune mediators to cause hepatocellular toxicity, and not with TNF and/or IFN. Additionally, some drugs might require bioactivation in order to synergize with cytokines to cause cell death, as was the case with sulindac. It was shown previously that sulindac sulfide but not sulindac synergizes with TNF to cause hepatocellular toxicity in vitro (Zou, et al., 2009). Future studies should be geared toward refining the approach described in this dissertation to account for the factors that might result in misclassification of drugs. One approach that should be pursued is to incorporate other inflammatory cytokines alone or in combination with TNF and or IFN into the in vitro assay described in this dissertation. IL-1 alpha (IL-1α), IL-1β and IL-17 are proinflammatory cytokines that play a role in liver injury induced by some drugs (Blazka, et al., 1996, Takai, et al., 2015). For example, flucloxacillin is associated with IDILI, but it did not synergize with TNF or IFN to cause death of HepG2 cells; however, a murine model of flucloxacillin-induced liver injury demonstrated that co-administration of recombinant IL-17 exacerbated flucloxacillininduced liver injury (Takai, et al., 2015). It would be interesting to determine if flucloxacillin can synergize with immune mediators other than TNF and IFN, such as IL-17, to kill HepG2 cells in vitro.

Since a few IDILI-associated drugs did not synergize with cytokines to kill HepG2 cells, it would be interesting to determine if cytochrome p450 (CYP)-mediated bioactivation is required for synergy with cytokines for those drugs. It should be noted that the vast majority of IDILI-associated drugs evaluated in this study were classified correctly based on their ability to synergize with TNF. This suggests that CYP-mediated bioactivation might not be required for the interaction between most IDILI-associated drugs and cytokines, although further investigation is needed to determine if this holds true with a larger set of drugs.

The results discussed in Chapter 2 indicate that cytotoxic synergy between drugs and TNF is enough to classify drugs according to their potential to cause IDILI, irrespective of the presence of IFN. The results discussed in Chapter 3, which focused exclusively on cytotoxic synergy between NSAIDs and cytokines, indicated that certain NSAIDs sensitize HepG2 cells to the harmful effects of IFN, whereas other NSAIDs do not. Interestingly, the NSAIDs that sensitize HepG2 cells to the harmful effects of IFN, the AA derivatives, are of most clinical concern with regard to IDILI whereas, the NSAIDs that do not sensitize HepG2 cells to IFN, the PA derivatives, are associated with IDILI that is of less clinical concern. It would be interesting if the ability of drugs generally to sensitize HepG2 cells to cytotoxicity mediated by IFN could distinguish between drugs that have a high propensity to cause IDILI and those that have some

IDILI liability but are of less clinical concern, as observed with the small set of NSAIDs discussed in Chapter 3.

Although inflammatory stress is an important risk factor associated with IDILI, it might not be important with regard to IDILI caused by all drugs, and thus consideration of other risk factors associated with IDILI should be taken when developing in vitro and in vivo models to identify drug candidates with the potential to cause IDILI. Other risk factors to consider include but are not limited to age, sex, underlying diseases (both inflammatory and not inflammatory), genetic polymorphisms related to drug metabolizing enzymes and/or genetic polymorphisms related to the immune system. Future efforts should focus on developing assays that incorporate such risk factors associated with IDILI to maximize the ability to identify drug candidates with the potential to cause IDILI before they reach the market and possibly before entering clinical trials.

The studies discussed in this dissertation implicate a role for caspases, MAPKs, ER stress and cytoplasmic free Ca⁺⁺ in the pathogenesis of IDILI, in particular, IDILI that results from the cytotoxic interaction between NSAIDs and immune mediators. The findings from the studies discussed in this dissertation are consistent with results from other studies, which implicate a role for these signaling pathways in the pathogenesis of various liver diseases including IDILI (Saberi, et al., 2014, Apostolova, 2013, Kao, et al., 2012, Gardner, et al., 2005). Although critical gaps in the understanding of how NSAIDs, particularly DCLF, synergize with the cytokines TNF and IFN have been filled, much remains to be elucidated. For example, an interesting observation discussed in Chapter 3 was that two different NSAIDs, DCLF and IBU, caused the same pattern of

activation of ERK, however, ERK played a dichotomous role in the NSAID/cytokine-induced cytotoxic interaction depending on the NSAID involved in its activation. This suggests that different drugs can influence the outcome of signaling through the ERK pathway either indirectly or by physically interacting with ERK itself or the substrates on which ERK acts. Further investigation is needed to determine precisely how DCLF and IBU differentially influence the outcome of signaling via the ERK pathway.

Chapter 4 discusses a possible role for cytoplasmic free Ca⁺⁺ in the cytotoxic interaction between DCLF and TNF and IFN. It is apparent that availability of cytoplasmic free Ca⁺⁺ is essential to the development of hepatocellular toxicity in response to cotreatment with DCLF in combination with cytokines since limiting the availability of cytoplasmic free Ca⁺⁺ protected cells from DCLF/cytokine-induced cytotoxicity. What remains to be elucidated is the cause of intracellular Ca⁺⁺ dysregulation in response to DCLF, as well as the specific time at which intracellular Ca⁺⁺ dysregulation occurs and leads to perpetuation of the UPR well as prolonged activation of the MAPKs, JNK and ERK. It is possible that early activation of the UPR in response to treatment with DCLF leads to dysregulation of intracellular Ca⁺⁺ resulting in a feedback amplification loop promoting persistent activation of the UPR, JNK and ERK. Further investigation is needed to confirm this.

The results from the studies involving 2-APB (Chapter 4) suggest that IP3 receptors play a role in the cytotoxic interaction between DCLF and cytokines. However, the mechanism by which IP3 receptor activation occurs in response to DCLF treatment and the signaling events that occur downstream of IP3 receptor activation leading to apoptosis remain to be determined. Activation of the UPR in response to DCLF results

in PERK activation followed by upregulation of the proapoptotic transcription factor, CHOP (Fredriksson, et al., 2014). One possibility is that upregulation of CHOP in response to DCLF treatment causes activation of ER oxidase 1 alpha (ERO1α), which can promote activation of IP3 receptors in response to ER stress followed by apoptosis (Li, et al., 2009). Upon activation, IP3 receptors physically interact with proteins located on the outer mitochondrial membrane to facilitate transfer of Ca⁺⁺ from the ER to the mitochondria. Excessive IP3-mediated release of Ca⁺⁺ can lead to overloading of Ca⁺⁺ in the mitochondrial matrix followed by mitochondrial permeability transition, resulting in apoptosis. Another possibility is that IP3-mediated release of Ca++ from the ER leads to activation of CaMKII which can activate the MAPKKK, ASK1, leading to sustained JNK activation and subsequently mitochondrial permeability transition and apoptosis. Although the involvement of mitochondrial permeability transition in the cytotoxic interaction between DCLF and cytokines has not been examined directly, results from a previous study suggest that it might be involved. Specifically, the observation that siRNA-mediated silencing of components of the apoptosome, caspase-9 and Apaf-1, protected HepG2 cells from DCLF/TNF-induced cytotoxicity suggests a role for mitochondrial permeability transition in the cytotoxic interaction between DCLF and cytokines (Fredriksson, et al., 2011). Whether or not DCLF causes IP3 receptormediated release of Ca++ from the ER leading to mitochondrial permeability transition in HepG2 cells remains to be determined; however, supporting this is the observation that DCLF causes dysregulation of intracellular Ca⁺⁺ and consequent mitochondrial permeability transition in human hepatocytes (Lim, et al., 2006).

Another unanswered question concerns the importance of ER stress with regard to cytotoxic synergy between other IDILI-associated drugs and cytokines. Interestingly, Fredriksson, et al. (2014) demonstrated that carbamazepine, another drug associated with IDILI, causes ER stress in HepG2 cells and that this is required for the cytotoxic interaction between carbamazepine and TNF. Induction of the UPR might be a common mechanism underlying the cytotoxic interaction between IDILI-associated drugs and cytokines. It would be interesting to determine whether other IDILI-associated drugs activate the UPR and whether this plays a role in in sensitization of hepatocytes to the cytotoxic effects of cytokines such as TNF and IFN. Moreover, if other IDILI-associated drugs synergize with cytokines to cause death of hepatocytes but do not do so by activating the UPR, it would be important to identify other mechanisms (stressors) responsible for sensitizing hepatocytes to the cytotoxic effects of cytokines.

Lastly, as mentioned in the introduction section of this dissertation, there are many hypotheses concerning the etiology of IDILI, and more than likely a combination of modes of action are involved in the pathogenesis. Although developing assays to identify drug candidates with the potential to cause IDILI is of utmost importance, it is imperative that future research also be directed toward investigating the interplay between various modes of action underlying the pathogenesis of IDILI (e.g. inflammatory stress and adaptive immunity). To date, the only animal models that recapitulate the severity of liver injury observed in cases of human IDILI were developed based on the inflammatory stress hypothesis in which rodents were administered a nonhepatotoxic dose of LPS in combination with a nonhepatotoxic dose of a drug associated with IDILI (Roth and Ganey, 2011). Recently, some animal models have

been developed based on activation of an adaptive immune response; however, the liver injury produced in these models is mild and does not recapitulate severe injury that is observed in human patients (Chakraborty, et al., 2015). Nonetheless, adaptive immune responses likely play a critical role in the precipitation of IDILI as demonstrated by the high prevalence of IDILI in patients with genetic polymorphisms in HLA genes (Lucena, et al., 2011). The study by Chakraborty, et al., (2015) demonstrated in Balb/c mice that inhibition of immune tolerance by depletion of myeloid derived suppressor cells sensitizes the liver to mild toxicity induced by rechallenge with the IDILI-associated drug halothane. What is interesting about this study is that the initial exposure to halothane produced more severe hepatotoxicity than the second exposure. The second exposure to halothane produced mild injury that appeared to be driven by the adaptive immune system. The etiology of the injury produced by the initial exposure to halothane was not investigated in this study but was pivotal to the mild injury that occurred upon halothane rechallenge. Dugan, et al., (2011) demonstrated that a single exposure of Balb/c mice to halothane leads to severe liver injury that is driven by the innate immune system. The injury observed after the first halothane exposure in the Chakraborty, et al., (2015) study mimicked the injury observed in the study by Dugan, et al., (2011), suggesting that an innate immune response elicited by the initial exposure to halothane contributed to the adaptive immune response initiated upon rechallenge with halothane. It would be interesting to determine if an interaction between the innate immune system and adaptive immune system is essential for the pathogenesis of human IDILI. Interestingly, Kupffer cells play an important role in promoting loss of immune tolerance in various liver diseases (Invernizzi, 2013). Whether or not innate immunity contributes

to adaptive immune-mediated IDILI in humans remains unknown but is worth investigating further. Furthermore, the in vitro studies discussed in this dissertation implicate a role for ER stress, MAPK activation and intracellular Ca⁺⁺ dysregulation in the cytotoxic synergy between IDILI-associated drugs and cytokines. It is critical to determine whether these mechanisms of hepatocellular sensitization to death mediated by cytokines hold true in vivo.

APPENDIX

Drug	Min	min TNF	min IFN	min TNF/IFN
Aspirin	11.02317	10.9841	15.15885	21.85225
Azithromycin	11.62381	12.98777	12.32817	14.83392
Buspirone	17.59238	18.56981	18.54376	17.9045
Idarubicin	13.92086	13.3255	12.22913	15.60874
Levofloxacin	14.04034	12.1065	13.70057	14.50974
Moxifloxacin	9.650601	9.826983	11.32122	14.01592
Pioglitazone	19.67819	20.40505	19.92209	20.75831
Promethazine	16.96038	19.44671	17.20356	22.08709
Rofecoxib	12.24869	12.21269	12.92278	15.93025
Sertraline	13.95237	16.37783	14.48685	16.59843
Bromfenac	13.81373	13.35347	13.48361	16.3288
Chlorpromazine	15.9557	18.0727	14.4343	17.16268
Diclofenac	15.64518	18.03256	16.18837	22.46181
Doxorubicin	19.05305	16.25846	16.41869	15.12666
Flucloxacillin	17.85148	17.51638	17.04674	16.90713
Flutamide	15.71064	15.67111	15.79347	16.69331
Ibuprofen	8.804186	8.880802	8.953888	15.81466
Isoniazid	15.69818	13.29336	15.98009	20.80651
Naproxen	8.721686	12.55691	10.78189	15.68234
Nimesulide	14.63728	14.17431	13.16604	15.99547
Potassium				
Clavulanate	17.40019	18.07494	17.33092	17.36303
Telithromycin	15.13821	14.31007	13.58245	17.4071
Trovafloxacin	12.0844	11.57897	10.58184	12.52037
Valproic Acid	17.87765	20.4039	19.21448	22.49163

Table 6. The minimum (min) of the LDH percentage values. These values were determined by the four-parameter logistic equation as described in the methods.

Drug	max	max TNF	max IFN	max TNF/IFN
Aspirin	11.02317	10.9841	19.70701	21.85225
Azithromycin	11.62381	12.98777	12.32817	29.15791
Buspirone	17.59238	18.56981	18.54376	17.9045
Idarubicin	13.92086	13.3255	12.22913	15.60874
Levofloxacin	14.04034	12.1065	13.70057	14.50974
Moxifloxacin	9.650601	9.826983	11.32122	14.01592
Pioglitazone	44.09206	45.64104	44.22409	43.60406
Promethazine	16.96038	19.44671	17.20356	22.08709
Rofecoxib	12.24869	12.21269	12.92278	15.93025
Sertraline	13.95237	16.37783	14.48685	16.59843
Bromfenac	13.81373	35.96762	17.71153	42.5107
Chlorpromazine	111.1036	97.917	93.2348	96.30114
Diclofenac	15.64518	38.99564	16.18837	51.18713
Doxorubicin	112.7848	94.77793	127.7975	101.111
Flucloxacillin	17.85148	17.51638	19.80186	16.90713
Flutamide	24.62606	25.01006	22.07863	20.98337
Ibuprofen	101.1707	105.1826	104.0844	105.1394
Isoniazid	57.67743	94.0967	48.93668	65.25762
Naproxen	101.6585	96.17086	99.30918	96.07838
Nimesulide	14.63728	106.5014	13.16604	102.5891
Potassium				
Clavulanate	17.40019	21.21038	17.33092	24.10388
Telithromycin	117.1374	99.17406	111.0956	115.919
Trovafloxacin	18.7321	45.5794	18.38844	68.70453
Valproic Acid	44.4982	84.16392	75.35409	89.68484

Table 7. Maximum (max) LDH percentage values. These values were determined by the four-parameter logistic equation as described in the methods.

Drug	Slope	Slope TNF	Slope IFN	Slope TNF/IFN
Aspirin	0	0	3.013419	0
Azithromycin	0	0	0	-1.75552
Buspirone	0	0	0	0
Idarubicin	0	0	0	0
Levofloxacin	0	0	0	0
Moxifloxacin	0	0	0	0
Pioglitazone	-16.0233	-11.8831	-14.0326	-30.0731
Promethazine	0	0	0	0
Rofecoxib	0	0	0	0
Sertraline	0	0	0	0
Bromfenac	0	-3.36002	-19.7211	-4.0419
Chlorpromazine	-10.0706	-7.6458	-12.6261	-5.26861
Diclofenac	0	-12.5147	0	-11.2072
Doxorubicin	-2.03372	-1.52064	-1.37644	-0.85869
Flucloxacillin	0	0	-5.00255	0
Flutamide	-0.22067	-0.35779	-0.50999	-3.2964
Ibuprofen	-6.14755	-2.1819	-5.49639	-2.18735
Isoniazid	-32.3153	-3.07052	-43.3983	-4.65097
Naproxen	-7.28776	-6.63365	-8.29965	-4.0413
Nimesulide	0	-14.9016	0	-15.2381
Potassium				
Clavulanate	0	-8.23058	0	-16.1012
Telithromycin	-4.20843	-3.14701	-3.9688	-2.29331
Trovafloxacin	-1.8714	-1.75052	-1.42378	-0.76885
Valproic Acid	-0.48261	-1.75394	-0.84953	-1.65951

Table 8. Concentration-response slope values. These values were determined by the four-parameter logistic equation as described in the methods. Due to the method of parameterization a negative slope means increasing function. For treatments that did not result in a statistically significant increase in percent LDH release from baseline, slope=0.

Drug	EC50	EC50 TNF	EC50 IFN	EC50 TNF/IFN
Aspirin	0	0	7.903784	0
Azithromycin	0	0	0	207.08716
Buspirone	0	0	0	0
Idarubicin	0	0	0	0
Levofloxacin	0	0	0	0
Moxifloxacin	0	0	0	0
Pioglitazone	81.91337	87.54133	86.76567	87.98228
Promethazine	0	0	0	0
Rofecoxib	0	0	0	0
Sertraline	0	0	0	0
Bromfenac	0	43.47215	41.72558	32.5106
Chlorpromazine	44.5165	40.6336	40.5259	36.5562
Diclofenac	0	28.50142	0	28.28117
Doxorubicin	35.359225	7.233752	52.2015	7.197095
Flucloxacillin	0	0	31.99518	0
Flutamide	27.66728	76.74721	33.45667	86.63006
Ibuprofen	72.79915	38.63694	75.69134	39.93189
Isoniazid	457.0833	507.2253	442.3663	272.2455
Naproxen	80.81034	32.85903	84.44202	29.74931
Nimesulide	0	36.87271	0	38.30741
Potassium				
Clavulanate	0	89.93895	0	78.03605
Telithromycin	129.71711	95.82117	140.46555	101.69113
Trovafloxacin	13.8738	7.97594	9.33336	8.52991
Valproic Acid	47.55449	60.68013	310.47438	53.10554

Table 9. Concentration-response EC50 values. These values were determined by the four-parameter logistic equation as described in the methods. For treatments that did not result in a statistically significant increase in percent LDH release from baseline, EC50=0.

Drug	EC10	EC10 TNF	EC10 IFN	EC10 TNF/IFN
Aspirin	0	0	0	0
Azithromycin	0	0	0	59.23607898
Buspirone	0	0	0	0
Idarubicin	0	0	0	0
Levofloxacin	0	0	0	0
Moxifloxacin	0	0	0	0
Pioglitazone	71.41698	72.7630205	74.190082	81.78325926
Promethazine	0	0	0	0
Rofecoxib	0	0	0	0
Sertraline	0	0	0	0
Bromfenac	0	22.6053931	0	18.87719122
Chlorpromazine	35.79033	30.4845085	34.053024	24.09032109
Diclofenac	0	23.9120577	0	23.24619544
Doxorubicin	12.00307	1.70544008	10.578278	0.557034513
Flucloxacillin	0	0	0	0
Flutamide	0	0	0	0
Ibuprofen	50.92171	14.1142229	50.749707	14.62394701
Isoniazid	427.0377	247.984686	420.52711	169.7423281
Naproxen	59.77633	23.5942366	64.801453	17.27245233
Nimesulide	0	31.8176865	0	33.16351557
Potassium				
Clavulanate	0	0	0	0
Telithromycin	76.95765	47.6693817	80.748376	39.01078794
Trovafloxacin	0	2.27332968	0	0.489570034
Valproic Acid	0.501105	17.3376558	23.375676	14.12942032

Table 10. EC10 values: the [drug]/Cmax value corresponding to 10% of the difference between the max and min (max – min). These values were determined by the equation listed in the methods.

Drug	D10	D10 TNF	D10 IFN	D10 TNF/IFN
Aspirin	0	0	0	0
Azithromycin	0	0	0	1
Buspirone	0	0	0	0
Idarubicin	0	0	0	0
Levofloxacin	0	0	0	0
Moxifloxacin	0	0	0	0
Pioglitazone	1	1	1	1
Promethazine	0	0	0	0
Rofecoxib	0	0	0	0
Sertraline	0	0	0	0
Bromfenac	0	1	0	1
Chlorpromazine	1	1	1	1
Diclofenac	0	1	0	1
Doxorubicin	1	1	1	1
Flucloxacillin	0	0	0	0
Flutamide	0	0	0	0
Ibuprofen	1	1	1	1
Isoniazid	1	1	1	1
Naproxen	1	1	1	1
Nimesulide	0	1	0	1
Potassium				
Clavulanate	0	0	0	0
Telithromycin	1	1	1	1
Trovafloxacin	0	1	0	1
Valproic Acid	1	1	1	1

Table 11. D10 values for each drug/cytokine treatment combination. D10 = 0 when the max – min \leq 10 LDH percentage points and D10 = 1 when the max – min > 10 LDH percentage points.

Drug	R10	R10 TNF	R10 IFN	R10 TNF/IFN
Aspirin	0	0	0	0
Azithromycin	0	0	0	333.8603414
Buspirone	0	0	0	0
Idarubicin	0	0	0	0
Levofloxacin	0	0	0	0
Moxifloxacin	0	0	0	0
Pioglitazone	80.0655076	84.4936389	84.5812117	87.25266593
Promethazine	0	0	0	0
Rofecoxib	0	0	0	0
Sertraline	0	0	0	0
Bromfenac	0	40.5689754	0	28.86086398
Chlorpromazine	35.9878347	31.5123484	34.7852044	25.32674658
Diclofenac	0	28.2927819	0	26.74169672
Doxorubicin	12.4368033	2.04040886	9.7017699	0.678420504
Flucloxacillin	0	0	0	0
Flutamide	0	0	0	0
Ibuprofen	51.6611796	14.3882751	51.2659082	15.49291833
Isoniazid	440.932549	268.137082	433.976149	208.6686853
Naproxen	60.4504777	24.3199933	65.8749377	18.3550262
Nimesulide	0	32.0085226	0	33.51641702
Potassium				
Clavulanate	0	0	0	0
Telithromycin	76.556936	50.5418105	81.3204968	39.29543299
Trovafloxacin	0	4.83702582	0	1.165938578
Valproic Acid	16.5957782	23.2583593	51.3249504	18.56832896

Table 12. R10 values: the [drug]/Cmax at which a 10 percent increase in the LDH response above baseline occurs. These values were computed using the equation listed in the methods. R10 was considered to be 0 when D10 \leq 10 LDH percentage points.

Drug	EC50 quotient	EC10 quotient	R10 quotient	Minmaxdiff
Aspirin	∩ Cost quotient	0	∩	0
Azithromycin	0	0	0	0
Buspirone	0	0	0	0
Idarubicin	0	0	0	0
Levofloxacin	0	_	0	0
		0		-
Moxifloxacin	0	0	0	0
Pioglitazone	0.935710824	0.981501101	0.947592134	0.82212
Promethazine	0	0	0	0
Rofecoxib	0	0	0	0
Sertraline	0	0	0	0
Bromfenac	0	0	0	22.61415
Chlorpromazine	1.095558848	1.174049846	1.142023254	-15.3036
Diclofenac	0	0	0	20.96308
Doxorubicin	4.888089196	7.038108762	6.095250595	-15.21225
Flucloxacillin	0	0	0	0
Flutamide	0	0	0	0.42353
Ibuprofen	1.884185187	3.607829584	3.590505415	3.935284
Isoniazid	0.901144521	1.722032603	1.644429582	38.82409
Naproxen	2.459303881	2.533513889	2.485628882	-9.322862
Nimesulide	0	0	0	92.32708
Potassium				
Clavulanate	0	0	0	3.13544
Telithromycin	1.353741663	1.614404124	1.514724844	-17.1352
Trovafloxacin	0	0	0	27.35273
Valproic Acid	0.783691301	0.028902715	0.713540366	37.13947

Table 13. EC50 quotient, EC10 quotient, R10 quotient and maxmindiff values for each drug/cytokine treatment combination. These values were determined as described in the methods.

Drug	TNF change
Aspirin	0
Azithromycin	0
Buspirone	0
Idarubicin	0
Levofloxacin	0
Moxifloxacin	0
Pioglitazone	0
Promethazine	0
Rofecoxib	0
Sertraline	0
Bromfenac	1
Chlorpromazine	0
Diclofenac	1
Doxorubicin	0
Flucloxacillin	0
Flutamide	0
Ibuprofen	0
Isoniazid	0
Naproxen	0
Nimesulide	1
Potassium	
Clavulanate	0
Telithromycin	0
Trovafloxacin	1
Valproic Acid	0

Table 14. The values for the categorical variable TNF change for each drug. TNF change = 1 when the drug/VEH curve is flat and the drug/TNF curve is sigmoidal and TNF change = 0 in all other situations.

Covariates	Beta
Intercept	-1.847
TNF change	2.959
EC50 VEH	-0.055
EC50 TNF	0.049
Delta VEH	0.068

Table 15. Coefficients for the model incorporating the covariates TNF change, EC50 VEH, EC50 TNF, and Delta VEH.

		95% confidence interval
Optimal cutoff threshold, k*	0.50	
True negative rate (specificity) using threshold k*	1	(0, 1)
True positive rate (sensitivity) using threshold k*	0.93	(0.79, 1)
AUC	0.96	(0.88, 1)

Table 16. The optimal cutoff threshold for the model incorporating the covariates TNF change, EC50 VEH, EC50 TNF, and Delta VEH.

Covariates	Beta
Intercept	-1.41
TNF change	2.763
EC50 VEH	0.002
EC50 TNF	0.025
Cmax	0.012

Table 17. Coefficients for the model incorporating the covariates TNF change, EC50 VEH, EC50 TNF, and Cmax.

		95% confidence interval
Optimal cutoff threshold, k*	0.34	
True negative rate (specificity) using threshold k*	0.9	(0.6, 1)
True positive rate (sensitivity) using threshold k*	0.93	(0.5, 1)
AUC	0.96	(0.9, 1)

Table 18. The optimal cutoff threshold for the model incorporating the covariates TNF change, EC50 VEH, EC50 TNF, and Cmax.

Covariates	Beta
Intercept	-1.918
Maxmindiff	0.118
EC50 VEH	-0.063
EC50 TNF	0.046
Delta VEH	0.089

Table 19. Coefficients for the model incorporating the covariates maxmindiff, EC50 VEH, EC50 TNF, and Delta VEH.

		95% confidence interval
Optimal cutoff threshold, k*	0.49	
True negative rate (specificity) using threshold k*	1	(0, 1)
True positive rate (sensitivity) using threshold k*	0.93	(0.79, 1)
AUC	0.96	(0.88, 1)

Table 20. The optimal cutoff threshold for the model incorporating the covariates maxmindiff, EC50 VEH, EC50 TNF, and Delta VEH.

Covariates	Beta
Intercept	-1.924
Maxmindiff	0.108
EC50 VEH	-0.066
EC50 TNF	0.05
Delta VEH	0.081
Cmax	0.003

Table 21. Coefficients for the model incorporating the covariates maxmindiff, EC50 VEH, EC50 TNF, Delta VEH, Cmax.

		95% confidence interval
Optimal cutoff threshold, k*	0.48	
True negative rate (specificity) using threshold k*	1	(0.7, 1)
True positive rate (sensitivity) using threshold k*	0.93	(0.79, 1)
AUC	0.99	(0.97, 1)

Table 22. The optimal cutoff threshold for the model incorporating the covariates maxmindiff, EC50 VEH, EC50 TNF, Delta VEH and Cmax.

Covariates	Beta
Intercept	-1.553
TNF change	3.353
EC50quotient	-0.091
Delta VEH	0.033
Cmax	0.026

Table 23. Coefficients for the model incorporating the covariates TNF change, EC50 quotient, Delta VEH and Cmax.

		95% confidence interval
Optimal cutoff threshold, k*	0.50	
True negative rate (specificity) using threshold k*	1	(0.4, 1)
True positive rate (sensitivity) using threshold k*	0.86	(0.64, 1)
AUC	0.96	(0.89, 1)

Table 24. The optimal cutoff threshold for the model incorporating the covariates TNF change, EC50 quotient, Delta VEH and Cmax.

Covariates	Beta
Intercept	-1.297
TNF change	3.683
R10 VEH	0.012
R10 TNF	-0.020
Delta VEH	0.034
Cmax	0.015

Table 25. Coefficients for the model incorporating the covariates TNF change, R10 VEH, R10 TNF, Delta VEH and Cmax.

		95% confidence interval
Optimal cutoff threshold, k*	0.40	
True negative rate (specificity) using threshold k*	1	(0.6, 1)
True positive rate (sensitivity) using threshold k*	0.86	(0.71, 1)
AUC	0.98	(0.94, 1)

Table 26. The optimal cutoff threshold for the model incorporating the covariates TNF change, R10 VEH, R10 TNF, Delta VEH and Cmax.

Covariates	Beta
Intercept	-1.165
Maxmindiff	0.168
R10 VEH	-0.004
R10 TNF	-0.021
Delta VEH	0.069

Table 27. Coefficients for the model incorporating the covariates maxmindiff, R10 VEH, R10 TNF and Delta VEH.

		95% confidence interval
Optimal cutoff threshold, k*	0.29	
True negative rate (specificity) using threshold k*	1	(0, 1)
True positive rate (sensitivity) using threshold k*	0.93	(0.8, 1)
AUC	0.97	(0.9, 1)

Table 28. The optimal cutoff threshold for the model incorporating the covariates maxmindiff, R10 VEH, R10 TNF and Delta VEH.

Covariates	Beta
Intercept	-1.577
TNF change	3.412
Delta VEH	0.036
Cmax	0.026

Table 29. Coefficients for the model incorporating the covariates TNF change, Delta VEH and Cmax.

		95% confidence interval
Optimal cutoff threshold, k*	0.49	
True negative rate (specificity) using threshold k*	1	(0.4, 1)
True positive rate (sensitivity) using threshold k*	0.86	(0.64, 1)
AUC	0.96	(0.89, 1)

Table 30. The optimal cutoff threshold for the model incorporating the covariates TNF change, Delta VEH and Cmax.

Covariates	Beta
Intercept	-1.566
TNF change	3.398
R10quotient	-0.125
Delta VEH	0.035
Cmax	0.026

Table 31. Coefficients for the model incorporating the covariates TNF change, R10 quotient, Delta VEH and Cmax.

		95% confidence interval
Optimal cutoff threshold, k*	0.50	
True negative rate (specificity) using threshold k*	1	(0.4, 1)
True positive rate (sensitivity) using threshold k*	0.86	(0.64, 1)
AUC	0.96	(0.89, 1)

Table 32. The optimal cutoff threshold for the model incorporating the covariates TNF change, R10 quotient, Delta VEH and Cmax.

Covariates	Beta	
Intercept	-1.644	
TNF change	3.188	
EC50quotient	2.149	
Cmax	0.028	

Table 33. Coefficients for the model incorporating the covariates TNF change, EC50 quotient and Cmax.

		95% confidence interval
Optimal cutoff threshold, k*	0.64	
True negative rate (specificity) using threshold k*	1	(0.5, 1)
True positive rate (sensitivity) using threshold k*	0.79	(0.64, 1)
AUC	0.96	(0.89, 1)

Table 34. The optimal cutoff threshold for the model incorporating the covariates TNF change, EC50 quotient and Cmax.

REFERENCES

REFERENCES

Adams, C., Brantner, V. 2006. Estimating the cost of new drug development: is it really 802 million dollars? Health Aff. (Millwood). 25, 420-428.

Aithal, G. 2004. Diclofenac-induced liver injury: a paradigm of idiosyncratic drug toxicity. Expert Opin. Drug Saf. 3, 519-523.

Aithal, G., Watkins, P., Andrade, R., Larrey, D., Molokhia, M., Takikawa, H., Hunt, C., Wilke, R., Avigan, M., Kaplowitz, N., Bjornsson, E., Daly, A. 2011. Case definition and phenotype standardization in drug-induced liver injury. Clin. Pharmacol. Ther. 89, 806-815.

Anderson, P. 1997. Kinase cascades regulating entry into apoptosis. Microbiol. Mol. Biol. Rev. 61, 22-46.

Apostolova, N., Gomez-Sucerquia, L., Alegre, F., Funes, H., Victor, V., Barrachina, M., Blas-Garcia, A., Esplugues, J. 2013. ER stress in human hepatic cells treated with Efavirenz: mitochondria again. J Hepatol. 59, 780-789.

Banks, A., Zimmerman, H., Ishak, K., Harter, J. 1995. Diclofenac-associated hepatotoxicity: analysis of 180 cases reported to the Food and Drug Administration as adverse reactions. Hepatology. 22, 820-827.

Beggs, K., Fullerton, A., Miyakawa, K., Ganey, P. and Roth, R. 2014. Molecular mechanisms of hepatocellular apoptosis induced by trovafloxacin-tumor necrosis factor-alpha interaction. Toxicol. Sci. 137, 91-101

Beggs, K., Maiuri, A., Fullerton, A., Poulsen, K., Breier, A., Ganey, P., Roth, R. 2015. Trovafloxacin-induced replication stress sensitizes HepG2 cells to tumor necrosis factor-alpha-induced cytotoxicity mediated by extracellular signal-regulated kinase and ataxia telangiectasia and Rad3-related. Toxicology. 331, 35-46.

Bennett, B., Sasaki, D., Murray, B., O'Leary, E., Sakata, S., Xu, W., Leisten, J., Motiwala, A., Pierce, S., Satoh, Y., Bhagwat, S., Manning, A., Anderson, D. 2001. SP600125, an anthrapyrazolone inhibitor of Jun N-terminal kinase. Proc. Natl. Acad. Sci. 98,13681-13686.

Berridge, M., Bootman, M., Lipp, P. 1998. Calcium--a life and death signal. Nature. 395, 645-648.

Bird, G., Williams, R. 1989. Detection of antibodies to a halothane metabolite hapten in sera from patients with halothane-associated hepatitis. J. Hepatol. 9, 366-373.

Bissell, D., Gores, G., Laskin, D., Hoofnagle, J. 2001. Drug-induced liver injury: mechanisms and test systems. Hepatology. 33, 1009-1013.

Black, M., Mitchell, J., Zimmerman, H., Ishak, K., Epler, G. 1975. Isoniazid-associated hepatitis in 114 patients. Gastroenterology. 69, 289-302.

Bode J., Ehlting C., Haussinger D. 2012. The Macrophage Response Towards LPS and its Control through the P38 MAPK-STAT3 Axis. Cellular Signaling. 24, 1185-1194.

Blazka, M., Elwell, M., Holladay, S., Wilson, R., Luster, M. 1996. Histopathology of acetaminophen-induced liver changes: role of interleukin 1 alpha and tumor necrosis factor alpha. Toxicol Pathol. 24, 181-9.

Boelsterli, U. 2002. Mechanisms of NSAID-induced hepatotoxicity: focus on nimesulide. Drug Saf. 25, 633-648.

Bollo, M., Paredes, R., Holstein, D., Zheleznova, N., Camacho, P., Lechleiter, J. 2010. Calcineurin interacts with PERK and dephosphorylates calnexin to relieve ER stress in mammals and frogs. PLoS One. 5, e11925.

Bogoyevitch, M. 2006. The isoform-specific functions of the c-Jun N-terminal Kinases (JNKs): differences revealed by gene targeting. Bioessays. 28, 923-934. Bort, R, Ponsoda, X, Jover, R, Gómez-Lechón, M, Castell, J. 1999. Diclofenac toxicity to hepatocytes: a role for drug metabolism in cell toxicity. J. Pharmacol. Exp. Ther. 288, 65-72.

Bourdi, M., Chen, W., Peter, R., Martin, J., Buters, J., Nelson, S., Pohl, L. Human cytochrome p450 2E1 is a major autoantigen associated with halothane hepatitis. Chem. Res. Toxicol. 9, 1159-1166.

Bramlage, P., Goldis, A. 2008. Bioequivalence study of three ibuprofen formulations after single dose administration in healthy volunteers. BMC Pharmacol. 8, 1-9.

Brandon, R., Eadie, M., Curran, A., Nolan, P., Presneill, J. 1986. A new formulation of aspirin: bioavailability and analgesic efficacy in migraine attacks. Cephalalgia 6, 19-27.

Brenner, C., Galluzzi, L., Kepp, O., Kroemer, G. 2013. Decoding cell death signals in liver inflammation. J. Hepatol. 59, 583-594.

Brnjic, S., Olofsson, M., Havelka, A., Linder, S. 2010. Chemical biology suggests a role for calcium signaling in mediating sustained JNK activation during apoptosis. Mol. Biosyst. 6, 767-774.

Buchweitz J., Ganey P., Bursian S., Roth R. 2002. Underlying endotoxemia augments toxic responses to chlorpromazine: is there a relationship to drug idiosyncrasy? J. Pharmacol. Exp. Ther. 300, 460-467.

- Cagnol, S., Chambard, J. 2010. ERK and cell death: mechanisms of ERK-induced cell death--apoptosis, autophagy and senescence. FEBS J. 277, 2-21.
- Cao, Z., Yin, W., Zheng, Q., Feng, S., Xu, G., Zhang, K. 2013. Caspase-3 is involved in IFN-γ- and TNF-α-mediated MIN6 cells apoptosis via NF-κB/Bcl-2 pathway. Cell Biochem. Biophys. 67, 1239-1248.
- Cao, Z., Zheng, Q., Li, G., Hu, X., Feng, S., Xu, G., Zhang, K. 2015. STAT1-mediated down-regulation of Bcl-2 expression is involved in IFN-γ/TNF-α-induced apoptosis in NIT-1 cells. PLoS One. 10, e0120921.
- Chakraborty, M., Fullerton, A., Semple, K., Chea, L., Proctor, W., Bourdi, M., Kleiner, D., Zeng, X., Ryan, P., Dagur, P., Berkson, J., Reilly, T., Pohl, L. 2015. Drug-induced allergic hepatitis developed in mice when myeloid-derived suppressor cells were depleted prior to halothane treatment. Hepatology. Published online ahead of print.
- Charli-Joseph, Y., Lima, G., Ramos-Bello, D., Aguilar, D., Orozco-Topete, R., Llorente, L. 2013. Genetic association of IFN-γ +874T/A polymorphism in Mexican patients with drug-induced Stevens-Johnson syndrome/toxic epidermal necrolysis. Arch. Dermatol. Res. 305, 353-357.
- Chen G., Goeddel D. 2002. TNF-R1 Signaling: A Beautiful Pathway. Science. 296, 1634-1635.
- Chen, N., Nomura, M., She, Q.B., Ma, W.Y., Bode, A.M., Wang, L., Flavell, R.A., and Dong, Z. 2001. Suppression of skin tumorigenesis in c-Jun NH2-terminal kinase-2-deficient mice. Cancer Res. 61, 3908–3912.
- Chen, S., Melchior, W., Guo, L. 2014. Endoplasmic reticulum stress in drug- and environmental toxicant-induced liver toxicity. J. Environ. Sci. Health C. Environ. Carcinog. Ecotoxicol. Rev. 32, 83-104.
- Cheng, L., You, Q., Yin, H., Holt, M., Franklin, C., Ju, C. 2009. Effect of polyl:C cotreatment on halothane-induced liver injury in mice. Hepatology. 49, 215-226.
- Cosgrove, B., Alexopoulos, L., Hang, T., Hendriks, B., Sorger, P., Griffith, L., Lauffenburger, D. 2010. Cytokine-associated drug toxicity in human hepatocytes is associated with signaling network dysregulation. Mol. Biosyst. 6, 1195-1206.
- Cosgrove, B., King, B., Hasan, M., Alexopoulos, L., Farazi, P., Hendriks, B., Griffith, L., Sorger, P., Tidor, B., Xu, J., Lauffenburger, D. 2009. Synergistic drug-cytokine induction of hepatocellular death as an in vitro approach for the study of inflammation-associated idiosyncratic drug hepatotoxicity. Toxicol. Appl. Pharmacol. 237, 317-330.
- Cousins, M., Plummer, J., Hall, P. 1989. Risk factors for halothane hepatitis. Aust. N. Z. J. Surg. 59, 5-14Lu J., Jones A.D., Harkema J.R., Roth R.A., Ganey P.E. 2012.

Amiodarone Exposure During Modest Inflammation Induces Idiosyncrasy-Like Liver Injury in Rats: Role of Tumor Necrosis Factor – Alpha. Toxicol. Sci. 125, 126-133.

Cowan, K., Storey, K. 2003. Mitogen-activated protein kinases: new signaling pathways functioning in cellular responses to environmental stress. J. Exp. Biol. 206, 1107-1115.

Crispe, I.N. 2009. The liver as a lymphoid organ. Annu. Rev. Immunol. 27, 147-163.

Czaja, M., Liu, H., Wang, Y. 2003. Oxidant-induced hepatocyte injury from menadione is regulated by ERK and AP-1 signaling. Hepatology. 37, 1405-1413.

Daly, A., Day, C. 2009. Genetic association studies in drug-induced liver injury. Semin. Liver Dis. 29, 400-411.

Dara, L., Ji, C., Kaplowitz, N. 2011. The contribution of endoplasmic reticulum stress to liver diseases. Hepatology. 53, 1752-1763.

Davis, R. 2000. Signal transduction by the JNK group of MAP kinases. Cell. 103, 239-252.

Deng, X., Liguori, M., Sparkenbaugh, E., Waring, J., Blomme, E., Ganey, P., Roth, R. 2008. Gene expression profiles in livers from diclofenac-treated rats reveal intestinal bacteria-dependent and -independent pathways associated with liver injury. J. Pharmacol. Exp. Ther. 327, 634-644.

Deng, X., Stachlewitz, R., Liguori, M., Blomme, E., Waring, J., Luyendyk, J., Maddox, J., Ganey P., Roth, R. 2006. Modest inflammation enhances diclofenac hepatotoxicity in rats: role of neutrophils and bacterial translocation. J. Pharmacol. Exp. Ther. 319, 1191-1199.

Deniaud, A., Sharaf el dein, O., Maillier, E., Poncet, D., Kroemer, G., Lemaire, C., Brenner, C. 2008. Endoplasmic reticulum stress induces calcium-dependent permeability transition, mitochondrial outer membrane permeabilization and apoptosis. Oncogene. 27, 285-299.

Desbois-Mouthon, C., Wendum, D., Cadoret, A., Rey, C., Leneuve, P., Blaise, A., Housset, C., Tronche, F., Le Bouc, Y., Holzenberger, M. 2006. Hepatocyte proliferation during liver regeneration is impaired in mice with liver-specific IGF-1R knockout. FASEB J. 20, 773-775.

Devuyst, O., Lefebvre, C., Geubel, A., Coche, E. 1993. Acute cholestatic hepatitis with rash and hypereosinophilia associated with ranitidine treatment. Acta. Clin. Belg. 48, 109-114.

Dong, Z., Bode, A. 2003. Dialogue between ERKs and JNKs: friendly or antagonistic? Mol. Interv. 3, 306-308.

Drosopoulos, K., Roberts, M., Cermak, L., Sasazuki, T., Shirasawa, S., Andera, L., Pintzas, A. 2005. Transformation by oncogenic RAS sensitizes human colon cells to TRAIL-induced apoptosis by up-regulating death receptor 4 and death receptor 5 through a MEK-dependent pathway. J Biol Chem. 280, 22856-22867.

Dugan, C., MacDonald, A., Roth, R., Ganey, P. 2010. A mouse model of severe halothane hepatitis based on human risk factors. J. Pharmacol. Exp. Ther. 333, 364-372.

Dugan, C., Fullerton, A., Roth, R., Ganey, P. 2011. Natural Killer Cells Mediate Severe Liver Injury in a Murine Model of Halothane Hepatitis. Toxicol. Sci. 120, 507-518.

Elahi, M., Asotra, K., Matata, B., Mastana, S. 2009. Tumor necrosis factor alpha -308 gene locus promoter polymorphism: an analysis of association with health and disease.Biochem. Biophys. Acta. 1792, 163-172.

Enslen, H., Brancho, D., Davis, R. 2000. Molecular determinants that mediate selective activation of p38 MAP kinase isoforms. EMBO J. 19, 1301-1311.

Farrar, M., Schreiber, R. 1993. The molecular cell biology of interferon-γ and its receptor. Annu. Rev. Immunol. 11, 571-611.

Fontana M., Vance R. 2011. Two Signal Models in Innate Immunity. Immunol. Rev. 243, 26-39.

Fredriksson, L., Herpers, B., Benedetti, G., Matadin, Q., Puigvert, J., de Bont, H., Dragovic, S., Vermeulen, N., Commandeur, J., Danen, E., de Graauw, M. van de Water, B. 2011. Diclofenac inhibits tumor necrosis factor-alpha-induced nuclear factor-kappaB activation causing synergistic hepatocyte apoptosis. Hepatology 53, 2027-2041.

Fredriksson, L., Wink, S., Herpers, B., Benedetti, G., Hadi, M., de Bont, H., Groothuis, G., Luijten, M., Danen, E., de Graauw, M., Meerman, J., van de Water B. 2014. Druginduced endoplasmic reticulum and oxidative stress responses independently sensitize toward TNFα-mediated hepatotoxicity. Toxicol. Sci. 140, 144-159.

Fribley, A., Zhang, K., Kaufman, R. 2009. Regulation of apoptosis by the unfolded protein response. Methods Mol Biol. 559, 191-204.

Fuchs, S., Fried, V., Ronai, Z. 1998. Stress-activated kinases regulate protein stability. Oncogene. 17, 1483-1490.

Gabrilovich, D., Nagaraj, S. 2009. Myeloid-derived suppressor cells as regulators of the immune system. Nat. Rev. Immunol. 9, 162-74.

Gao, B., Jeong, W., Tian, Z. 2008. Liver: An organ with predominant innate immunity. Hepatology. 47, 729-736.

Gandhi A., Guo T., Ghose R. 2010. Role of c-Jun N-terminal kinase (JNK) in Regulating Tumor Necrosis Factor-alpha (TNF-a) Mediated Increase of Acetaminophen (APAP) and Chlorpromazine (CPZ) Toxicity in Murine Hepatocytes. Toxicol. Sci. 35, 163-173.

García Rodríguez, L., Williams, R., Derby, L., Dean, A., Jick, H. 1994. Acute liver injury associated with nonsteroidal anti-inflammatory drugs and the role of risk factors. Arch. Intern. Med. 154, 311-316.

Gardner, O., Shiau, C., Chen, C., Graves, L. 2005. Peroxisome proliferator-activated receptor gamma-independent activation of p38 MAPK by thiazolidinediones involves calcium/calmodulin-dependent protein kinase II and protein kinase R: correlation with endoplasmic reticulum stress. J. Biol. Chem. 280, 10109-10118.

Gorina, R., Petegnief, V., Chamorro, A., Planas, A. 2005. AG490 prevents cell death after exposure of rat astrocytes to hydrogen peroxide or proinflammatory cytokines: involvement of the Jak2/STAT pathway. J. Neurochem. 92, 505-518.

Gottesdiener K., Agrawal N., Porras A., Wong P., Rogers J., Gertz B., Redfern J., Marbury T. 2003. Effects of Renal Insufficiency and Hemodialysis on the Pharmacokinetics of Rofecoxib. Am. J. Ther. 10, 252-258.

Gross, A., McDonnell, J., Korsmeyer, S. 1999. BCL-2 family members and the mitochondria in apoptosis. Genes Dev. 13, 1899-1911.

Gumbhir – Shah, K., Cevallos, W., DeCleene, S., Halstenson, C., Korth – Bradley, J. 1997. Absolute bioavailability of bromfenac in humans. Ann. Pharmacother. 31, 395-399.

Gunawan, B., Liu, Z., Han, D., Hanawa, N., Gaarde, W., Kaplowitz, N. 2006. C-Jun Nterminal kinase plays a major role in murine acetaminophen hepatotoxicity. Gastroenterology. 131, 165-178.

Gurumurthy, P., Krishnamurthy, M., Nazareth, O., Parthasarathy, R., Sarma, G., Somasundaram, P., Tripathy, S., Ellard, G. 1984. Lack of relationship between hepatic toxicity and acetylator phenotype in three thousand South Indian patients during treatment with isoniazid for tuberculosis. Am. Rev. Respir. Dis. 129, 58-61.

Hassan, F., Morikawa, A., Islam, S., Tumurkhuu, G., Dagvadorj, J., Koide, N., Naiki. Y., Mori, I., Yoshida, T., Yokochi, T. 2008. Lipopolysaccharide augments the in vivo lethal action of doxorubicin against mice via hepatic damage. Clin Exp Immunol. 151, 334-340.

Hasselblatt, P., Rath, M., Komnenovic, V., Zatloukal, K., Wagner, E.F. 2007. Hepatocyte survival in acute hepatitis is due to c-Jun/AP-1-dependent expression of inducible nitric oxide synthase. Proc. Natl. Acad. Sci. 104, 17105-17110.

Heinze, G., Ploner, M., Dunkler, D., Southworth, H. 2013. Logistf: Firth's bias reduced logistic regression. R package version 1.21.

Hellwig, C., Rehm, M. 2012. TRAIL signaling and synergy mechanisms used in TRAIL-based combination therapies. Mol. Cancer Ther. 11, 3-13.

Hershey, G., Schreiber, R. 1989. Biosynthetic analysis of the human interferon-gamma receptor. Identification of N-linked glycosylation intermediates. J. Biol. Chem. 264, 11981-11988.

Hirata, K., Takagi, H., Yamamoto, M., Matsumoto, T., Nishiya, T., Mori, K., Shimizu, S., Masumoto, H., Okutani, Y. 2008. Ticlopidine-induced hepatotoxicity is associated with specific human leukocyte antigen genomic subtypes in Japanese patients: a preliminary case-control study. Pharmacogenomics J. 8, 29-33.

Hoffman, B., Liebermann, D.A. 2008. Apoptotic signaling by c-MYC. Oncogene. 27, 6462-6472.

Horras C., Lamb C., Mitchell K. 2011. Regulation of Hepatocyte Fate by Interferongamma. Cytokine Growth Factor Rev. 22, 35-43.

Hughes, H., Biehl, J., Jones, A., Schmidt, L. 1954. Metabolism of isoniazid in man is related to the occurrence of peripheral neuritis. Am. Rev. Tuberc. 70, 266-273.

Hussain, S., Harris, C. 2006. P53 biological network: at the crossroads of the cellular-stress response pathway and molecular carcinogenesis. J. Nippon Med. Sch. 73, 54-64.

Hussaini, S., Farrington, E. 2014. Idiosyncratic drug-induced liver injury: an update on the 2007 overview. Expert Opin. Drug Saf. 13, 67-81.

Invernizzi, P. 2013. Liver auto-immunology: the paradox of autoimmunity in a tolerogenic organ. J. Autoimmun. 46, 1-6.

Jeschke, M., Gauglitz, G., Song, J., Kulp, G., Finnerty, C., Cox, R., Barral, J., Herndon, D., Boehning, D. 2009. Calcium and ER stress mediate hepatic apoptosis after burn injury. J. Cell Mol. Med. 13, 1857-65

Johnson, G., Lapadat, R. 2002. Mitogen-activated protein kinase pathways mediated by ERK, JNK, and p38 protein kinases. Science. 298, 1911-1912.

Jo, S., Cho, W., Sung, S., Kim, H., Won, N. 2005. MEK inhibitor, U0126, attenuates cisplatin-induced renal injury by decreasing inflammation and apoptosis. Kidney Int. 67, 458-66.

Kao, E., Shinohara, M., Feng, M., Lau, M., Ji, C. 2012. Human immunodeficiency virus protease inhibitors modulate Ca2+ homeostasis and potentiate alcoholic stress and injury in mice and primary mouse and human hepatocytes. Hepatology. 56, 594-604.

Kaplowitz, N. 2005. Idiosyncratic drug hepatotoxicity. Nat. Rev. Drug Discov. 4, 489-499.

Kim, J., Sharma, R. 2004. Calcium-mediated activation of c-Jun NH2-terminal kinase (JNK) and apoptosis in response to cadmium in murine macrophages. Toxicol. Sci. 81, 518-527.

Kim, S., Yoon, H., Shin, D., Park, S., Kim, Y., Park, J., Jee, Y. 2012. TNF-α genetic polymorphism -308G/A and antituberculosis drug-induced hepatitis. Liver Int. 32, 809-814.

Kindmark, A., Jawaid, A., Harbron, C., Barratt, B., Bengtsson, O., Andersson, T., Carlsson, S., Cederbrant, K., Gibson, N., Armstrong, M., Lagerström-Fermér, M., Dellsén, A., Brown, E., Thornton, M., Dukes, C., Jenkins, S., Firth, M., Harrod, G., Pinel, T., Billing-Clason, S., Cardon, L., March, R. 2008. Genome-wide pharmacogenetic investigation of a hepatic adverse event without clinical signs of immunopathology suggests an underlying immune pathogenesis. Pharmacogenomics J. 8, 186-195.

Kisseleva T., Bhattacharya S., Braunstein J., Schindler C. 2002. Signaling Through the JAK/STAT Pathway, Recent Advances and Future Challenges. Gene. 285, 1-24.

Klaunig, J., Goldblatt, P., Hinton, D., Lipsky, M., Chacko, J., Trump, B. 1981. Mouse liver cell culture. I. Hepatocyte isolation. In Vitro. 17, 913-925.

Kramer, J., Sagartz, J., Morris, D. 2007. The application of discovery toxicology and pathology towards the design of safer pharmaceutical lead candidates. Nat. Rev. Drug Discov. 6, 636-649.

Kyriakis, J., Avruch, J. 2001. Mammalian mitogen-activated protein kinase signal transduction pathways activated by stress and inflammation. Physiol. Rev. 81, 807-869. Review.

Lail-Trecker, M., Peluso, C., Peluso, J. 2000. Hepatocyte growth factor disrupts cell contact and stimulates an increase in type 3 inositol triphosphate receptor expression, intracellular calcium levels, and apoptosis of rat ovarian surface epithelial cells. Endocrine. 12, 303-314.

Laine, L., Goldkind, L., Curtis, S., Connors, L., Yanqiong, Z., Cannon, C. 2009. How common is diclofenac-associated liver injury? Analysis of 17,289 arthritis patients in a long-term prospective clinical trial. Am. J. Gastroenterol. 104, 356-362.

- Larson, A., Polson, J., Fontana, R., Davern, T., Lalani, E., Hynan, L., Reisch, J., Schiødt, F., Ostapowicz, G., Shakil, A., Lee, W. 2005. Acetaminophen-induced acute liver failure: results of a United States multicenter prospective study. Hepatology. 42, 1364-1372.
- Lee, W., Squires, R., Nyberg, S., Doo, E., Hoofnagle, J. 2008. Acute liver failure: Summary of a workshop. Hepatology. 47, 1401-1415.
- Li, D., Liu, J., Mao, Y., Xiang, H., Wang, J., Ma, W., Dong, Z., Pike, H., Brown, R., Reed, J. 2005. Calcium-activated RAF/MEK/ERK signaling pathway mediates p53-dependent apoptosis and is abrogated by alpha B-crystallin through inhibition of RAS activation. Mol. Biol. Cell. 16, 4437-4453.
- Li, N., McLaren, J., Michael, D., Clement, M., Fielding, C., Ramji, D. 2010. ERK is integral to the IFN-γ-mediated activation of STAT1, the expression of key genes implicated in atherosclerosis, and the uptake of modified lipoproteins by human macrophages. J. Immunol. 185, 3041-3048.
- Li, G., Mongillo, M., Chin, K., Harding, H., Ron, D., Marks, A., Tabas, I. 2009. Role of ERO1-alpha-mediated stimulation of inositol 1,4,5-triphosphate receptor activity in endoplasmic reticulum stress-induced apoptosis. J. Cell Biol. 186, 783-792.
- Liang, S., Zhang, W., McGrath, B., Zhang, P., Cavener, D. 2006. PERK (eIF2alpha kinase) is required to activate the stress-activated MAPKs and induce the expression of immediate-early genes upon disruption of ER calcium homoeostasis. Biochem. J. 393, 201-209.
- Lim, M., Lim, P., Gupta, R., Boelsterli, U. 2006. Critical role of free cytosolic calcium, but not uncoupling, in mitochondrial permeability transition and cell death induced by diclofenac oxidative metabolites in immortalized human hepatocytes. Toxicol. Appl. Pharmacol. 217, 322-31.
- Liu, J., Mao, W., Ding, B., Liang, C. 2008. ERKs/p53 signal transduction pathway is involved in doxorubicin-induced apoptosis in H9c2 cells and cardiomyocytes. Am. J. Physiol. Heart Circ. Physiol. 295, H1956-H1965.
- Liu, Z., Kaplowitz, N. 2002. Immune-mediated drug-induced liver disease. Clin. Liver Dis. 6, 755-774.
- Lucena, M., Molokhia, M., Shen, Y., Urban, T., Aithal, G., Andrade, R., Day, C., Ruiz-Cabello, F., Donaldson, P., Stephens, C., Pirmohamed, M., Romero-Gomez, M., Navarro, J., Fontana, R., Miller, M., Groome, M., Bondon-Guitton, E., Conforti, A., Stricker, B., Carvajal, A., Ibanez, L., Yue, Q., Eichelbaum, M., Floratos, A., Pe'er, I., Daly, M., Goldstein, D., Dillon, J., Nelson, M., Watkins, P., Daly, A. 2011. Susceptibility to amoxicillin-clavulanate-induced liver injury is influenced by multiple HLA class I and II alleles. Gastroenterology. 141, 338-347.

Luyendyk J., Maddox J., Cosma G., Ganey P., Cockerell G., Roth R. 2003. Ranitidine treatment during a modest inflammatory response precipitates idiosyncrasy-like liver injury in rats. J. Pharmacol. Exp. Ther. 307, 9-16.

Maiuri A., Breier, A., Gora, L., Parkins, R., Ganey, P., Roth, R. 2015. Cytotoxic Synergy Between Cytokines and NSAIDs Associated with Idiosyncratic Hepatotoxicity is Driven by Mitogen-activated Protein Kinases. Toxicol. Sci. Published online ahead of print.

Mansouri, A., Ridgway, L., Korapati, A., Zhang, Q., Tian, L., Wang, Y., Siddik, Z., Mills, G., Claret, F. 2003. Sustained activation of JNK/p38 MAPK pathways in response to cisplatin leads to Fas ligand induction and cell death in ovarian carcinoma cells. J. Biol. Chem. 278, 19245-19256.

Maundrell, K., Antonsson, B., Magnenat, E., Camps, M., Muda, M., Chabert, C., Gillieron, C., Boschert, U., Vial-Knecht, E., Martinou, J., Arkinstall, S. 1997. Bcl-2 undergoes phosphorylation by c-Jun N-terminal kinase/stress-activated protein kinases in the presence of the constitutively active GTP-binding protein Rac1. J. Biol. Chem. 272, 25238-25242.

Mebratu, Y., Tesfaigzi, Y. 2009. How ERK1/2 activation controls cell proliferation and cell death: Is subcellular localization the answer? Cell Cycle 8, 1168-1175.

Metushi, I., Cai, P., Dervovic, D., Liu, F., Lobach, A., Nakagawa, T., Uetrecht, J. 2015a. Development of a novel mouse model of amodiaquine-induced liver injury with a delayed onset. J. Immunotoxicol. 12, 247-260.

Metushi, I., Hayes, M.A., Uetrecht, J. 2015b. Treatment of PD-1(-/-) mice with amodiaquine and anti-CTLA4 leads to liver injury similar to idiosyncratic liver injury in patients. Hepatology. 61, 1332-1342.

Morita M., Watanabe Y., Akaike T. 1995. Protective Effect of Hepatocyte Growth Factor on Interferon-gamma-Induced Cytotoxicity in Mouse Hepatocytes. Hepatology. 21, 1585-1593.

O'Connor, N., Dargan, P., Jones, A. 2003. Hepatocellular damage from non-steroidal anti-inflammatory drugs. QJM 96, 787-791.

Nagy, G., Kardon, T., Wunderlich, L., Szarka, A., Kiss, A., Schaff, Z., Bánhegyi, G., Mandl, J. 2007. Acetaminophen induces ER dependent signaling in mouse liver. Arch. Biochem. Biophys. 459, 273-279.

Noguchi, K., Kitanaka, C., Yamana, H., Kokubu, A., Mochizuki, T., Kuchino, Y. 1999. Regulation of c-Myc through phosphorylation at Ser-62 and Ser-71 by c-Jun N-terminal kinase. J. Biol. Chem. 274, 32580-32587.

Nowak, G. 2002. Protein kinase C-alpha and ERK1/2 mediate mitochondrial dysfunction, decreases in active Na+ transport, and cisplatin-induced apoptosis in renal cells. J. Biol. Chem. 277, 43377-43388.

Oh-hashi, K., Naruse, Y., Tanaka, M. 2002. Intracellular calcium mobilization induces period genes via MAP kinase pathways in NIH3T3 cells. FEBS Lett. 516, 101-105.

Orrenius, S., Zhivotovsky, B., Nicotera, P. 2003. Regulation of cell death: the calcium-apoptosis link. Nat. Rev. Mol. Cell Biol. 4, 552-565.

Ostapowicz G., Fontana R., Schiodt F., Larson A., Davern T., Han S., McCashland T., Shakil A., Hay J., Hynan L., Crippin J., Blei A., Samuel G., Reisch J., Lee W. 2002. Results of a prospective study of acute liver failure at 17 tertiary care centers in the United States. Ann. Intern. Med. 137, 947-954.

Pardoll, D. 2012. The blockade of immune checkpoints in cancer immunotherapy. Nat. Rev. Cancer. 12, 252-264.

Parker, R., Flint, O., Mulvey, R., Elosua, C., Wang, F., Fenderson, W., Wang, S., Yang, W., Noor, M. 2005. Endoplasmic reticulum stress links dyslipidemia to inhibition of proteasome activity and glucose transport by HIV protease inhibitors. Mol. Pharmacol. 67, 1909-1919.

Pearson, G., Robinson, F., Beers Gibson, T., Xu, B., Karandikar, M., Berman, K., Cobb, M. 2001. Mitogen-activated protein (MAP) kinase pathways: regulation and physiological functions. Endocr. Rev. 22, 153-183.

Pirmohamed, M., Lin, K., Chadwick, D., Park, B. 2001. TNFalpha promoter region gene polymorphisms in carbamazepine-hypersensitive patients. Neurology. 56, 890-896.

Pinsky, M., Vincent, J., Alegre, M., Dupont, E. 1993. Serum cytokine levels in human septic shock. Chest 103, 565-575.

Porter, A., Jänicke, R. 1999. Emerging roles of caspase-3 in apoptosis. Cell Death Differ. 6, 99-104.

Ramm, S., Mally, A. 2013. Role of drug-independent stress factors in liver injury associated with diclofenac intake. Toxicology 312,83-96.

Reid, J., Mandrekar, S., Carlson, E., Harmsen, W., Green, E., McGovern, R., Szabo, E., Ames, M., Boring, D., Limburg, P. 2008. Comparative bioavailability of sulindac in capsule and tablet formulations. Cancer Epidemiol., Biomarkers Prev. 17, 674-679. R Core Team. 2015. R: A language and environment for statistical computing. R Foundation for Statistical Computing, Vienne, Austria.

Ritz, C., Streibig, J. 2005. Bioassay Analysis using R.J. Statist. Software, Vol 12, Issue 5.

Roberts R., Ganey P., Ju C., Kamendulis L., Rusyn I., Klaunig J. 2007. Role of the Kupffer cell in mediating hepatic toxicity and carcinogenesis. Toxicol. Sci. 96, 2-15. Robin, X., Turck, N., Hainard, A., Tiberti, N., Lisacek, F., Sanchez, J., Müller. 2011. pROC: an open-source package for R and S+ to analyze and compare ROC curves. BMC Bioinformatics. 12, 77.

Ron, D., Walter, P. 2007. Signal integration in the endoplasmic reticulum unfolded protein response. Nat. Rev. Mol. Cell Biol. 8, 519-529.

Rosini, P., De Chiara, G., Lucibello, M., Garaci, E., Cozzolino, F., Torcia, M. 2000. NGF withdrawal induces apoptosis in CESS B cell line through p38 MAPK activation and Bcl-2 phosphorylation. Biochem. Biophys. Res. Commun. 278, 753-759. Roth, R., Ganey, P. 2011. Animal models of idiosyncratic drug-induced liver injury-current status. Crit. Rev. Toxicol. 41, 723-739.

Roulston, A., Reinhard, C., Amiri, P., Williams, L. 1998. Early activation of c-Jun N-terminal kinase and p38 kinase regulate cell survival in response to tumor necrosis factor alpha. J. Biol. Chem. 273, 10232-10239.

Roux, P., Blenis, J. 2004. ERK and p38 MAPK-activated protein kinases: a family of protein kinases with diverse biological functions. Microbiol. Mol. Biol. Rev. 68, 320-44.

Rutkowski, D., Kaufman, R. 2004. A trip to the ER: coping with stress. Trends Cell Biol. 14, 20-28.

Saberi, B., Ybanez, M., Johnson, H., Gaarde, W., Han, D., Kaplowitz, N. 2014. Protein kinase C (PKC) participates in acetaminophen hepatotoxicity through c-jun-N-terminal kinase (JNK)-dependent and -independent signaling pathways. Hepatology. 59, 1543-1554.

Sadzak, I., Schiff, M., Gattermeier, I., Glinitzer, R., Sauer, I., Saalmüller, A., Yang, E., Schaljo, B., Kovarik, P. 2008. Recruitment of Stat1 to chromatin is required for interferon-induced serine phosphorylation of Stat1 transactivation domain. Proc. Natl. Acad. Sci. USA. 105, 8944-8949.

Sato, Y., Tsukada, K., Matsumoto, Y., Abo, T. 1993. Interferon-gamma Inhibits Liver Regeneration by Stimulating Major Histocompatibility Complex Class II Antigen Expression by Regenerating Liver. Hepatology. 18, 340-346.

Schenten, D., Medzhitov, R. 2011. The control of adaptive immune responses by the innate immune system. Adv. Immunol. 109, 87-124.

Seki, E., Brenner, D., Karin, M. 2012. A liver full of JNK: signaling in regulation of cell function and disease pathogenesis, and clinical approaches. Gastroenterology. 124, 307-320.

- Setiawati, E., Deniati, S., Yunaidi, D., Handayani, L., Harinanto, G., Santosos, I., Purnomo, Sari, A., Rimainar, A. 2009. Bioequivalence study with two naproxen sodium tablet formulations in healthy subjects. J. Bioequivalence Bioavailability 1, 28-33.
- Shaw, P., Ditewig, A., Waring, J., Liguori, M., Blomme, E., Ganey, P., Roth, R. 2009b. Coexposure of mice to trovafloxacin and lipopolysaccharide, a model of idiosyncratic hepatotoxicity, results in a unique gene expression profile and interferon gammadependent liver injury. Toxicol. Sci. 107, 270-280.
- Shaw, P., Ganey, P., Roth, R. 2009a. Tumor necrosis factor alpha is a proximal mediator of synergistic hepatotoxicity from trovafloxacin/lipopolysaccharide coexposure. J. Pharmacol. Exp. Ther. 328, 62-68.
- Shaw P., Ganey P., Roth R. 2010. Idiosyncratic Drug-Induced Liver Injury and the Role of Inflammatory Stress with an Emphasis on an Animal Model of Trovafloxacin Hepatotoxicity. Toxicol. Sci. 118, 7-18.
- Shaw P., Hopfensperger M., Ganey P., Roth R. 2007. Lipopolysaccharide and trovafloxacin coexposure in mice causes idiosyncrasy-like liver injury dependent on tumor necrosis factor-alpha. Toxicol. Sci. 100, 259-266.
- She, Q., Chen, N., Dong, Z. 2000. ERKs and p38 kinase phosphorylate p53 protein at serine 15 in response to UV radiation. J. Biol. Chem. 275, 20444-20449.
- Shen, H., Pervaiz, S. 2006. TNF receptor superfamily-induced cell death: redox-dependent execution. FASEB J. 20, 1589-1598.
- Shuai, K., Liu, B. 2003. Regulation of JAK-STAT signalling in the immune system. Nat. Rev. Immunol. 11, 900-911.
- Spraggs, C., Budde, L., Briley, L., Bing, N., Cox, C., King, K., Whittaker, J., Mooser, V., Preston, A., Stein, S., Cardon, L. 2011. HLA-DQA1*02:01 is a major risk factor for lapatinib-induced hepatotoxicity in women with advanced breast cancer. J. Clin. Oncol. 29, 667-673.
- Stark G., Kerr I., Williams B., Silverman R., Schreiber R. 1998. How Cells Respond to Interferons. Annu. Rev. Biochem. 67, 227-264.
- Stephanou, A., Latchman, D. 2003. STAT-1: a novel regulator of apoptosis. Int. J. Exp. Pathol. 84, 239-244.
- Stepniak, E., Ricci, R., Eferl, R., Sumara, G., Sumara, I., Rath, M., Hui, L., Wagner, E. 2006. c-Jun/AP-1 controls liver regeneration by repressing p53/p21 and p38 MAPK activity. Genes Dev. 20, 2306-2314.

Stevens, J., Baker, T. 2009. The future of drug safety testing: expanding the view and narrowing the focus. Drug Discov Today. 14, 162-167.

Stonāns, I., Stonāne, E., Russwurm, S., Deigner, H., Böhm, K., Wiederhold, M., Jäger, L., Reinhart, K. 1999. HepG2 human hepatoma cells express multiple cytokine genes. Cytokine 11, 151-156.

Sun, F., Chen, Y., Xiang, Y., Zhan, S. 2008. Drug-metabolizing enzyme polymorphisms and predisposition to anti-tuberculosis drug-induced liver injury: a meta-analysis. 2008. Int. J. Tuberc. Lung Dis. 12, 994-1002.

Svegliati-Baroni, G., Ridolfi, F., Caradonna, Z., Alvaro, D., Marzioni, M., Saccomanno, S., Candelaresi, C., Trozzi, L., Macarri, G., Benedetti, A., Folli, F. 2003. Regulation of ERK/JNK/p70S6K in two rat models of liver injury and fibrosis. J. Hepatol. 39, 528-537.

Szalai, G., Krishnamurthy, R., Hajnóczky, G. 1999. Apoptosis driven by IP(3)-linked mitochondrial calcium signals. EMBO J. 18, 6349-6361.

Takai, S., Higuchi, S., Yano, A., Tsuneyama, K., Fukami, T., Nakajima, M., Yokoi, T. 2013. Involvement of immune- and inflammatory-related factors in flucloxacillin-induced liver injury in mice. J Appl Toxicol. 35, 142-51.

Taudorf, S., Krabbe, K., Berg, R., Pedersen, B., Møller, K. 2007. Human models of low-grade inflammation: bolus versus continuous infusion of endotoxin. Clin. Vaccine Immunol. 14, 250-255.

Teoh, N., Farrell, G. 2003. Hepatotoxicity associated with non-steroidal anti-inflammatory drugs. Clin. Liver Dis. 7, 401-413.

Tewari, R., Sharma, V., Koul, N., Sen, E. 2008. Involvement of miltefosine-mediated ERK activation in glioma cell apoptosis through Fas regulation. J. Neurochem. 107, 616-627.

Timmins, J., Ozcan, L., Seimon, T., Li, G., Malagelada, C., Backs, J., Backs, T., Bassel-Duby, R., Olson, E., Anderson, M., Tabas, I. 2009. Calcium/calmodulin-dependent protein kinase II links ER stress with Fas and mitochondrial apoptosis pathways. J. Clin. Invest. 119, 2925-2941.

Trey C., Davidson C.S. 1970. The Management of Fulminant Hepatic Failure. Prog. Liver Dis. 3, 282-98.

Tuijos, S., Fontana, R. 2011. Mechanisms of drug-induced liver injury: from bedside to bench. Nat. Rev. Gastroenterol. Hepatol. 8, 202-211.

Tukov F., Maddox J., Amacher D., Bobrowski W., Roth R., Ganey P. 2006. Modeling Inflammation – Drug Interactions in Vitro: A Rat Kupffer cell – Hepatocyte Coculture System. Toxicology in Vitro. 20, 1488-1499.

Uetrecht, J. 1999. New concepts in immunology relevant to idiosyncratic drug reactions: the "danger hypothesis" and innate immune system. Chem. Res. Toxicol. 12, 387-395.

Ulisse, S., Cinque, B., Silvano, G., Rucci, N., Biordi, L., Cifone, M., D'Armiento, M. 2000. Erk-dependent cytosolic phospholipase A2 activity is induced by CD95 ligand cross-linking in the mouse derived Sertoli cell line TM4 and is required to trigger apoptosis in CD95 bearing cells. Cell Death Differ. 7, 916-924.

Unzueta, A., Vargas, H. 2013. Nonsteroidal anti-inflammatory drug-induced hepatotoxicity. Clin. Liver Dis. 17, 643-656.

Urano, F., Wang, X., Bertolotti, A., Zhang, Y., Chung, P., Harding, H., Ron, D. 2000. Coupling of stress in the ER to activation of JNK protein kinases by transmembrane protein kinase IRE1. Science. 287, 664-666.

Uzi, D., Barda, L., Scaiewicz, V., Mills, M., Mueller, T., Gonzalez-Rodriguez, A., Valverde, A.M., Iwawaki, T., Nahmias, Y., Xavier, R., Chung, R., Tirosh, B., Shibolet, O. 2013. CHOP is a critical regulator of acetaminophen-induced hepatotoxicity. J. Hepatol. 59, 495-503.

Vanderlinde, R. 1985. Measurement of total lactate dehydrogenase activity. Ann. Clin. Lab. Sci. 15, 13–31.

Varinou, L., Ramsauer, K., Karaghiosoff, M., Kolbe, T., Müller, M., Decker, T. 2003. Phosphorylation of the Stat1 transactivation domain is required for full-fledged IFN-gamma-dependent innate immunity. Immunity. 19, 793-802.

Verrier, F., Deniaud, A., Lebras, M., Métivier, D., Kroemer, G., Mignotte, B., Jan, G., Brenner, C. 2004. Dynamic evolution of the adenine nucleotide translocase interactome during chemotherapy-induced apoptosis. Oncogene. 23, 8049-8064.

Viechtbauer, W. 2010. Conducting meta-analyses in R with the metafor package. J. of Statistical Software. 36, 1-48.

Vodovotz Y., Kim P., Bagci E., Ermentrout G., Chow C., Bahar I., Billiar T. 2004. Inflammatory Modulation of Hepatocyte Apoptosis by Nitric Oxide: in Vivo, in Vitro, and in Silico studies. Curr. Mol. Med. 4, 753-762.

Volpes R., Van Den Oord J., De Vos R., Depla E., De Ley M., Desmet V. 1991. Expression of Interferon-gamma Receptor in Normal and Pathological Human Liver Tissue. Hepatology. 12, 195-202.

Wajant H., Pfizenmaier K., Scheurich P. 2003. Tumor necrosis factor signaling. Cell Death. Differ. 10, 45-65.

Wang W., Liao X., Chen J., Li D., Lin C., Yan Y., Tang Y., Jiang J. 2011. Sodium Valproate Induces Mitochondria-dependent Apoptosis in Human Hepatoblastoma Cells. Chinese Med. J. 124, 2167-2172.

Wang, X., Martindale, J., Holbrook, N. 2000. Requirement for ERK activation in cisplatin-induced apoptosis. J. Biol. Chem. 275, 39435-39443.

Watkins P. 2005. Idiosyncratic Liver Injury: Challenges and Approaches. Toxicologic Pathology 33, 1-5.

Wen, Z., Zhong, Z., Darnell, J.E. 1995. Maximal activation of transcription by Stat1 and Stat3 requires both tyrosine and serine phosphorylation. Cell. 82, 241-250.

Westerink, W., Schoonen, W. 2007a. Cytochrome p450 enzyme levels in HepG2 cells and cryopreserved primary human hepatocytes and their induction in HepG2 cells. Toxicol. In Vitro 21, 1581-1591.

Westerink, W., Schoonen, W. 2007b. Phase II enzyme levels in HepG2 cells and cryopreserved primary human hepatocytes and their induction in HepG2 cells. Toxicol. In Vitro 21, 1592-1602.

Wu, D., Cederbaum, A. 2008. Cytochrome P4502E1 sensitizes to tumor necrosis factor alpha-induced liver injury through activation of mitogen-activated protein kinases in mice. Hepatology. 47, 1005-1017.

Wullaert, A., Van, L., Heyninck, K., Beyaert, R. 2007. Hepatic tumor necrosis factor signaling and nuclear factor-kappaB: effects on liver homeostasis and beyond. Endocr. Rev. 28, 365-386.

Xu, J., Henstock, P., Dunn, M., Smith, A., Chabot, J., Graff, D. 2008. Cellular Imaging Predictions of Clinical Drug-Induced Liver Injury. Toxicol. Sci. 105, 97-105.

Yamamoto, K., Ichijo, H., Korsmeyer, S. 1999. BCL-2 is phosphorylated and inactivated by an ASK1/Jun N-terminal protein kinase pathway normally activated at G(2)/M. Mol Cell Biol. 19, 8469-8478.

Yan, W., Frank, C., Korth, M., Sopher, B., Novoa, I., Ron, D., Katze, M. 2002. Control of PERK elF2alpha kinase activity by the endoplasmic reticulum stress-induced molecular chaperone P58IPK. Proc. Natl. Acad. Sci. 99, 15920-15925.

Ye, J., Rawson, R., Komuro, R., Chen, X., Davé, U.P., Prywes, R., Brown, M., Goldstein, J. 2000. ER stress induces cleavage of membrane-bound ATF6 by the same proteases that process SREBPs. Mol. Cell. 6, 1355-1364.

Yoshida, H., Matsui, T., Hosokawa, N., Kaufman, R., Nagata, K., Mori, K. 2003. A time-dependent phase shift in the mammalian unfolded protein response. Dev. Cell. 4, 265-271.

Zhang, Y., Cho, Y., Peterson, B., Zhu, F., Dong, Z. 2004. Evidence of STAT1 phosphorylation modulated by MAPKs, MEK1 and MSK1. Carcinogenesis. 25, 1165-1175.

Zimmerman, H. 1999. Hepatotoxicity: the adverse effects of drugs and other chemicals on the liver. 2nd ed. Philadelphia: Lippincott, Williams and Wilkins.

Zou, W., Beggs, K., Sparkenbaugh, E., Jones, A., Younis, H., Roth, R., and Ganey, P. 2009. Sulindac metabolism and synergy with tumor necrosis factor-alpha in a drug-inflammation interaction model of idiosyncratic liver injury. J. Pharmacol. Exp. Ther. 331, 114-121.

Zou W., Roth R., Younis H., Malle E., Ganey P. 2011. Neutrophil – Cytokine Interactions in a Rat Model of Sulindac-Induced Idiosyncratic Liver Injury. Toxicology. 290, 278-285.